

multi-Risk sciEnce for resilienT commUnities undeR a changiNgcLimate

Codice progetto MUR: **PE00000005** – CUP LEAD PARTNER: E63C22002000002



Deliverable title: Multi-criteria metrics and methodology for integrated exposure assessment

Deliverable ID: 5.2.2

Due date: November, 2023 (M12)

Submission date: November 30th, 2023

AUTHORS

Mario Losasso (Task leader), Valeria D'Ambrosio, Enza Tersigni, Maria Fabrizia Clemente, Sara Verde, Antonio Sferratore, Pasquale De Toro, Martina Bosone, Bruna Di Palma, Paola Galante, Federica Visconti, Marilena Bosone, Ferdinando Di Martino, Vittorio Miraglia (UNINA DIARC); Maria Polese, Andrea Prota, Gabriella Tocchi, Carlo Del Gaudio (UNINA DIST); Anna Maria Zaccaria, Antonino Rapicano (UNINA DISS); Francesco De Paola, Giuseppe Speranza (UNINA-DICEA); Federico Porcù, Tiziano Maestri, Erika Brattich, Giorgia Proietti Pelliccia, Mohammad Reza Shirzad (UNIBO); Chiara Scaini, Antonella Peresan (OGS); Paola Vannucchi (Task co-leader), Daniele Maestrelli (UNIFI); Paolo Prati, Dario Massabò (UNIGE).

Technical references.....	5
Document history	6
Table of contents	7
List of Tables	7
List of Figures	7
1. Executive summary.....	11
2. Conceptual frameworks	13
2.1. Urban and Metropolitan Settlements: systemic approach and multi-scalar urban components 13	
2.1.1. The District scale	14
2.2. Hazard, vulnerability and exposure of urban systems	16
2.3. From the concept of exposure to integrated exposure.....	18
2.3.1. Definitions and integration factors for exposure under multi-risk conditions.....	19
2.3.2. Vulnerability aspects in characterizing exposure	23
2.3.3. Typo-morphological aspects of urban settlements considering integrated exposure factors	24
2.3.3.1. Characteristics of urban settlements	25
2.3.3.2. Urban analysis.....	26
2.4. Metrics, index and indicator.....	30
2.4.1. Metrics, index and GIS-based indicators	30
2.5. Multi-criteria approaches for exposure assessment.....	32
2.5.1. Heat wave.....	35
2.5.2. Flooding	37
2.5.3. Coastal erosion	38
2.5.4. Earthquake.....	40
3. Knowledge of Urban and Metropolitan Settlements oriented to exposure assessment	45
3.1. Urban Settlement system analysis	45
3.1.1. The urban physical system	45
3.1.2. The socio-ecological system.....	48
3.1.3. The geo-morphological system	51
3.1.4. Settlement models	54
3.1.4.1. Combination of layout patterns and morphological variations of settlements	55

3.2. Characterization of urban settlements: typo-morphological, environmental and spatial-functional analysis.....	56
3.3. Identification of recurring urban patterns of buildings and open spaces.....	60
3.3.1. Buildings	60
3.3.2. Open spaces.....	64
3.3.3. Definition of an algorithm in a GIS environment for the recognition of recurring urban patterns in urban settlements	68
3.3.4. Urban settlements knowledge through integrated taxonomies: the contribution of Local Climate Zones	69
3.4. A clustering proposal of existing urban settlements.....	72
3.5. The impending hazards in urban context.....	78
3.5.1. Score-based procedure for the identification of relevant hazards.....	80
3.6. Citizen-centered exposure data collection for multi-risk exposure development	86
4. Urban critical context and Urban Hotspot.....	89
4.1. Urban critical context and hotspot identification criteria	89
4.1.1. Challenges and methods to hotspot assessment.....	92
4.1.2. Relevant implications for hotspot assessment	94
4.2. The use of indicators to identify urban critical context/hotspots taking into account heatwaves and air pollution	95
4.2.1. Heatwave.....	96
4.2.2. Aerosol pollution	103
4.2.3. Relevant indicators to characterize heat waves and aerosol pollution hazards and exposure	105
4.2.4. Composite effect of heat waves and air pollution	106
4.3. Hotspot example identification and assessment using GIS based approaches	107
4.3.1. Identification of flooding risk hotspots	108
4.3.2. Identification of heatwave risk hotspots.....	111
4.3.3. An example of heatwave hotspot assessment.....	112
5. Composite indicators for multi-risk exposure assessment	117
5.1. Composite indicators.....	117
5.1.1. Identification of Critical Urban Context or HotSpot using multi-risk composite-index	118
5.1.2. Step-by-step methodology to identify Critical Urban Contexts (CUC) or HotSpots (HS) within an urban settlement	119
5.1.2.1. Example application for identification of CUC.....	119
5.1.2.2. Example application for identification of HS	125
5.1.3. Selecting relevant sub-indicators: the use of risk storylines	128
5.1.3.1. Example application for the construction of composite-index based on risk-storyline	130

5.2. Multi-criteria Decision Analysis as a tool supporting effective risk management.....	133
---	-----

References	135
------------------	-----

Cartographic documents	167
------------------------------	-----

Authors contribution	168
----------------------------	-----

Technical references

Project Acronym	RETURN
Project Title	multi-Risk sciEnce for resilientT commUnities undeR a changiNg climate
Project Coordinator	Domenico Calcaterra UNIVERSITA DEGLI STUDI DI NAPOLI FEDERICO II domcalca@unina.it
Project Duration	December 2022 – November 2025 (36 months)

Deliverable No.	DV2.2
Dissemination level*	
Work Package	WP2 - Multi-risk-oriented modeling of urban systems
Task	T2.2 – Integrated physical and socio-ecological exposure to multiple hazards
Lead beneficiary	UNINA
Contributing beneficiary/ies	Partner short name, Partner short name, Partner short name, etc.

* PU = Public

PP = Restricted to other programme participants (including the Commission Services)

RE = Restricted to a group specified by the consortium (including the Commission Services)

CO = Confidential, only for members of the consortium (including the Commission Services)

Document history

Version	Date	Lead contributor	Description
0.1	17.03.2023	Mario Losasso (UNINA), Paola Vannucchi (UNIFI)	First draft
0.2	07.06.2023	Mario Losasso (UNINA), Paola Vannucchi (UNIFI)	Critical review and proofreading; Task Extended description
0.3	20.11.2023	All the authors	
0.4		Mario Losasso (UNINA), Maria Polese (UNINA)	Edits for approval
1.0	30.11.2023		Final version
1.0	15.09.2025	Mario Losasso (UNINA), Maria Polese (UNINA), Maria Fabrizia Clemente (UNINA)	Final editing for publication on RETURN platform

Table of contents

List of Tables

Table 1. Exposure indicator sample.	31
Table 2. Thematic classification methods for value ranges used in GIS environments.	31
Table 3. MCDAs methods comparison regarding exposure assessment.	33
Table 2. MCDAs methods used for different hazards.	41
Table 5. Sub-systems and components of urban settlements.	Errore. Il segnalibro non è definito.
Table 6. An example of environmental, technological, and functional-spatial analysis used to assess the integrated exposure of built-up areas.	47
Table 7. Hazard classification.	79
Table 8. Hotspot definitions.	90
Table 9. List of indicators for assessment of heat hazard, vulnerability and exposure (Tuomimaa et al., 2023).	102
Table 10. Indicators to characterize heatwaves and aerosol pollution hazards.	105
Table 11. Real estate market value and lease value of residential buildings in each OMI zone of Somma Vesuviana.	120
Table 12. Seismic hazard and integrated vulnerability indicators and related normalized value for each urban district (i.e., OMI zone). The final value of the seismic risk index is reported in the last column (R_index).	123
Table 13. Flood hazard and integrated vulnerability indicators and related normalized value for each urban district (i.e., OMI zone). The final value of the flood risk index is reported in the last column (R_index).	124

List of Figures

Figure 1. The urban system as an ecosystem. (Source: Duvigneaud and Denaeyer-De Smet, 1977).	13
Figure 2. Multi-scalar approach. Accounting for the interactions among different sub-systems, a proposal for the identification of administrative boundaries to outline macro-meso-micro scale entities to be investigated. The identification of urban districts is not only in administrative boundaries, but also in accounting for built up pattern homogeneity, natural and administrative boundaries, geomorphological features, infrastructure system, road patterns, homogeneous economic value, construction period, and technical-constructive features.	14
Figure 3. Extrapolation from satellite data of built-up areas, to be defined later in their scaling (Source: Author's elaboration based on Corbane, C., Rodriguez, D., Sabo, F., Politis, P., Syrris, V. Large scale mapping of human settlements from Earth. Observation data with JEO-batch of the JRC Earth Observatory Data and Processing Platform, EU Joint Research Centre, Disaster Risk Management Unit).	15
Figure 4. An example of Urban Districts identification in west Naples' Macro-area. (Source: Bologna, Losasso, Mussinelli, Tucci, 2021).	16
Figure 5. INFORM Risk Model. (scaling (Source: Author's elaboration based on DRMKC, European Commission Disaster Risk Management, https://drmkc.jrc.ec.europa.eu/inform-index).	20
Figure 6. Graphical presentation of the Hazard & exposure dimension (Source: INFORM Risk Model, https://drmkc.jrc.ec.europa.eu/inform-index/INFORM-Risk)	21

Figure 7. Maps of exposure: population density (Source: Galderisi & Limongi, 2021).	22
Figure 8. Paul Klee, A sheet from the city book, 1928.	24
Figure 9. Map of Miletus and map of Athens in its geographical context	25
Figure 10. Map of the city of Aleppo before the destruction of the civil war (Source: Davolio, 2019).	26
Figure 11. The historic center of Polignano a Mare in the studies of Gianfranco Caniggia.	27
Figure 12. Drawings from S. Bisogni, A. Renna, Il disegno della città di Napoli, 1974 (1964).	28
Figure 13. Naples Spatial History. Figure-background plan and Red-blue plan from the Greek-Roman city to the contemporary city	28
Figure 14. Typological and Spatial Analysis. On the left: The primary elements in the dense structure of the city. On the right: Interior and exterior urban spaces	29
Figure 15. S. Muratori. Atlas (unpublished) of the territory. Padania Romana (Source: Lombardini, 2017).	30
Figure 16. a) The Florence urban settlement as depicted in the 1:10.000 Tuscany geological map (CARG 1:10.000 section n. 275040). The city of Florence well fits with the hypothetical urban settlement proposed in the Scenario n. 5. b) An example of 3D geo-model produced for a portion of the Florence urban area. The 3D model highlights the subsurface stratigraphy and structural setting.	54
Figure 17. Grid pattern (a), radial plan (b) and linear plan city model (c).	55
Figure 18. Real cases approach to identify basic patterns and subsequent tracing of their variations in urban context.	56
Figure 19. Example of identifying of urban districts.	57
Figure 20. Example of reading by homogeneous criteria and identifying systems for a typical critical context (top left: orographic system; top right: settlement system; bottom left: natural system, bottom right: complex system)	59
Figure 21. Recurring building typologies in urban fabrics and their dimensional characteristics.	61
Figure 22. Stone wall", example data sheet of the prevailing construction technique catalogue.	61
Figure 23. Classification of prevailing construction techniques according to the different building typologies identified.	62
Figure 24. Parameters for the identification of recurring residential building typologies.	63
Figure 25. Thematic map of prevailing building typology by census area.	63
Figure 26. Distribution of prevalent building construction periods recorded with respect to census areas.	64
Figure 27. Generic urban patterns: (a) from right to left: pavilions, slabs, terraces, terrace-courts, pavilion-courts and courts; (b) deduced generic urban patterns for Italian cities (Source: Bassolino et al., 2021; Verde et al., 2021).	65
Figure 28. Classification of urban patterns: (a) high-density urban patterns; (b) medium and low-density urban patterns; (c) squares and open spaces; (d) medium green areas and green areas (Source: Bassolino et al., 2021; Verde et al., 2021).	67
Figure 29. Comparison between the values of descriptive indicators of urban morphology accuracy between the different input model of data and simulation tools. Test on the urban patterns of the city of Naples (Source: Bassolino et al., 2021).	68
Figure 30. Map of building density and green areas by census section (Source: Verde et al., 2021).	69
Figure 31. Schematic representation of the adopted methodology (a); taxonomic analysis of Soccavo district and database structure. Each element reports its LCZ classification (highlighted in light blue), taxonomy classes (highlighted in blue) and the corresponding design strategies according to NCCAP Database.	71
Figure 32. Classification of Italian municipalities based on urban degree (left) and urban centeredness degree (right).	73
Figure 33. Italian municipalities classified based on number of inhabitants (left) and altimetric zone (right).	74

Figure 34. Distribution of municipalities in Italy based on combination of population class and urban degree (a); population class and urban centeredness degree (b); urban degree and urban centeredness degree (c).	75
Figure 35. Distribution of municipalities and population in Italy based on the urban degree (a); number of municipalities based on urban centeredness degree classification (b); percentage of municipalities – classified in cities, towns/suburbs and rural areas based on urban degree – in different altimetric zones.	76
Figure 36. Clusters obtained combining information on urban degree and urban centeredness degree.	77
Figure . Maps showing: the number of industrial sites classified as major accident hazard sites located in each municipality (left) and the social vulnerability index value calculated at municipal level (right).	78
Figure 37. Number of deaths (a) and economic damages expressed as a share of GDP (Gross Domestic Product) (b) caused in Italy by natural disasters during last century. Source EM-DAT https://www.emdat.be/ .	81
Figure 38. ECDF of seismic hazard intensity measure (left) and seismic hazard scores for each municipality (right).	82
Figure 39. ECDFs of riverine flood hazard (left) considering the percentage of residential area (top) and the percentage of industrial area (bottom) potentially inundated as intensity measure; maps show the riverine flood hazard scores for residential areas (left) and industrial areas (right) in each municipality.	83
Figure 40. ECDFs of tsunami hazard (left) considering the percentage of residential area (top) and the percentage of industrial area (bottom) potentially inundated as intensity measure; maps show tsunami hazard scores for residential areas (left) and industrial areas (right) in each municipality.	84
Figure 41. ECDF of heat wave hazard adopting the monthly average maximum temperature as proxy of the intensity (left) and values of heat wave score for each municipality in Italy (right).	85
Figure 42. Building typologies identified while implementing CEDAS in a pilot area in northeastern Italy.	87
Figure 43. Sketch of the approach to be implemented within the SMILE project: the data collected by citizens and the satellite images will be processed by a machine learning engine to update the current exposure layers.	88
Figure 44. Process definition and model hypothesis to outline hotspot areas in critical contexts. The application of strategies and actions for risk mitigation (adaptation, vulnerability and exposure reduction, and resilience enhancement) should be tested to assess impact reduction.	89
Figure 45. Climate change related issues and challenges for the multi-risk assessment (Source: Gallina et al., 2016).	93
Figure 46 . Multi-risk assessment process. The definition of risk curves depends on the combination of different indexes related to single risks. The risk assessment process is developed using spatial information on hazards, elements at risk and vulnerability with the use of GIS based tools and remote sensing. (Source: Risk City Application of GIS for multi-hazard risk assessment in an urban environment Cees van Westen, ISL, 2004).	94
Figure 47. Left, European Air Quality Index categories and related pollutant range values; right, health messages associated with each category (source: European Environment Agency)	96
Figure 48. Heat index calculation and consequences on human health. Green refers to possible fatigue, and heat cramp. Light orange refers to high fatigue, and respiratory difficulties. Dark orange refers to possible heat stroke and insolation. Red refers to highly probable heat stroke.	97
Figure 49. Humindex calculation: relative humidity in the abscissa and temperature on the ordinate axis.	98
Figure 50. Wind chill calculation and value. Source: Britannica, 2023.	99
Figure 51. Geographic coverage of PM10 measurements for the OECD and G20 countries in AirBase. (Turner et al., 2016).	104
Figure 52. Climate change: its influence on extreme weather events, air pollution and aeroallergens, and effects on respiratory health. PM: particulate matter; COPD: chronic obstructive pulmonary disease. (De Sario et al. 2014)	107

Figure 53. Hazard (H), exposure (E) and risk (R), the concept of a risk hotspot (Jalayer F, et al. (2014) Probabilistic GIS-based method for delineation of urban flooding risk hotspots).....	108
Figure 54. Flowchart describing the conceptual development of the proposed methodology for delineation of urban flooding hotspots (Jalayer F, et al. (2014) Probabilistic GIS-based method for delineation of urban flooding risk hotspots).	109
Figure 55. Main components of the TWI calculation (Jalayer F, et al. (2014) Probabilistic GIS-based method for delineation of urban flooding risk hotspots).	110
Figure 56. Mapping UMT units using ortho-rectified aerial photography, an example in Addis Ababa. Note Fig. 4a (source www.bing.it/maps) is not the original orthophoto based on which the UMT in Fig. 4b is generated (Jalayer F, et al. (2014) Probabilistic GIS-based method for delineation of urban flooding risk hotspots).....	111
Figure 57. a) Hypothesis of the Roman centuriatio in V. Valerio, “La carta di Napoli e dintorni degli anni 1817/1819, Napoli 1983”. Nola is located in the red square b)	112
Figure 58. a) Heat wave days. Data processed from Capodichino weather station data (Source: https://www.ilmeteo.it/portale/archivio-meteo/Napoli) b) Historical series of rainfall data recorded in Cicciano from 2008 to 2020 (Source: http://centrofunzionale.regione.campania.it/#/pages/dashboard) integrated with data from Annali dell’Ufficio Idrografico e Mareografico di Napoli (1928-1999) c) The diagram of Bagnoulus Gaussen highlights on Nola a period of dryness, from May to August, coinciding with the stretch of the graph in which the curve of precipitation falls below that of temperatures.	113
Figure 59. Conceptual framework for integrated exposure assessment	114
Figure 60. Integrated exposure assessment for the case of heat wave.....	114
Figure 61. GIS-based framework.	115
Figure 62. a) population density b) vulnerable population (< 5 years > 65anni).	116
Figure 63. Heat wave HotSpot Areas Identification based on the exposure value.....	116
Figure 64. Delimitation of OMI zones allowing to identify urban districts in Somma Vesuviana. Each zone is identified by an alphanumeric code that categorizes the zone as Central (B), Semi-central (C), Suburb (D) and rural (R).	120
Figure 65. Vs30 map (left) proposed by Mori et al. (2020) and slope map (right) for the municipality of Somma Vesuviana (bounded with red polyline).	121
Figure 66. Hydrogeographic network and flood hazard maps for the medium probability flood scenario provided by ISPRA for Somma Vesuviana	122
Figure 67. Integrated risk index values for Somma Vesuviana’s districts.	125
Figure 68. Impact scenario of pluvial flooding (on the left) and of heat wave (on the right).	127
Figure 69. Urban hotspots. In the described example the urban hotspots are identified based on a quantitative approach and aggregation rules specific for the study area.	128
Figure 70. Example of impact chain showing the sequence of impacts due to the occurrence of a tsunami triggered by an earthquake in an urban context characterized by the presence of an industrial site handling dangerous substances.....	130

1. Executive summary

Multi-risk conditions affect urban and metropolitan settlements, characterized in their complexity by the interaction between biophysical (urban settlements, water, soil, etc.), infrastructural, geological and geomorphological as well as socioeconomic subsystems. Here a condition resulting from the simultaneous occurrence of hazards, both climatic and non-climatic, interacting with each other with the consequent aggravation of overall and cascading risks is identified as multi-hazard (IPCC, AR6, 2022).

The co-presence of multiple hazards and the simultaneous occurrence of multi-hazard conditions can trigger the attainment of tipping points (breaking points), potentially responsible for undermining the balance of socio-ecological (IPCC, AR6, 2022), environmental and urban systems.

Compound risks are defined as "risks resulting from the interaction of hazards, which may be characterized by single extreme events or multiple coincidental or sequential events interacting with exposed systems" (IPCC, 2022, Glossary of terms, p. 303).

The identification of settlement contexts and hotspot areas, characterized by the concentration or overlap of detected risks and impacts, makes the application of counter measures (adaptation, vulnerability and exposure reduction, and resilience enhancement strategies and actions) a priority.

Within these contexts/areas, multicriteria assessments must be developed that are the operational translation of the objectives, such that they can be measured to implement a comparison between various alternatives. Criterion construction requires the definition of: meaning of a specific criterion (semantics); how the criterion is measured (metrics); how the criterion affects evaluation of alternatives (criterion response function).

The multiplicity and complexity of interactions among different elements and systems that constitute the urban system, as well as urban functions ensuring its livability, safety, and sustainability, make the modeling of urban settlements a challenge. The taxonomic description of the various systems forming urban settlements, as well as the ontologies useful for explaining the interrelationships between the various parts, are the subject of DV 5.2.1 "Risk-Oriented Taxonomy and Ontology of Urban Subsystems and Functional Models".

On the other hand, the understanding of risk and multi-risk conditions in settlements depends on a series of factors related to the system's exposure with respect to the hazard and risks it faces. This exposure is inextricably linked to the contextual conditions in which it occurs and is integrated with the vulnerabilities of the assets and systems that are part of the settlement.

This deliverable DV 5.2.2 "Multi-criteria metrics and methodology for integrated exposure assessment" addresses the theme of integrated exposure assessment, proposing a series of approaches useful for identifying critical contexts and hotspots in urban areas with reference to potential multi-risk conditions that may occur.

The first part of the document (Chapter 2) is dedicated to laying the base to the **conceptual frameworks** to approach the study of urban settlements, including introduction of the variable relevant scales that should be accounted for in a multi-scalar approach.

Multi-Hazard: This is defined as the condition resulting from the simultaneous or sequential occurrence of hazards, including climatic ones, which interact with each other, leading to an aggravation of the overall risk and the potential trigger of cascading effects (*compound risks*).

Integrated Exposure: means that exposure is not only understood as the presence of people or *assets* in risk areas but is **integrated with the vulnerability** of the exposed elements. Factors influencing vulnerability are considered and should be accounted for in a proper exposure assessment.

Assessment Approaches: Multi-Criteria Decision Analysis (MCDA) allows for measuring and comparing complex objectives. Metrics, indices, and MCDA approaches are examined for exposure to hazards.

The following chapter (Chapter 3) is dedicated to the “**knowledge**” of the Urban and Metropolitan settlements. Besides recalling part of the taxonomic description already introduced in DV 5.2.1, some other features such as the Settlement models, the Socio-ecological systems and the Geo-morphological systems contributing to the context identification, as well as recurrent urban patterns, are described. Next, a proposal for clustering urban settlements based on common characteristics is introduced.

Urban and metropolitan settlements are studied as complex systems, composed by subsystems: the **urban physical system** (e.g., building typologies and *layout*), the **socio-ecological system** (e.g., demographic characteristics and social vulnerability), and the **geo-morphological system**.

Recurrent urban patterns (building and open space) are identified and classified to characterize settlements homogeneously and analyze potential risk impact. Moreover, a **clustering** methodology is proposed to group Italian municipalities based on common characteristics, using *open-source* data such as the degree of urbanization (Eurostat classification) and the degree of urban centrality (SNAI methodology), in addition to the number of inhabitants and the altimetric zone. This allows for identifying contexts with similar risk profiles.

A **score-based procedure** is defined to classify and compare the incidence of different hazards (seismic, flood, tsunami, heatwave) at the municipal level, overcoming the limitations of comparing hazard maps alone.

The subsequent chapter (Chapter 4) presents the concept of urban critical context and hotspots. Also, literature examples for indicator-based identification of urban critical context or GIS-based identification of urban hotspots are presented.

The concept of **Critical Urban Context (CUC)** and **Urban Hotspot** are defined as areas characterized by the concentration or overlap of risks and impacts. Methods for their identification using indicators and **GIS-based** approaches are presented, with examples related to heatwaves, air pollution, and flood risk.

Finally, Chapter 5 presents the use of **composite indicators or index** for multi-risk exposure assessment, providing a step-by-step methodology for identifying Critical Contexts or *Hotspots*.

This chapter is complemented with practical step by step examples illustrating the application of the methodology for critical urban context or hotspots identification as well as the selection of relevant indicators needed for the assessment in the considered contexts and in multi-risk conditions. The tool of “**risk storylines**” guide the selection of relevant indicators in complex multi-risk scenarios, helping to understand cascading effects.

Finally, an application example is presented for the identification of Critical Contexts (CUC) in the municipality of Somma Vesuviana, calculating an **integrated risk index** for seismic and flood risk, aggregating hazard and integrated exposure indicators. The MCDA approach is finally highlighted as a crucial tool to support effective risk management decisions.

2. Conceptual frameworks

2.1. Urban and Metropolitan Settlements: systemic approach and multi-scalar urban components

Urban settlements are complex systems composed by physical, social and ecological components, characterized by specific functions and organized in hierarchical levels (de Rosnay, 1977). In urban settlements, the human habitat (composed, among others, of residential buildings, productive activities, service facilities, infrastructures and networks, green areas, etc.) interacts continuously and in a multi-scale perspective on a morpho-environmental, spatio-functional and technical-performance levels with both the biotic and abiotic components co-present in the reference environmental system, defining multiple spatial relationships that include the mobility and flows of people, the supply of water and energy resources, the exchange of raw materials and goods, the emission of pollutants and material waste. It is also from these relationships that the specificities of settlements are determined (Castellari et al., 2014).

Based on these considerations, the complexity, number and heterogeneity of the phenomena involved in urban and metropolitan settlements require innovative systemic and multi/inter-disciplinary knowledge approaches (Losasso, 2013). In this sense, a multi- and inter-disciplinary, a-scalar and inter-sectoral methodological approach enables the optimization of all the aspects involved in the different areas of transformative intervention and in the dimensions of process, project and product, which are also inextricably interrelated, combining traditional and innovative methodologies.

The city is intended as an open "living biological organism" (see figure 1) in a systemic perspective that integrates input and output flows, referring to a set of complex and heterogeneous processes of production, transformation, use and dissipation of materials and energy. Material and immaterial flows pass-through cities enabling life, supplying urban production and growth, but at the same time exert strong pressures on the natural environment consuming matter and energy, producing climate-changing gas emissions and waste (Russo, 2018).

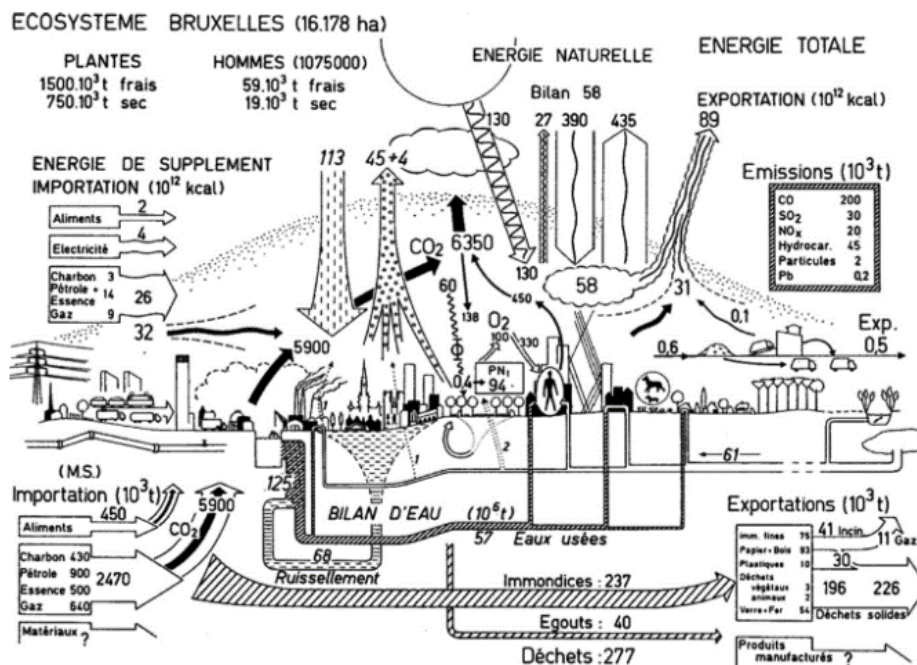


Figure 1. The urban system as an ecosystem. (Source: Duvigneaud and Denaeyer-De Smet, 1977).

In the new climate regime, linear models of production-consumption-waste impose a transition to a carbon-neutral society as well as a green and circular economy (UN Habitat, 2011; IPCC, 2022). Regeneration processes on "portions of the city," set the *district* as the "size of the minimum area of intervention in order to

rely on economies of scale and to support major investments," in which it is possible to "qualify or construct not only buildings, but also community, neighborhood services and sustainable living" (AUDIS, GBC Italia & Legambiente, 2011). The scale of urban districts is therefore outlined as an appropriate scalar dimension for the transition both in reference to potential environmental, natural and anthropogenic risks and to potential actions to mitigate, adapt and increase the resilience of urban systems.

2.1.1. The District scale

The district dimension, conceptual and spatial, is between the urban scale and the more detailed scale of homogeneous urban components and building blocks. The district scale is therefore the most suitable to address dynamic downscaling and upscaling processes aimed at defining mutual dependencies among the different levels and the complexity that characterize contemporary cities configuring itself as a scientific basis on which to test the feasibility of decision-making processes and design solutions (Losasso, 2021).

The recognition and consequent perimeter of the extended territorial areas within which to develop the preliminary investigations, identified as macro-areas, must be based on geomorphological and meteo-climatic analyses. Macro-areas correspond, in fact, to the territorial areas whose settlement characters are restituted through thematic interpretations that include administrative boundaries, the perimeter of the examined area, degrees of urban centrality and polarities, and information on current and expected climate. Within the macro-areas (or Territorial Areas) it is possible to identify Urban Districts, referring to an intermediate scale of settlement between the city and the neighborhood and corresponding to areas with recognizable settlement features and natural boundaries (Bologna et al., 2021). The perimeter of the Urban Districts, which can differ from the administrative boundaries, is also based on the characteristics of the built environment (prevailing building types, density of construction, building materials, period of construction, prevailing functions etc.), urban infrastructure (road pattern, physical limits, etc.), environmental and natural-landscape aspects (natural limits, etc.); these conditions contribute, in fact, to define the exposure and vulnerability to hazards. Figure 3 shows an interesting example of extrapolation from satellite data of built-up areas that can be used to characterize exposure in a multi-scalar approach.

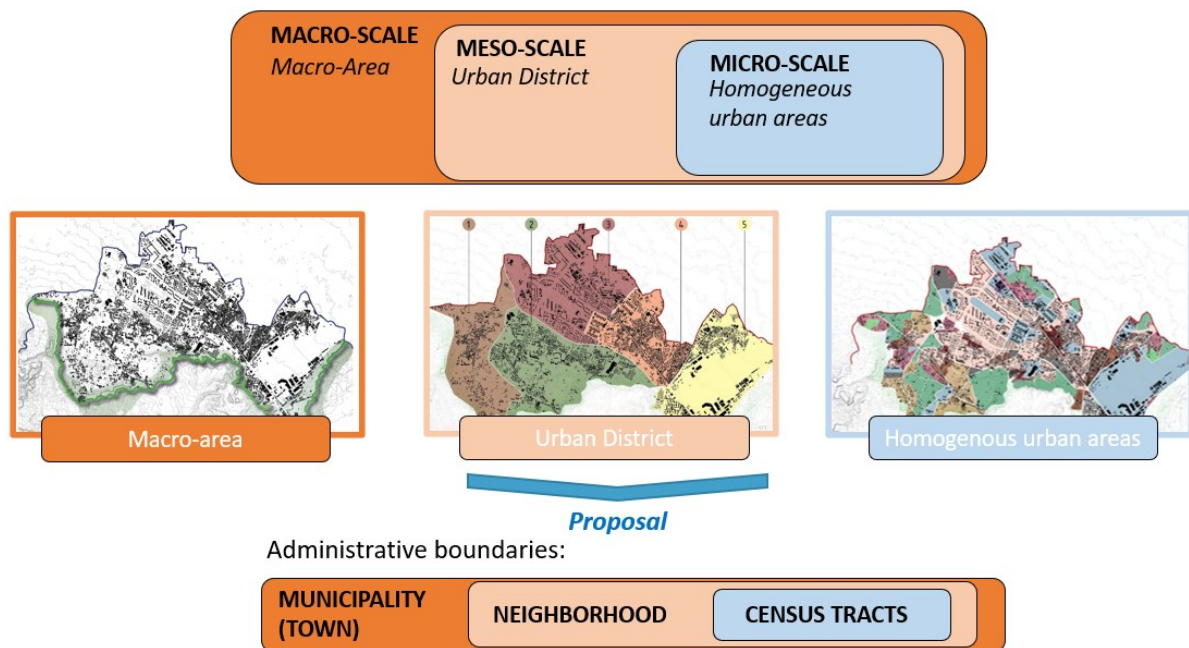


Figure 2. Multi-scalar approach. Accounting for the interactions among different sub-systems, a proposal for the identification of administrative boundaries to outline macro-meso-micro scale entities to be investigated. The identification of urban districts is not only in administrative boundaries, but also in accounting for built up pattern homogeneity, natural and administrative boundaries, geomorphological features, infrastructure system, road patterns, homogeneous economic value, construction period, and technical-constructive features.

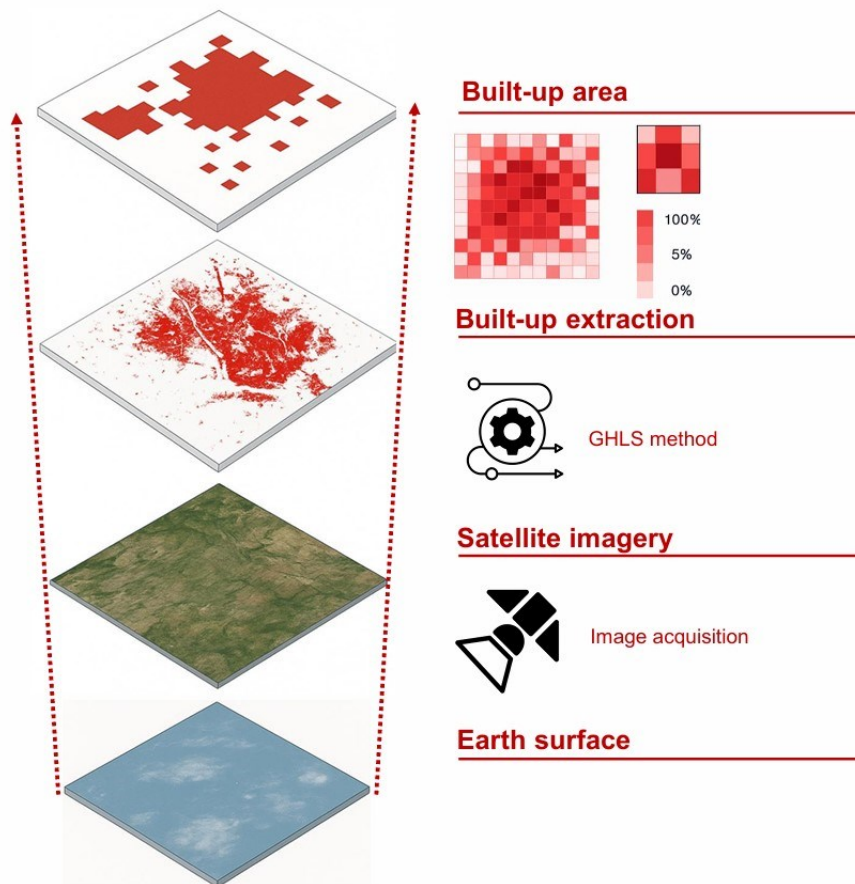


Figure 3. Extrapolation from satellite data of built-up areas, to be defined later in their scaling (Source: Author's elaboration based on Corbane, C., Rodriguez, D., Sabo, F., Politis, P., Syrris, V. Large scale mapping of human settlements from Earth. Observation data with JEO-batch of the JRC Earth Observatory Data and Processing Platform, EU Joint Research Centre, Disaster Risk Management Unit).

Urban Districts are structured on the basis of different information layers, including elements of urban taxonomies, ontologies, and specific parts of the urban fabric, in a progressive scalarity approach up to building blocks. In this sense, the Districts represent urban units of conforming reference size, designed as a scalar reference for effective interventions in preventing and reducing urban risk reduction (Losasso et al., 2021). The scale of the Districts is intermediate between macro-areas and homogeneous areas, the reference is to areas of 20,000-50,000 inhabitants, contextually defined by multiple aspects that include natural boundaries,

geomorphological features, infrastructure system, administrative boundaries, homogeneous urban fabrics, road patterns, homogeneous economic value, construction period, and technical-constructive features.

As an example, Figure 4 shows urban districts identification for the west Naples' Macro-area.

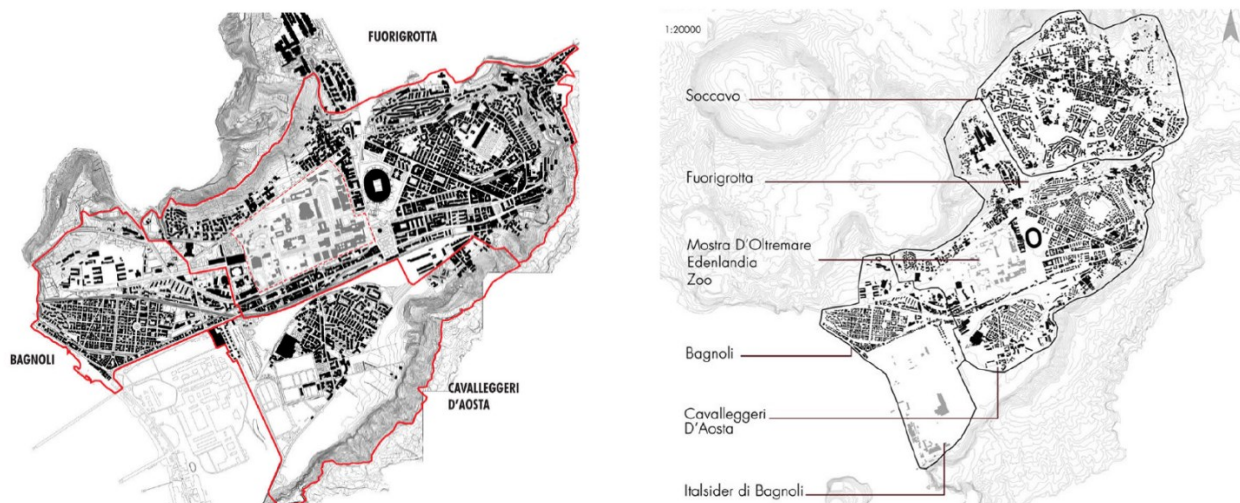


Figure 4. An example of Urban Districts identification in west Naples' Macro-area. (Source: Bologna, Losasso, Mussinelli, Tucci, 2021).

In this scenario, the research intends to adopt a demonstrator approach linked to experimental development actions in the field of knowledge and multi-scalar projects (macro-areas, urban districts, urban and building components of more limited dimensions) and process (proof of concepts, strategic programs, actions, tools, pilot projects). In the knowledge phase, therefore, in addition to the traditional analytical methods of interpreting urban contexts, interpretative readings are also required in order to consider type-morphological aspects capable of capturing relevant aspects connected to exposure and vulnerabilities.

2.2. Hazard, vulnerability and exposure of urban systems

Natural hazards are natural processes or phenomena that may cause loss of life, injury or other health impacts, property damage, social and economic disruption or environmental degradation (UNISDR, 2018). The potential negative impact on societies, human environment and natural systems following an actual occurrence of a natural hazard is referred to as disaster risk. Disaster risk is not only associated with the occurrence of the natural phenomenon but also with the exposure of human and economic assets to such phenomenon and their vulnerability conditions that may favour or facilitate disaster when such phenomenon occur. As a matter of fact, risk can be defined as the result of the interaction of three components: hazard, exposure and vulnerability (IPCC, 2014; UNISDR, 2018).

Hazard is the phenomenon that carries the potential for adverse consequences on human and natural systems. It is characterized by its location, likelihood of occurrence, intensity or magnitude and duration. Indeed, it can be sudden onset events (e.g., flash floods, storms, mudflows, landslides, earthquakes) or creeping processes (e.g., droughts, salinisation) (IPCC, 2014; UNDRR, 2016). Natural hazards (e.g., earthquakes, droughts, floods) are hazardous phenomena that have natural origins, but hazards could also be anthropogenic in origin (e.g., oil spills, terrorist attacks). The exposure is represented by the presence of people, infrastructure, housing, production capacities, species or ecosystems, and other tangible human assets in places and settings that could be adversely affected by one or multiple hazards (IPCC, 2014; UNDRR, 2016). If a hazard occurs in an area with no exposure, then there is no risk (e.g., typhon hitting the Pacific Ocean, such as typhon Lekima in 2013). Exposure may vary both in space and time: people and economic assets become concentrated in areas exposed to hazards through processes such as population growth, migration, urbanization and economic development. Vulnerability expresses the propensity or predisposition of an individual, a community, infrastructure, assets or systems (including ecosystems) to be adversely affected by hazards (UNDRR, 2016). As a matter of fact, risk not only depends on the severity of hazard or the number of people or assets exposed, but also the

susceptibility of people and assets to the negative effects induced by hazards play a crucial role. Together with exposure, vulnerability can explain why some non-extreme hazards can lead to extreme impacts and disasters, while some extreme events do not. Vulnerability encompasses a variety of concepts and elements including the lack of capacity of the urban system to cope and adapt to hazards impacts as well (Birkmann et al., 2013; IPCC, 2014). Coping capacity refers to the ability of people, organizations and exposed systems, using available skills and resources, to manage adverse conditions, risk or disasters (Poljanšek et al., 2019). Evidence has shown that some processes or conditions, often development-related, may influence the level of risk in urban areas by increasing levels of exposure and vulnerability or reducing capacity. Risk drivers may include poverty and inequality, climate change and variability, unplanned and rapid urbanization and the lack of disaster risk considerations in land management and environmental and natural resource management, as well as compounding factors such as demographic change, non-disaster risk-informed policies, the lack of regulations and incentives for private disaster risk reduction investment, complex supply chains, the limited availability of technology, unsustainable uses of natural resources, declining ecosystems, pandemics and epidemics (UNISDR, 2018).

Many of the effects associated with climate change exacerbate or alter existing hydrometeorological hazards, such as droughts, floods, storms and heat waves. Climate change is exacerbated by the anthropogenic emission of greenhouse gases and leads to alterations in global climate patterns with shifts in local precipitation, temperature and weather patterns. This causes climate-related hazards to become more intense, longer and more frequent. Climate change also stresses critical ecosystems and is likely to exacerbate gradual processes of environmental degradation. Ecological conditions affect natural barriers that can mitigate the impacts of a disaster and protect communities providing natural defences against natural hazards. For instance, wetland ecosystems function as natural sponges that trap and slowly release surface water, rain, snowmelt, groundwater and floodwaters. Dunes and reefs create physical barriers between communities and coastal hazards.

Also atmospheric aerosols are connected to climate change, through direct and indirect effects that interact in complex ways ultimately affecting the climate. It is known that aerosols can directly influence the Earth's energy balance by either scattering or absorbing sunlight, changing the radiative forcing. Some aerosols, like sulphate particles, tend to scatter sunlight back into space, leading to a cooling effect on the Earth's surface. Others, like black carbon (soot), absorb sunlight and contribute to warming.

The aerosols can also act as cloud condensation nuclei, providing surfaces for water vapor to condense into cloud droplets. The presence of aerosols can affect cloud properties, including their brightness and lifespan.

Another parameter influenced by aerosols is the cloud reflectivity (Albedo effect): the changes in cloud albedo can affect the amount of solar radiation reaching the Earth's surface. In addition, some aerosols enhance the longevity of clouds, affecting precipitation patterns and regional climate.

While aerosols have both warming and cooling effects, their net impact on the climate depends on various factors, including the type of aerosols, their concentration, and the specific atmospheric conditions. It's important to note that efforts to mitigate climate change often focus on reducing greenhouse gas emissions, as these gases have a more significant and longer-lasting impact on global warming. However, understanding the role of aerosols is crucial for accurately predicting and managing climate change and its forthcoming impacts.

Risk assessment allows to estimate the severity of human, economic, environmental as well as social impacts expected for given scenarios (i.e., disaster event defined in terms of its magnitude and probability of occurrence) in a region of interest based on hazard, exposure and vulnerability conditions. The assessment of the risk enables decision makers to understand the nature and extent of disaster risk, to formulate prevention and mitigation policies and implement consequential preparedness or response actions. Disaster prevention indicates the set of activities and measures to avoid existing and future risks. As certain hazards cannot be eliminated, prevention aims at reducing vulnerability and exposure in such contexts in order to reduce the risk of disaster. Mitigation measures are actions put in place to reduce the severity and/or the extent of the adverse impacts of hazardous events. They may include engineering techniques and hazard-resistant construction as well as improved environmental and social policies and public awareness. Also the preparedness actions are carried out within the context of disaster risk management and aim to build the capacities needed to efficiently manage all types of emergencies and achieve orderly transitions from response to sustained recovery (UNISDR, 2018). Risk analysis also allows to identify the most suitable measures to prevent or mitigate the effect of climate change on climate-related hazards. In a climate change context, adaptation means reducing

the vulnerability to effects of climate change, taking appropriate action to prevent or minimize the damage they can cause, or taking advantage of opportunities that may arise. Examples of adaptation measures include interventions adopted for large-scale infrastructure changes, such as construction of defences to protect against sea-level rise, as well as promotion of behavioural shifts, such as inducing individuals to reduce their food waste. Climate change mitigation refers to actions aimed to make the impacts of climate change less severe. For example, by preventing or reducing the emission of greenhouse gases (GHG) into the atmosphere. In such case, mitigation is achieved either by reducing the sources of these gases (e.g., by increasing the share of renewable energies, or establishing a cleaner mobility system) or by enhancing the storage of these gases (e.g. by increasing the size of forests).

Hazardous events may occur simultaneously or cumulatively over time and in this case the potential interrelated effects may amplify the overall risk. The case of landslides triggered by an earthquake (Chang, et al., 2007; Lee, et al., 2008) or a tsunami triggered by an earthquake (Mimura, et al., 2011) are the typical examples of one hazard that triggers another one. In other cases, one event may cause several different threats which are considered jointly, as in the case of a volcanic eruption with ash and lapilli fallout and lava flows (Zuccaro, et al., 2008; Thierry, et al., 2008) or storm surge and high wind occurred during a hurricane (Gill and Malamud 2014). The occurrence of a natural hazard can also trigger technological accidents. Such events are known as 'Natech' (Natural Hazards Triggering Technological Accidents) and, although they are relatively rare, the consequences of these phenomena can be catastrophic. Examples of such events occurred during last decades are the Kocaeli earthquake in 1999 which was a devastating disaster hitting one of the most industrialized regions of Turkey, (Girgin, 2011), the hurricanes Rita and Katrina in 2005 that caused the release of hazardous materials from offshore oil and gas facilities (Cruz and Krausmann, 2008), and the Great East Japan earthquake and tsunami in 2011 (Krausmann and Cruz, 2013). Natech accidents can be also triggered by natural events characterized by low-severity and high-frequency, such as extreme temperatures, which caused a relevant number of accidents in the past (Ricci et al., 2021; Casson Moreno, 2019). The interaction between two different hazards that occur close in time may also cause changes in vulnerability conditions. As a matter of fact, when two hazards act on the same exposed elements, vulnerability of the exposed elements may be altered by the first one and, in turn, their capacity to response to the second hazard may dramatically change. For instance, the presence of a load on a system such as the snow on a roof could determine an increment of the vulnerability during a seismic event (Garcia-Aristizabal et al., 2013). Therefore, to enable stakeholders to understand the relative importance of different risks for a given region and implement suitable disaster risk reduction measures multi-risk analysis becomes an essential tool. The latter requires to account for both hazards interactions, with a deep investigation of possible chains of events and the estimation of the related probability of occurrence (e.g., Iannacone et al., 2023) and vulnerability interactions, modelling the dynamic change in the performance of an exposed systems. Accordingly, also the exposure assessment should consider all possible hazards the urban system is exposed to. Moreover, the evaluation of risks related to different sources should account also for their possible interactions with special care to avoiding potential unwanted effects of certain risk reduction measures on other hazard typologies, defined as 'asynnergies' (de Ruiter et al., 2021).

2.3. From the concept of exposure to integrated exposure

Knowledge of risks is the first step towards conscious implementation of disaster risk reduction in urban and metropolitan settlements and to effectively mitigate the impact of potential hazards either on the physical system, the population or the functions/services. In scientific literature, the use of the term 'multi-hazard' is usually closely linked to the concept of risk reduction. In fact, in recent years there has been a growing awareness of the need to manage, and therefore to know and investigate, multiple risks involving impacts on assets, resources and people. The analysis of potential impacts is based on a spatial approach that considers a base area and the hazards that may occur within this area (including cascading, compound, aggregate effects, etc.).

In multi-hazard approaches, compared to single-hazard approaches, it must be considered that:

- the characteristics of hazards differ according to the specificities of the hazards and thus the methods for analyzing them also differ;

- hazardous events are often interrelated and influence each other, resulting in phenomena often described as interacting, compound, cascading, etc;
- hazards give rise to different risks and impacts depending on which elements are at risk, making the analysis of exposure and vulnerability factors fundamental, although the methods for assessing them vary depending on the hazards.

The multi-hazard approach to evaluate integrated exposure takes into account not only individual hazards, such as those related to natural events (earthquakes, floods, storms, heat waves) or anthropogenic events (industrial accidents, terrorist attacks, pandemics), as well as their potential interaction, but also considers the interconnections and interactions between different urban assets, such as transport, critical infrastructure, public health, etc. Assessing multi-hazard integrated exposure allows for more effective emergency management, as it takes into account the interrelationships between different aspects of the city and can lead to holistic solutions in risk planning and mitigation. Integrated exposure in this context implies a systemic and multidimensional approach to understanding and managing urban risks.

2.3.1. Definitions and integration factors for exposure under multi-risk conditions

According to the recent report by the insurance group AXA and the institute Ipsos (Future Risks Report 2023, Special 10th edition), the major risks perceived by a sample of experts and the population for the next five to ten years have been identified to be globally confronted. In fact, the 'Future Risks Report' includes among the main global risks those arising from climate change, energy, depletion of natural resources and biodiversity, together with those linked to social tensions, financial and macroeconomic instability and pathogenic conditions (AXA FUTURE RISKS REPORT, 2023).

As is well known, risk represents the potential for adverse consequences for human or ecological systems, recognising the diversity of values and objectives associated with such systems (IPCC, AR6 Synthesis Report - SYR, 2023). Relevant adverse consequences include those on lives, livelihoods, health and well-being, economic, social, and cultural assets and investments, infrastructure, services (including ecosystem services), ecosystems and species. For example, in the context of climate change impacts, risks result from dynamic interactions between climate-related hazards with the exposure and vulnerability of the affected human or ecological system to the hazards. Hazards, exposure, and vulnerability may each be subject to uncertainty in terms of magnitude and likelihood of occurrence, and each may change over time and space due to socio-economic changes and human decision-making (IPCC, AR6 Synthesis Report - SYR, 2023).

The exposure represents: the presence of people; livelihoods; species or ecosystems; environmental functions, services, and resources; infrastructure; or economic, social, or cultural assets in places and settings that could be adversely affected (IPCC, AR6 Synthesis Report - SYR, 2023) and, otherwise, properties, systems, or other elements present in hazard zones that are thereby subject to potential losses (Inter-agency Network for Education in Emergencies – INEE, <https://inee.org/>). Measures of exposure can include the number of people or types of assets in an area (UNDRR - United Nations Office for Disaster Risk Reduction, Sendai Framework Terminology on Disaster Risk Reduction, <https://www.undrr.org/terminology>). These can be combined with the specific vulnerability of the exposed elements to any hazard to estimate the quantitative risks associated (Inter-agency Network for Education in Emergencies – INEE, <https://inee.org/>).

Exposure in the urban environment is connected not only with vulnerabilities and hazards, but also with the typical conditions of urban settlements. According to the definitions of IPCC in AR6 (2023) the categorisation of areas as “urban” by government statistical departments is generally based either on population size, population density, economic base, provision of services, or some combination of the above. Urban systems are networks and nodes of intensive interaction and exchange including capital, culture, and material objects. Urban areas exist on a continuum with rural areas and tend to exhibit higher levels of complexity, higher populations, and population density, intensity of capital investment, and a preponderance of secondary (processing) and tertiary (service) sector industries.

The extent and intensity of these features varies significantly within and between urban areas (IPCC, AR6 Synthesis Report - SYR, 2023). In this complex context, in which hazard and vulnerability are correlated to exposure, is thus relevant to integrate the exposure of natural and physical assets with the social vulnerability to hazards in order to gain an overview of all contributing factors, particularly to prioritise risk management interventions.

To this end, a useful approach is the one adopted in the INFORM risk model (DRMKC, European Commission Disaster Risk Management, <https://drmkc.jrc.ec.europa.eu/inform-index>). In INFORM the risk is evaluated as a composite index depending on three dimensions: hazard & exposure, vulnerability and lack of coping capacity.

$$\text{Risk} = \text{Hazard \& Exposure} \times \text{Vulnerability} \times \text{Lack of coping capacity}$$

As shown also in Figure below, hazard & exposure are joined in a single dimension reflecting the probability of physical exposure associated with specific hazards.

There is no risk if there is no physical exposure, no matter how severe the hazard event is. Therefore, the hazard and exposure dimensions are merged into hazard & exposure dimension. As such it represents the load that the community has to deal with when exposed to a hazard event. The dimension comprises two categories: natural hazards and human-induced hazards, aggregated with the geometric mean, where both indexes carry equal weight within the dimension (European Commission, DRMKC – INFORM, <https://drmkc.jrc.ec.europa.eu/inform-index>). Figure 6 shows a more detailed graphical representation of the Hazard & exposure dimension along with its components and possible indicators used for the evaluation.

The contribution of the different dimensions to risk is conceptualized in a counterbalancing relationship: the “risk of what” (natural and human hazard), and the “risk to what” (population), as shown figuratively in Figure 5.

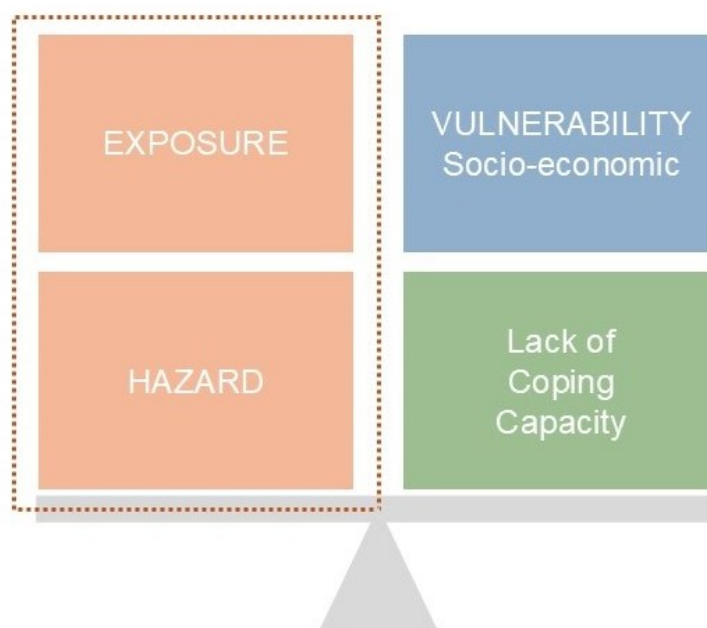


Figure 5. INFORM Risk Model. (scaling (Source: Author's elaboration based on DRMKC, European Commission Disaster Risk Management, <https://drmkc.jrc.ec.europa.eu/inform-index>).

Dimensions	Hazard & exposure					Vulnerability				Lack of coping capacity			
Categories	Natural		Human			Socio-Economic		Vulnerable groups		Institutional		Infrastructure	
Components	Earthquake Tsunami Flood Tropical cyclone Drought	Current conflict intensity	Projected conflict intensity	Development deprivation (50%)	Inequality (25%)	Aid dependency (25%)	Uprooted people	Other vulnerable groups	DRR	Governance	Communication	Physical infrastructure	Access to health system

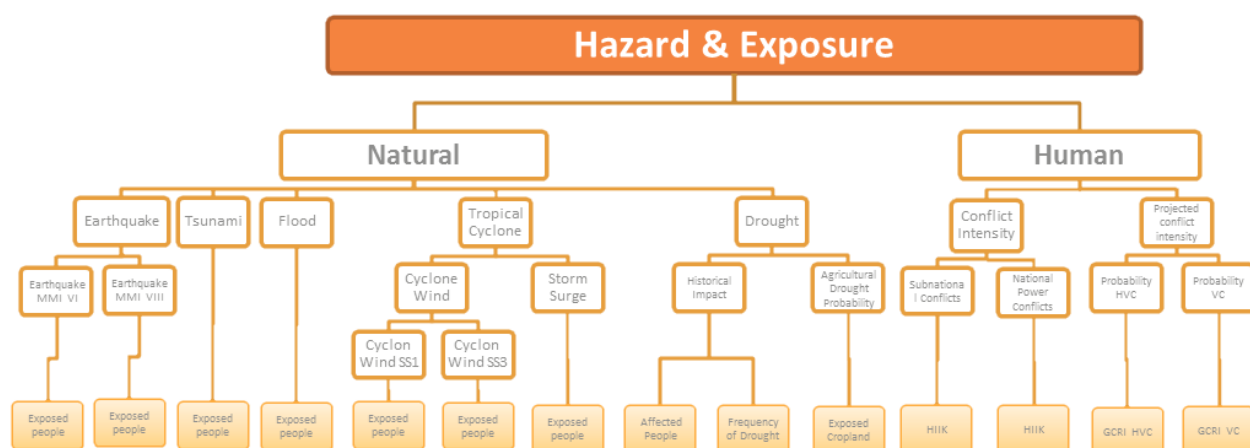


Figure 6. Graphical presentation of the Hazard & exposure dimension (Source: INFORM Risk Model, <https://drmkc.jrc.ec.europa.eu/inform-index/INFORM-Risk>)

Exposure has many definitions, that evolved during the last decades in the different scientific fields. according to United Nations International Strategy for Disaster Reduction (UNISDR United Nations International Strategy for Disaster Risk Reduction, Terminology on disaster risk reduction, Geneve, 2009), exposure is defined as «the people, property, systems, or other elements present in hazard zones that are thereby subject to potential losses» (UNISDR, United Nations International Strategy for Disaster Risk Reduction, Terminology on disaster risk reduction, Geneve, 2009). Increases in vulnerability and exposure are responsible for the overall increase in risk, and therefore require particular attention in the formulation of policies and actions to reduce disaster risk.

Both exposure and vulnerability are dynamic, vary across temporal and spatial scales, and depend on economic, social, geographic, demographic, cultural, institutional, governance-related, and environmental factors. Moreover, factors affecting exposure and vulnerability vary considerably by hazard context, disaster stage and national setting (Rufat et al., 2015). High exposure and vulnerability are linked to skewed development processes, such as those associated with environmental mismanagement, rapid demographic changes, rapid and unplanned economic processes, urbanization in hazardous areas, poor governance, and the scarcity of livelihood options for the people, particularly the poor (Cardona et al, 2012).

Measuring vulnerability and exposure requires an integrated understanding of components and how these factors are combined: a relevant integration can be identified in vulnerability and exposure assessment methods. The assessment of vulnerability and exposure range from global to local-scale participatory

approaches, which need to be integrated using appropriate platforms. The appropriateness of methods used for these assessments depends on the purpose of the analysis, time and geographic scale involved, the resources available, the number and type of actors, and economic and governance aspects. Such differences and how they can be overcome to promote integration of the different dimensions of vulnerability and exposure needs be addressed and could be examined using case studies.

Exposure and vulnerability information allow to develop risk indicators and monitor risk, so vulnerability and exposure information are often used as indicators of relative risk and the evolution of risk over time and geographic dimension. Thus, greater emphasis needs to be placed on the collection and analysis of vulnerability and exposure information, to inform the development of risk indicators and the process of monitoring risk over time and space. Several indicators of physical and socio-economic vulnerability/exposure require statistically robust information regarding the nature of the built environment (e.g., building stock, lifelines, critical facilities), which is often not available even in developed nations. The employment of advanced models to predict the geographical distribution, susceptibility to damage and loss, and value of the elements exposed to the hazards will be fundamental in a site-specific analysis.

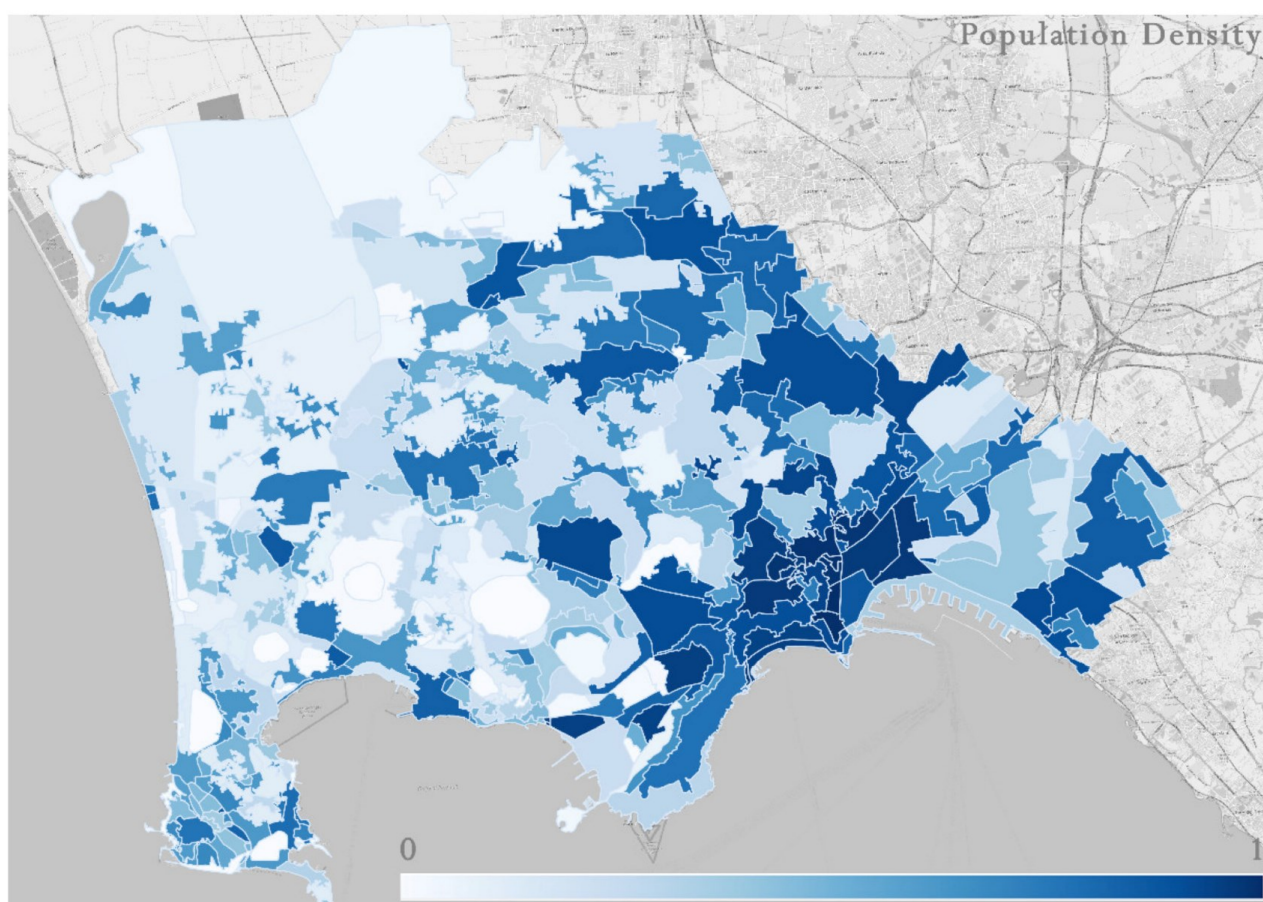


Figure 7. Maps of exposure: population density (Source: Galderisi & Limongi, 2021).

Exposure assessment consists in the identification and distribution of elements located within the area of potential hazard:

- the built environment (e.g. residential houses, commercial buildings, critical infrastructure (e.g. hospital, heliports, ports) and facilities, public services;
- people and the social system (e.g. main characteristics of exposed people and institutions);
- economic assets (e.g. agriculture, livestock, shops, productive facilities, ecc.);
- natural environment (e.g. flora, fauna, conservation areas).

Exposure analysis mostly consists in the estimation of the quality (according to vulnerability models) and quantity of assets pertaining to these systems located in hazardous areas; generally, also the assessment of the associated economic value is performed. The evaluation of exposure has improved thanks to the fast development of satellite and remote sensing technologies and the estimation of economic value should be done for the tangibles (e.g. infrastructure, buildings, production of goods and services) as well as for the intangibles (e.g. population's welfare, cultural heritage, environmental elements) values (Galderisi & Limongi, 2021).

2.3.2. Vulnerability aspects in characterizing exposure

The identification of assets exposed to hazards is a crucial step in determining disaster risk of urban systems. “Asset” generically represents everything that might be exposed to hazards and that can undergo the negative consequences due to the impacting hazard, determining the risk: population, buildings and infrastructure, environment, economic activities, essential facilities are all “assets at risk”. Buildings and infrastructures exposed at a given hazard may be damaged or destroyed due to the occurrence of a hazard, people may be injured or killed, essential facilities and transportation facilities as well as economic activities may be hampered or interrupted. The more assets are exposed the more the risk is likely to be high. On the contrary, in areas without exposed assets, hazards cannot generate risk. It is therefore important to identify and quantify all assets located in hazard prone areas (i.e., how many buildings are there, how many people live and work there and what essential facilities are present – e.g., lifelines, services and emergency response units).

However, the simple listing of exposed elements is not enough for modelling the exposure of urban system to natural hazards. Exposure has a close relationship with vulnerability. While the exposure identifies the exposed assets, the vulnerability defines the susceptibility of such assets to impacts of hazards. Thus, they are both essential to evaluate the level of disaster losses and impacts experienced in urban systems. Vulnerability reflects the intrinsic performance of an element at risk against particular hazard based on its physical, social, economic or environmental factors. Such performance could be different also for elements belonging to the same asset category (e.g., buildings), determining a different level of vulnerability for each element. Thus, when assessing exposure to a particular hazard, it is necessary to assess not only the number of elements of a given asset exposed but also to detect related features that may affect their response to hazard. For instance, seismic vulnerability of buildings expresses their susceptibility to sustain a certain level of damage due to ground shaking of a given intensity. Seismic vulnerability is usually different for different building types (e.g., masonry and reinforced concrete buildings) due to their different typological and structural features that lead to a different performance against earthquakes. The seismic exposure is generally expressed by building inventory, that provides the number of exposed buildings belonging to different classes of structures or vulnerability classes (e.g., number of buildings with masonry structure) and their distribution at territorial scale. Therefore, for a proper exposure assessment, the main factors affecting vulnerability of exposed assets to several hazards should be properly accounted for. Addressing vulnerability together with exposure is also crucial to ensuring effectiveness in disaster management measures, allowing to understand which elements exposed to hazards most affect the level of risk and why. It is worth mentioning that integrated exposure modelling (i.e., exposure integrated with vulnerability information – i.e., vulnerability factors and risk drivers) is a different task than vulnerability modelling. In fact, the exposure modelling allows to know the distribution of exposed asset at territorial level and their characteristics that mostly affect their performance against one or more hazards, while the vulnerability modelling provide probabilistic estimates of expected damages/impacts under a hazardous event of a given intensity.

Urban system is complex and encompasses several assets, both tangible (most of the physical elements) and intangible ones (e.g., the cultural values, the wellbeing of communities, psychological conditions, and sociological behaviour), that may be susceptible to significant impacts from hazards. Also, as mentioned before, many urban processes or conditions are officially recognized as risk drivers that may increase the exposure and the vulnerability and reduce the coping capacity of urban systems as well (e.g., climate change, unplanned and rapid urbanization, unsustainable uses of natural resources). Accordingly, integrated exposure assessment should not only consider physical aspects (i.e., physical characteristics of elements at risk that affect their physical vulnerability directly linked to a particular hazard) but also social, economic, environmental and institutional ones.

2.3.3. Typo-morphological aspects of urban settlements considering integrated exposure factors

In urban and metropolitan settlements, risk exposure results from a combination of factors. This can therefore be described as integrated exposure and, in this specific case, an investigation may be carried out into the interpretation of certain urban morphologies and their corresponding influence on impacts, either exacerbating or mitigating their effects. For example, grid layouts, characterized by high building density, often present permeabilities that help mitigate heat waves or the run-off of water in the event of flooding.

The definition of "urban settlements" given in the "Report on the state of scientific knowledge on impacts, vulnerability and adaptation to climate change in Italy" (Castellari et al., 2014) identifies the distinctive characteristics, universally valid, and the variable case-by-case specificities of the urban settlements. The opportunity for a typo-morphological approach is rooted in the dichotomy between universal and specific characters as part of a research aimed at identifying "contextual" ways of mitigating and adapting to integrated exposure factors.



Figure 8. Paul Klee, A sheet from the city book, 1928.

This approach presupposes the sharing of the hypothesis according to which the preservation of the built heritage is to be pursued not only as part of the defence of the human and environmental system but also in its specific consistency and organizational structure, as the outcome of a collective expression or "human thing par excellence", in which lies the sense of belonging of a community to a site, to a territory: "the city is the locus of collective memory" (Rossi, 1966).

The typo-morphological analysis, aided by a perceptive reading of complex territorial structures, represents an essential orientation tool as it traces compositional rules that govern the aggregation of parts of homogeneous cities and the relationships between them. Understanding the nature of material heritage exposed to risks means identifying the identity structure of that heritage, knowing its constitutive and evolutionary rules and, through those, evaluating the fragilities of the exposed assets. Until now this kind of knowledge has been useful in guiding conservation and valorisation interventions or even informing new constructions. The climate crisis accentuates of the need to modulate adaptation and mitigation actions towards a desired "contextuality" and systematic nature of the interventions.

Referring to the classification of risks introduced in Science for Disaster Risk Management 2020 (Casajus Valles, A., et al., 2021), which identifies a taxonomy of risks divided into 5 categories - Geophysical, Hydrogeological, Meteorological, Climatological, Human-made, it can be observed that the degree of exposure of urban settlements is generically uniform as regards the geophysical and hydrogeological characteristics of the soil, therefore inherent to factors of location. On the other hand, shape and size of buildings and open

spaces, together with their reciprocal organization and correlation, significantly affect the degree of exposure to meteorological and climatological risks and often represent the contributing cause of Human-made risks.

2.3.3.1. Characteristics of urban settlements

The distinctive characteristics of universally valid urban settlements concern: the heterogeneity of the constituent elements (residential buildings, productive activities, service equipment, infrastructures and networks, green areas, water bodies, etc.); the biunivocal relationship of interdependence that exists between the settlement and the surrounding territory, which generates what today we would call inter-scalarity phenomena.

These characteristics have been evident since the beginning of the urban phenomenon and represent its reason for existence as well as a distinctive feature. The spread of urban settlement in the various geographical regions proceeds in parallel with the establishment of agriculture as a productive activity for sustenance. The agricultural surplus, the need to conserve food products in safe places, the possibility of exchanging food products with artisanal products or with other products grown elsewhere, motivate the emergence of conurbations with different degrees of self-sufficiency. This took shape precisely through the contextual presence of complementary activities that took shape in the settlement: commercial, artisanal, residential, sacred. Often surrounded by defensive systems, the settlements were connected to each other by commercial infrastructures: roads, ports, caravans that guaranteed their subsistence (Benevolo, 1963).

The settlements were characterized by the presence within the defensive enclosure of open spaces intended for community assemblies or more generally for meetings which acted as a counterpoint to dense areas occupied by residential and public buildings. The existence of an urban design that presides over the organization and distribution of urban parts distinguishes "foundation" urban settlements from spontaneous agglomerations. The "free city of Greece" represents a moment of high awareness of the urban settlement towards its internal structure and its relationship with the surrounding territory. The well-known settlements of Miletus and Athens show the distinctive characters in an archetypal form and therefore more perceptible. The plan of the city of Miletus, as planned by Hippodamus in the 5th century BC, precisely identifies the size and layout of the residential insulae and the linked system of commercial, civil and religious areas. The "geographical" structuring of the polis of Athens which includes a vast agricultural territory delimited by natural hills and the port area of Piraeus, remains emblematic for issues concerning the relationships on a territorial scale of a city (see Figure 9).

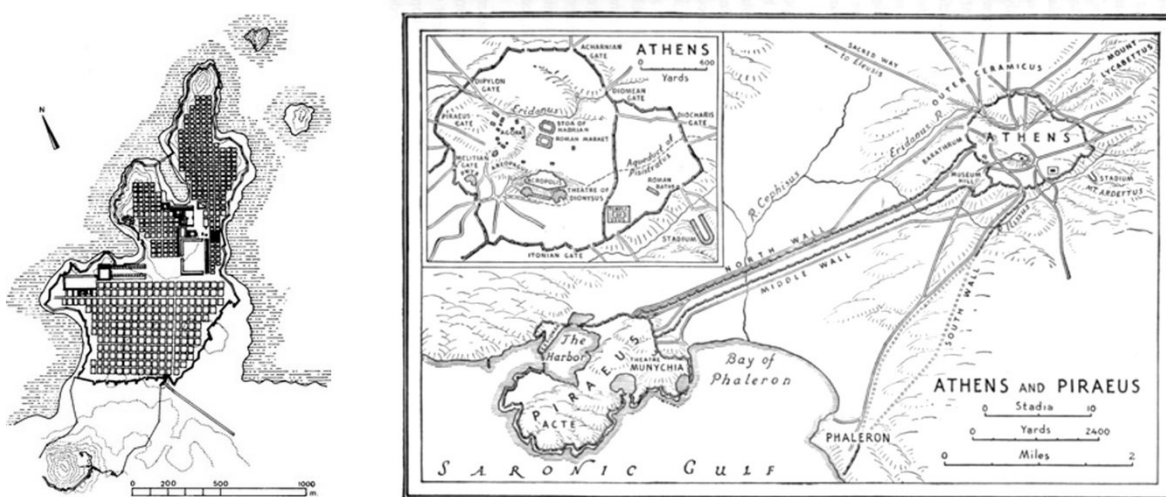


Figure 9. Map of Miletus and map of Athens in its geographical context

The geomorphological characteristics of the site represent the reason for the location of the settlements - the fertile nature of the soil, the richness of the subsoil, the proximity to waterways or protected bays, the sweetness of the stone - and influence its development and decline, affecting characteristics of the urban form (morphology) and to inform the nature of its buildings (typology).

The identity structures of settlements are deposited in the specific characteristics. Even though each urban settlement is unique from the point of view of built form, it is possible to identify formal recurrences that refer to geomorphological issues (orography and nature of the soil), underlying geometries (linear, grid, radial), density (ratio between volume and space occupation), to building typologies. These recurrences, mostly due to the reiteration of customs and migrations of urban ideas (Ferlenga, 2014) open the way to classifications which, proceeding by induction, through the analysis of specific case studies, inform deductive logical systems which through codification of simple settlement models allow us to investigate and understand complex settlements generated by the combination of different models.

Through the recognition of similar characteristics, urban analysis allows us to orient ourselves in the multiple forms that urban settlements take on when specific characteristics vary.

2.3.3.2. Urban analysis

Urban analysis as a technical-operational tool represents the result of Urban Studies which substantiated the disciplinary re-foundation of the architectural discipline after the Second World War. Starting from the radical criticism of the functionalist reduction in architecture, the aim was to affirm the autonomy of the built form and elected the city as an instrument of explanation and comparison.

Within these studies, the literature identifies two main lines of research which have as their object the built form described through analytical drawings.

The first, attributable to the figure of Aldo Rossi, focuses on the analysis of the city as a totality, in which all the components participate in the construction of a fact, the "city as an architecture", the city as a work of art and collective expression. In the city there are two constitutive components: the residential areas and the primary elements, which as "permanencies", participate in the evolution of the city over time and are identified with the facts constituting the city. The recognition of the homogeneous parts (hence the neighbourhoods) and for each of these the identification of primary elements and residential areas constitutes the objective and outcome of the urban analyses attributable to this trend.



Figure 10. Map of the city of Aleppo before the destruction of the civil war (Source: Davolio, 2019).

The second way, attributable to the figure of Saverio Muratori and Gianfranco Caniggia (see Figure 11), aims to reconstruct the reasons for urban forms starting from the typological variations of building aggregates. In this type of study, the point of view is focused on minor construction (residences) and the objective seems to be the recognition of a genetic-evolutionary code of the permanence of settlement characteristics and building typologies. These studies reveal a sort of line of continuity that sees the evolution of settlements taking place

through subsequent "adaptations" of the types to external agents. It is useful to note that, since the origin of the evolutionary process, orientation criteria aimed at mitigating climatic issues have directed the arrangement and aggregation of types. The redesign of the typological plans of the ground floors of entire urban parts, complete with the indication of the stairwells, constitutes the representative work of this line of research.



Figure 11. The historic center of Polignano a Mare in the studies of Gianfranco Caniggia.

Both approaches contain questions of inter-scalarity that are precious for the study of contemporary landscapes, and today appear complementary.

The urban analyses were commissioned to substantiate recovery or reconstruction interventions of the historical heritage but also influenced settlement patterns of new buildings with particular reference to the public housing districts built after the Second World War.

The "explosion" of the urban phenomenon marked the end of the oppositional dialectic between city and countryside by establishing new interrelations between city and territory (Corboz, 1986), producing the emerging geographies of the metropolitan suburbs, of the peri-urban, of widespread urbanisations, of mixed production tertiary (Lanzani, 2013). Accordingly, the object of urban investigation goes beyond the boundaries of historical and consolidated settlements to address the "new landscapes", legitimized by the use and recognition by the communities. The new settlements, built very quickly compared to the slow times of the historic city, seem to sever the links with the settlement rules, generating spaces of friction, especially in places of interference between heterogeneous landscapes. In this Territory of architecture (Gregotti, 1986) which becomes a palimpsest (Corboz, 1986) the geographical context as the "background" of the urban settlement finds its structuring function in relation to the different materials. Knowledge of its form and consistency becomes essential for a reading aimed at understanding the heterogeneous urban facts. Perceptive reading becomes a decisive key to accessing the "landscape as a structure of the territory" (Pagano 2016), rehabilitating the three-dimensionality of urban settlements too often studied only through plan drawing. From this point of view, the urban studies of Lynch, De Carlo, Renna and Bisogni reveal themselves to be precursors of a perspective that seems useful today more than ever.

The reading method developed by A. Renna and S. Bisogni in their degree thesis, using the perceptive approach together with the typo-morphological one, seems to bring together the issues and allow the discovery of the connections between the different settlements and the contexts. The structure of the research reveals the knowledge of an inter-scalarity which does not proceed as a unidirectional cascade but which indicates a cyclical method encompassing: Breakdown of the perceptive field of the study area into simple elements, Definition of boundary conditions, Reconstruction of partial units, Reconstitution of global unity.

As example, the drawings in Figure 12 highlight the preminence of the morphology of the site over the formal nature of the settlement: the understanding of the orographic structure precedes the analysis of the typological levels: *structural density, structural condition, structural form and analysis of the road structure: density of the road network, shape of the road network.*

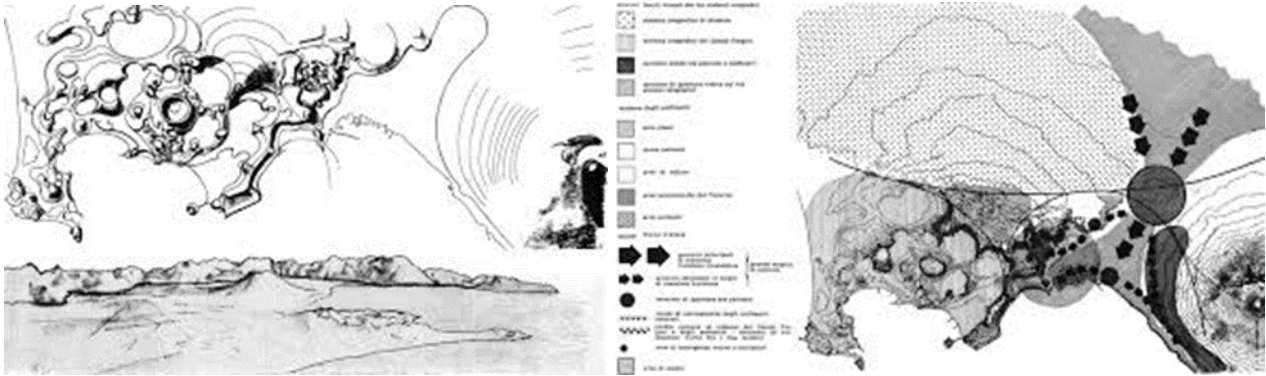


Figure 12. Drawings from S. Bisogni, A. Renna, *Il disegno della città di Napoli*, 1974 (1964).

Another method of analysis, which can be defined as complementary and integrative if related to the consolidated urban and typological studies by Caniggia and Rossi schools and that establishes significant synergies with the topographical reading by Renna and Bisogni, is the one proposed, recently, by Uwe Schröder and his research group of RWTH Aachen University in the German context. The urban systems are observed as artefacts and analysed in order to reveal their structure, described through the figure-background plan (Rowe, Koetter, 1978) and the red-blue plan, in their historical and spatial evolution (Schröder, 2015). In this approach, the typology is investigated in relationship to its capacity for 'formation' (Pareyson, 1954) of the spaces of the urban systems. Therefore, the spaces within urban systems are classified into warm/red or cold/blue spaces based on the degree of internality or externality, on the architectural or morphological nature of the horizontal and vertical boundaries, on the urban or rural connotation, on the 'dedication' [Widmung], inclusive or exclusive that spaces assume in relationship to their predominantly public or private use. The analysis proposed by Red-Blue Plan is of strong inter-scalar meaning. At the territorial scale, the Spatial History is represented by paralleling the significant phases of the evolution of the urban systems, through the use of historical maps, in a diachronic form (see e.g. Figure 13).



Figure 13. Naples Spatial History. Figure-background plan and Red-blue plan from the Greek-Roman city to the contemporary city

At the intermediate and detailed scale, red and blue can assume two different gradations to identify, in the built, respectively with dark and light red, internal/internal spaces and internal/external spaces: the former are closed on all sides and covered, the seconds closed not on all sides and not covered. Blue and light blue are also distinguished depending on the rural and landscape or urban connotation of the spaces that are not architecturally delimited and open. The theoretical reference derived from Raumgestaltung German theory (Schmarsow, 1894) but also from architectural Spatialism, among others by Sigfried Giedion (Giedion, 1941),

Bruno Zevi (Zevi, 1948) and Christian Norberg-Schulz (Norberg-Schulz, 1975). From a methodological-operational point of view, it could be interpreted as an update and a data increase of what in the *La Nuova Topografia di Roma* (1748) by Giovanni Battista Nolli and in the *Mappa topografica della città di Napoli e de' suoi contorni* (1775) by Giovanni Carafa, Duke of Noja, where the most important buildings of the city reveal their typological structure through the representation of entrance halls, porticoes and courtyards, bringing out the relevant and original character of dense but, following Benjamin's definition, often porous urban systems.

This method of analysis could be useful because finalised to insert the third dimension in the reading of the urban system, adding information (permeability of soil, section ratio of spaces etc.) that have potentially impact on risk conditions.



Figure 14. Typological and Spatial Analysis. On the left: The primary elements in the dense structure of the city. On the right: Interior and exterior urban spaces

Following a clarification of the risks to which the built heritage is exposed, it appears useful to carry out a classification of settlement models capable of linking the geometric settlement scheme and densities to geomorphological characteristics and subsequently proceeding with the examination of the formal and perceptive structure of the contexts that may result complex and even critical depending on a combination of endogenous and exogenous factors.

The urban analysis, through a correlation of perceptive and typo-morphological approaches, will offer the opportunity to clarify the gradual exposure of the built heritage.

The examination of the critical contexts within the respective landscape units will facilitate an appropriate modulation of mitigation and adaptation measures in coherence with the objectives of identity reconstruction. With a view to valorising and increasing the sense of belonging deposited in the identity structures of places, this type of approach allows the preparation of systemic strategies for the "care" of contemporary landscapes.



Figure 15. S. Muratori. Atlas (unpublished) of the territory. Padania Romana (Source: Lombardini, 2017)

2.4. Metrics, index and indicator

The approaches for assessing exposure, impacts and their potential reduction on people, assets and resources resulting from the combination of different types of hazards include, on the one hand, the modelling of climate hazards through projection scenarios and, on the other hand, the physical and socio-economic characteristics of urban settlements that affect exposure and vulnerability factors. The assessment of these determining components in the evaluation of risk impacts must consider multiple dimensions: the physical-environmental impact of climate hazards, the ability of the system to recover after an extreme event and to adapt to changes in the long run, and the socio-economic characteristics of the system that contribute to adaptation efforts.

Quantitative approaches are, therefore, essential to improve the understanding of environmental, social, and economic effects for the purpose of risk mitigation. In quantitative approaches to risk analysis, deterministic indices and indicators are essential tools for assessing vulnerability and exposure to impacts in urban settlements. The selection and the development of indices and indicators used in quantitative assessments of vulnerability, exposure and hazard factors must be supported by a review of existing literature and the availability of data. Indicators reduce the complexity of multidimensional issues through their proportional quantification, allowing complex ideas, processes, and scaling to be analysed, compared, and communicated. In this way, a risk assessment based on indices and indicators can integrate data from different disciplines (Fleming et al., 2023).

The selection and analysis of indicators for estimating the vulnerability and exposure components of urban settlements provides parameters that can be measured and monitored over time. These tools and processes provide a solid basis for assessing the evolution of these determinants and implementing short- and long-term climate risk management strategies (D'Ambrosio, 2016).

2.4.1. Metrics, index and GIS-based indicators

The *Exposure* is related to the presence of people, structures, infrastructures, livelihoods or services in the urban system that could be adversely affected and exposed to impacts and is directly associated with the *Vulnerabilities* of "n" subsystems (physical, socioeconomic, etc.) of the urban settlement. Following the IPCC AR5 and AR6 models (IPCC, 2014; IPCC, 2023) for assessing the impact of climate phenomena, this relation is summarized in the following formula used to assess the impact:

$$I = f(H; E; V_1; V_2; \dots; V_n)$$

where E is the exposure, H is the hazard and $V_1; V_2; \dots; V_n$ are the vulnerabilities of the n subsystems. In many cases the vulnerabilities of the various subsystems are aggregated into a single indicator of vulnerability of the entire urban settlement; then, the previous formula for the impact can be reduced to:

$$I = f(H; E; V)$$

where V is the vulnerability of the urban settlement.

To assess exposure, indices are constructed to measure the value exposed to risk in specific units of measurement (for example, measures of surfaces in hectares or square meters, measures of volumes in cubic metres, measures of population density in number of inhabitants per square kilometer, etc.).

Starting from these indices it is possible to build indicators, appropriately partitioning the index measurement domain into classes and assigning a label to each class, with a specific semantic meaning.

For example, suppose that the index measures the population density in a specific area of the urban settlement analyzed, in a range between 100 and 20,000 residents per square kilometer, and that you wish to obtain an exposure indicator made up of three classes: labeled, respectively, low density, medium density and high density, specifying that the area is not very dense if the number of inhabitants is less than 500 residents per square kilometer and very dense if it is greater than or equal to 5000 residents per square kilometer.

The following table synthetize this exposure indicator.

Table 1. Exposure indicator sample.

Label	Minimum	Maximum	Rule
Low density	100	500	$\text{Exposure} < 500$
Medium density	500	5000	$500 \leq \text{Exposure} < 5000$
High density	5000	50000	$\text{Exposure} \geq 5000$

In GIS-based models an indicator can be obtained applying a thematic classification process, where a thematic class is a class equipped with a symbol, as well as a label. All entities belonging to the class are displayed with the class symbol on the map.

The lower and upper ends of the index ranges are called breaks. A thematic classification method for value ranges must be used to determine the breaks of each class in an appropriate manner. The following table lists the main thematic classification methods for value ranges used in GIS environments for thematic classification.

Table 2. Thematic classification methods for value ranges used in GIS environments.

Method	Description	Reason for choice
Manual	The breaks of each class are specified by the user	This method is adopted when the breaks of each class are already known and set in scientific literature, in legal norms or by appropriate calibration processes
Equal interval	The domain value of the indicator is partitioned in equally wide ranges.	This method is adopted when we want that each class match exactly an equal width subset of the attribute domain regardless of the number of thematic elements that will belong to the class. This width is given by the extent of the domain divided by the number of classes
Quantile	The breaks of each class are determined so that each class has approximately the same number of elements.	This method is adopted if the number of elements belonging to each thematic class is required to be approximately the same.

Natural breaks	The breaks of each class are determined so that the sum of the standard deviations values calculated for all the classes is as low as possible	This method is adopted when we require that the elements belonging to a thematic class have values as similar as possible to each other and as dissimilar as possible from the ones of elements belonging to other classes. This method is the for default thematic classification method; it provides the best semantic distinction between the classes.
Standard Deviation	The amplitude of the value intervals in each class is given by a sub-multiple of the standard deviation of the attribute values.	Thes method is used when it is necessary to exploring whether the distribution of attribute values is random (that is, frequency distribution follows a Gaussian trend) or if it is not for anthropic, historical, regulatory reasons. which broke this causality.

The natural break method is the most used thematic classification method. It is based on the Jenks algorithm (Jenks, 1977), an iterative algorithm that determines optimal break values by minimizing the average standard deviations in each class. Recently a study of thematic classification methods in climatic risk analysis applied to classify heat islands is given in (Lu et al, 2021).

In order to build integrated exposure indices or indicators, it is necessary to prepare a normalization process that allows the individual indices and exposure indicators to be compared. This process can follow different approaches. A first feasible approach is to normalize the input indices. For example, let's suppose we have two types of exposure, made up of two measurement indices: extension of urban green areas in hectares, and density of residents in number of inhabitants per square kilometer. If you intend to obtain an integrated exposure index for normalization processes, it is necessary to make the two indices dimensionless, normalizing them to the same interval, for example [0,1]. Therefore, if the extension of urban green areas is within a range between 0 and 10 hectares, it is possible to divide the value of the index by the width of this interval, i.e. by 10, obtaining a dimensionless value between 0 and 1.

If the index or indicator of the integrated exposure depends on the input indices n based on a known function, it is possible to obtain this index is calculated using this function.

Another way to obtain the integrated exposure index/indicator is to use a rule-based process in which IF..THEN rules are defined. For example:

IF the number of residential buildings in poor condition is greater than 10 and the population density is greater than 5000 inhabitants per square kilometer, **THEN** the integrated exposure is "Very high".

A typical functional or rule-based approach is one that allows to obtain composite indicators starting from intermediate indicators, providing a hierarchical model of the indicators.

2.5. Multi-criteria approaches for exposure assessment

In recent years, the frequent occurrence of extreme weather events caused by rising temperatures has increased the risk of flooding and earthquake disasters, and their occurrence is increasing worldwide (Blackett, 2023; Sadhukhan et al., 2022). These disasters significantly threaten human survival and affect social development (Sen et al., 2021; Wang et al., 2020; Khosravi et al., 2019), making the interconnections between economic, environmental, and social processes increasingly evident.

The United Nations Office for Disaster Reduction (UNDRR) and its partners launched the "Make Cities Resilient" campaign in 2010 and defined resilience as "the ability of exposed systems, communities or societies to withstand, absorb, adapt, transform, and recover promptly and effectively from the effects of hazards, which includes protecting and restoring basic structure and functions through risk management" (Dilanthi & Pournima, 2019).

As early as 1990, Funtowicz and Ravetz pointed out that decisions on environmental problems are particularly characterized by uncertainty, high stakes, urgency, and controversy (Funtowicz and Ravetz 1990). In the field of environmental decision-making, Multi-Criteria Decision Aid (MCDA) can address problems involving more than one objective. Several theoretical (e.g., Munda 1995; Castells and Munda 1999) and empirical (e.g., Janssen 1992; Andreoli and Tellarini 2000; Mendoza and Prabhu 2000) studies have shown that MCDA provides a useful tool for decision aid in this field, as it allows for multiple objectives, the use of different types of data, and the involvement of different stakeholders. The choice of a particular method depends on the specific problem and user requirements. Since the number of existing methods is already quite large and continues to increase, choosing the "right" method is not an easy task.

Several authors have compared multi-criteria algorithms regarding their consistency, relative accuracy, speed, etc.

De Montis et al. (2004) proposed a comparison of seven different MCDA methods (MAUT, AHP, Evamix, ELECTRE III, Regime, NAIAD and programming methods) through a list of quality criteria for assessing their usability considering the most relevant sustainable development issues. The authors grouped the quality criteria according to three main aspects:

- operational components of MCDA methods (characteristics of the method derived from its theoretical basis),
- applicability of MCDA methods in the user's context (e.g., criteria referring to project constraints in terms of cost and time, or criteria referring to the structure of the problem-solving process, considering, for example, the possibility of stakeholder participation)
- applicability of MCDA methods considering the structure of the problem (possibility of including indicators with specific characteristics needed for problem solving, the type of data to be used and their availability).

Starting from the methodology proposed in De Montis et al. (2004) for comparing different MCDA methods, the aim is to investigate the existing literature about the use of different MCDAs in assessing the exposure related to four hazard categories: flooding, coastal flood, heat wave, earthquake. In this document is presented a first step of this research with the aim of using the obtained result to propose a new set of criteria for comparing the usability of MCDA methods in the exposure assessment.

Table 3. MCDAs methods comparison regarding exposure assessment

ANP	The Analytic Network Process (ANP) method was introduced by Saaty in 1996. It is an essential tool for articulating the understanding of a decision-making problem as it allows for the comparison of two elements against a third element in the system, assessing the relative influence of one element on the other with respect to an underlying control criterion. PNA is used to derive relative priority scales of absolute numbers from individual judgements (or real measures normalised in relative form) that also belong to a fundamental scale of absolute numbers and is useful for transforming intuitive informed judgements into real responses that are reflected in actual measurements in the real world (Saaty, 2004).
AHP	The Analytic Hierarchy Process (AHP) is one of the most used MCDA is a special case of the ANP. It was developed by Thomas L. Saaty in 1980, to organize and analyse numerous models and expert opinion-based complex choices, changing them in a hierarchical structure. By identifying the elements of decision-making such as goal, criteria (indicators) and alternatives (sub-indicators), AHP allows to prioritize and relating them to each other and simplifying the analysis and decision-making. The weight of elements in a certain level of decision-making is gained through a weighted linear summation method based on pairwise comparison.
Fuzzy AHP	The Fuzzy Analytic Hierarchy Process method (F-AHP) was proposed from Buckley (1985), combining AHP and fuzzy logic theory to solve the ambiguity, uncertainty, and inaccuracy in AHP (Schwarz, 2010) due to the inclusion of subjectivity in decision-making and inconsistent limits.
AHPSort II	Ishizaka et al. (2012) presented "AHPSort," a preference-based method for AHP sorting. Sorting cars (Gujansky et al., 2014) and risk levels (Xie et al., 2019) are two uses for it. Given the Decision Maker's preferences for "limiting" or "central profiles" of each class's benchmark, it helps the Decision Maker organise a set of alternatives into many classes. The number of pairwise comparisons required in AHP increased quadratically with the number of possibilities; however, AHPSort minimises this requirement. The Decision Maker must provide AHPSort with advance notice of the number and standard of the classes in which the options will be categorised and grouped. The "AHP-K" (and "AHP-K-veto") variant, in which items are automatically grouped based on the number of ordered classes, can be used in the absence of such data.



	<p>A second version of the AHPSort, known as "AHPSort II," was introduced by Miccoli and Ishizaka (2017), in line with the wave of methodological advances in the literature. This version significantly reduced the number of pairwise comparisons required by the Decision Maker and, consequently, the cognitive effort associated with it. It merely compares a small number of typical points across the performance range of the alternatives, after which the scores of the actual ones are interpolated. The authors describe how the AHPSort-II variation would require just 1.54% of the pairwise comparisons that would have been required with the originally presented AHP, resulting in a significant reduction of the cognitive input of the Decision Makers in an environmental sorting application. This contribution may undoubtedly be considered significant because it allows the AHP to be realistically applied to a wide range of options, as opposed to the earlier recommendation that the AHP be used to evaluate just alternatives using the approach that was first introduced (Saaty et al., 2003).</p>
TOPSIS	<p>Technique for Order of Preference by Similarity to the Ideal Solution is a MCDA method developed by Hwang and Yoon in the 1981. It is used in different fields of scientific research to support decision-makers between different alternatives of specific projects. It is based on the concept that the chosen alternative should have the shortest Euclidean distance from the positive ideal solution and the longest Euclidean distance from the negative ideal solution. The positive ideal solution is defined as the sum of all the best values that can be reached for each attribute, while the negative ideal solution consists of all the worst values reached for any attribute. Based on the comparison of the relative distance, an alternative priority can be defined.</p>
WSM - Weighted Sum Model	<p>The weighted sum model (WSM) (Fishburn, P.C. (1967), also known as Simple Scoring Method, Simple Additive Weighting (SAW) (Churchman et al., 1954; Salehi and Izadikhah, 2014), Weighted Linear Combination (WLC) (Malczewski and Rinner, 2015) or Factor Rating (Sorooshian, 2018). The WSM was used in a number of studies to calculate a value by adding up the attribute values and multiplying them by the appropriate weights. Every selection criterion in WSM has a score allocated to the alternatives, and each criterion's weight is taken into account before the weighted total. For this reason, the MADM technique is attacked for being the sum of disparate types of data, without a way for determining attribute weights, and having a built-in problem with the generation of dependence information that is not logically ordered among the attributes. It is clear from this that the incapacity of the WSM and other MADM to interpret data from many sources is one of their main limitations. For example, these are not applicable in situations where decision-making groups or experts are not aware of or familiar with specific criteria (or at least one criterion) in decision-making situations involving multiple criteria due to incomplete or limited awareness, knowledge, expertise, or other reasons. Therefore, there are two sets of criteria used in the decision-making process: the decision criteria derived from a shared information source, usually a group of experts, and the specific criteria derived from a separate information source.</p>
Weighting methods of Shannon's entropy (Entropy)	<p>A common statistical quantifier for characterising intricate systems is the Shannon entropy. It can identify aspects of nonlinearity in model series, which helps to provide a more trustworthy explanation for the nonlinear dynamics of various points of analysis. This improves our understanding of the characteristics of complex systems that are nonequilibrium and complex (Yao et al., 2020). Most complex systems, but not all of them, also have the property of having heterogeneous distributions of linkages in addition to complexity and nonequilibrium (Jolliffe, 2002). Shannon entropy is the term for the idea of entropy that he used in information theory for computer science data communication (Shannon, 1949, 2001). The term "entropy" describes a system's degree of ambiguity and randomness (Bugata and Drotar, 2020). It won't be difficult to predict the class of new data if we assume that all of the existing data belong to a single class. In this instance, entropy is 0. Entropy, which is a number between 0 and 1, reaches its maximum value when all probabilities are equal (Galar and Kumar, 2017; Rajaram et al., 2017). The degree to which this incidence has a low likelihood determines what class it belongs in, depending on the variables (Sabatini, 2000; Conforte et al., 2019).</p>
ELECTRE	<p>ELECTRE, was developed by Roy in 1985. The acronym stands for "ELimination Et Choix Traduisant la REalité" and express the ability of this methods family of a) managing criteria of both quantitative and qualitative nature, b) using very heterogeneous scales, c) avoiding overcompensation effects through the use of the concordance index and the existence of veto thresholds, d) considering imperfect knowledge of the data and arbitrariness in the construction of criteria, e) finally, considering the reasons for and against outranking. It comes in four main revisions (ELECTRE I, II, III, and IV) (Roy, 1991) as well as two other versions (ELECTRE IS and TRI) (De Montis et al., 2005). The processing of a system of pairwise comparisons of the options forms the foundation of the ELECTRE technique. It is based on a system of preference relations (SPR) according to which if an activity is thought to be at least as good as another, it will rank higher than the other (Roy, 1996).</p>
VIKOR	<p>The VIKOR (VlseKriterijumska Optimizacija I Kaompromisno Resenje) technique (Otay & Kahraman, 2022), introduced by Opricovic in 1998, aims to rank and select the most suitable alternatives (Wang & Chang, 2005) that define the percentage of closeness to the optimum option or so-called "compromise option." (Babashamsi et al., 2016).</p>
GRA	<p>One of the most common models of grey system theory is Grey Relational Analysis (GRA), often known as Deng's Grey Incidence Analysis model. Professor Deng Julong first suggested GRA (Ju-Long, 1982). GRA determines whether or not data sequences are closely related by analysing the geometric curves' degree of similarity. The sequences are more relevant the more similar the curves are, and vice versa (Liu et al., 2017). Different kinds of "grey relational degree" values, also known as "degree of grey</p>



	incidence," are included in GRA models. A quick explanation of one of the models' variations is given below. Deng's GRA model has been widely used in numerous study disciplines because it reflects the inter-influences among the elements analysed based on the correlation coefficient of specific points (Tan and Deng, 2012).
COPRAS	The COPRAS is a new MCDM method used to maximize and minimize the criteria value. This method selects the best option or a set of alternatives that helps in decision-making by considering the ideal (positive) and worst (negative) solutions and acts as an evaluation ranking in terms of the meaning and usefulness of the options (Ghased et al., n.d.; Roozbahani et al., 2020). In other words, it is an instrument-based ranking approach that works with the idea of weighted arithmetic operations, taking into account the nature of the criteria (Ramana et al., 2022; Stefano et al., 2015).

2.5.1. Heat wave

Continued heat waves will undoubtedly threaten sustainable social development and people's safety, especially increased mortality (Guo et al., 2017; Yang et al., 2019; Li et al., 2021). Therefore, in the context of global warming, it is necessary to strengthen the knowledge of extreme environmental risks for city residents and develop adaptation strategies for decision makers to improve urban resilience (Li et al., 2019b).

In addition, in order to take mitigation measures, it is important to identify places where heat risk is strongest based on a local-level assessment (Estoque et al., 2020) where the urban heat island effect can accelerate the formation of extreme heat and further threaten the health of urban residents (Gao, Hou, & Chen, 2019; Li & Zhou, 2019; Patz, Campbell-Lendrum, Holloway, & Foley, 2005).

The Intergovernmental Panel on Climate Change (IPCC) has used the Heat Wave Duration Index (HWDI) to assess heat risk (Radinović & Ćurić, 2012), while some studies have assessed vulnerability from a social response perspective (Sheridan & Dixon, 2017; Zhu et al., 2014). But in both cases, there is no systematic approach to understanding heat wave-induced risk (Azhar, Saha, Ganguly, Mavalankar, & Madrigano, 2017).

Following IPCC report (2018), climate change risk is determined by three aspects: hazard, vulnerability, and exposure.

Some studies have identified indicators to assess the impact of heat waves on human health, such as temperature-humidity index (WBGT) and the Universal Thermal Climate Index (UTCI) (Emmanuel, 2005; Matthews, 2018; Wang, Tian, Kim, & Yin, 2019) but they were introduced into the hazard field without any reference to the framework proposed by the IPCC and especially with a specific focus on the local scale.

Moreover, the effects of heat waves on human health are closely related to factors involving aspects related to people's physiological state and economic conditions, but also to aspects related to the quality of services in urban settings (Johnson, Stanforth, Lulla, & Luber, 2012; Schmidtlein, Deutsch, Piegorsch, & Cutter, 2008; Stillman, 2019). Duqne, assessing vulnerability requires consideration of several complex location-dependent physiological variables and other social and environmental factors (Aubrecht and Ozceylan 2013a, b).

Vulnerability is considered a function of the level of exposure to heat waves, the level of sensitivity to a heat wave, and the level of adaptive capacity of the population (McCarthy et al. 2001, Oppenheimer et al. 2014, Wilhelmi and Hayden 2010). Exposure is often related to local climate and urban meteorology, as well as to the pattern of land use in the urban area. By it is meant the nature and degree of exposure of a system to heat waves. Population density turns out to be the most widely used indicator to assess it (Estoque et al., 2020).

Sensitivity is influenced by differences in socio-economic status or cultural aspects of the population (Lundgren and Jonnson, 2012) and focuses on people who are more susceptible to heat waves: the elderly and people with diseases result with a higher level of mortality (Chen et al, 2015; Sun et al., 2014), as well as the very young, socially isolated people, and workers engaged in agriculture (Zhu et al., 2014). "Adaptive capacity" concerns the ability of individuals or regions to cope with extreme heat, thereby reducing its vulnerability. (Zhu et al. 2014) and is related to individual precaution awareness and regional economic and medical capacity (Rinner et al., 2010). Differences in exposure, sensitivity, and adaptive capacity will create vulnerable population segments.

Both the exposure and sensitivity components are based on quantitative data from models, measurements, or aggregate data, while adaptive capacity is assessed through both qualitative (interviews) and quantitative data from surveys (Wilhelmi and Hayden 2010). Thus, vulnerability is a function of events occurring in natural and human systems, influenced by external factors (such as climate change, economic factors, etc.) and by factors

within the system (such as a person's or system's adaptive capacity) (Lundgren and Jonnson, 2012). For this reason, the impacts of heat waves vary widely across locations and at different scales (Knowlton et al. 2009; Page et al. 2012) due to variability in localized microclimates resulting from the complexity of their physical and built environments (Bassil et al. 2009), socioeconomic development (Rey et al. 2009), and adaptation strategies (Huang et al. 2011).

In the study of natural hazards, census data on demographics and socioeconomic factors are the most commonly used to find critical vulnerability points (Wilhelmi and Hayden 2010). But this approach does not take into account the micro scale (e.g., the neighborhood or block) at which it would be useful to assess vulnerability to identify realistically related mitigation and prevention strategies for territories (Schmidtlein, Deutsch, Piegorsch, & Cutter, 2008). Therefore, Wilhelmi and Hayden (2010) propose a study in which they try to assess local vulnerability to extreme heat by exploring the relationship between people and place.

Öberg (2009) used a tool developed by the Swedish Land Mapping, Cadastre and Registration Authority, Lantmäteriet, to identify vulnerable groups during heat waves, based on geographic information systems (GIS). The author identified three groups of the most vulnerable population segments (women older than 65 years, children younger than 3 years, and people with heart or lung disease, as well as people with allergies that affect breathing) by mapping their distribution in the Swedish city of Växjö, where the test was conducted. Reid et al. (2009) used census data to map vulnerability to extreme heat in the United States and create a cumulative heat vulnerability index. In the study, 10 variables were mapped and analyzed for heat-related morbidity/mortality, including demographic and socioeconomic variables (age, poverty, education, living alone, and race/ethnicity) and other variables such as land cover, prevalence of diabetes, and access to air conditioning. Using a principal components analysis, they found four factor loadings of the heat vulnerability variables that explain the variance among the variables: - social/environmental vulnerability (below poverty line, race other than white, less than a high school diploma, no access to green space) - social isolation (living alone, being over 65 and living alone) - prevalence of air conditioning (no central air conditioner, no air conditioning) - proportion of elderly/diabetes (diabetes, age over 65).

As argued by El-Zein and Tonmoy (2015), the most common method of aggregation in the literature, which is occasionally based on multi-attribute utility theory (MAUT), usually creates rankings by building a global utility function via weighted summation. Nevertheless, Indicator-Based Vulnerability Assessments (IBVA) rarely, if ever, satisfies the related criteria for additive independence and full understanding of system interactions by analyst. The authors create a comparison between the structures of IBVA problems and Multi-Criteria Decision Analysis (MCDA) problems. They demonstrate how a set of methods known as Outranking Methods, which were created in MCDA to address criteria incommensurability, data uncertainty, and preference imprecision, provide IBVA with a viable substitute for multiplicative or additive aggregation. They construct thresholds of difference, reformulate IBVA problems within an outranking framework, and apply an outranking approach, ELECTRE III, to evaluate the relative vulnerability of 15 local government areas in metropolitan Sydney to heat stress. The findings supported the ranking outcomes' robustness and suggested that assessments with a combination of qualitative, semi-quantitative, and quantitative indicators, threshold effects, and ambiguities regarding the precise relationships between indicators and vulnerability are better suited for an outranking approach.

Qureshi and Rachid (2021) provided an interesting review of academic research on multi-criteria DST approaches for urban heat mitigation, highlighting that for evaluate the Urban Heat Stress (UHS) the following methods were applied: Analytical Hierarchy Process (SWOT) (Sangkakool et al., 2018), Multi-criteria outranking approach (MCDA and IBVA) (El-Zein & Tonmoy, 2015), Enhanced Fuzzy Delphi Method (EFDM) (Mahdiyar et al., 2018), Fuzzy decision-making trial and evaluation laboratory (FDEMATEL) (Tabatabaee et al., 2019), Multi-criteria method by linear regression (Foissard et al., 2019), The technique for order of preference by similarity to ideal solution (TOPSIS) (Kotharkar et al., 2020), Spatial Multi-Criteria Evaluation (SMCE) (Januadi Putra et al., 2019), Fuzzy Analytic Hierarchy Process, Fuzzy TOPSIS (Asghari et al., 2017). Interestingly, some interpret heat wave evaluation from the perspective of heat wave mitigation through the adoption of nature-based solutions (such as green roofs) (Mahdiyar et al., 2018; Sangkakool et al., 2018; Tabatabaee et al., 2019).

2.5.2. Flooding

It is now increasingly recognized that cities are the places most exposed to climate threats (Mabrouk and Haoying, 2023). Decreasing their vulnerability and increasing their resilience is an increasingly urgent goal that requires thinking systemically and over the long term, taking a multidisciplinary approach. In this context, it becomes crucial and necessary to address the issue of flood risk starting from the study and analysis of flood exposure factors.

Mabrouk & Haoying (2023) point out that flood exposure and vulnerability are interrelated aspects that influence each other (Le Cozannet et al., 2013; Kovacs et al, 2017): flood exposure negatively affects vulnerability just as certain vulnerability factors (socioeconomic index, financial capacity of inhabitants, living conditions) can lead to variation in exposure based on geographic variations and social and political standards (Barthel et al., 2013). The authors propose a classification system for at-risk districts based on the use of fuzzy AHP-VIKOR, WSM and TOPSIS (FAVWT as abbreviation) concepts to classify at-risk districts, reporting accuracy as the main reason for their choice: the study ignores socioeconomic indicators but the combination of these concepts succeeds in simultaneously considering methods released at different times and meeting all previously ignored indicators. Forty-four indicators related to flood risk were identified and evaluated by one hundred and thirteen Egyptian climate experts and then classified using fuzzy AHP. The results of this study demonstrate the correlation between urban form and the spatial distribution of flood risk, showing that it increases near traditional downtown patterns and decreases when moving to dispersed patterns in the city periphery. So urban form is taken as an indicator that, when combined with other non-spatial indicators, is particularly significant in analyzing flood trends.

Gudiyangada Nachappa et al. (2020) proposed a comparison of the predictive performance of three different modeling approaches, including MCDA models (AHP and ANP), ML models (RF and SVM), and ensemble modeling based on DST optimization (RF-SVM, AHP-ANP) to map flood susceptibility. The results showed that ML models (SVM and RF) were better than MCDA methods (AHP and ANP) and, most importantly, the RF model achieved the highest accuracy among all ML and MCDA models, highlighting that the weakness of MCDAs is the uncertainty associated with criteria weighting based on expert knowledge. In addition, the interrelational connections in the structure of the PNA made its performance more satisfactory than that of the AHP model.

Azizi et al. (2023) used the novel-ensemble MCDM framework to assess flood vulnerability for 26 watersheds in Ardabil province, starting with the calculation of exposure, sensitivity, and resilience factors (Balica & Wright, 2010; Tingsanchali & Promping, 2022; White et al., 2005) to floods and identifying 19 criteria. To this end, they developed and compared four different aggregation frameworks by integrating the Complex Proportional Evaluation of Alternatives (COPRAS) (Zavadskas & Kaklauskas, 2002) and the UK Department for International Development (DFID) approach (Balica & Wright, 2010; White et al., 2005) with the widely used weighting methods of Shannon entropy (Entropy) and analytical hierarchy process (AHP).

In contrast to this study, Peng & Zhang (2022) argue and demonstrate that the combined AHP-CRITIC-game-theory weighting is more reasonable than the AHP and AHP-Entropy Weighting Method (EWM) methods for determining the weight of indicators. Their urban flood risk assessment model is based on the selection of six flood hazard and vulnerability assessment indicators, and a risk map was generated based on the GIS platform. For the case study examined, Jinshui District, the results showed that the risk is higher in areas with lower elevation and higher economic development.

The recent study by Chaulagain et al. (2023) proposes the flood susceptibility mapping of Kathmandu metropolitan city based on the identification of the most flood susceptible local administrative unit using a multicriteria decision analysis model, including analytical hierarchical process (AHP) and weighted linear combination in geographic information system (GIS). Six hazard criteria were identified: slope, elevation, drainage density, precipitation, land use and land cover, and distance from the river (the latter was the most significant criterion, followed by precipitation and land use and land cover). The results confirmed that this model is a robust technique for weighing flood indicators by providing valuable support to local governments in implementing the local adaptation action plan, budgeting, policy formulation, formulation of flood preparedness and response strategies, and implementation of programs in the affected area. It also provides a valuable starting point for other cities that are preparing for climate resilience improvement.

Sharifi et al (2021) conducted an interesting study in which urban resilience is related to three different urban form patterns: traditional, semi-planned and planned. Nine selected neighborhoods of Shiraz, an ancient Iranian city, were categorized based on these three patterns and their resilience to three main stressors was evaluated: earthquakes, extreme heat events and floods. Also in this study, the method used is based on the combination of Shannon entropy and the VIKOR method is used to rank the resilience of each neighborhood to each of the three stressors. The results show that, overall, the physical form of planned neighborhoods is more conducive to urban resilience. In contrast, the urban form of traditional neighborhoods was found to be less resilient. However, some variations were found depending on the type of stressor considered. The paper concludes by emphasizing the need to consider social and economic factors in future studies on the resilience of urban forms.

Tu et al. (2023) propose a new multicriteria decision-making method (MCDM) G1-EW-MGLA (GEM)-AHPSort II, combining the AHPSort II method, the G1-EW method and the MGLA method, to assess flood resilience in Hubei Province, China. The authors motivate the choice of this combination of methods by analyzing the convenience of their use based on the following criteria: capability of handling multiple alternative classification problems, adequacy in supporting group decision-making, agility in the decision process, and reliability in the results. Specifically, the authors propose a framework of indicators for assessing regional flood resilience from the perspective of objective and management factors in order not only to assess the flood resilience of each city, but also to understand the potential differences in the performance of each city under the different assessment indicators. The study shows that although the assessment results may attribute the same level of resilience for different cities, yet there may be great differences in the performance of different assessment indicators. This aspect becomes of great importance to local government departments, which, by studying and analyzing assessment results and indicator data, can improve regional resilience to flood disasters.

Zhu et al. (2021) propose a framework based on the use of the VIKOR method together with the Grey Relational Analysis (GRA) method classification method assuming that VIKOR performs better than the TOPSIS method because it not only considers the distance between each alternative and the positive and negative ideal solutions, but also takes into account the relative importance of both distances (Li et al., 2019b). Moreover, it is particularly suitable from a decision-making perspective because it also considers the balance between the whole and the individual, making the decision-making process more reasonable. To attribute mathematical robustness to the rank provided by VIKOR, GRA is then applied to estimate correlations between the city under study and other cities taken as benchmarks for comparison. The indicators used in this framework are physical, social and economic and are divided by considering the three phases of the flood disaster cycle (before, during and after).

In the study by Li et al. (2019b) the VIKOR method is also used but in a more extended form than the traditional model to improve the handling of hybrid information and to achieve a higher group consensus than traditional VIKOR methods with equal weights. In addition, to increase the flexibility of linguistic judgments of experts, fuzzy hesitant in urban flood resilience indicators an integrated indicator system for flood resilience assessment with hybrid information was considered. The method was tested in 5 southeastern coastal cities of P. R. China, ranking them according to the results.

2.5.3. Coastal erosion

Coastal erosion vulnerability assessment is widely used to assess the degree of coastal zone loss caused by erosion and plays an important role in coastal natural resource protection, planning, management and decision making. Several studies have attempted to quantify the vulnerability of coastal systems in recent decades. combining various sets of parameters and doing single and multivariate analyses. Almost all of these studies follow some basic steps, including scaling, weighting and combining elements of one or more categories of coastal vulnerability factors. However, each study used a unique method for each step.

As pointed out by Tanim et al. (2022), the damage caused by sudden catastrophic events highlights the urgency of adopting systemic approaches for an integrated vulnerability assessment of coastal systems (Ahmed et al., 2021), considering the coexistence of all vulnerability factors associated with the various subsystems of coastal regions and simultaneously analyzing socio-environmental and biophysical aspects. It is from this perspective that urban planning, nature conservation and emergency management strategies must be reorganized.

Generally, the factors that are considered in the vulnerability analysis of coastal areas, in relation to their quantitative and qualitative characteristics, can be classified into: physical characteristics, hydroclimate, environmental factors, socio-economic perspectives, and shoreline vulnerability (Tanim et al., 2022). From the simultaneous combination of these five groups of vulnerabilities and using the Multi-Criteria Decision Making (MCDM) approach, the same authors developed two integrated indices of socio-environmental coastal vulnerability (CVI-50 and CVI-90), referring to average and extreme factor conditions, respectively. The Probabilistic Principal Component Analysis (PPCA) was used to obtain a data-based CVI against which the CVI-50 and CVI-90 were compared. To assign the weights of the different vulnerability groups needed to estimate the final index, this study employs an entropic weighting technique, avoiding the risk of subjectivity in individual judgments (present in most cases where MCDMs are used). Finally, a geospatial analysis was used to process data derived from both the MCDM and PPCA in order to assess the vulnerability to natural hazards of six coastal counties in South Carolina. Validation of the results shows that the CVI-50 methods underestimate biophysical vulnerability to coastal hazards while both CVI-90 and PPCA present more robust results for vulnerability from biophysical and socioeconomic factors, confirming the greater importance placed on decision-makers' opinions in using MCDM while the PPCA technique is more suitable for assessing high-dimensional vulnerability.

The study by Cao et al. (2022) proposes a coastal erosion vulnerability assessment system for the Great Bay area of the Pearl River Estuary based on the integrated use of 12 indices and the analytic hierarchy process (AHP) method, Technique for Order Preference by Similarity to an Ideal Solution (TOPSIS) method, independent weight method, Jenks natural breaks method (Jenks), exposure-sensitivity-adaptation (ESA) model and obstacle degree. The 12 indices are divided into 5 categories: coastal characteristics, hydrodynamic forces, economy, population and coastal reconstruction. The results show that coastal characteristics, coastal shallows and protective capacity are key elements in controlling erosion.

Fu et al. (2022) assessed coastal erosion vulnerability through the coastal erosion vulnerability (CVI) method and identified 8 assessment indicators. The weight of the overall index was calculated using the Delphi method and the entropy weight method. To quantitatively assess the temporal and spatial distribution of coastal erosion vulnerability, the global index was combined with the CVI and geographic information system (GIS) technology. The eastern coast of Qiongdong was studied, identifying 5 degrees of vulnerability and allowing an assessment of the overall performance of the area with respect to erosion vulnerability. A number of factors were identified as major controlling factors influencing coastal erosion vulnerability in the study area (such as that the interannual downward erosion rate of the beach, and the rate of change of the isobath and the coastal dynamic factor), providing an important methodological reference for the development and management of the coastal zone in the study area.

Also, in the research of Hossain et al. (2022), the coastal vulnerability index (CVI) was calculated using Gornitz's CVI model and the Analytical Hierarchy Process (AHP) method were used to understand the spatial distribution of physical vulnerability along the coastal stretch between the Indian Subarnarekha estuary (Balasore district, Odisha) and the mouth of the Haldi River (Purba Medinipur, West Bengal). Six geological parameters, such as elevation, slope, bathymetry, coastal geomorphology, shoreline change, and coastal land use, and four physical process variables, such as mean sea level (MSL), mean tidal range, significant wave height, and storm surge height were taken as input data for the ArcGIS ver. 10.5 tool through which coastal vulnerability mapping with respect to coastal hazards was developed. The results of the study showed that both models simulated similar results of probable inundation extent of two different storm surge scenarios of wave heights ≤ 3 m and ≤ 5 m. The method used is particularly useful for coastal planners, decision makers and administrators to identify and implement risk reduction policies.

The study by Ghosh and Mistri (2022) aimed to assess the multi-hazard coastal vulnerability of the Matla-Bidya interest area of the Indian Sundarbans Delta, considering exposure, sensitivity, and adaptability. Again, the analytical hierarchy process (AHP) was used to calculate coastal vulnerability from 26 indicators using in combination with remote sensing data and geospatial techniques.

Ahmed et al. (2021) proposed an integrated approach for coastal erosion vulnerability assessment in the eastern coastal region of Bangladesh. Thirteen spatial criteria were identified with respect to two components of vulnerability, namely physical and socioeconomic vulnerability. The analytical hierarchy process (AHP) was used to weight the criteria, which were then combined to generate individual vulnerability indices. Finally, integration of these indices with the physical and social vulnerability indices allowed the overall vulnerability

map to be developed. Geospatial techniques were used to examine the pattern of vulnerability to the effects of coastal erosion. Receiver operating characteristics (ROC) technique was used to validate the results.

Finally, Serafim et al. (2019) developed a coastal vulnerability index (CVI) to assess the vulnerability of the coast of Santa Catarina State (southern Brazil) to incident wave climate from the integration of the adaptive capacity index (ACI), composed of socioeconomic and local variables, and the susceptibility index (SI), composed of physical variables. Coastal dynamics resulting from nearshore wave processes were analyzed through numerical models and integrated with other variables in a geographic information system (GIS). The analytical hierarchy process (AHP) was used to obtain the hierarchy of variables for the index, considering five classes of vulnerability. The results of the AHP showed greater relevance of physical variables than socioeconomic and locational variables, highlighting the importance of including such variables, such as waves, in the definition of coastal zone management measures.

2.5.4. Earthquake

In the last decade, a growing number of researchers have become increasingly interested in the use of Multi-Criteria Decision Making methods in earthquake studies (Jamal-ud-din et al., 2023; Flores et al. 2021; Walker et al. 2021), integrating qualitative and quantitative indicators to manage the complexity of decision making.

In the past, some studies, such as the Zebardast's one (2013), focused on assessing social vulnerability using factor analysis to identify its sub-dimensions, with their primary variables, to be included in the Analytic Network Process (ANP). The results of the factor analysis were used in the ANP to assign weights to the different social vulnerability variables in order to calculate both factor scores for each sub-dimension and the composite social vulnerability index (SOVI). This approach has been applied and validated in Iran's counties and resulted robust for constructing a composite SOVI. Here the SOVI was considered as a factor capable of guiding and directing natural disaster management strategies by local authorities and the national government.

Rezaie and Panahi's (2015) research highlighted the importance of considering qualitative and quantitative indicators to study the seismic vulnerability of an area. AHP and GIS spatial modeling are identified as preferred methods. AHP to categorize and weight the indicators considering them simultaneously and evaluating the importance of each in relation to the others. GIS to manage, integrate, and analyze data derived from the indicators. The proposed method was used for developing a seismic vulnerability map from the simultaneous analysis of four factors of geotechnical, structural, social and physical distance. The author suggested that acquiring data through field studies and integrating these four different categories of information makes the map closer to reality.

Also Armaş et al. (2017) emphasized the adoption of interdisciplinary approaches to developing a global seismic hazard vulnerability index. The experimentation was done through a spatial approach in Bucharest, Romania, the most earthquake-prone capital city in the European Union, by developing a global seismic hazard vulnerability index based on a multicriteria analysis, to process spatial socioeconomic data, and analytical methods (the improved displacement coefficient method and custom-defined vulnerability functions) to estimate damage patterns, incorporated in a GIS environment. The results show that mitigation efforts can be improved through interdisciplinary approaches that compensate for uncertainty in model inputs due to less detailed data sets. In this way, useful and robust seismic vulnerability indices can be obtained to spatially identify building vulnerability models.

Xu et al. (2016) used an iterative method based on the application of the multicriteria model and the corresponding GIS solution method to solve the multicriteria problem of locating urban earthquake evacuation shelters, demonstrating the effectiveness of their approach from an urban planning perspective.

Nyimbili et al. (2018) integrated the Hierarchical Analytical Process (AHP), the Technique of Sorting Preference by Similarity to the Ideal Solution (TOPSIS), and GIS to produce seismic hazard and risk maps in the Küçükçekmece region of Istanbul, Turkey. Topography, distance to the epicenter, soil classification, liquefaction and fault/focal mechanism were identified as the main factors that most influence the impact of earthquakes. Seismic hazard maps prepared by this method showed high correlation and compatibility.

Jena and Pradhan (2020) also pioneered and tested a method for assessing seismic risk in Aceh, Indonesia, from the combination of cross-validation artificial neural network (fourfold ANN-CV) with a hybrid method

of hierarchical process analytic-Technique of order of preference by similarity to ideal solution (AHP-TOPSIS). The authors motivate the choice of neural networks based on the fact that they are recognized in the literature for their ability to improve city-scale probability mapping. In addition, special emphasis was placed on predictive accuracy in probability mapping through the identification of specific indicators. This mapping was then used for hazard assessment. Second, social and structural factors were identified to develop a vulnerability map. Finally, a risk assessment was obtained by multiplying the hazard and vulnerability indices by these factors and calculating the population and areas at risk. The results show excellent levels of accuracy and consistency.

Manyaga et al. (2020), through a review of 36 academic papers about the use of MCDM planning and management of natural disasters, highlighted that there is a lack in this field particularly in pre and post disaster phases. In this context, MCDM are interpreted as tools able to support the effective planning, to forecast imminent disasters and to prepare accordingly, thus mitigating the loss to human life. The study reveals that, especially when it comes to earthquakes, the availability and accessibility of reliable and up-to-date geospatial data supports decision making and facilitates disaster management.

Roy et al. (2021) selected 19 variables, including physical, environmental, and socioeconomic geography, and utilised the analytical hierarchy process (AHP) to assess the hazard, vulnerability, and exposure indices in the Bangladeshi Mekhna River estuary area. They used the area under the curve (AUC) to confirm the accuracy of assessing the level of erosion risk.

Jamal-ud-din et al. (2023) used the Analytical Hierarchal Process (AHP) and Weighted Linear Combination (WLC) methods to assess seismic vulnerability, relying on 24 indicators separated into four vulnerability components (systematic, structural, socio-economic and geological).

Aghataher et al. (2023) pioneered a hybrid method in Tehran based on modifying a rainfall optimization algorithm (ROA) into a gradient descent-based algorithm (GROA) and integrating the latter with a fuzzy analytical hierarchical process (FAHP). Finally, a geographic information system (GIS) was used to identify areas where a discontinuity in emergency response occurs after a destructive earthquake. The results of this study confirm that the use of GROA can improve the existing approach, avoiding local optimism and optimizing the process of identifying key locations for emergency response.

Table 4. MCDAs methods used for different principal hazards.

HAZARD	USED METHOD	AUTHOR
Heat wave	Multi-criteria outranking approach (The authors compared the structures of Indicator-Based Vulnerability Assessments problems and MCDA problems). ELECTRE III	El-Zein and Tonmoy (2015)
	AHP based on SWOT (Strength, Weakness, Opportunities, Threats) analysis.	Sangkakool et al. (2018)
	The authors developed an Enhanced Fuzzy Delphi Method (EFDM) for identifying criteria.	Mahdiyar et al. (2018)
	Multi-criteria linear regression method was used to build a model of the Urban Heat Island.	Foissard et al. (2019)
	TOPSIS	Kotharkar et al. (2020)
	AHP to analyze the parameters involved in the UHI phenomenon.	Sangiorgio et al. (2020)
	Delphi methods used to identify the most important criteria. Fuzzy AHP to weigh the selected criteria. Fuzzy TOPSIS technique for choosing the most suitable heat stress index.	Asghari et al. (2017)
	Spatial Multi-Criteria Evaluation (SMCE)	Januadi Putra et al. (2019)
	The enhanced fuzzy Delphi method (EFDM) and fuzzy decision-making trial and evaluation laboratory (FDEMATEL) approaches.	Tabatabaee et al. (2019)
Flooding	A combination of fuzzy AHP-VIKOR, WSM, and TOPSIS concepts (FAVWT as an abbreviation) in ranking risky districts	Mabrouk & Haoying, (2023)
	Dempster Shafer Theory (DST), Support vector machine (SVM), Analytical Hierarchical Process (AHP), Analytical Network Process (ANP)	Gudiyangada Nachappa et al. (2020)



	Novel-ensemble MCDM frameworks: the complex proportional assessment of alternatives (COPRAS) and the UK Department for International Development (DFID) approach was integrated with widely used weighting methods of Shannon's entropy (Entropy) and Analytical Hierarchy Process (AHP).	Azizi et al. (2023)
	GIS, Game theory, Combination weighting	Peng & Zhang (2022)
	GIS based MCDA using AHP	Chaulagain et al. (2023)
	AHP, TOPSIS	Sharifi et al. (2021)
	G1-EW-MGLA (GEM)-AHPSort II method is proposed by combining AHPSort II method, G1-EW method, and MGLA method.	Tu et al. (2023)
	VIKOR, GRA	Zhu et al. (2021)
	Hesitant fuzzy VIKOR, Information aggregation	Li et al. (2019b)
Coastal erosion	MCDM approach, to develop two integrated indices of socio-environmental coastal vulnerability (CVI-50 and CVI-90). Probabilistic Principal Component Analysis (PPCA) to obtain a data-based CVI. Entropic weighting technique to assign the weights of the different vulnerability groups. Geospatial analysis to process data derived from both the MCDM and PPCA.	Tanim et al. (2022)
	The analytic hierarchy process (AHP) method, Technique for Order Preference by Similarity to an Ideal Solution (TOPSIS) method, independent weight method, Jenks natural breaks method (Jenks), exposure-sensitivity-adaptation (ESA) model and obstacle degree method are used in conjunction with 12 evaluation indices to construct a coastal erosion vulnerability evaluation system.	Cao et al. (2022)
	Coastal Erosion Vulnerability method and 8 assessment indicators to assess coastal erosion vulnerability. Delphi method and the entropy weight method to weight the overall index. Geographic Information System (GIS) technology in combination with the global index and the CVI to quantitatively assess the temporal and spatial distribution of coastal erosion vulnerability.	Fu et al. (2022)
	Gornitz's CVI model to calculate the Coastal Vulnerability Index (CVI). The Analytical Hierarchy Process (AHP) method to understand the spatial distribution of physical vulnerability. ArcGIS ver. 10.5 tool to develop the coastal vulnerability mapping with respect to coastal hazards.	Hossain et al. (2022)
	The analytical hierarchy process (AHP) to calculate coastal vulnerability from 26 indicators using in combination with remote sensing data and geospatial techniques.	Ghosh and Mistri (2022)
	AHP to weight the criteria. Geospatial techniques to examine the pattern of vulnerability to the effects of coastal erosion. Receiver Operating Characteristics (ROC) technique to validate the results.	Ahmed et al. (2021)
	AHP to obtain the hierarchy of socioeconomic, local and physical variables for the Coastal Vulnerability Index (CVI). GIS to analyze coastal dynamics resulting from nearshore wave processes and other variables.	Serafim et al. (2019)
Earthquake	AHP to weigh five main criteria that have the strongest influence on the impact of earthquakes, which were also used as input into the TOPSIS method. GIS (ESRI ArcGIS) to produce earthquake hazard maps.	Nyimbili et al. (2018)
	GIS-supported iterative method	Xu et al. (2016)
	AHP and Weighted Linear Combination (WLC) methods are used to identify earthquake vulnerability.	Jamal-ud-din et al. (2023)
	AHP-TOPSIS	Jena and Pradhan (2020)
	AHP and PROMETHEE	Nassereddin et al. (2019)
	Fuzzy multicriteria model (FUMCO)	Opricovic & Tzeng (2003)

	GIS-based earthquake-triggered hybrid framework for suitability analysis using a Fuzzy Analytical Hierarchical Process (FAHP) and Gradient Rain Optimization Algorithm (GROA).	Aghataher et al (2023)
	AHP and GIS	Rezaie and Panahi (2015)
	Hybrid Factor Analysis and Analytic Network Process (F'ANP) model	Zebardast (2013)
	Improved Displacement Coefficient Method and custom-defined vulnerability functions) incorporated in GIS method	Armaş et al. (2017)

Here is an example of how different criteria should be considered for the assessment of each phenomenon:

Heat Wave

- Land Use and Vegetation cover to assess the presence of heat islands.
- Urban Geometry to consider specific parameters such as building height, street distribution and the presence of solar glare.
- Human Activities that contribute to heat islands, such as vehicular traffic and industrialisation.

Floods

- Topography and Hydrography to assess the areas most susceptible to flooding.
- Land Use/Land Cover can be included to understand how human activities influence flood risk.
- Critical Infrastructure as their location can be an important criterion for assessing flood risk.

Coastal Erosion

- Coastal Topography to assess areas most vulnerable to erosion.
- Climate and Tides informations can be crucial in understanding the extent of coastal erosion.
- Presence of Infrastructure can be included to assess the impact on erosion.

Earthquakes

- Economic losses associated to the cost of buildings repair/reconstruction.
- Impact on population (injured/deaths)
- Business interruption
- Time to recover

However, the key to using multi-criteria methods is the careful definition of relevant criteria and appropriate weighting according to the specific situation and priorities of the stakeholders involved in the assessment.

There are several multi-criteria methods used for the assessment of earthquakes, floods, heat islands and coastal erosion. Some of them are most commonly used considering specific hazard:

Heat Wave

- Topsis (Technique for Order of Preference by Similarity to Ideal Solution) is used to assess the severity of heat waves as it helps to rank alternatives according to their distance from the ideal solution.
- MCDM (Multi-Criteria Decision Making) as generic approach that can be customised to assess various aspects of heat islands, such as temperature, land use, etc.

Flooding

- MCDA (Multi-Criteria Decision Analysis) as generic approach that can be adapted to flood assessment, allowing simultaneous assessment of multiple criteria.
- GIS (Geographic Information System), together with multi-criteria techniques, can provide a spatial assessment of flood risk by integrating geographical data and multi-criteria decisions.

Coastal Erosion

- AHP is successfully applied to evaluate and rank the various criteria associated with coastal erosion.
- Geographic Information System (GIS) technology in combination with the global index and the CVI to quantitatively assess the temporal and spatial distribution of coastal erosion exposure.

Earthquakes

- PROMETHEE (Preference Ranking Organisation Method for Enrichment Evaluation) helps to compare alternatives based on multiple criteria, considering stakeholder preferences and facilitating the evaluation of emergency response systems.
- AHP (Analytic Hierarchy Process) allows criteria to be structured and prioritised according to relative importance, facilitating the assessment of earthquake complexity.
- Fuzzy Logic can be used to address the uncertainty and lack of accurate data associated with earthquakes, offering a more flexible assessment.

In many cases, it is also possible to combine several methods to achieve a more complete and accurate assessment.

3. Knowledge of Urban and Metropolitan Settlements oriented to exposure assessment

3.1. Urban Settlement system analysis

3.1.1. The urban physical system

Starting from the development of the observation component of the urban system and according to national regulatory guidelines, National Climate Change Adaptation Strategy (SNACC, 2015) and Climate Change Adaptation Plan (PNACC, 2022), an exposure-oriented taxonomic reading of urban settlements should be identified, consistent with potential actions for adaptation and risk mitigation.

In the framework of the cited documents, actions have been divided into two main types: type A or soft actions and type B or non-soft or green and grey actions.

Soft actions are those that do not require direct structural and material interventions, but are still instrumental in their implementation, contributing to the building of adaptive capacity through increased knowledge or the development of a favourable organisational, institutional and legislative context.

The macro categories of information actions, development of organisational and participatory processes, and governance belong to the soft types.

Grey and green actions, on the other hand, both have a component of materiality and structural intervention. However, the latter differ clearly from the former by proposing 'nature-based' solutions, i.e., the sustainable use or management of natural 'services', including ecosystem services, in order to reduce the impacts of climate change. Finally, grey actions are those related to improving and adapting facilities and infrastructures to climate change, which can in turn be subdivided into actions on facilities, materials and technologies, or on infrastructures or networks (PNACC, 2022, p.73).

According to these guidelines, 3 sub-systems can be identified for the sectoral subdivision of urban settlements: the green sub-system and the grey sub-system which refer to the physical characteristics of the urban system, the soft sub-system which refers to the functions and services and processes provided. The subsystem constituted by the population must be added to these to understand the vulnerability and exposure relationships established between this and the soft, grey and green subsystems.

For a further understanding of the risk-oriented taxonomy of urban settlements, DV 5.2.1 should be referred to. In the paragraph below, we provide a description aimed at understanding the relationship between exposure factors and the subsystems and components constituting the urban system.

This reading distinguishes the physical component on the one hand and the functional/service component on the other in accordance with the cognitive approaches of urban science and architecture. Moreover, this differentiation allows the elaboration of a knowledge model of the urban system based on the integration of the three identified macro-systems (soft, hard and population) to systematically represent urban conditions and the interconnections between natural elements and those influenced by the anthropic component.

The physical part of the urban settlements is made up of two sectoral sub-systems: Green and Grey, composed of sub-areas identified on the basis of type-morphological, environmental and spatial characteristics. The Grey domain is composed of the physical systems that structure the urban settlement, i.e.: built-up areas, technological systems and networks. The Green domain is composed of the physical systems of Green and Blue systems (designed to provide natural services, including ecosystem services) and of Vegetated areas and Non-vegetated areas, which include elements such as parks, beaches, dune systems, river banks, uncultivated areas, etc.).

The soft system does not refer to physical structuring and material aspects but to service supply and process development (including the development of organisational, institutional, legislative, information, participatory, governance contexts, economy etc.).

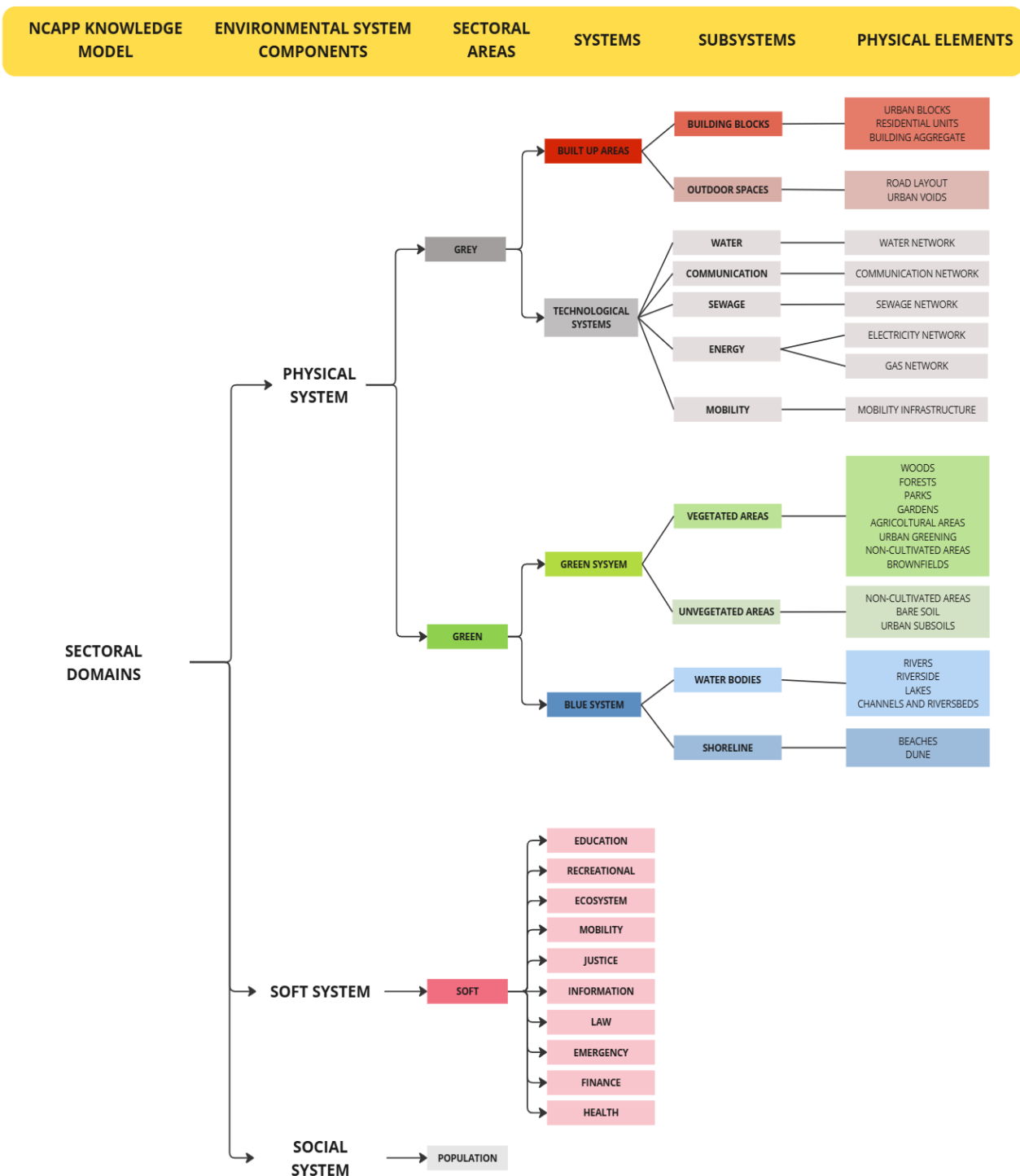


Figure 1. Sub-systems and components parts of urban settlement system (elaboration based on PNACC, 2022).

The identified sub-systems allow for a harmonisation of knowledge bases to establish the use of shared approaches and to use common types of data and analysis models to represent the impact of hazards of different nature (seismic, volcanic, climatic, etc.). This phase constitutes an important aspect to be considered in the process of prevention, mitigation, preparedness and response to catastrophes in multi-risk assessment models (environmental, natural and anthropogenic hazards).

The knowledge of the urban system in relation to specific hazards aims to identify specific characteristics and performances of the built environment, enabling the elaboration of databases useful to define strategies, framing quantitative and qualitative data and information. The aim of the analyses is to identify relations

between settlement design principles and processes of construction and formation of the built space in the functional, socio-productive and urban identity response, considering the need to acquire multiple quantitative data of the physical system together with qualitative data of a synthetic nature and other non-measurable aspects (Losasso et al., 2021).

In terms of design, in order to develop effective risk-oriented solutions, it will be essential to address the factors that influence the behavior of urban areas in relation to the presence and contribution of natural components such as the rate of soil artificialization, the overall density of tree masses and their leaf area, summer wind patterns, and the phenomena of polluting and climate-altering emissions that alter atmospheric behavior (MATTM, 2014, pp. 649-650). This contributes to the protection and restoration of active ecosystems capable of providing effective solutions for reducing the risks arising from climate change, such as contributing to the storage, infiltration, retention, and runoff of rainwater during flooding events and cooling during heat waves through evapotranspiration and shading provided by vegetation surfaces, thereby increasing resilience (WEC, 2024).

Taxonomy therefore supports the identification of physical elements, soft components, and social systems potentially impacted by climate risks, in order to reduce vulnerabilities and exposure factors. The implemented knowledge models coherent with the taxonomy must consider the identity and characterization factors of places, the interpretation of their environmental, cultural, functional, and critical characteristics. Thus developed, the knowledge models are configured as complex processes, due to the multiplicity of information and data that, at different scales (building-open space, neighbourhoods-district), relate type-morphological, physical, functional and performance aspects. These analyses are functional to accurately understand the integrated exposure of the built-up areas. Urban settlements are thus organized based on different levels of information, in a progressive scaling from urban districts to building blocks.

Table 5. An example of environmental, technological, and functional-spatial analysis used to assess the integrated exposure of built-up areas.

SECTORAL AREA	SYSTEM	SUBSYSTEM	Environmental analysis	Technological analysis	Functional-spatial analysis
Grey sectoral area	Built-up areas	Building blocks	Energy demand	Construction techniques	Settlement analysis (orientation of layouts, features of urban elements)
			Thermal behaviour in summer	Building type	Urban structure (schwartzplan, private/public space)
			Thermal behaviour in winter	Age of construction	Land use
			CO ₂ emissions	Form factors	Flows (energy, materials, waste)
			Solar radiation	Façade ratio	
			Natural ventilation	Number of stories	
			Atmospheric precipitation	Height	
		Outdoor spaces	Direct solar radiation	Soil permeability	Settlement analysis
			CO ₂ emission of open spaces		
			Sky View Factor	Materials and techniques for paving	Urban structure
			Natural ventilation		

			Relative humidity		
			Air temperature		
			Surface temperature		
			Mean radiant temperature		
			Albedo		
			Thermal comfort		
				Materials and techniques for shading elements	
					Land use
					Flows

3.1.2. The socio-ecological system

Urban areas are characterized by complex and dynamic interactions between society and ecosystems. They are ideal to study the links between people and nature to better understand the socio-ecological dynamics and responses to environmental changes (Catton, 1982). Studies on such areas, however, have partially captured the coupled socio-ecological nature of urban environments (Frank et al., 2017). Biologists focused on the structures of ecosystems in cities while social scientists examined cities based on their social construction and complex and variable definitions (Sassen, 2008).

Social science research has started to investigate the impact of the natural environment on urban life with the inclusion of principles of human ecology, developed by the sociologists of the Chicago School between the 20s and 50s of the last century (Hawley, 1950). These urban studies have significantly influenced the definition of human-ecological interactions in cities. For example, the positive effects of urban green spaces on the human population (i.e., health, physical activity, psychological well-being) and social cohesion have been explored (Barbosa et al. 2007).

The assumption that urban areas are dynamic hubs where changes are the result of economic, political, social, and ecological interactions, has pushed researchers to focus more on the connections between biological characteristics and the complex socio-ecological relationships of cities (Breuste et al., 2013; Elmqvist et al., 2013; Grove et al., 2013). This has allowed, of course, the overcoming of sectoral thinking and approaches and the opening of new lines of discussion and research on urban areas.

Research on urban metabolism is a domain in which the natural and social sciences find obvious points of convergence. Urban metabolism - the process of production, flow and consumption of materials and energy in cities - is a topic used in urban studies to investigate infrastructure, energy efficiency, recycling of materials and waste management in urban ecosystems. This approach has allowed scholars to more clearly represent the interconnectedness between urban ecosystems, the socio-natural processes that shape them and the relationships of power, becoming effective in showing "how urban environmental and social change are mutually determined and how these metabolic processes provide cues for creative pathways towards more democratic urban environmental policies" (Hayen 2014). Studies on urban metabolism have centered, for example, on the lifestyle of urban residents and their ability to adapt to stressful urban conditions (Zhang, 2013). Additionally, they have examined indicators to assess the liveability of man-made environments (Kennedy et al., 2011) and on issues related to urban water, pollution, gentrification, food safety, and the environment (Heynen, 2014; Loftus, 2012; Gabriel, 2014).

The approaches aimed at uniting the ecological and social dimensions of cities find synthesis in the description of them as 'complex Socio-Economic Systems' (SES). Redman et al. (2004) define SES as a "coherent system of biophysical and social factors that regularly interact in a resilient, sustained manner; a system that is defined at several spatial, temporal, and organizational scales, which may be hierarchically linked; a set of critical resources (natural, socioeconomic, and cultural) whose flow and use is regulated by a combination of ecological and social systems; and a perpetually dynamic, complex system with continuous adaptation".

Social-ecological systems are linked systems of people and nature, emphasizing that humans must be seen as a part of, not apart from, nature (Berkes and Folke, 1998). The social component refers to all human activities that include economy, technology, politics and culture. On the other hand, the ecological component refers to the biosphere, that is, to the part of the planet on which life develops.

More specifically, the social system is the patterned network of relationships constituting a coherent whole that exist between individuals, groups, and institutions. Interactions take place through behaviors, actions, and specific activities (economic, political, educational, etc.), within the framework of regulatory rules and other types of constraints that limit the variety of acts allowed to each subject with respect to others (Gallino, 1988).

Parsons (1951) organized social systems in terms of action units, where one action executed by an individual is one unit. Social systems rely on a system of language, and culture must exist in a society in order for it to qualify as a social system. Luhmann (1984) based his definition of a "social system" on the mass network of communication between people and defined society itself as an "autopoietic" system, meaning a self-referential and self-reliant system that is distinct from its environment. Luhmann considered social systems as belonging to three categories: societal systems (such as religion, law, art, education, science, etc.), organizations (defined as a network of decisions which reproduce themselves) and interaction systems (systems that reproduce themselves on the basis of co-presence rather than decision making).

Examples of social systems include nuclear family units, communities, cities, nations, college campuses, religions, corporations, and industries. The organization and definition of groups within a social system depend on various shared properties such as location, socioeconomic status, race, religion, societal function, or other distinguishable features.

Among the main properties of a social system, we find:

- the constituent units of a social system are not individuals themselves, but rather the actions and behaviors that they engage in due to their specific social position that binds them to their particular role;
- a social system is always "open": its "boundaries" are stable and penetrable by exchanges of resources and information with the external, physical, social environment of other social systems;
- all living systems, including social systems, have the ability to develop by reacting to changes in inputs from outside;
- to survive, any social system must overcome functional problems such as obtaining external resources, keeping their members above the minimum required to achieve their goals, adapting to varying changes in the physical and social environment around them, and avoiding internal conflicts;
- social systems are endowed with morphogenetic capabilities, that is, they include processes that tend to continuously modify the structure and state of the system, to differentiate and complicate its form, etc.

The balance of a Social System can be disturbed by changes in any of its components (ecological, economic, political, social, etc.), which often involve/generate conflicts: wars between peoples; conflicts between social groups; between the political system and civil society; between the human system and the natural environment, ecological problems, etc; technical conflicts (digital divide, etc.). The so-called "climatic migrations", which push thousands of people away from their territories to defend themselves from the effects of global warming, are a clear indicator of the deep conflict between the human and environmental systems.

The ecological system (or ecosystem) is a biological community consisting of all the living organisms (including humans) in a particular area and the nonliving components, such as air, water, and mineral soil, with which the organisms interact. Examples of ecological systems include forests, grasslands, agricultural systems, lakes, streams, wetlands, estuaries, and coral reefs (Likens, G. 1992). Ecosystem processes cycle water and nutrients, build soils, produce the oxygen we breathe, remove carbon dioxide and other greenhouse gases from the atmosphere, and perform many other functions that are important for the health of people and the planet. The ecological system is usually described in terms of:

- Extent and distribution
- Diversity and biological balance
- Ecological processes
- Physical and chemical attributes

– Ecological exposure contaminants

The extent and distribution of ecological systems influence the types of animals and plants that are present; the physical, chemical, and biological processes in the system; and the resiliency of the systems to perturbations (Wilson, 1992). The extent refers to the physical area covered by an ecological system. It can be reflected as an area or as a percentage of a baseline or of the total area. Extent indicators typically are based on physical and biological characteristics that are observable by remote sensing, but some ecosystems have indistinct boundaries. Distribution includes the pattern or arrangement of ecological systems and depends on the scale of analysis (e.g., local or national). Extent and distribution of ecological systems can be assessed through the analysis of the following parameters: i) land cover (the actual or physical presence of vegetation on the land surface) and land use (the purpose of human activity on the land, generally designated through zoning or regulation); ii) forest type, extent and fragmentation, that involves both the extent of forest and its spatial pattern, and the degree to which forested areas are being broken into smaller patches and pierced or interspersed with non-forest cover; iii) urbanization and population change, as increasing population often means increased urbanization, including conversion of forest, farm, and other lands for housing, transportation, and commercial purposes; iv) wetlands acreage, that support a variety of fish and wildlife species and contribute to the aesthetic and environmental quality.

The health of an ecological system can often be judged by its biological diversity and balance. Diversity can be viewed in terms of both the number of species present in an ecological system and the extent to which some species are threatened and endangered. Biological balance refers to the interrelationships among organisms, including the structure of food webs and the ability of ecological systems to sustain themselves over time. Balance is a dynamic characteristic rather than a fixed state. Diversity and biological balance may influence the functioning and stability of ecological systems. Scientists generally agree that as the number of species in any particular type of ecological system declines, that system can potentially lose its resilience (i.e., its ability to rebound after it has been stressed (McCann, 2000)). In addition, biological diversity may contribute to quality of life, as the diversity of some species contributes to the diversity of important human commodities (e.g., different tree species for different woods, such as pine, walnut, or hickory, or different fish species for food, such as tuna, red snapper, or catfish). Trends in the types and numbers of species that live within ecological systems and how they interact with each other can be investigated through the analysis, for example, of bird populations, freshwater benthic macroinvertebrate communities, intactness of the native freshwater fish fauna and non-indigenous species.

Ecological systems are sustained by a number of biological, physical, and chemical processes, including primary production (conversion of the sun's energy into organic matter through photosynthesis), and the associated cycling of carbon, nutrients (nitrogen, phosphorus), hydrogen/oxygen, and other elements from the physical environment (air, water, land) through biological organisms and back into the physical environment. Collectively, ecological processes produce organic matter, transfer carbon and nutrients, drive soil formation, and enable organisms to reproduce. They also play an important role in providing ecological services—for example, providing natural resources, such as food, fiber, and timber, and regulating air and water quality. An indicator of quality of ecological processes is, for example, the carbon storage in forest biomass (biological material) is an essential attribute of stable forest ecosystems and a key link in the global carbon cycle.

Physical and chemical attributes influence and sustain ecological systems. They have driven the evolutionary history of species, and they continue to drive ecological processes, shape the conditions in which species live, and govern the very nature of ecological systems. Physical attributes can include temperature, hydrology, and physical habitat, as well as major physical events that reshape ecological systems, such as fires, floods, and windstorms. Chemical attributes can include pH, dissolved oxygen concentrations, and nutrients (e.g., nitrogen and phosphorus). The percentages of acid deposition (e.g., nitrate and sulfate) resulting from air pollution (that can have serious effects on both terrestrial and aquatic ecosystems), nitrogen and phosphorus loads in large rivers (critical nutrients for plants and animals, and terrestrial ecosystems and headwater streams), sea level, sea surface temperature, global mean temperature and precipitation, can be all considered as physical or chemical attributes.

Environmental contaminants, such as chemicals introduced into the environment intentionally (as with fertilizers, pesticides, and herbicides) or unintentionally (through accidental spills or leaks of chemicals used in home and commercial applications), can harm plant and animal communities. At sufficient exposure levels, environmental contaminants can begin to have toxic effects on individuals within animal or plant populations.

When a sufficient number of individuals are affected, contaminant exposure can change the structure and function of ecological systems. Ecological exposure to contaminants is tracked using biomarkers of contaminant exposure. Biomarkers measure either the levels of a contaminant (or its byproducts) in plant or animal tissue or the organism's biological response to the contaminant. Examples include: tissue levels of pesticides, PCBs, and mercury, which have been used for many years to evaluate exposures in the brown pelican, bald eagle, lake trout, and a host of other fish and wildlife species; pathological anomalies in plant or animal tissue, such as damage to plant tissue from ground-level ozone; tumors in fish exposed to sediment contaminated with polycyclic aromatic hydrocarbons.

Human societies, economies and cultures are constitutive parts of the biosphere which transform it both locally and globally. People, economies, societies and cultures depend on the biosphere which shapes them, therefore they both co-evolve. Socio-ecological systems emerge from this interaction in which its components interact and are conditioned in a dynamic and constant way. A central aspect of these interactions involves ecosystem services, that is, the benefits that society obtains from ecosystems, which constitutes the basis of their development and sustainability. The interaction between actors of both subsystems further complicates the matter and increases the vulnerability of the system. In fact, stressors (i.e., factors that perturb the ecosystem) can be both natural (e.g., hurricanes, floods) or human-induced (e.g., toxic chemicals, nutrients, or introduced invasive species). Extent and distribution can be impacted by both natural forces and human activities happening over different time and spatial scales. For example, extent and/or distribution of ecological systems can change over long time periods, such as those associated with climate and geological forces (like the formation of glaciers), or more quickly as a result of human activities such as: direct shifts in land use (for example, filling wetlands or developing a subdivision where a forest used to be); altering hydrological cycles (for example, constructing a dam); exposure to pollutants, such as acid rain, which can acidify lakes and streams and kill certain trees in high elevations; building highways through a forest; developing waterfronts in a manner that splits bordering marshlands apart. Similarly, decreases and increases in biological balance can be results of changing in land use, water management, environmental pollution, and intentional or unintentional introduction of new species into ecosystems. Ecological processes suffer impacts of human activities—including pesticide use, chemical use, waste generation, land use changes, and water quality management, among others—that affect the rates, types, and timing of ecological processes. For instance, many pesticides, chemicals used in industry, pollutants, and waste products can interfere with species reproduction, one of the most important ecological processes. Changes in land use that alter the extent and distribution of ecological systems can directly affect ecological processes in particular areas, often causing associated changes in primary production, nutrient cycling, and erosion and sediment transport. For example, changing forested land to urban or agricultural lands influence the amounts and types of primary producers, the infiltration of water into soils, and the storage and cycling of carbon and nutrients. Factors that alter the critical chemical and physical characteristics of ecological systems include temperature, pH electrochemical (redox) potential, and the transparency of air and water. Activities and events that can alter physical and chemical characteristics include climate change, water contamination, and changes in water runoff, snowpack, ground water, and light regimes.

Environmental degradation (i.e., the deterioration of the environment through depletion of resources such as air, water and soil; the destruction of ecosystems and the extinction of wildlife) may affect frequency and intensity of extreme climate events, such as forest fires, hurricanes, heat waves, floods, droughts, and storms. Also, ecosystems disfunctions and degradation affects the socio-ecological resilience, i.e., the capacity of linked social–ecological systems to absorb recurrent disturbances in order to retain essential structures, processes and relationships. Deforestation and desertification have demonstrable effects on local rainfall patterns and are complicit with the occurrence of drought. Also, ecological conditions affect natural barriers that can moderate the impacts of a disaster and protect communities providing natural defenses against hazards. For instance, wetland ecosystems function as natural sponges that trap and slowly release surface water, rain, snowmelt, groundwater and floodwaters. Dunes and reefs create physical barriers between communities and coastal hazards.

3.1.3. The geo-morphological system

The geo-morphological system of urban areas is relevant given the increasing vulnerability of these areas to various natural hazards, exacerbated by factors such as climate change and urbanization.

The geological makeup of an area – encompassing aspects like soil composition, rock types, and the presence of fault lines – directly influences its susceptibility to hazards. For instance, areas built on soft or loosely packed soils are more vulnerable to seismic activities due to soil liquefaction. Similarly, the presence of certain rock types might predispose a region to higher risks of landslides or erosion.

Cities built in areas with complex geological histories may face unique challenges. For example, urban areas situated near active volcanoes, such as Naples, are not only at higher risk of eruption, but also of landslides or earthquakes. The geological nature of an area can also dictate the availability and quality of groundwater, impacting urban water supply, and influencing land subsidence, which can further exacerbate hazard vulnerability.

In coastal cities, geological factors such as land subsidence and the type of coastal rock or sediment can significantly influence susceptibility to sea-level rise and storm surges. For instance, cities like Venice are sinking due to a combination of factors such as excessive groundwater extraction, exacerbating the risk of flooding, sea level rise, sediment segregation and anthropic wave production.

Geomorphological features like river systems, coastal lines, mountains, and valleys play a significant role in determining a city's vulnerability to natural hazards.

Urban areas in floodplains, for instance, are more susceptible to flooding. The topography of a region, studied under geomorphology, can influence how water accumulates or disperses during heavy rainfall events, which is critical for urban flood management. Similarly, cities located in mountainous or hilly areas need to consider the risk of landslides, especially when land-use changes, such as deforestation or construction, alter the natural landscape.

The coastal geomorphology is vital for understanding and managing risks related to coastal hazards like tsunamis, hurricanes, and coastal erosion. Coastal cities must consider their geomorphological setting to develop effective coastal defense and adaptation strategies.

Integrating geological and geomorphological considerations into urban planning is critical for sustainable and safe urban development. This integration can inform the decision-making process regarding land use, infrastructure development, and disaster mitigation strategies.

For example, geological and geomorphological assessments can guide building codes and construction practices in earthquake-prone areas or inform the design of flood defense systems in areas vulnerable to flooding. They can also aid in identifying safe locations for critical infrastructure like hospitals, power plants, and evacuation routes.

Advancements in technology and data collection have significantly enhanced our ability to understand and apply geological and geomorphological information in urban planning. Geographic Information Systems (GIS), remote sensing, and computer modeling provide valuable tools for mapping hazard-prone areas, simulating hazard impacts, and developing risk reduction strategies. These technologies enable urban planners and decision-makers to make informed decisions based on a comprehensive understanding of the geology and geomorphology of their urban settings.

As climate change alters weather patterns and increases the frequency and severity of certain natural hazards, the importance of understanding urban geology and geomorphology becomes even more pronounced. Rising sea levels, increased rainfall intensity, and more frequent extreme weather events will continue to challenge urban areas. Incorporating geological and geomorphological knowledge into climate change adaptation strategies will be vital for reducing future hazard exposure and enhancing urban resilience.

In the first instance the urban areas can be described through a general scenario that reports the first order geomorphological characteristics as defined in the taxonomy.

Exemplification

Here below the five scenarios proposed in the frame of the tasks are reported:

Scenario 1_climatic, hydraulic, and biological risks Settlement characteristics: Widespread flat settlement located along a dune coast with the presence of a beach and pine forest intersected by canals and a river. Built fabric: Historic center characterized by compact fabric; dense residential fabric of recent expansion adjacent

to transportation infrastructure on a territorial scale. Risks: Climatic risks with phenomena of drought and coastal erosion, hydraulic risks with flood and river flooding events, and biological risks with marine pollution.

Scenario 2_geophysical, hydraulic, climatic, and biological risks Settlement characteristics: Flat inland settlement in a volcanic-origin basin surrounded by hilly reliefs with the presence of cavities used for extraction. Built fabric: Historic center characterized by compact fabric; widespread residential fabric of recent expansion adjacent to transportation infrastructure on a territorial scale. Risks: Geophysical risks of volcanic, seismic, and landslide types, hydraulic risks with the presence of sudden floods, climatic risks with heatwaves and heavy rains, biological risks with atmospheric and soil pollution.

Scenario 3_climatic, biological, and na-tech risks Settlement characteristics: Coastal plain settlement with a beach characterized by an industrial area served by rail infrastructure. Built fabric: Fragmented fabric of recent construction, articulated along urban roads predominantly orthogonal to the coastline. Risks: Climatic risks from coastal erosion, biological risks from marine pollution, and na-tech risks due to the presence of numerous industrial structures in the coastal area.

Scenario 4_geophysical, hydraulic, climatic, and biological risks Settlement characteristics: Historic settlement between a hilly relief with a monumental forest and a densely built false plain. Complex topographic layout with the presence of valleys and underground cavities. Built fabric: Historic center located on a hillside and characterized by compact fabric. Risks: Geophysical risks from landslides, hydraulic risks from sudden floods, climatic risks with heatwaves and heavy rains, biological risks with atmospheric and soil pollution.

Scenario 5_geophysical, hydraulic, climatic, and biological risks Settlement characteristics: Flat inland settlement in a tectonic-origin basin surrounded by mountainous reliefs with the presence of a river. Built fabric: Historic center characterized by compact fabric; widespread residential fabric of recent expansion adjacent to transportation infrastructure on a territorial scale. Risks: Geophysical risks of seismic type with site amplification, liquefaction, soil stability, hydraulic risks with the presence of sudden floods, climatic risks with heatwaves and heavy rains, biological risks with atmospheric and soil pollution.

Taking as example the fifth scenario, we can exemplify those geo-morphological features that expose urban settlements to hazard. In the following paragraph we propose a description of the risk-related factors associated with such setting. The scenario well fits with several urban settlements of the Italian peninsula e.g., particularly with the city of Florence. We therefore adopt this urban settlement as a reference for this exemplification. The city of Florence is strongly interdigitated with the cities of Prato and Pistoia and is located in a tectonic basin (called, using a geological term, a "semi-graben"; Neuendorf, 2005) bordered on the northern side by tectonic (normal) faults. Furthermore, the basin, and so the city of Florence, is cut through by the Arno river and its tributaries. Additionally, the Florence basin is a large productive district, hosting key infrastructures and cultural tourism. All these above mentioned aspects bear a strong link with the geo-morphological sphere. The geology of the Florence urban settlement (Figure 16a) is in fact characterized by the presence of Quaternary tectonic boundary faults (associated with secondary transversal faults) potentially capable of rising seismic hazard. The exposure to such risk is therefore high. The presence of the Arno river exposes the city to high flood risk (as testified by historical record, e.g., the 1966 flood; e.g., Coli et al., 2013). Despite the city being located in the basin, the presence of boundary scarps associated with the faults imply the possibility of landslide risk (Morelli et al., 2021). Due to its morphology and conformation, the basin is subject to climatic risk (primarily associated with heat-waves; Morabito et al., 2012). Furthermore, being Florence a large productive district, this makes the urban settlement exposed to biological risk associated with contaminants and air pollution (Palli et al., 2008). As testified by this example, the correct characterization of the urban area in the frame of its geo-morphological settlement is key for the correct quantification of multi-risk exposure. In this frame, a further tool enhancing this characterization that can constitute the first step to build a digital twin is a 3D digital model of the subsurface (Figure 16b). Such model may not only provide a clear picture of the subsurface but may also help to highlight the relationships with the surface elements exposed to multi-risk.

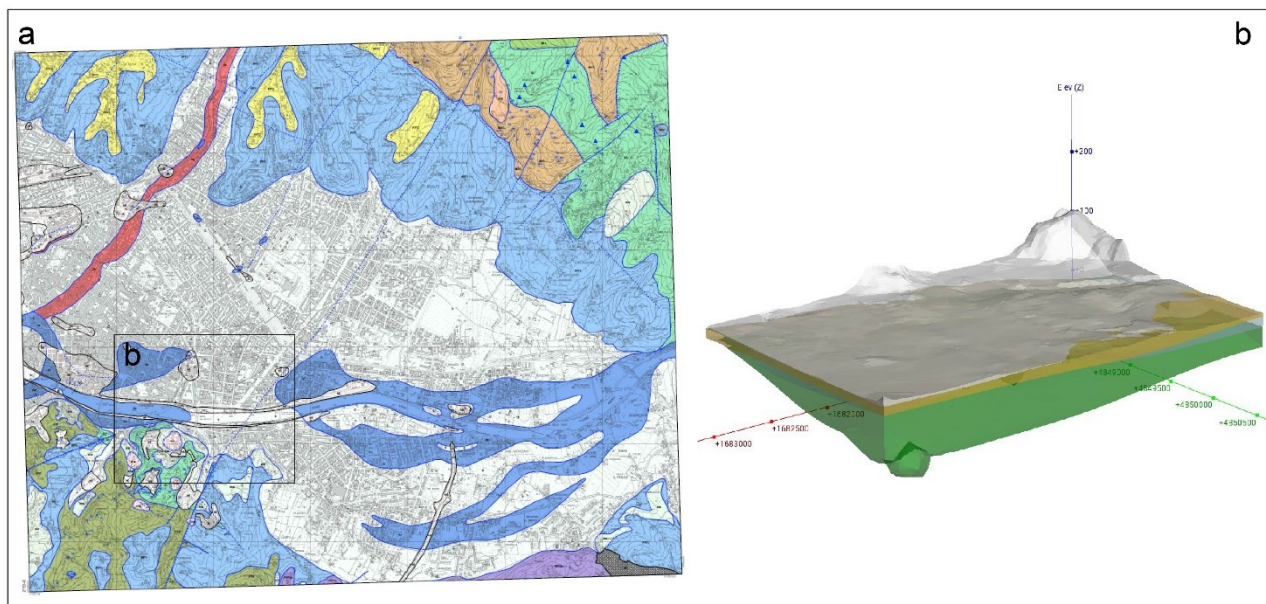


Figure 16. a) The Florence urban settlement as depicted in the 1:10.000 Tuscany geological map (CARG 1:10.000 section n. 275040). The city of Florence well fits with the hypothetical urban settlement proposed in the Scenario n. 5. b) An example of 3D geo-model produced for a portion of the Florence urban area. The 3D model highlights the subsurface stratigraphy and structural setting.

3.1.4. Settlement models

In the process of morphological reading, the representation of the physical and functional layout of urban and rural settlements can be entrusted to settlement systems, constituted as a set of urban areas, territorial endowments, living and production spaces capable of ensuring urban and ecological quality to the inhabited areas. Leaning on structuring factors such as "elements of a hydro geomorphological [...] or infrastructural nature, which are recognized as having a fundamental morphogenetic role that has influenced settlement morphologies", settlement systems are defined in their consistency, uses, functionality, methods of implementation of interventions and governance policies by territorial and urban planning.

For the identification of settlement contexts, the characterizing conditions (urban fabrics, road layouts, geomorphologic conditions, natural limits, critical infrastructures, green systems, etc.) that may be relevant for the assessment of the impacts of possible hazards should be considered, since they present different conditions of response to them according to their characteristics and, therefore, exposure. In relation to multi-hazard conditions - varying from time to time - urban hotspots can be identified in which the consequences (the effects) of the combination of vulnerability, exposure and hazard are condensed as transition factors from risk conditions to impacts.

The study of the layout plan of a settlement is the first aspect to investigate in this type of approach. In this regard, three categories of ancient layouts can be distinguished, deriving from construction canons and models that have inspired city constructions, guiding urban planners in development and renewal: **the grid, the radial plan, and the linear structure.**

The **grid** or **checkerboard pattern** (Figure 17a) involves the creation of road axes (main and secondary) intersecting at right angles to form blocks that take the shape of squares or rectangles. In Europe, the systematization of this type is attributed to the Greek architect and urban planner Hippodamus of Miletus, who recommended its application in the construction of newly founded colonies. Additionally, its frequent implementation is also attributed to the typical model of the Roman castrum, the encampment of Roman legions, ideally of a quadrangular shape cut by two main axes: the *cardo*, in the north-south direction, and the *decumanus*, in the east-west direction. The two axes divided the castrum into four quarters, further subdivided into smaller lots. In the United States, the grid pattern is the basic rule for urban planning, and in Italy, it is found in the historic centers of many Greco-Roman-founded cities, such as Naples, Turin, Aosta, and Castelfranco Veneto.

The **radial plan** (Figure 17b), with diverging roads radiating from a central nucleus, is the result of a typical urban evolution in medieval Europe. In Dutch cities like Amsterdam and Haarlem, the radial pattern is still clearly visible, characterized by a central square surrounded by concentric canals, where each expansion of the city implies a new circle of walls and canals. Milan is also an example of a city with a radio-centric plan. In this case, the settlement system is characterized by a series of main roads branching out in various directions from a central inhabited core. This core tends to expand progressively along the axes and concentric circles, often accompanied by walls or canals in the past and now marked by large ring roads.

The **linear plan city model** (Figure 17c) is characteristic of cities that develop along a generating axis, with transverse roads intersecting it. This type of city typically develops along a road and takes on a narrow and long shape. The concept was conceived by the Spanish Soria at the end of the 19th century with the Ciudad Lineal, a settlement of defined width built on a central axis whose length could be potentially unlimited. The same happens in many coastal urban centers, especially if surrounded in the rear by elevations. The inhabited center of Genoa, for example, can only expand mainly along the coast and, as long as possible, on the elevations, taking on a fan shape.

The three layout patterns of grid, linear, and radial (see Figure 17) can give rise to other families of similar settlements. For example, Greek-Roman layouts, 19th-century fabrics, agricultural layouts and layouts from the second half of the 20th century belong to the grid category; ridge, matrix road and coastal road settlements belong to the linear category; foundation settlements and 19th-century neighbourhoods belong to the radial category.

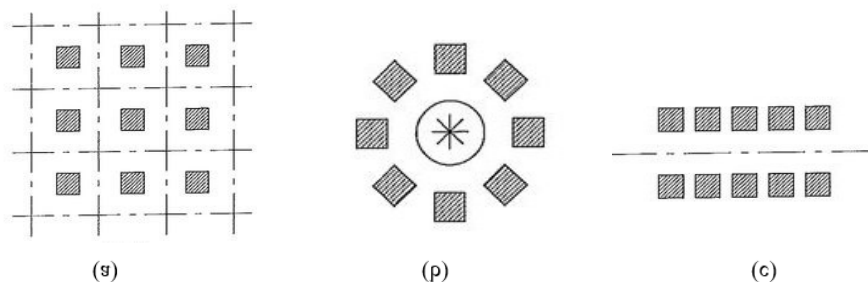


Figure 17. Grid pattern (a), radial plan (b) and linear plan city model (c).

3.1.4.1. Combination of layout patterns and morphological variations of settlements

The three layout patterns described above are neither unique nor exclusive. In fact, most cities have varied plans, depending on different interventions that have overlapped over time, also in relation to morphological and geographical dynamics affecting the tectonic support in which they root.

The study of the settlement nature approximately reveals this process of urban development adaptation to **morphological variations** of the territory and **combinations of grid, radial, and linear layout patterns**. The latter derive from conditions that have tended to arise recently because of expansion processes: the intersection between linear systems – which can rely on different linear structuring factors – determines densified nodes at the welding points, sometimes recognizable for the settlement of specialized functions. The intersection between concentrated systems generally takes place along the outgoing axes, determining a band of lower density and structuring than the original concentrated systems and, negatively, free areas undergoing erosion and interclusion. The intersection between a concentrated system and one or more linear systems, finally, causes the linear system to assume a role of urban gate compared to the concentrated system, which thus becomes "second plan" compared to the surrounding territory.

The assumption is that a settlement system is always a complex system, the outcome of settlement and transformative processes, of which it is possible to recognize **parameters of affinity and differentiation** that allow for a more complete understanding. Affinity parameters refer to the three layout patterns of the settlement system measurable through some structuring factors such as density, size, and proportion. On the other hand, differentiation parameters refer to changing factors that influence the transformations of the settlement system,

namely morphological variations related to the orographic (geomorphological) and natural systems and combinations of layout patterns.

Through the "comparative orthophotos" reported in Figure 18 it is possible to apply this interpretation to real cases, starting from the identification of basic patterns and subsequent tracing of their variations.

The selected and collected orthophoto represented in the abacus are then composed and assembled in urban contexts representing their contemporary reality.

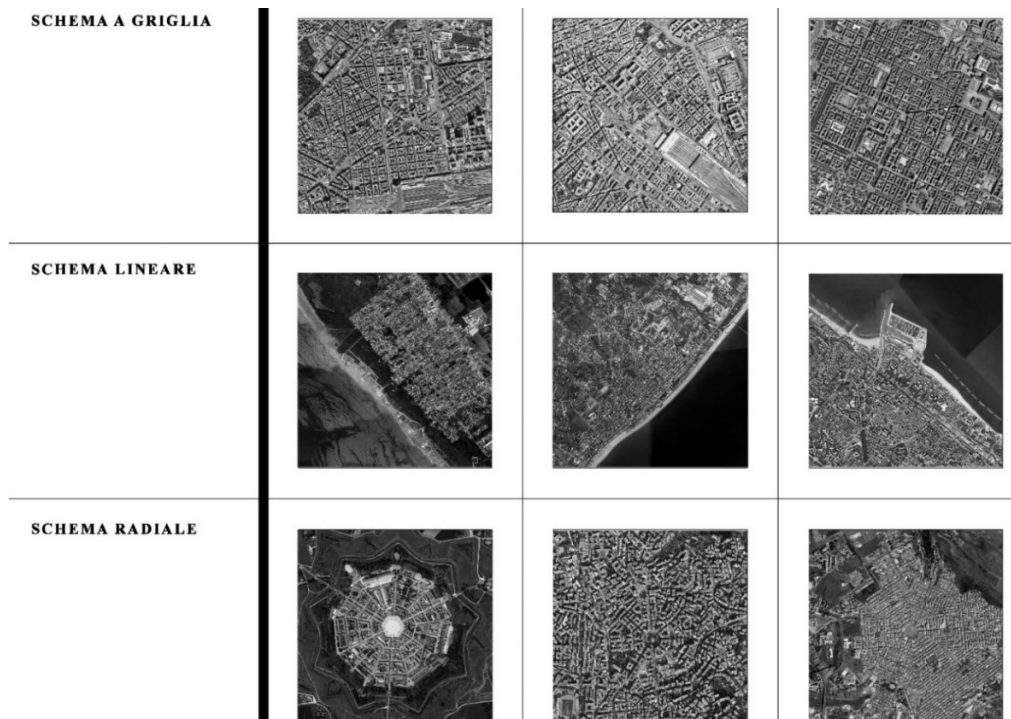


Figure 18. Real cases approach to identify basic patterns and subsequent tracing of their variations in urban context.

3.2. Characterization of urban settlements: typo-morphological, environmental and spatial-functional analysis

The knowledge and description of urban and metropolitan settlements in relation to specific multi-hazard conditions contributes to the identification of "critical contexts" and "hotspot areas", characterized by the concentration or overlap of risks and impacts, for which the application of countermeasures (adaptation strategies and actions, to reduce vulnerability and exposure, and increase resilience) is a priority.

With reference to (Bologna et al., 2021), the size of the contexts that can be studied with reference to their critical conditions with respect to risks corresponds with the definition of "urban districts", territorial areas possessing between 20,000 and 60,000 inhabitants (Figure 19: Example of identification of urban districts).

Starting from the premises given in Sections 4.1.5 and 5.1.5, critical contexts are representative of conditions that occur within the contemporary urban reality and, from the point of view of system characterization, present a settlement complexity given by the juxtaposition of the previously described settlements models and variations related to the morphology of territories.



Figure 19. Example of identifying of urban districts.

From the point of view of interpretive reading, these areas are described through the analysis of three main systems selected as capable of synthesizing *type-morphological, environmental and spatial-functional* issues and which can be considered as *identifying criteria and factors of homogeneity precisely of critical contexts*:

- the *orographic system* describes the characteristics, articulation and distribution of land reliefs and depressions, both surface and submarine ones. Orography substantially determines the consistency and influence of certain weathering agents such as winds, for example, and influences the choice of settlement principles for the development of urban systems. The two-dimensional representation of the orographic system is entrusted to contour lines, continuous curved lines joining points topographically located at the same elevation, that is, at equal vertical distance from a horizontal reference plane to which zero elevation has been assigned (Figure 37, top-left: orographic system).

Soil consistency, i.e., the geo-morphological characteristics described in Section 3.1.3, together with the specificities of the orographic system contribute to determining the presence of geo-physical and hydro-geological risk factors in certain territorial areas that can be selected and defined as critical in relation to these parameters.

- *natural system* is understood here as the combination of the categories of physically identifiable elements that make up the natural environment such as, for example, forests, beaches, seas, lakes, rivers, and in general those related to, for example, water resources, land use, and biodiversity. Also included in this system are man-made elements such as monumental forests and gardens, botanical gardens, reclamation canals, and reservoirs, to name a few. In the representation of this system, green and blue are chosen as reference color fields that recall the most shared perceptual modes related to water and vegetation (see Figure 37 – bottom-left: natural system).

In light of the current environmental crisis, the presence of these elements is an indication of richness ecosystem and is a parameter for the measurement of alterations or permanences that affect exacerbating or mitigating different types of risk such as, for example, hydro-geological, climatic and anthropogenic.

- the *settlement system* synthesizes the components related to the built fabric and the routes intended for the road system with respect to the system conditions that connote its contemporary configuration from the combination of the settlement models identified as the origin of the settlements and the variations imposed by the orographic and natural systems.

The representation of the settlement system is entrusted to surfaces that correspond to the extent of the fabrics and to lines that recall the course of the tracks. Variations in the fabrics and tracks are expressed through monochromatic diversifications: for the built fabric, the type and density of the pattern describe the density and orientation of the built-up area; for the tracks, the thickness of the lines identifies the functional classification, while the type of line clarifies whether it is a road or a railroad, for example (see Figure 20 – top-right: settlement system).

The characteristics of settlements, in terms of, for example, their positioning, arrangement, orientation, functions and density, also in relation to the characters of the orographic and natural systems with which they relate, contribute to the determination of anthropogenic risk factors, as well as to the increase or mitigation of hydro-geological and climatic risk factors, to name but a few.

Having identified the **prevailing characteristics** of the systems selected, additional specific factors such as, for example, density, in both physical and social terms, fabric and path orientation, and functional domains, also intervene in the analysis of critical contexts, which have a relevant influence on multi-hazard assessments, but represent the precise specification of a "case-by-case" investigation that will be further explored in the next phase of research activities.

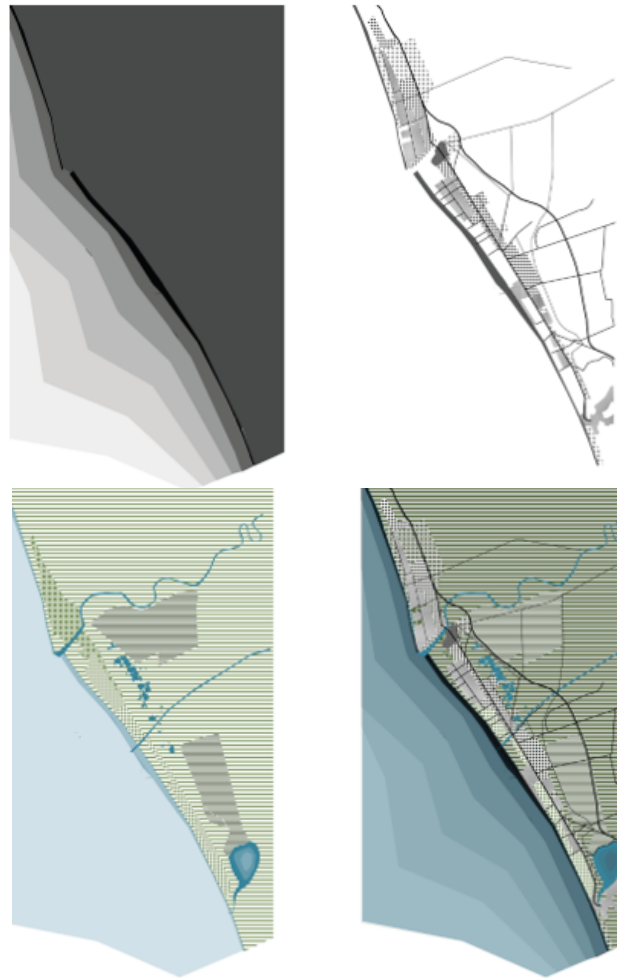


Figure 20. Example of reading by homogeneous criteria and identifying systems for a typical critical context (top left: orographic system; top right: settlement system; bottom left: natural system, bottom right: complex system)

An initial selection of contexts led to the identification of four pilot cases, from which it will be possible to identify additional areas for further investigation.

Context 1_weather-climate, hydraulic and biological hazards.

Diffuse flat settlement located along a dune coast in the presence of sandy shoreline and pine forest furrowed by canals and river.

Historic center characterized by compact fabric; dense residential fabric of recent expansion on highway.

Presence of meteo-climatic hazards with dry weather and coastal erosion phenomena, hydraulic hazards with river flooding and overflow events, and biological hazards with marine pollution phenomena.

Context 2_geophysical, hydraulic, meteo-climatic and biological hazards.

Flat inland settlement in basin of volcanic origin sandwiched between hilly reliefs with presence of cavities for mining use.

Historic center characterized by compact fabric; widespread residential fabric of recent expansion on provincial road.

Presence of volcanic, seismic and landslide geophysical hazards, hydraulic hazards with presence of flash floods, weather-climate hazards with heat waves and heavy rains, biological hazards with air and soil pollution.

Context 3_weather-climate, biological and na-tech hazards.

Coastal plain settlement with sandy shore characterized by industrial area served by railroad tracks.

Fragmented fabric of recent construction articulated along urban roads with predominantly orthogonal to the coast.

Presence of weather-climatic hazards from coastal erosion, biological hazards from marine pollution, and natech hazards due to the presence of numerous industrial artifacts in coastal area.

Context 4_ geophysical, hydraulic, meteo-climatic and biological risks.

Historic settlement sandwiched between a hill relief with monumental forest and a densely built-up falsopiano.

Complex topographic trend with presence of valleys and underground cavities.

Historic center arranged on hillside and characterized by compact fabric.

Presence of geophysical hazards from landslides, hydraulic hazards from flash floods, weather-climatic hazards with heat waves and heavy rains, biological hazards with air and soil pollution.

3.3. Identification of recurring urban patterns of buildings and open spaces

The proposed experimental methodological approach was developed as an advancement of the PLANNER (PLANNER-Piattaforma per LA GestioNe dei rischi Naturali in ambiEnti uRbanizzati”, POR CAMPANIA FESR 2014/2020) research project (D'Ambrosio et al., 2023). The framework was initially implemented to analyse the outdoor/indoor microclimatic behaviour and buildings CO₂ emission reduction but it can be also useful to recognise the urban patters of building and open spaces to support a risk-oriented knowledge of urban systems. The objective set as the assumption of the research is the definition of methodologies capable of describing the performance behaviour of residential buildings and open spaces over the entire national territory, in terms of response to climatic and microclimatic stimuli related to the increase in urban temperatures, with reference to medium-term climate projections, as a consequence of the ongoing climate change.

To achieve this objective, methodological approaches were developed through the construction of a complex knowledge apparatus (normative, bibliographic and best practice references), the use of GIS-based tools, parametric software and dedicated tools, as well as data exchange processes, in order to allow the development of a classification of the two physical subsystems - residential buildings and open spaces - capable of describing their energy and performance behaviour in different climatic conditions.

3.3.1. Buildings

In order to classify the physical subsystem relating to residential buildings, basic building typologies recurring on a national scale were first identified. The categories chosen constitute a non-exhaustive, but representative selection of the most frequent cases detectable in urban areas. The recurring residential building typologies were defined on the basis of the literature (Corrado et al., 2014; Aymonino, 1977; Caniggia and Maffei, 1979): they refer to four categories - detached house one/two-family, in-line building, block building and tower building - to which are associated specific dimensional characteristics (surface area, number of floors, total height and Window-to-wall ratio) as shown in Figure 21.





Building typologies	Surface area (sqm)	Number of floors	Height (m)	Window-to-wall ratio (WWR)
 Detached house one/two family	100/floor	2	8	0,12
 In-line building	400/floor	4	16	0,12
 Block building	600/floor	6	24	0,12
 Tower building	300/floor	12	48	0,12

Figure 21. Recurring building typologies in urban fabrics and their dimensional characteristics.

The intersection and comparison of the data obtained from literature and current Italian legislation has allowed the identification of the construction techniques most used in the Italian context. In particular:

- the UNI/TR 11552 standard 'Abacus of structures constituting the opaque envelope of buildings. Thermophysical parameters' (Ente Nazionale di Normazione, 2014) provided an abacus of the envelopes most commonly used in existing buildings and their main thermophysical parameters;
- the 'Sample Vulnerability Census of Current Buildings' (Department of Civil Protection, 2000) provided information on the main building techniques present in specific Italian regions;
- the 'TABULA' project (*Typology Approach for BUiLding stock energy Assessment*) and the 'EPISCOPE' project (*Energy Performance Indicator Tracking Schemes for the Continuous Optimisation for Refurbishment Processes in European Housing Stocks*) (Corrado et al., 2014) provided a reference with respect to the most widespread residential building typologies in Europe and at national level.

The catalogue of commonly used techniques thus developed is consisting of eighteen commonly used construction techniques: 8 types of vertical opaque closures; 7 types of horizontal opaque closures; 3 types of vertical transparent closures. The related thermophysical parameters, such as transmittance, phase shift and attenuation, were determined with the help of a simulation software validated by the Italian Thermotechnical Committee (see Figure 22).

MPI02 – Stone wall					
Layer	d (cm)	ρ (kg/m ³)	c (J/(kg K))	λ (W/mK)	R (m ² K/W)
1 - Interior plaster	2	1400	1000	0,700	-
2 - Bricks and stones	40 - 100	2500	1000	2,400	-
3 - Exterior plaster	2	1800	1000	0,900	-
U _m = 2 W/m ² K			Construction period = until 1945		

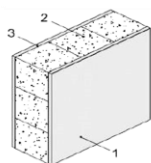


Figure 22. Stone wall”, example data sheet of the prevailing construction technique catalogue.

Moreover, the most widespread construction periods have been classified considering the entry into force of restrictive requirements on energy efficiency of buildings in the Italian national legislation, the main historical events that have occurred in Italy that have caused changes in the world of building production and, finally the periods identified by the National Institute of Statistics (ISTAT) in the Permanent population and housing census.

The classification of the construction periods is as follows:



- until 1945: period from the beginning of the 20th century to the period between the two world wars;
- from 1946 to 1975: phase of the Reconstruction and the economic boom in Italy;
- from 1976 to 1990: first Italian legislative provisions on the energy efficiency of buildings;
- from 1991 onwards: restrictive requirements on energy performance for new buildings.

The construction techniques identified were correlated to the four recurring building typologies in urban fabrics; each recurring building type has been characterized in each of the four periods with specific commonly used construction techniques (the only exception is the Tower building, not present in Italy before 1945). In Figure 23 is shown the classification of prevailing construction techniques with respect to building typologies.





Building typologies	Construction period	Wall Code	Roof Code	Floor Code	Windows Code
 Detached house one/two family 100 sqm/floor 2 floors WWR = 0,12	Until 1945	MPI02	CIN05	SOL13	IVS01
	From 1945 to 1975	MIP01	CIN04	SOL13	IVS01
	From 1976 to 1990	MCV01	COP03	SOL03	IDA01
	From 1991 onwards	MCV02	COP03	SOL03	IDG01
 In-line building 400 sqm/floor 4 floors WWR = 0,12	Until 1945	MPI02	CIN05	SOL13	IVS01
	From 1945 to 1975	MIP01	COP01	SOL13	IVS01
	From 1976 to 1990	MCV02	COP03	SOL03	IDA01
	From 1991 onwards	MPF03	COP03	SOL03	IDG01
 Block building 600 sqm/floor 6 floors WWR = 0,12	Until 1945	MPI02	CIN05	SOL13	IVS01
	From 1945 to 1975	MIP01	CIN04	SOL13	IVS01
	From 1976 to 1990	MCV02	COP03	SOL03	IDA01
	From 1991 onwards	MPF03	COP03	SOL03	IDG01
 Tower building 300 sqm/floor 12 floors WWR = 0,12	Until 1945	-	-	-	-
	From 1945 to 1975	MCO03	COP03	SOL13	IVS01
	From 1976 to 1990	MCV02	COP03	SOL03	IDA01
	From 1991 onwards	MPF03	COP03	SOL03	IDG01

Figure 23. Classification of prevailing construction techniques according to the different building typologies identified.

A GIS-based classification method was thus applied to detect the prevailing building typology and prevalent construction periods in census areas. The framework was implemented on a GIS platform and tested on the urban fabric of the municipality of Naples. The reasons for choosing this urban fabric are the complexity and diversity of the urban forms that characterise it. In fact, the city of Naples represents a dense urban fabric characterised by different urban settings, ranging from historical consolidated urban areas to recently built-up settlement fabrics. For each of the recurring building typologies, the value ranges of its prevailing characteristics were defined: Surface area, Height and Shape index. They are shown in Figure 24.



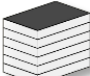

Building typologies	Surface area (sqm)	Height (m)	Shape Index
 Detached house one/two family	≥ 75 and < 250	$\geq 3,5$ and < 9	$\geq 0,030$
 In-line building	≥ 75	≥ 9 and < 36	$\geq 0,010$
 Block building	≥ 300 and < 1500	≥ 9 and < 36	$\geq 0,020$ and $< 0,055$
 Tower building	≥ 250	≥ 36	$\geq 0,010$

Figure 24. Parameters for the identification of recurring residential building typologies.

In order to assign the prevailing building typology to each residential census area, the polygonal vector thematism of the buildings included in the topographic database was used; the DTM and DSM rasters were used for the assessment of building heights and volumes. The shape index of each building was estimated by calculating the ratio between the surface area and the square of the building perimeter. This value varies in a range between 0 and 1; the closer it is to 1, the more regular the shape of the building; conversely, the closer it is to 0, the more irregular the shape of the building. Each census area is classified with the most prevalent building typology among those to which the buildings located in it are assigned. Census areas in which there is no specific prevalence of one or two building types have been labelled 'Not identifiable' as they are not assigned to a specific building type. 'Mixed' is used to classify those census areas where there is more than one prevalent building type. Figure 25 shows the thematic map with the distribution of prevailing building types by census areas. Empty census zones are non-residential census zones with no buildings, which are excluded from the classification.

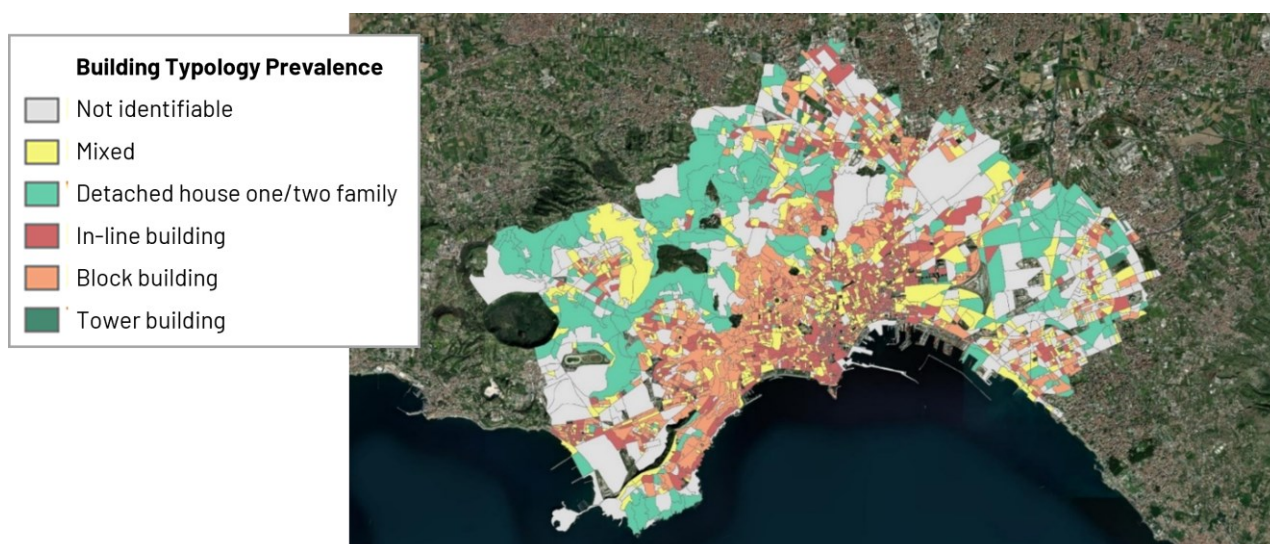


Figure 25. Thematic map of prevailing building typology by census area.

In order to assign to each census area the prevalent construction period of the buildings located in it, a breakdown of the construction period was made into four epochs (Until 1945, From 1946 to 1980, From 1981 to 1990, From 1991 onwards) by grouping the construction periods according to the entry into force of restrictive requirements on the energy efficiency of buildings in Italian legislation and the main periods of change in the world of building production in Italy. The census area was assigned the construction period of the majority of the buildings located in it. A further class of construction period labelled 'Mixed' has been

added to the census areas in which there is no prevalence of buildings constructed in the same period. Figure 26 shows the thematic map of the prevailing construction periods per census area.

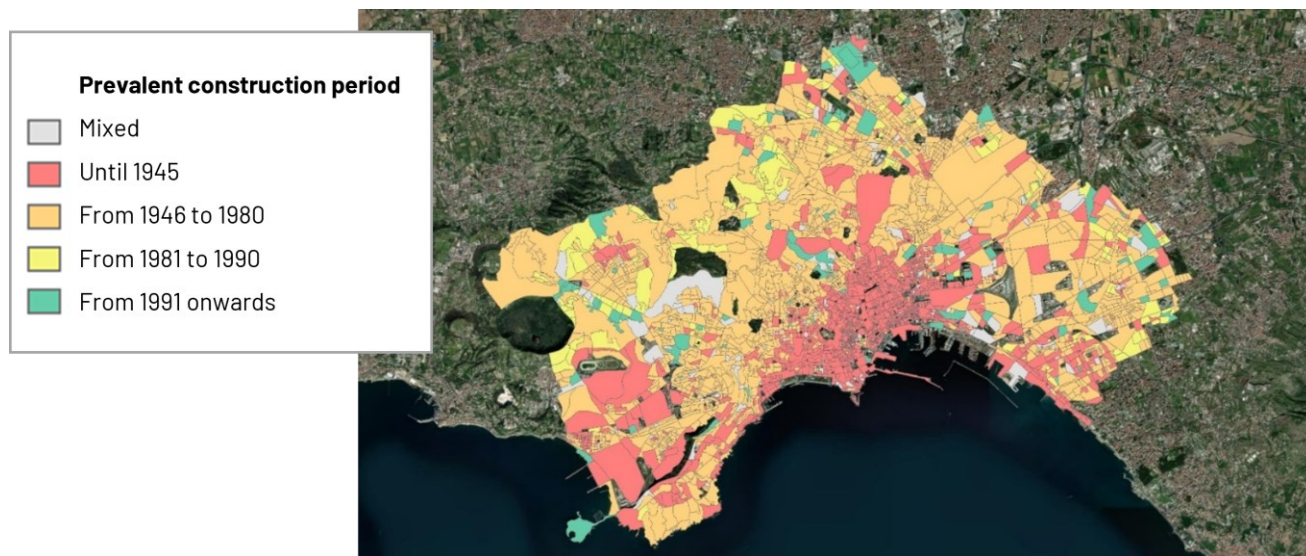


Figure 26. Distribution of prevalent building construction periods recorded with respect to census areas.

The recurring building typologies thus classified were used in PLANNER Research as a starting point to simulate pre- and post-intervention energy requirements and CO₂ emissions and indoor comfort conditions also with reference to medium-term climate projections (D'Ambrosio et al., 2023).

The framework proposed in this paragraph has been realised for its application to Italian urban settlements. As a demonstrative example, its application to the case of Naples is reported.

3.3.2. Open spaces

A classification of the physical subsystem of outdoor spaces was developed through the identification of recurring types of urban forms. This classification aims to identify the critical aspect of outdoor spaces with respect to heat wave impacts in urban settlements and the potential effectiveness resulting from the use of climate adaptive design solutions (Bassolino et al., 2021).

The first phase of this process involved defining generic urban forms capable of enabling an easy measurement of the microclimatic behaviour and performance of open spaces. It aimed to describe the interactions between these spaces, the environmental components and the elements constituting the urban environment. Realizing a definition for recurring urban forms of outdoor spaces relies on the premise of engaging in an abstraction process. In this process, canonical models of urban forms aggregations should be able to delineate the outdoor spaces within cities and describe the microclimatic environmental behaviour that ensues.

The classification process was based on the studies carried out by C. Ratti, D. Raydan, K. Steemers in 2003 in the publication "Building form and environmental performance: archetypes, analysis and an arid climate (Energy and Buildings, n. 35, Elsevier Science)", from which emerges the demonstration of how different urban geometries determine different effects on the built environment. In fact, six simplified urban forms are considered, which were identified by L. Martin, L. March in 1972 in "Urban spaces and Structures (Cambridge University Press, UK)", based in turn on archetypes of building forms, describing the effects they have in relation to energy and environmental behaviour.

In order to restrict the complexity of urban patterns that characterize the urban and metropolitan settlements and to analyse and consequently compare the environmental impact on the different types of geometry and urban morphology among the increase in urban temperatures and the phenomenon of heatwaves. In this classification (see figure 27), the idea is to utilize urban pattern that take into account the archetypes of urban configurations. The goal is to construct geometric models that are representative of different various urban morphologies based on dimensional ratios commonly described and presented within the selected

representative cities (chosen at the beginning of the research project as the different test bed of the different climate conditions through Italy).

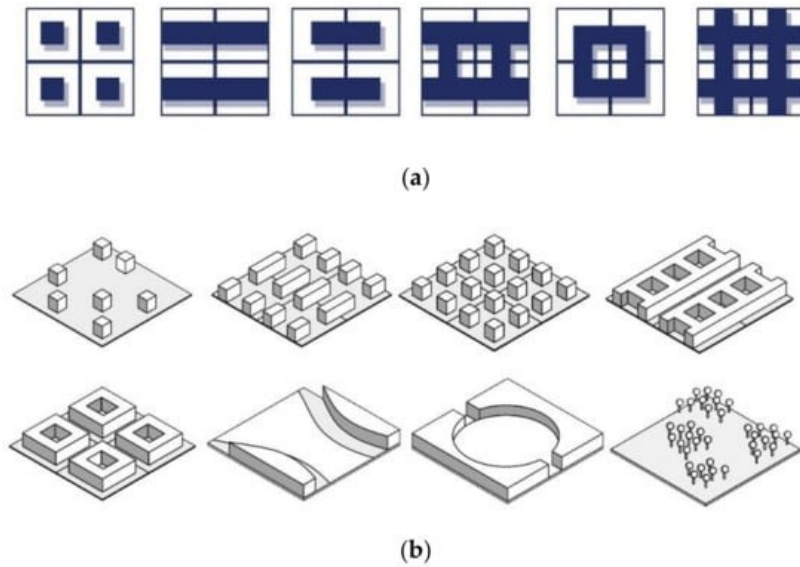


Figure 27. Generic urban patterns: (a) from right to left: pavilions, slabs, terraces, terrace-courts, pavilion-courts and courts; (b) deduced generic urban patterns for Italian cities (Source: Bassolino et al., 2021; Verde et al., 2021).

The definition of urban pattern was, then, made on the basis of scientific literature, from reading of recurring urban morphologies detected with satellite data within the reference cities for the climate macroregions defined by the PNACC. Based on these assessments, it was possible to define a catalogue of typed urban patterns aimed at describing the microclimatic behaviour of outdoor spaces in urban settlements (Verde et al., 2021). The definition of urban pattern has been carried out first of all by making a first typological classification of the spaces:

- Urban patterns;
- Squares and open spaces;
- Green areas.

A subclassification has been defined for each category. Urban patterns are divided according to the different types of aggregation of buildings such as:

- Terrace-courts;
- Pavilion-courts;
- Terraces;
- Pavilion/towers;
- Sprawl-pavilion.

As discriminants for their classification the following were considered:

- The distance between buildings;
- The buildings height.

The further classification was carried out through:

- The building density (cum/sqm);
- The territorial coverage ratio.

This procedure leads to the definition of a sub-classification:

- High-density patterns;
- Medium-density patterns;
- Low-density patterns.

A different classification was made for the squares and the open spaces, for which the following were taken into account as classification factors:

- The buildings perimeter percentage (BPP);
- The buildings height (m).

Finally, a classification for green areas was necessarily adopted to highlight the different characteristics as eco-systemic value with a dual classification. First, these were classified according to the percentage of tree cover and the type:

- Agricultural green;
- Uncultivated green;
- Urban green;
- Wooded areas.

Subsequently, a subdivision was made which classified the green areas according to the tree cover percentage (TCP) into:

- Medium green areas ($0 < TCP \leq 25\%$; $25\% < TCP \leq 50\%$; $TCP > 50\%$);
- Green areas ($TCP \geq 90\%$).

During the second stage, an indicator system that could characterise and parameterize comparable geometric and urban morphological features was chosen, further structuring the classification process. The chosen indicators, drawn from those employed within the GIS process for determining the climate and exposure vulnerability model in the PLANNER research, include:

- the ratio of built surface to open spaces;
- the average building height;
- the sky view factor;
- the hillshade.

The classification is reported in Figure 28.

class	typical urban forms	distance between buildings [m]	buildings height [m]	building density [mc/mq]	territorial coverage ratio
high density urban patterns	terrace-courts	≤ 3.5	> 12	2.61	0.36
		> 3.5	> 12	3	0.36
	pavilion-courts	≤ 7	> 12	2.36	0.47
		> 7	> 12	2	0.4
	terraces	≤ 7	> 12	0.96	0.37
		> 7	> 12	0.64	0.33
medium density urban pattern	terraces	≤ 7	≤ 12	0.55	0.37
		> 7	≤ 12	0.6	0.33
	pavilions/towers	≤ 7	≤ 12	0.17	0.23
		≤ 7	> 12	0.29	0.23
		> 7	≤ 12	0.17	0.23
		> 7	> 12	0.29	0.23
low density urban pattern	sprawl-pavilions	> 7	> 6	0.06	0.04

(a)

(b)

class	typical urban forms	distance between buildings [m]	height of buildings [m]	built perimeter's percentage [%]	class	typical urban forms	category	tree cover percentage
squares and open spaces	squares 	> 50.7	< 6	50% < BPP < 75% 75% < BPP < 90% BPP > 90%	medium green areas and green areas	green areas 	agricultural	TCP ≤ 25% 25% < TCP ≤ 50% TCP > 50%
			> 6; < 12	50% < BPP < 75% 75% < BPP < 90% BPP > 90%				
			> 12	50% < BPP < 75% 75% < BPP < 90% BPP > 90%				
	open spaces 	< 50.7	< 6	0% < BPP < 25% 25% < BPP < 40% BPP > 40%		green areas 	uncultivated	TCP < 25% 25% < TCP < 50% TCP > 50%
			> 6; < 12	0% < BPP < 25% 25% < BPP < 40% BPP > 40%				
			> 12 m	0% < BPP < 25% 25% < BPP < 40% BPP > 40%				
	open spaces 	< 50.7	< 6	0% < BPP < 25% 25% < BPP < 40% BPP > 40%		green areas 	urban green	TCP < 25% 25% < TCP < 50% TCP > 50%
			> 6; < 12	0% < BPP < 25% 25% < BPP < 40% BPP > 40%				
			> 12 m	0% < BPP < 25% 25% < BPP < 40% BPP > 40%				
	open spaces 	< 50.7	< 6	0% < BPP < 25% 25% < BPP < 40% BPP > 40%		green areas 	wooded areas	TCP ≥ 90%
			> 6; < 12	0% < BPP < 25% 25% < BPP < 40% BPP > 40%				
			> 12 m	0% < BPP < 25% 25% < BPP < 40% BPP > 40%				

Figure 28. Classification of urban patterns: (a) high-density urban patterns; (b) medium and low-density urban patterns; (c) squares and open spaces; (d) medium green areas and green areas (Source: Bassolino et al., 2021; Verde et al., 2021)..

Afterwards, a data exchange process was carried out to compare the environmental and microclimatic performance between real urban forms of the reference cities and the typified recurring urban forms. This was done by running testing and verifying through data exchange between GIS-based tools and parametric design tools and testing the process on the city of Naples (Bassolino and Verde, 2023).

In order to achieve homogenous outputs amongst the various ICT tools in accordance with the system of indicators, a process of comparison, simulation, and data interchange between GIS-based tools and parametric tools in the Grasshopper environment was carried out.

This involved categorizing segments of actual urban patterns in the city of Naples, classified according to diverse characteristics capable of capturing the existing morphological diversity (e.g., roadway width, distance between buildings, average building height, type of aggregation, presence of open spaces or green areas). These real patterns were then matched with generated recurrent urban patterns, and corresponding values for the selected indicators of urban morphology were identified.

Urban patterns, both real and recurrent, have been enclosed within a dial sized 100 × 100 m, also to effectively size the models of typical urban patterns and to easily carry out simulation operations.

To compare the performance behavior between actual urban fabrics and standardized models of urban patterns, the initial step involved identifying the values of urban morphology indicators for representative sections identified within the city of Naples. This was accomplished through the GIS model developed for calculating vulnerability to heatwave events. Subsequently, this process occurred first based on the three-dimensional reconstruction of real city models using information within the GIS, and then based on geometric models of standardized urban patterns. Next, using the parametric platform Grasshopper within the McNeel Rhinoceros software and the LadyBug plug-in, corresponding values of urban morphology indicators were computed. This replicated the calculation processes carried out in the GIS environment through the definition of generative algorithms. The indicator values obtained through parametric design software were initially compared with those obtained in the GIS model for the city of Naples. Following that, assessments were conducted by comparing the values derived from the three-dimensional "real" model with those from the "parametric" three-dimensional model, with a maximum allowable margin of error set at 35%. The resulting data underwent thorough verification and were confirmed as valid (see Figure 29).



















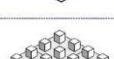



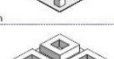


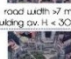
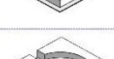



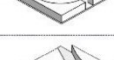






climatic macro-regions	urban patterns	typical urban forms	GIS data output	real urban condition 3D model	3D model data output	accuracy error GIS/3D data output	parametric 3D model	parametric 3D model data output	accuracy error 3D/parametric 3D data output	
2 PADANA PLAIN, HIGH ADRIATIC SIDE AND COASTAL AREAS OF SOUTHERN CENTRAL OF ITALY reference city: NAPLES 	 road width < 3.5 m 0 m < building av. H < 15 m		full-empty ratio 31 average height 10 m sky view factor 733 hillshade 133		full-empty ratio 3661 average height 10 m sky view factor 731 hillshade 102	full-empty ratio 231 average height 01 sky view factor 01 hillshade 201		full-empty ratio 3661 average height 10 m sky view factor 696 hillshade 20	full-empty ratio 01 average height 01 sky view factor 191 hillshade 151	
	 3.5m < road width < 7 m building av. H < 6 m		full-empty ratio 61 average height 3 m sky view factor 734 hillshade 136		full-empty ratio 6781 average height 3 m sky view factor 977 hillshade 123	full-empty ratio 121 average height 01 sky view factor 251 hillshade 121		full-empty ratio 3661 average height 3 m sky view factor 90 hillshade 12394	full-empty ratio 01 average height 01 sky view factor 31 hillshade 11	
	 3.5m < road width < 7 m 6 m < building av. H < 9 m		full-empty ratio 501 average height 7 m sky view factor 30 hillshade 125		full-empty ratio 47681 average height 7 m sky view factor 257 hillshade 9120	full-empty ratio 51 average height 01 sky view factor 171 hillshade 331		full-empty ratio 36001 average height 7 m sky view factor 334 hillshade 10600	full-empty ratio 321 average height 01 sky view factor 231 hillshade 11	
	 3.5m < road width < 7 m 6 m < building av. H < 9 m		full-empty ratio 361 average height 7 m sky view factor 43 hillshade 119		full-empty ratio 37691 average height 7 m sky view factor 642 hillshade 10369	full-empty ratio 01 average height 01 sky view factor 331 hillshade 151		full-empty ratio 36061 average height 7 m sky view factor 467 hillshade 10667	full-empty ratio 31 average height 01 sky view factor 321 hillshade 31	
	 3.5m < road width < 7 m 6 m < building av. H < 30 m		full-empty ratio 261 average height 15 m sky view factor 26 hillshade 103		full-empty ratio 26441 average height 15 m sky view factor 225 hillshade 7777	full-empty ratio 21 average height 01 sky view factor 141 hillshade 321		full-empty ratio 40061 average height 15 m sky view factor 263 hillshade 6064	full-empty ratio 31 average height 01 sky view factor 201 hillshade 251	
	 road width < 7 m building av. H < 30 m		full-empty ratio 461 average height 30 m sky view factor 24 hillshade 74		full-empty ratio 47671 average height 30 m sky view factor 2016 hillshade 7517	full-empty ratio 01 average height 01 sky view factor 151 hillshade 21		full-empty ratio 40001 average height 30 m sky view factor 2035 hillshade 7124	full-empty ratio 201 average height 01 sky view factor 11 hillshade 61	
	 squares		full-empty ratio 101 average height 0 m sky view factor 150 hillshade 150		full-empty ratio 941 average height 0 m sky view factor 5019 hillshade 11453	full-empty ratio 61 average height 01 sky view factor 151 hillshade 31		full-empty ratio 6001 average height 0 m sky view factor 467 hillshade 10065	full-empty ratio 31 average height 01 sky view factor 51 hillshade 141	
	REGIONS: EMILIA ROMAGNA LAZIO CAMPANIA PUGLIA MOLISE UMBRIA BASILICATA VENETO TOSCANA ABRUZZO MARCHE CALABRIA	 open spaces		full-empty ratio 201 average height 0 m sky view factor 56 hillshade 119		full-empty ratio 30251 average height 0 m sky view factor 565 hillshade 9920	full-empty ratio 341 average height 01 sky view factor 11 hillshade 201		full-empty ratio 34471 average height 0 m sky view factor 491 hillshade 9920	full-empty ratio 171 average height 01 sky view factor 151 hillshade 01
		 green areas		full-empty ratio 01 average height 0 m sky view factor 66 hillshade 155		full-empty ratio 0001 average height 0 m sky view factor 775 hillshade 11400	full-empty ratio 01 average height 01 sky view factor 131 hillshade 351		full-empty ratio 0001 average height 0 m sky view factor 656 hillshade 12400	full-empty ratio 01 average height 01 sky view factor 91 hillshade 01

Figure 29. Comparison between the values of descriptive indicators of urban morphology accuracy between the different input model of data and simulation tools. Test on the urban patterns of the city of Naples (Source: Bassolino et al., 2021).

3.3.3. Definition of an algorithm in a GIS environment for the recognition of recurring urban patterns in urban settlements

A process was formulated within a GIS environment to identify recurring urban patterns in open spaces, that involved defining the morphological traits of recurrent urban patterns and analyzing their environmental performance under varying climatic conditions. The effectiveness of this process was tested using the city of Naples as a sample case (Bassolino and Verde, 2023).

The initial step involved recognizing urban morphology and automatically linking recurrent urban patterns. This process involved calculating the density parameter, which represents the ratio of built volume (measured in cubic meters) to unbuilt area (measured in square meters). The data were extracted from thematic classifications of built and open spaces within the topographic database (DBT). Then, the corresponding value was associated with the classification of recurrent urban patterns, calculated based on the area and height values of buildings in the digital surface model (DSM) and the digital terrain model (DTM) of the city of Naples.

To obtain the density parameter for built structures, calculations were made at the atomic unit of the census section. Parameters such as average building height and the covered area within distinct building polygons were determined, along with defining the percentage values of surface treated as green. The "Volume" attribute was derived from the product of building area and height. Subsequently, an "intersect" operation enabled the overlapping of building polygons with census section polygons, and a summarization operation facilitated associating the average volume value with the census sections. Finally, building density (D) was calculated as the ratio of the building's volume (cubic meters) to the census section's area (square meters).

This first classification was not able to take into account the green areas. For this reason, the process was further detailed.

This second phase of sub-classification aimed to identify census sections with a prevalence of green-treated areas. For this purpose, it was needed a "training set" operation, testing sections with known surface treatment

and building density to classify areas as "green" if occupied by at least 80% vegetation or as "medium green" if the area ranged from 55% to 80%.

Another sub-classification focused on areas with a density exceeding 17 cubic meters per square meter, indicating very tall buildings. Initially classified as very dense fabric, these sections were later reclassified as "medium dense fabric," where the soil is occupied up to 55% by building surfaces. Additionally, a sub-classification based on the percentage of green surface within census sections was integrated, obtained through intersection with the green areas layer in the topographical database.

The obtained data demonstrates that, through the generation of classification processes centered on building density, which include the presence and prevalence of areas treated as green, it is possible to identify the predominant urban pattern within the information clusters represented by census sections (see Figure 30).

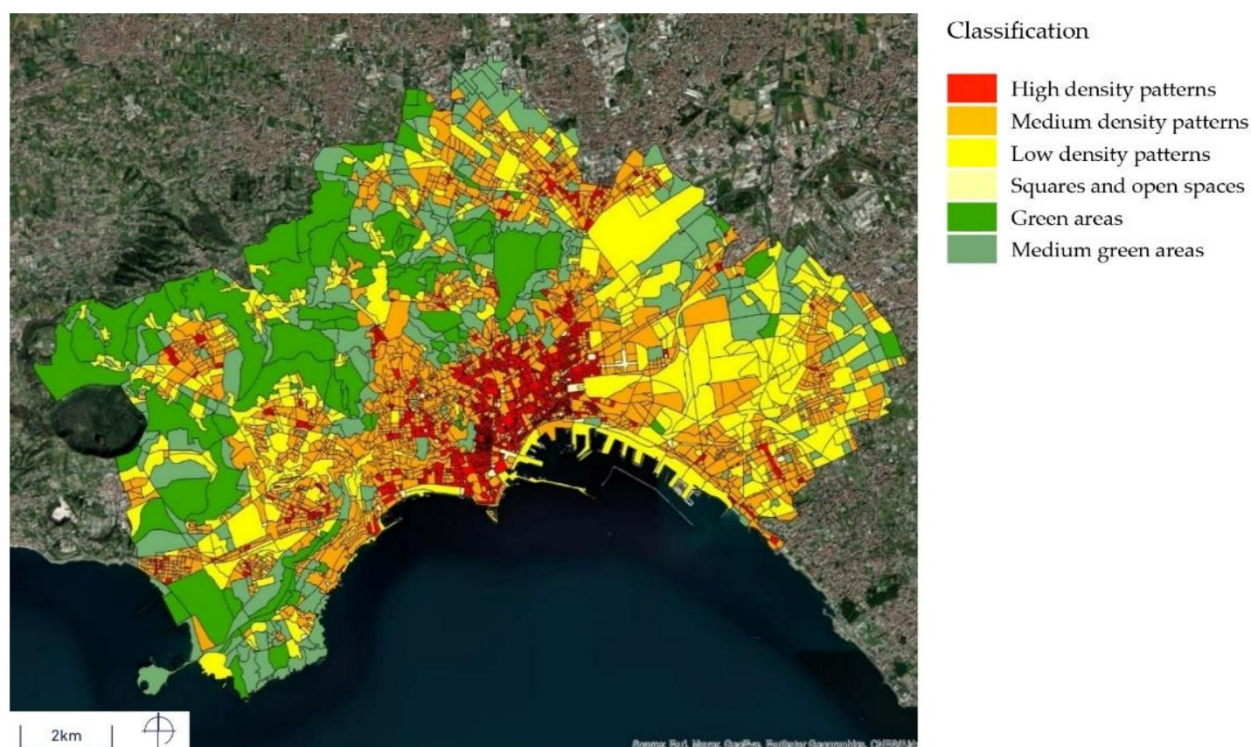


Figure 30. Map of building density and green areas by census section (Source: Verde et al., 2021).

3.3.4. Urban settlements knowledge through integrated taxonomies: the contribution of Local Climate Zones

The physical and functional complexity of the urban settlements amplifies the negative effects of climatic hazards such as heat waves, floods, droughts, and sea level rise. To counter climate risks, strategies must be based on in-depth knowledge of the relevant morphoclimatic context and the relationship between environmental factors and the morphological and functional characteristics of urban contexts, adopting a scientific-based, multidisciplinary approach geared towards the territorialization of adaptation measures (CMCC, 2023; IPCC, 2022).

Recent advances in Earth observation systems and machine learning techniques have produced high-resolution datasets on topography, urban land cover, and population, as well as on current and future climate risks. However, these tools provide autonomous descriptions of the hazards and risk components considered (Mills et al., 2017). Considering the need for systemic and integrated approaches in the current multi-risk scenario, to understand the complexity of such conditions it is necessary to simplify the input data, facilitating

calculations without losing the variability that characterizes urban fabrics and their physical and socioeconomic interactions (D'Ambrosio et al. 2023; Turchetti, 2023).

Several studies have analyzed urban parameterization to identify relationships between environmental factors and morphological features (Oke, 1988). Following Chandler (Chandler, 1970), Ellefsen (Ellefsen, 1984), and Oke (Oke, 2006), the classification of Local Climate Zones (LCZ) by Stewart and Oke (Stewart and Oke, 2012) has become an established reference (Demuzere, Bechtel, et al., 2019). The LCZ defines regions of territory that are homogeneous in terms of surface cover, materials, and human activities; 10 classes concern built-up areas and 7 concern land cover types. Each class is associated with standardized geometric, surface, thermal, and metabolic parameters. Among the most promising methodologies for the development of classification are GIS-based approaches integrated with open-source databases (Levlovics et al., 2013; Hidalgo et al., 2019).

Moreover, several authors have also used LCZ to integrate climate knowledge and urban design, outlining adaptation and risk reduction actions in relation to morphological and environmental characteristics (Middel et al., 2014; Mills et al., 2017; Nazarian et al., 2019; Maharof et al., 2020; Musco et al., 2020; Liu et al., 2023; Li et al., 2025).

Accordingly, this contribution intends to propose an approach that integrates the morphometric analysis of LCZs with the taxonomic analysis of the urban system derived from the PNACC and developed within RETURN project, aiming to offering an operational tool to support decisions at the local level. The case study concerned the district of Soccavo, in the Metropolitan City of Naples.

The methodology consists of three main phases (see Fig. 31):

- data collection, mapping, and refining of Local Climate Zones through GIS-based approaches;
- integration of LCZs with urban taxonomies and spatial analysis of results;
- selection and cataloging of strategies and actions in relation to taxonomy elements and existing sets, and definition of the integrated database.

As an early result, summary sheets have been defined for each LCZ, showing the prevalence of taxonomy element in terms of surface coverage. Afterwards, climate adaptation strategies from the NCCAP Database have been linked to different taxonomy elements. Each strategy, supported by an operational objective and a monitoring indicator set in terms of effectiveness and progress, has been therefore coupled with different class of elements in the physical system taxonomy as a hypothetical application. To further support the link between PNACC objectives and design interventions, various sets of actions were analyzed as related to these objectives. The result is a catalog, for each objective, of possible design proposals associated with the most effective LCZ application in terms of climate risk reduction.

The integration provided multiple benefits: on the one hand, LCZs allow the effectiveness of adaptation strategies to be verified through the potential variation of the parameters associated with the classification; on the other hand, the taxonomy provides a detailed analysis of the physical composition of urban settlements and refines the larger-scale schematization of urban fabrics carried out by the LCZs, identifying the elements most suitable for implementing the planning guidelines set out in the PNACC.

The proposed framework supports the integration of LCZs and urban taxonomies as an operational support for planning and risk management, providing an informed, integrated database representing climate criticalities, morphological, typological and environmental settlement features, and possible design strategies. The identification of critical points through LCZ-taxonomic analysis need further, detailed investigations; however, the process highlighted a stable degree of homogeneity of the proposals for each LCZ in relation to the PNACC objectives, suggesting promising results in terms of replicability in different contexts.



71

3.4. A clustering proposal of existing urban settlements

Urban settlements throughout Italian territory are characterized by different typo-morphological features, settlement patterns, demographic, social, economic and institutional conditions. A clustering of such urban settlements may help understanding which are the most common urban settlement types in Italy and their characteristics. Tocchi et al. (2025) propose a clustering methodology that groups urban settlements based on open-source data, used as proxies of urban vulnerability and exposure.

Below, the preparatory material used to develop the methodology, further elaborated in Tocchi et al. (2025), is presented.

A first step for a national scale clustering of urban settlements is the assessment of data availability and the definition of the scale of analysis. Publicly available data on built environment and population in urban areas is often provided with reference to the administrative level. The twenty regions in Italy are the first-level administrative divisions. Each region is divided into a certain number of provinces, the second-level administrative divisions of the Italian territory, and each province is composed of many municipalities. The first clustering proposal of Italian country presented herein is performed considering the municipality as urban settlement boundaries and using only open-source data. More specifically, the following information are taken into account for the clustering:

- Degree of urbanization
- Urban centeredness degree
- Number of inhabitants
- Altimetric zone

The Degree of urbanization is a classification that indicates the character of an area based on the share of local population living in urban clusters and in urban centers. According to Eurostat (the statistical office of the European Union), municipalities are classified into three types of area: thinly populated area (rural area); intermediate density area (towns and suburbs/small urban area), and densely populated area (cities/large urban area). Methodology proposed by Eurostat is adopted for the classification of local administrative units (municipalities) in the mentioned areas that uses as a criterion the geographical contiguity in combination with the share of local population living in the different type of clusters (https://ec.europa.eu/eurostat/statistics-explained/index.php?title=Degree_of_urbanisation_classification_-_2011_revision). The typology is defined by classifying grid cells of 1 km² to one of the three following clusters, according to their population size and density: i) high-density cluster, characterized by contiguous grid cells of 1 km² with a density of at least 1500 inhabitants per km² and a minimum population of 50 000; ii) urban cluster characterized by contiguous grid cells of 1 km² with a density of at least 300 inhabitants per km² and a minimum population of 5000; iii) rural grid cell, i.e., grid cell outside high-density clusters and urban clusters. In a second step, municipalities are then classified to one of three types of areas:

- Densely populated area also called cities or large urban area, if at least 50 % live in high-density clusters.
- Intermediate density area also called towns and suburbs or small urban area, if less than 50 % of the population lives in rural grid cells and less than 50 % live in high-density clusters.
- Thinly populated area or rural area if more than 50 % of the population lives in rural grid cells.

The classification of the Italian municipalities adopting to the above-mentioned Eurostat procedure is shown in Figure 20 (left) and it is provided by ISTAT (National institute of statistics in Italy).

The identification of the urban centeredness degree starts from a reading of the Italian territory as a polycentric territory, i.e., a territory characterized by a network of municipalities or aggregations of municipalities (centers of offer of services) around which areas characterized by different levels of peripherality gravitate. These centers offer a wide range of essential services, capable of generating important catchment areas, even remotely, and of acting as "attractors" (in the gravitational sense). The level of peripherality of the other areas

with respect to the network of urban centers influence may determine difficulties of access to basic services as well as lower quality of life of citizens and their level of social inclusion. The methodology adopted for the definition of the urban centeredness degree of municipalities is the one proposed within the National strategy for internal areas (SNAI, "Strategia nazionale per le aree interne" in Italian), a territorial policy aimed at improving the quality of services to citizens and economic opportunities in internal territories, i.e., those areas characterized by a significant distance from the main service offering centers and at risk of marginalization. The proposed methodology consists of two main phases:

1. Identification of the urban hubs, according to a criterion of capacity to offer some essential services.
2. Classification of the remaining municipalities into 4 bands: peri-urban areas; intermediate areas; peripheral areas and ultra-peripheral areas, based on the distances from the hubs measured in mileage time.

More specifically, the choice of hubs (which can be also defined as service offering centers) is based on the service offering indicators concerning high school educational services (e.g., offer includes high schools, technical and professional institutes and other types of higher institutions), health services (e.g., presence of several health and emergency facilities, presence of healthcare facilities with at least 250 beds) and rail transport services (e.g., train stations characterized by more than 6000 travelers on average per day and a high number of trains on average per day). Some neighboring municipalities are classified as intermunicipal hubs; this means that several contiguous municipalities are able, in a network system, to offer the identified level of services. The other municipalities are classified based on an accessibility indicator calculated in terms of minutes to reach the nearest hub. Thus, the distance expressed in minutes from the nearest hub is less than 20 minutes for the peri-urban areas, equal to approximately 20 e 40 minutes for the intermediate areas, between 40 and 75 minutes for the peripheral areas and more than 75 minutes for ultra-peripheral territories. Figure 31 (right) shows the Italian municipalities classified based on the associated urban centeredness degree.

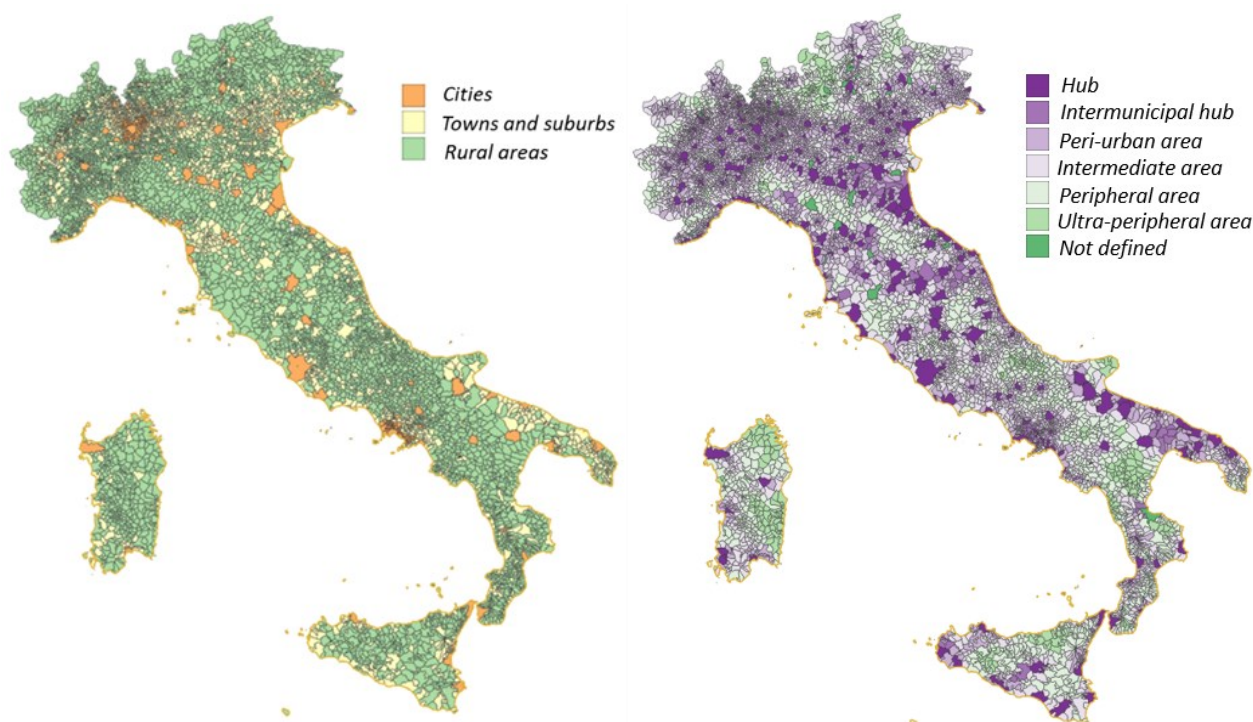


Figure 3232. Classification of Italian municipalities based on urban degree (left) and urban centeredness degree (right).

Municipalities can be also classified based on the residential population (i.e., the number of inhabitants within the municipality, derived by ISTAT). Specifically, seven population classes are defined: population less than 500 inhabitants ($C_{pop}=1$); population between 501 and 2000 inhabitants ($C_{pop}=2$); population between 2001 and 5000 ($C_{pop}=3$); population between 5001 and 10000 ($C_{pop}=4$); population between 10001 and 50000 ($C_{pop}=5$); population between 50001 and 250000 ($C_{pop}=6$); population higher than 250000 inhabitants ($C_{pop}=7$). The

number of classes can be also reduced considering only three classes: high populated municipalities ($C_{pop}=6$ or 7); medium populated municipalities ($C_{pop}=4$ or 5); low populated municipalities ($C_{pop}=1, 2$ or 3).

ISTAT also classifies Italian municipalities on the basis of their altimetric threshold values into five zones. The classification criteria are contained in the 1958 publication (Istat, Statistical districts, Methods and norms, series C - n. 1 August 1958). Altitude zones are distinguished mountain, hill and lowland. The mountain zones are characterized by reliefs higher than 600 m.a.s.l.; hill zones include areas characterized by an altitude ranging between 300 and 600 m.a.s.l.; lowland zones are zones situated at lower than 300 m.a.s.l. Altitude is derived from DEM (Digital elevation model) elaborated by ISPRA (Italian Institute for Environmental Protection and Research) for a 20 m grid. Starting by DEM values, statistics about average, sum, minimum and maximum altitude in the defined zones (i.e., within the municipal boundaries) are obtained using a zonal statistic tool through a GIS software. The altimetric zone of the municipality is then derived based on the surface prevalence criterion, i.e., based on the altimetric zone which most of the municipality surface belong to. The above-mentioned zones have been further divided, to take into account the moderating action of the sea on the climate, respectively in altimetric zones of internal mountain, internal hill, coastal mountain, coastal hill and coastal lowland. Figure 32 shows Italian municipalities classified in population classes and the altimetric zones.

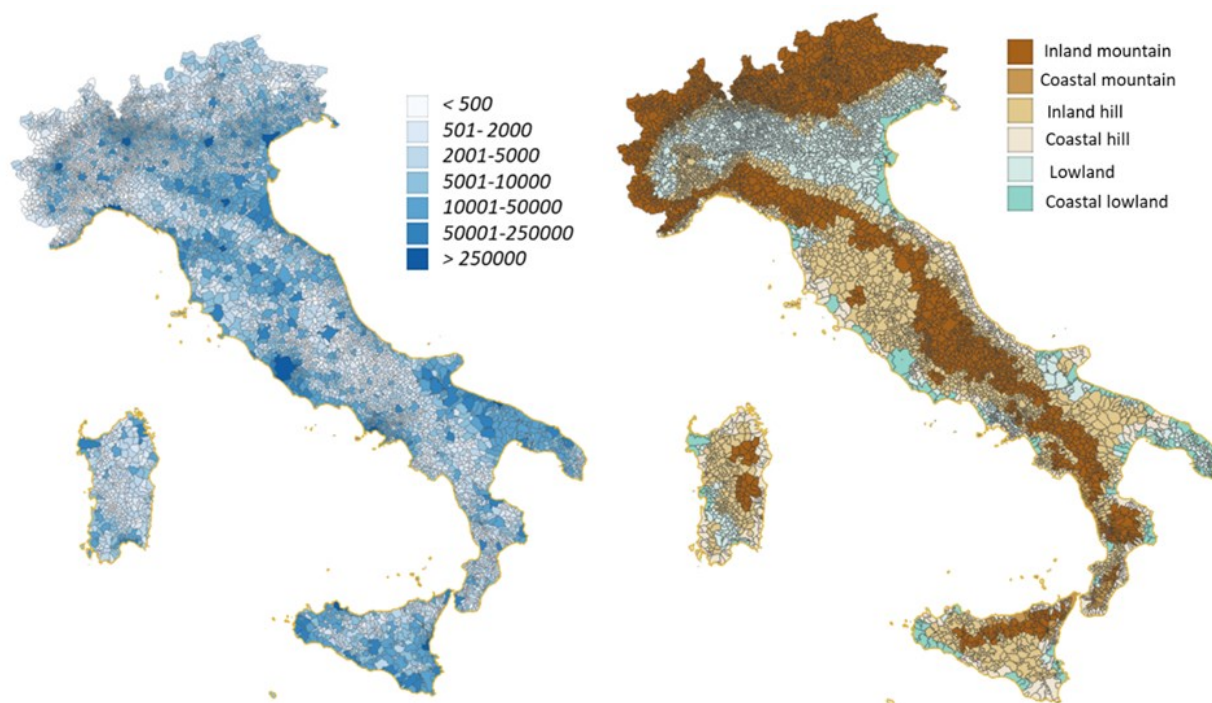
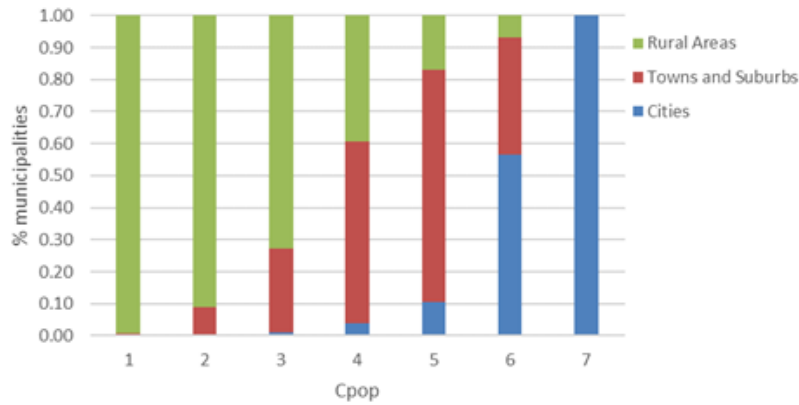
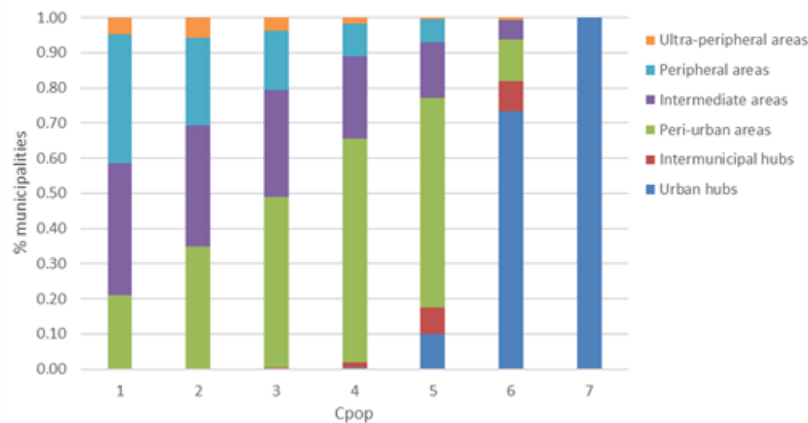


Figure 3333. Italian municipalities classified based on number of inhabitants (left) and altimetric zone (right).

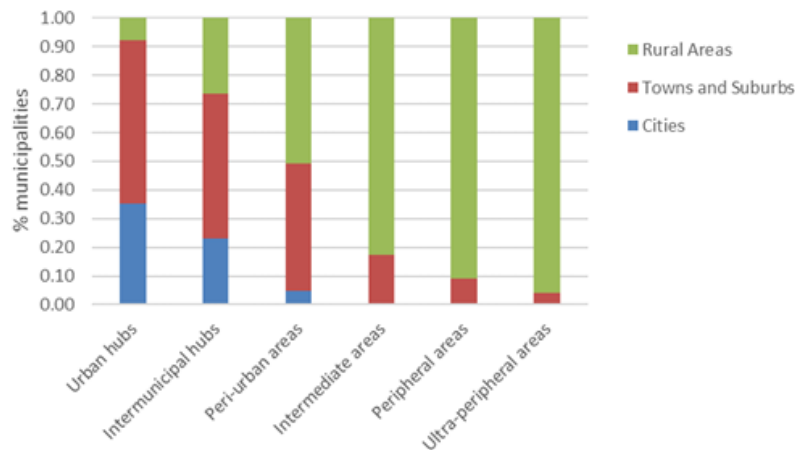
A first analysis of the classification obtained using the mentioned open-source data point out that, as expected, cities are usually characterized by large population while population tends to be lower in rural areas (Figure 33a). The same trend is observed considering population and urban centeredness degree (i.e., the higher the centeredness degree, the higher the population). Most intermediate areas, peripheral areas and ultra-peripheral areas are classified as rural areas. Almost all peri-urban areas are classified as rural areas or towns/suburbs, while most urban hubs and intermunicipal hubs are classified as cities or towns/suburbs (i.e., they generally are high densely populated).



(a)



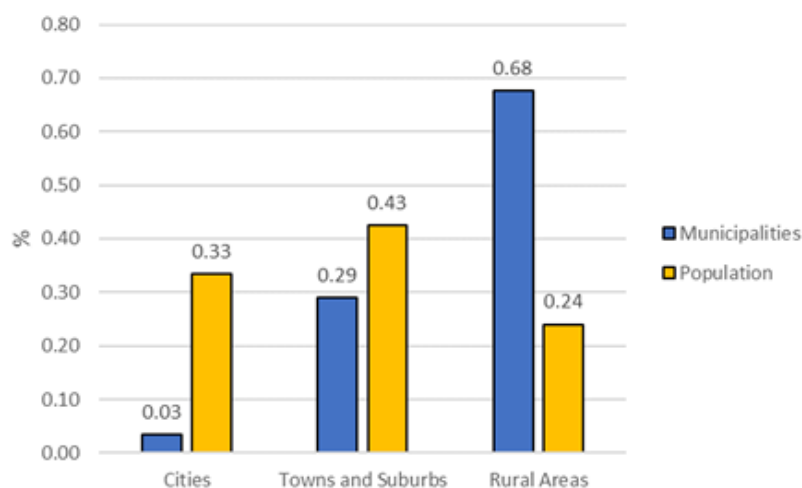
(b)



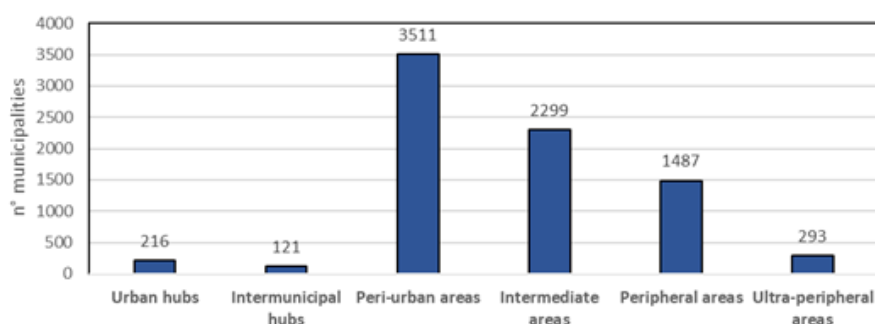
(c)

Figure 3434. Distribution of municipalities in Italy based on combination of population class and urban degree (a); population class and urban centeredness degree (b); urban degree and urban centeredness degree (c).

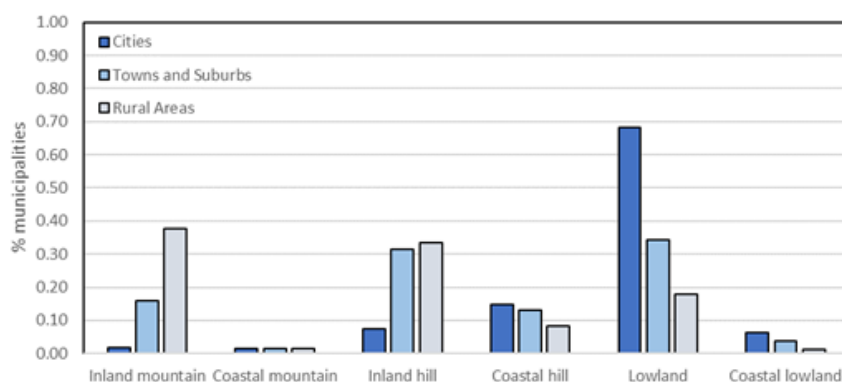
Many municipalities in Italy are classified as peri-urban areas (3511 municipalities - the 44%). A percentage of 68% of municipalities are classified as rural areas while only 3% are cities. Although they represent only a small percentage, as they are densely populated areas, 33% of the whole population live in cities. Most cities are located in lowland areas, towns and suburbs are located mostly in lowland and inland hill areas while rural areas are mostly located in inland mountain and inland hill areas (Figure 34c).



(a)



(b)



(c)

Figure 3535. Distribution of municipalities and population in Italy based on the urban degree (a); number of municipalities based on urban centeredness degree classification (b); percentage of municipalities – classified in cities, towns/suburbs and rural areas based on urban degree – in different altimetric zones.

Using the information on degree of urbanization, urban centeredness degree, population class and altimetric zones, a clustering of the Italian municipalities is carried out. A first step clustering is obtained combining information about the degree of urbanization and the urban centeredness degree, obtaining 12 clusters for the Italian municipalities (Figure 35). If also the information about population class was considered in the clustering, 29 clusters are obtained. Considering also information about altimetric zone, the 7953 municipalities (ISTAT, 2018) are clustered in 98 clusters. This means that in Italy there are 98 different urban settlement types, according to clustering criteria adopted. The cluster that encompasses the largest number of municipalities is the cluster representing low densely populated mountain rural areas (1630, the 20% of Italian

municipalities). However, the representativeness of this cluster is much lower if we consider the residential population as evaluation parameter. The 17% of Italian population live in highly populated urban hubs cities (more than 250000 inhabitants) located in lowland areas. The cluster of towns/suburbs in lowland peri-urban areas with a population between 5000 and 50000 inhabitants (i.e., medium population class) is the most representative one both in terms of number of municipalities (521, the 7%) and in terms of population (11% of people live in these areas).

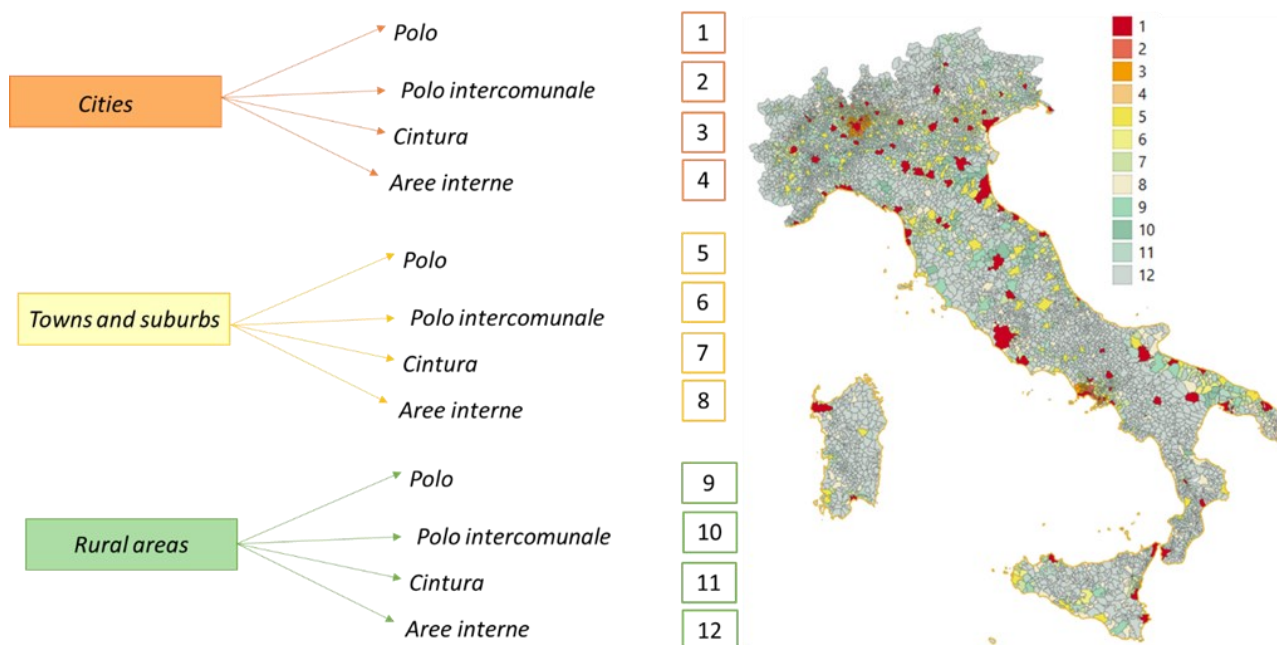


Figure 3636. Clusters obtained combining information on urban degree and urban centeredness degree.

Clustering proposal can be also refined considering also other parameters publicly available accounting for i) the presence of a major accident hazards sites, as defined by Directive 2012/18/EU (Seveso-III directive), i.e., sites where industrial plans handling dangerous substances and a potential industrial accidents is likely to strongly affect population exposed, ii) the presence of socially vulnerable population, which usually shows higher probability of being disproportionately affected by natural hazards. The inventory of industrial sites is provided in Italy by ISPRA. Figure 36 (left) shows the municipalities where one or more industrial sites classified as major accident hazard sites are located.

Social vulnerability refers to the increased likelihood of some social groups to suffer negative consequences of natural hazards, due to their lack of capacity to react and manage the effect of hazard related processes (Oliver-Smith, 1999; McCarthy, et al., 2001; Cutter, et al., 2003; Wisner, et al., 2004; Adger, 2006; Barros, et al., 2014). In research literature, different socio-economic and demographic factors have been identified as social vulnerability components. The main parameters adopted to assess social vulnerability are gender, age, education, socioeconomic status, public health condition, employment status, and access to resources. To measure social vulnerability, indicator-based approach are the most used methods (Cutter et al., 2003; Yoon, 2012). In Frigerio et al. (2018) variables for quantifying social vulnerability in Italy are identified based on a literature review and taking into account also the data availability. These variables are representative of 7 demographic and socio-economic indicators relevant to the specific context, that can increase or decrease social vulnerability, i.e., family structure, education, socioeconomic status, employment, age, population growth, race/ethnicity. All those variables can be derived from ISTAT and can be aggregated to obtain a social vulnerability index (e.g., Frigerio et al., 2018; Tocchi et al., 2023). Figure 36 (right) shows the social vulnerability index value calculated for Italian municipalities.

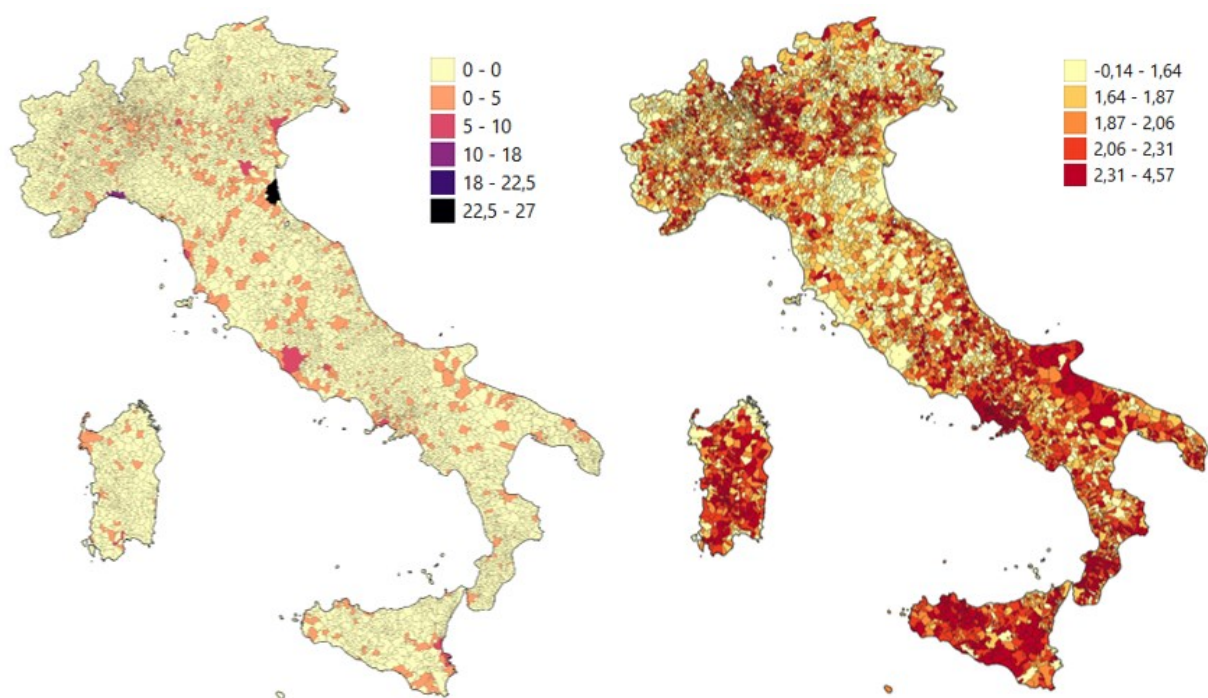


Figure 3737. Maps showing: the number of industrial sites classified as major accident hazard sites located in each municipality (left) and the social vulnerability index value calculated at municipal level (right).

3.5. The impending hazards in urban context

Numerous regions of the world are vulnerable to different types of hazards. Effective risk management and reduction requires as a first step an improvement of understanding of risks; this entails a thorough comprehension of the contributing factors from which the risk depends: hazard, vulnerability and exposure (UNISDR, 2005). However, multi-risk analysis present inherent challenges, especially due to the disparate characteristics of distinct hazards. As a result, it is increasingly being recognized the need to investigate and manage various types of hazards that contribute to risks, posing a threat to assets, services, and individuals (Kappes et al., 2012).

Internationally, numerous organizations have developed different taxonomies of hazards that can potentially have impacts on assets, individuals, and resources in urban and metropolitan settlements. Consequently, various hazards classifications have been examined in order to clarify how the concept evolved in the field of multi-risk assessment. This led to the identification of a trend in the classification techniques in terms of the weight attributed to the interaction between hazards and current climate change. Next, the main taxonomies analysed are reported.

The **Sendai Framework for Disaster Risk Reduction 2015-2030** (UNDRR, 2015) developed a hazard classification for aiding in risk assessment processes. It includes hazards associated to natural disasters as well as ones related to the environment and technology (UNDRR, 2020). Within this taxonomy, the identified hazards are categorized into 8 major groups:

- Biological,
- Hydrometeorological,
- Technological,
- Geohazard,
- Chemical,
- Environmental,
- Extraterrestrial,
- Societal.

Within each of these groups, the specific hazard phenomena are identified, for a total of more than 300 phenomena. It is significant to observe that in this classification, climatic events – and consequently, **climatic hazards** – **are not included**. Extreme climate events are included in the hydrometeorological group rather than having their own category, indicating a **taxonomy** that is **still unaware of the amplification factors determined by climate change**.

The European Commission has developed a comparable classification to the one made by the UNDRR in 2015.

This classification was disclosed in the report "**Science for disaster risk management 2020 - Acting today, protecting tomorrow**" and it divided hazards in 5 groups:

- Geophysical,
- Hydrogeological,
- Meteorological,
- Climatological,
- Human-made.

By adding a **category specifically devoted to climate events**, this taxonomy marks the beginning of a **shift in focus towards the role of climate variables as both precursors and intensifiers of other hazard types**.

In this framework characterized by the evolving of climate impacts, the **Technical Expert Group on Sustainable Finance** (TEG, 2020) has formulated a **specific classification for climate-related events**. This classification aims to guide users of the EU Taxonomy in understanding events with the most significant impact on the biophysical system.

In this case, climatic hazards are categorized into 4 macro-categories, encompassing hazardous phenomena related to:

- Water,
- Temperature,
- Wind,
- Mass movements.

Each category includes both acute (extreme) and chronic (gradual onset) climatic events, excluding those arising from secondary climatic events (including chemical, biological, ecological, and epidemiological risks).

In the context of climate change, specifically climatic hazards, the most recent and relevant classification has been developed by the **Intergovernmental Panel on Climate Change (IPCC)** in its **Sixth Assessment Report (AR6)**. Hazards are identified in the report as **Climate Impact Drivers (CIDs)** (IPCC, 2021).

The 7 macro-categories identified in the report are as follows:

- Heat and cold,
- Wet and dry,
- Wind,
- Snow and ice,
- Coastal,
- Oceanic,
- Other.

The report outlines 35 Climate Impact Drivers distributed with varying intensity across different global regions. The framework of Climate Impact Drivers developed in AR6 supports **an assessment of changing climatic conditions relevant to sectoral impacts and risk assessment**.

Table 6. Hazard classification

UNDRR (2020)	European Commission (2020)	TEG (2020)	IPCC – WGI AR6
Biological	Geophysical	Temperature-related	Heat and cold
Hydrometeorological	Hydrogeological	Wind-related	Wet and dry
Technological	Meteorological	Water-related	Wind

Geohazard	Climatological	Solid mass-related	Snow and ice
Chemical	Human-made		Coastal
environmental			Oceanic
Extraterrestrial			other
Societal			
Source:			
<i>Hazard definition & classification review - Sendai Framework for Disaster Risk Reduction 2015–2030</i>	<i>Science for disaster risk management 2020 - Acting today, protecting tomorrow</i>	<i>Technical Expert group on sustainable finance</i>	<i>Climate Change 2021 – The Physical Science Basis</i>

A review of the state of the art and existing taxonomies related to hazards that determine impacts on urban settlements reveals a shift of focus among international organisations on the classification of climate hazards identified as triggers and amplifiers of other types of hazards of natural or anthropogenic origin (Ghosh, 2018). In particular, the distinction is highlighted between hydrometeorological hazards, i.e. natural processes or phenomena of atmospheric, hydrological or oceanographic nature that may cause loss of life, damage to resources or property, or environmental degradation (UNISDR, 2004), and climate hazards, understood as physical conditions of the climate system (such as, for example, extreme events) that can be directly linked to impacts (positive or negative) on human or ecological systems and assessable through a series of indices and indicators (IPCC, 2021).

Understanding hazards plays a pivotal role in the knowledge and management of climate change impacts. Hazard event classifications aid in better comprehending the nature of climate risks, their interconnections, and their impact across various sectors, including urban settlements. These classifications are crucial for identifying appropriate response actions to address and mitigate climate impacts, concurrently reducing social, economic, and environmental vulnerability and exposure.

3.5.1. Score-based procedure for the identification of relevant hazards

An urban context is characterized by its settlement conditions and impeding hazards. Several hazards could threaten urban settlements (see also section 6.1.1). According to EM-DAT (the international disaster database - <https://www.emdat.be/>), extreme temperature (i.e., heat waves), earthquakes, landslides and floods are the hazards that generated largest human and economic impacts during last century (Figure 37). Italian country is also exposed to Volcanic and Tsunami hazards; such type of perils are very localized or very extreme events (i.e., rare events), and even if they did not cause relevant impacts in the last century, they could be responsible of devastating effects in case of occurrence.

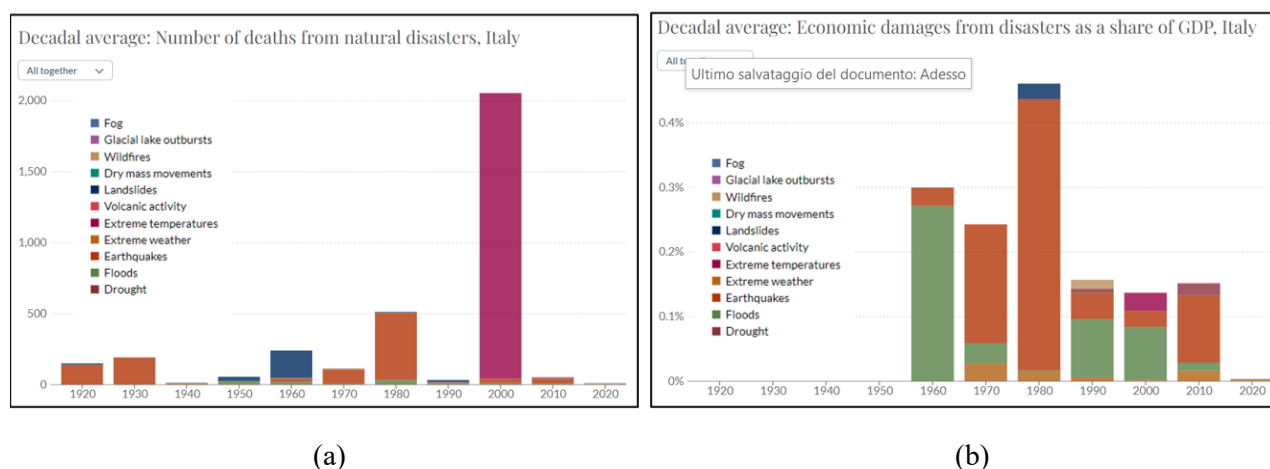


Figure 3838. Number of deaths (a) and economic damages expressed as a share of GDP (Gross Domestic Product) (b) caused in Italy by natural disasters during last century. Source EM-DAT <https://www.emdat.be/>

Due to the variability of geomorphological, climatic and hydrological features, the incidence of different hazards throughout the Italian territory varies, as their potential to generate significant impacts. Hazard maps, when available, provide information on the location, intensity and frequency of hazards, allowing to locate areas where given events are characterized by highest intensity. Hence, the hazard maps related to different type of perils represent a useful tool to identify impending hazard in urban areas. However, given the different nature and frequency of different hazards it is not straightforward to compare their incidence based on the sole hazard maps. Therefore, a score-based procedure is proposed to allow the ranking of different hazards and to infer which hazards could be more relevant in a given urban context. The procedure is applied to urban contexts at the municipality scale. For each relevant peril, the value of the corresponding intensity measure on the hazard map at given return period is considered. Such measure of intensity is subsequently transformed into a normalized score. Normalization allows to transform variables into pure, dimensionless, numbers. Several normalization techniques can be adopted. In order to obtain a score that reflects the relative position of the intensity value with respect to a range defined by highest and the lower intensity, normalization is performed using the empirical cumulative distribution functions (ECDFs). ECDF expresses the probability that a random variable X will take a value lower or equal to a given value x , i.e., $P(X \leq x)$, based on sample observations. Adopting as sample observations the value of the selected hazard-intensity measures at the municipal scale for all Italian municipalities, and applying the normalization process, all indicators assume a value between 0 and 1, where 0 is associated to the municipality (or the municipalities) characterized by the lower hazard-intensity measure in Italy, while 1 is associated to the municipality (or the municipalities) characterized by the higher value. Through the scoring, a ranking of all Italian municipalities with respect to a given hazardous event is carried out.

Ideally, such scoring procedure can be applied to all relevant hazard in Italy, adopting as input available hazards maps or maps of parameters that can be considered as proxies of hazard intensity. The seismic hazard intensity is derived from a measure of earthquake-induced ground shaking at the municipal centroid, which is quantified according to a selected hazard map. In Italy the official reference is the MPS04 model proposed by Stucchi et al. (2004; 2011). Seismic hazard is obtained by the PSHA. The results of the PSHA were elaborated by INGV (Istituto Nazionale di Geofisica e Vulcanologia) and presented in terms of maps showing the value of peak ground acceleration (PGA) and spectral acceleration at reference elastic periods ($S_a(T)$) corresponding to an exceedance probability in a given period of time or, equally, to an assigned return period, considering rocky soils ($V_{s30} > 800$ m/s, class A, NTC18). Nine different hazard maps of Italy were realized by INGV for nine different return periods (2500, 1000, 475, 200, 140, 100, 72, 50 and 30 years) or probabilities of exceedance in 50 years (2%, 5%, 10%, 22%, 30%, 39%, 50%, 63% and 81%). To evaluate the score for seismic related hazard, the PGA value for 475-year return period (or 10% probability of exceedance in 50 years) is selected as intensity measure in this application as it is the reference used in most building codes for seismic design. The model provides the seismic actions for each point of a 5x5 km mesh covering all the Italian territory. The PGA value at municipal centroid is obtained as weighted average on distance, considering the closer grid points. Figure 38 shows the ECDF obtained for seismic hazard intensity measure and the map showing the seismic hazard score calculated for each municipality.

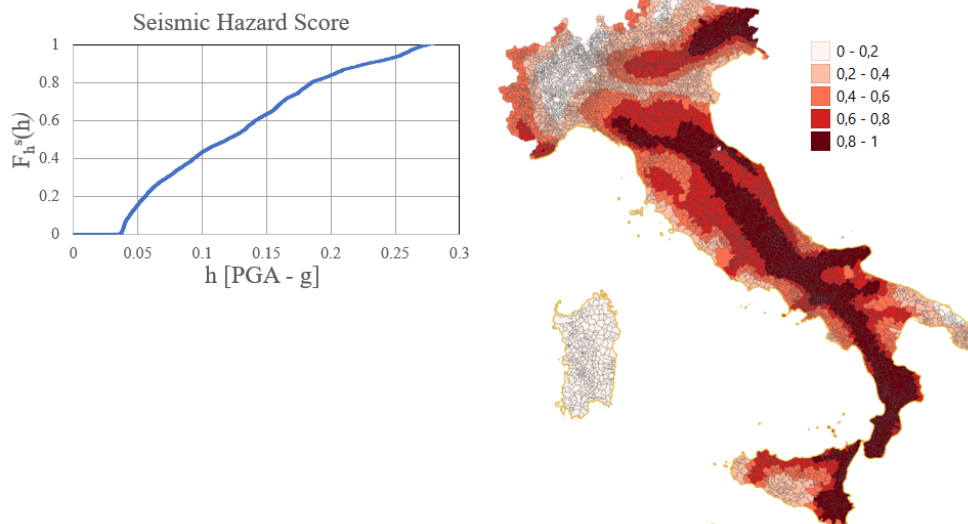


Figure 3939. ECDF of seismic hazard intensity measure (left) and seismic hazard scores for each municipality (right).

Concerning flood hazard, ISPRA (Istituto Superiore per la Protezione e la Ricerca Ambientale) provides riverine flood hazard maps containing the perimeter of the geographical areas in Italy that could be affected by floods. Such maps, bounded by the District Basin Authorities, are derived for three probability scenarios: low probability event (extreme events with a return period more than 300 years), medium probability scenario (events with return period of 100 years or greater) and high probability scenario (frequent events). For this application, the percentage of an urban area expected to be inundated in a medium probability scenario (with a mean return period between 100 and 200 years) is considered as riverine flood intensity measure. This scenario is selected as frequent events with a return period between 20 and 50 years are characterized by low intensity and may be not suitable to account for the effect of climate change (that tends to increase the frequency of higher intensity events); on the other hand, events with a return period greater than 300 years can be considered as too rare flood events. The land use of potentially inundated areas within a municipality can greatly affect the type and the level of expected impacts. Therefore, in evaluating the area potentially inundated according to the considered scenario also the land use is taken into account. More specifically, areas destined to residential, industrial or rural uses are distinguished within the municipality through a GIS software. This information is available from ISTAT in shapefile format. The overlapping of land use maps with flood extension map allows to evaluate the percentage of residential, industrial and rural area potentially inundated in each municipality. Such percentage is adopted as input of the score-based procedure. Figure 39 shows the ECDFs obtained for riverine flood hazard considering residential and industrial areas and the maps with relative scores.

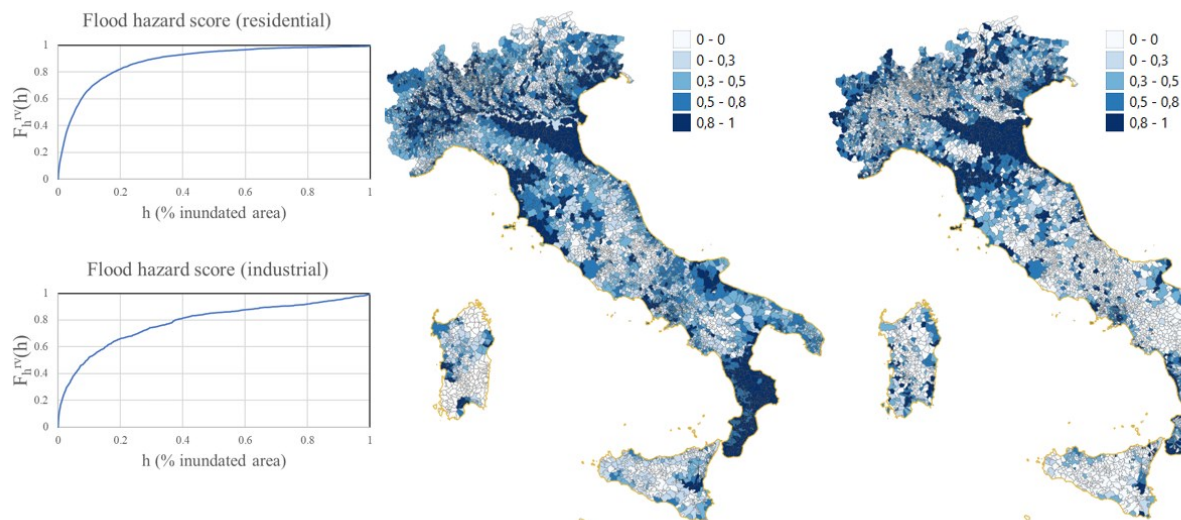


Figure 4040. ECDFs of riverine flood hazard (left) considering the percentage of residential area (top) and the percentage of industrial area (bottom) potentially inundated as intensity measure; maps show the riverine flood hazard scores for residential areas (left) and industrial areas (right) in each municipality.

The probabilistic hazard model for earthquake-induced tsunamis (S-PTHA, Seismic –Probabilistic Seismic Hazard Assessment) produced by the project TSUMAPS-NEAM (2016-2018, Agreement N° ECHO/SUB/2015/718568/PREV26), co-financed by DGECHO and coordinated by INGV, is the most recent and homogeneous, at continental scale, information available today about tsunami hazard along the *Northeastern Atlantic, the Mediterranean and connected seas* coasts (<http://www.tsumaps-neam.eu/>). The model adopts the MIH (Maximum Inundation Height) quantity as the intensity parameter for tsunamis, i.e., the maximum height reached by the water above the resting sea level along profiles orthogonal to the coast. The limitations of such a continental-scale model mainly concern its spatial resolution, which allows neither the in-depth analysis of specific source areas nor the detailed ingress assessment and the delimitation of areas potentially inundated by tsunamis. Thus, the tsunami inundation maps, which identify the Italian coastal areas potentially exposed to tsunamis generated by earthquakes, provided by ISPRA are used for this application. The maps were developed within the formal framework of the National Alert System for Earthquake Generated Tsunamis (SiAM - Sistema Allertamento Maremoti), established in 2017 (Directive of the President of the Council of Ministers, 17 February 2017). Tsunami inundation maps and related warning zones (representing the envelope of all the areas subject to inundation resulting from any possible known sources of earthquake-induced tsunamis) were defined by using an empirical methodology and they are publicly available (<http://sgi2.isprambiente.it/tsunamimap/>). SiAM's guidelines indicate that the reference MIH_{ref} value, corresponding to MIH with an average return time of 2500 years on the 84th percentile hazard curve at a given POI (Point Of Interest), should be adopted in definition run-up and alert level. Also, a safety factor, indicated as k , is applied to estimate the run-up taking into consideration potential local changes in MIH_{ref} , which can lead to locally significant variations. This coefficient allows to transform MIH_{ref} into an estimate of the maximum expected *run-up*, here indicated as R_{max} . To allow a reliable choice of k , TSUMAPS-NEAM estimated a relationship between mean MIH_{ref} and the maximum run-up R_{max} in some representative areas, through detailed modelling of numerous tsunamis with different features. According to these results, a value of k equal to 3 was selected. Based on the estimated maximum run-up value (R_{max}) for a given coastal sector, the corresponding value of maximum ingress distance (D) was evaluated. The relationship used provides 200 m of D for every meter of R , applied to all coastal areas; in correspondence of the river mouths, to take into account the tsunami's wave rise in the river bed, a different attenuation law was adopted, where 1 m of R corresponds to 400 m of ingress along the river bank, while laterally the attenuation considered is 1 m every 100 m distance from the riverbed. Accordingly, tsunami inundation maps (Alert Zone, "Zona di Allertamento") were defined considering run-up classes of R equal to 1, 2, 5, 10, 15, 20 and 25 m, associated with Advisory (Orange alert, with expected run-up at the shoreline less than 1 m) and Watch (Red alert, with expected run-up greater than 1 m) alert levels. Subsequently, three tsunami alert buffer zones were delineated for the Italian coastal areas under tsunami threat, namely Zone-1 (Orange alert), Zone-2 (Red alert) and Unique

Zone (Orange/Red alerts together). For the score-based application, the Unique Zone, encompassing both Advisory and Watch levels inundation areas (downloaded at: <http://sgi.isprambiente.it/tsunamiweb/Download.aspx>) is adopted. Distinguishing between inundated residential, industrial and rural areas, three different scores are obtained. Figure 40 shows the ECDFs and maps with tsunami scores.

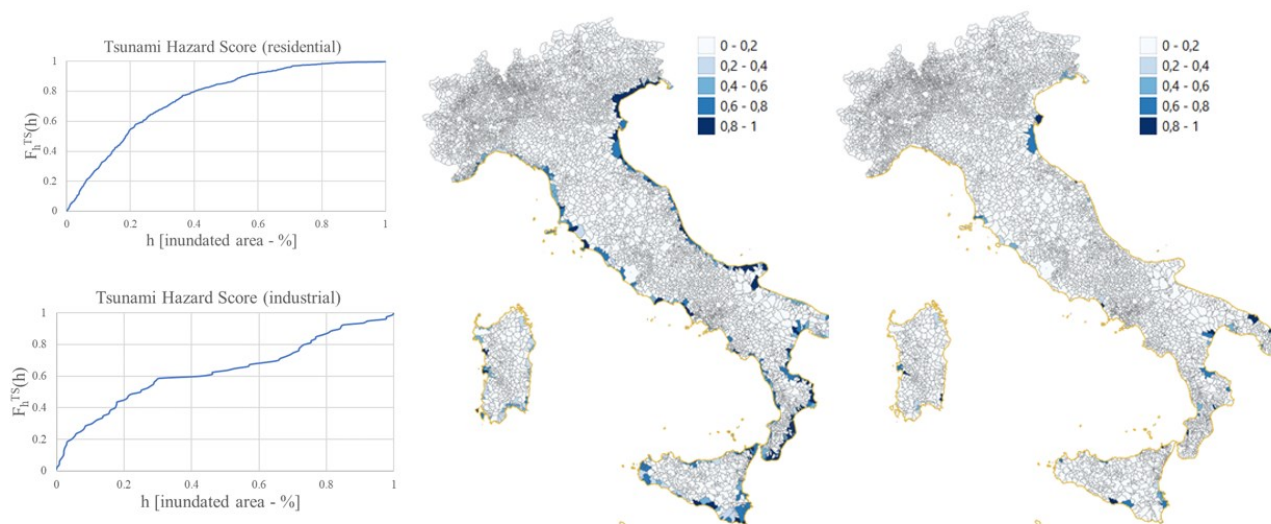


Figure 4141. ECDFs of tsunami hazard (left) considering the percentage of residential area (top) and the percentage of industrial area (bottom) potentially inundated as intensity measure; maps show tsunami hazard scores for residential areas (left) and industrial areas (right) in each municipality.

Concerning heat waves, there are no hazard maps available. Heatwaves vary according to the location of a particular region and the time of year and there is no universal way of defining or measuring heatwaves. A definition based on the Heat Wave Duration Index is that a heat wave occurs when the daily maximum temperature exceeds the average maximum temperature by 5 °C for more than five consecutive days; average maximum temperature is determined for the period 1961–1990 (Frich et al., 2002). The same definition is used by the World Meteorological Organization. According to such definition, the average monthly maximum temperature in the months of July and August recorded in the last 5 years (2018 – 2022) is adopted as proxy of heat wave intensity. This information is provided by ISPRA on a 5km grid covering all the territory, through the spatial interpolation of meteorological stations recordings (<http://www.scia.isprambiente.it/>). Temperature values at municipal centroid are evaluated as weighted average of grid values considering their distance from the centroid. The average value of such temperature values (i.e., average monthly maximum temperature in the considered months) at municipal centroid is assumed as input of for the score-based procedure. Figure 41 shows the ECDF obtained and the scoring map.

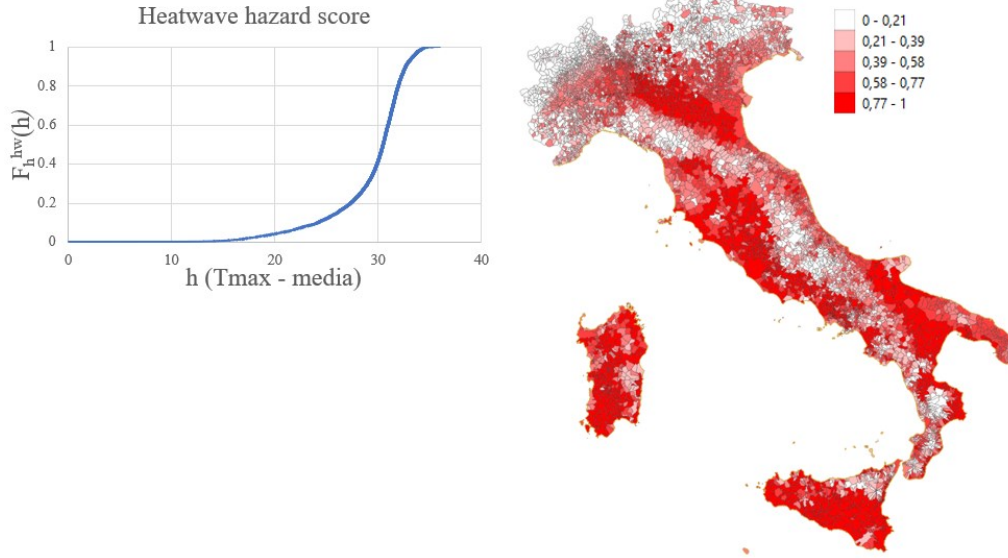


Figure 4242. ECDF of heat wave hazard adopting the monthly average maximum temperature as proxy of the intensity (left) and values of heat wave score for each municipality in Italy (right).

Similar procedures can be applied also considering volcanic, landslides and pluvial floods hazards. Area exposed to volcanic hazard can be derived from the perimeter of areas potentially subject to dangerous phenomena, used in Civil Protection emergency planning (e.g., red zone and yellow zone of Vesuvius and Phlegraean Fields). To build the score, for example, the percentage of residential/industrial areas included in the red zones and yellow zones within a given municipality may be used. Landslides hazard maps are produced by ISPRA and are publicly available. The following hazard levels are considered: very high (P4), high (P3), medium (P2) and low (P1). Landslide prone areas at the different hazard level are identified based on the analysis of the PAI (Hydrogeological Management Plan, "Piano di Assetto Idrogeologico" in Italian) constraints and rules (e.g., land use constraints, requirements). Thus, landslide hazard score can be obtained considering the weighting sum of areas potentially affected by landslides of different hazard level, according to the following equation:

$$Score_{landslide} = (A_{P4} \cdot w_{P4}) + (A_{P3} \cdot w_{P3}) + (A_{P2} \cdot w_{P2}) + (A_{P1} \cdot w_{P1})$$

Where A_{P4} , A_{P3} , A_{P2} and A_{P1} are the areas, expressed in km^2 , potentially affected by P4, P3, P2 and P1 landslides hazard level respectively, and w_{P4} , w_{P3} , w_{P2} and w_{P1} are the weight associated with each hazard from P4 to P1. The suggested values for such weights are 0.4, 0.3, 0.2 and 0.1 respectively for w_{P4} , w_{P3} , w_{P2} and w_{P1} , according to a criterion of decreasing importance.

Pluvial flood-prone areas can be defined as the low elevated areas within the urban watershed where excess runoff accumulates (Schanze, 2018). To characterize pluvial flooding, not only the event intensity and duration (i.e., precipitation depths) but also the physical and social urban features should be investigated. In fact, urban pluvial floods are affected by several local factors such as, for example, the presence and maintenance conditions of the storm drainage system, the existence of underground infrastructures, and the extent of impervious surfaces within the urban watershed (Di Salvo et al., 2017). Thus, pluvial flooding is usually investigated through detailed hydrologic and hydrodynamic simulations. However, those kinds of analyses are usually computationally expensive and require intensive resources. For this reason, other simplified approaches (e.g., Seleem et al., 2021) can be used. Still, their application at large scale throughout the whole Italian territory could be time consuming and would require very refined input data (e.g., DEM of 1 x 1 m horizontal resolution and 20 cm vertical accuracy).

3.6. Citizen-centered exposure data collection for multi-risk exposure development

Citizens are the core of society and play a crucial role in Disaster Risk Reduction (DRR): their actions can actually contribute to amplify or mitigate risks. Societal awareness and action are relevant for all risk components, from hazard to exposure, and for all stages of impact mitigation, from prevention to emergency. This is demonstrated by the increasing number of activities that involve citizens into the alert and response phase (e.g. by assessing perceived ground shaking or identifying building damages). However, there are very few applications in which citizens collect information about the exposed assets and their relationships within the urban systems. Their contribution, when combined with existing exposure assessment frameworks, can increase the temporal and spatial resolution of exposure and support the definition of risk mitigation plans. In addition, citizens learn about the exposure of the areas where they live and, indirectly, become more aware of potential risks (Peresan et al., 2023).

The CEDAS (building CEnsus for seismic Damage ASsessment) methodology explores the possibilities of collecting exposure data with the contribution of trained citizens, including students and the general public. The method consists in training citizens to collect exposure data by means of a google form, tailored to the specific context and knowledge level of participants. It was first implemented in 2021 and 2022, involving more than 300 students from 7 high schools in northeastern Italy. The CEDAS approach consists of three main phases:

1. Training phase: students or citizens are trained, providing them the basic notions on how to assess the characteristics of exposed assets and to statistically analyze the collected data, thus performing citizen science activities.
2. Collection phase: students or citizens collect data using the google form in presence or, if there are any restrictions, remotely based on aerial images of the area, such as those provided by Google Maps and StreetView.
3. Analysis phase: validation of the collected data against known sources (e.g. land use plans) and analysis of the collected data, so as to identify the most common building typologies and characterize the building stock in the study areas.

The google form used for data collection was developed specifically for the project. The list of parameters collected by the CEDAS form implemented in northeastern Italy is provided synthetically here (for further details, refer to Scaini et al., 2023):

- General data on building address and location
- Building use
- Building age, material and construction typology
- Building position and geometry
- Roof type
- Conservation state
- Presence of specific features (e.g. soft floor, irregular height, prominent terraces or roofs)

CEDAS has proven effective for a selected case-study related to earthquakes (Scaini et al., 2022) and allowed collecting exposure data and identifying common building typologies in northeastern Italy (see Figure 42). Building features specific to the study areas, such as reconstructed or retrofitted buildings after the 1976 events, or emerging building typologies (e.g. ecological houses), could be identified by the citizens. Results demonstrate that trained citizens and scientists can fruitfully collaborate in increasing risk-related knowledge and, subsequently, societal resilience in seismic-prone areas.

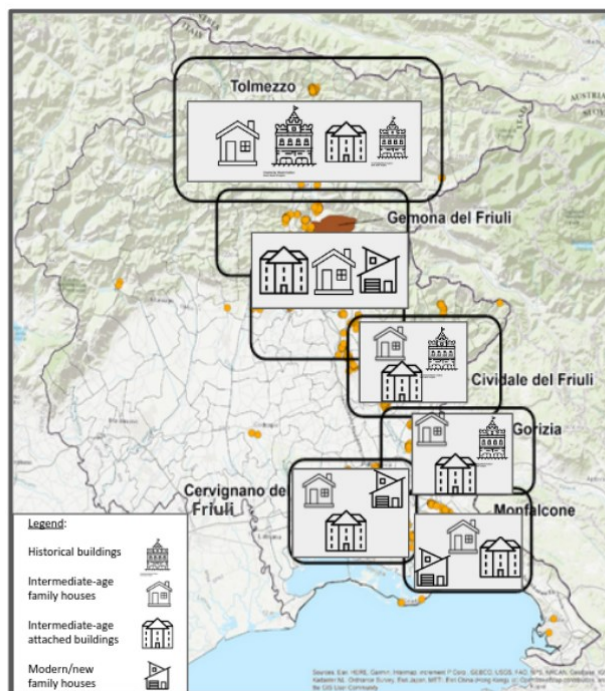


Figure 4343. Building typologies identified while implementing CEDAS in a pilot area in northeastern Italy.

The CEDAS method is potentially applicable to a wide range of contexts, including multiple hazards. Currently it is being implemented by OGS in a multi-hazard context, to assess exposure to earthquake-related hazards such as seismically-induced landslides (Alvioli et al., 2023) or tsunamis (Peresan et al., 2022). The data collection form was updated to accommodate additional indicators such as ground floor elevation and presence of openings, which are relevant to assess exposure to the aforementioned hazards. The method is also being expanded to account for the contribution of other non-expert participants, not only from schools but, for example, volunteering citizens. In addition, the current activities are involving experts in different topics such as civil protection volunteers and practitioners, taking into account their different level of expertise and their knowledge of the specific context.

Current research efforts at OGS are devoted to generalize the approach by validating the data collected by citizens and combining them with aerial images and machine learning. Machine learning methods are already used for damage recognition, but their potential for exposure assessment is still poorly explored despite the increasing availability of potential source data (e.g., from remote sensing). Data collected by citizens will serve as a training dataset for artificial intelligence applications, towards a data driven exposure development. The expected result is a methodology that allows to develop dynamic exposure layers that grasp the changes in the building stock with the help of citizens and automated classification (Figure 43). This approach will be synergically implemented into the SMILE (Statistical MachIne Learning for Exposure development) Project funded by the PRIN 2022 call within the PNRR program.

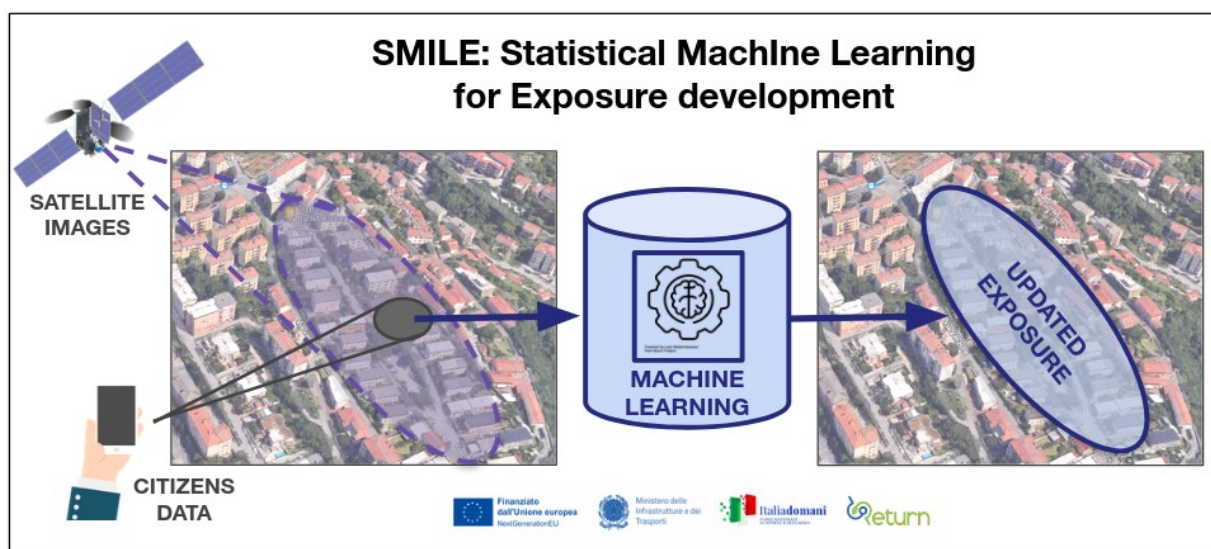


Figure 4444. Sketch of the approach to be implemented within the SMILE project: the data collected by citizens and the satellite images will be processed by a machine learning engine to update the current exposure layers.

The implementation of CEDAS in different contexts will allow to identify which exposure data can be collected by citizens and include them in the exposure framework proposed within RETURN. In particular, the experience of CEDAS can contribute to designing a template for exposure data collection that account for the citizens' active role. CEDAS can therefore contribute to the definition of multi-criteria metrics for the assessment of urban exposure and risks, accounting for their physical and social dimension within a citizen-centered perspective.

4. Urban critical context and Urban Hotspot

4.1. Urban critical context and hotspot identification criteria

Once multi-hazard, multi-exposure, multi-vulnerability, and multi-risk scenarios are assessed it is possible to identify critical urban contexts at urban district level. Aiming to achieve a thorough understanding of the complex relationship between vulnerability, exposure, and hazards, a systemic approach is demanded. As reported in section 4.1.5, a critical urban context can be conceptualized as a complex system that fails to ensure the expected performances across multiple dimensions. As well, in section 5.1 urban critical contexts has been defined by specific taxonomies (urban blocks, building types, construction techniques, soil characteristics, etc.) concerning both the hard (grey and green systems), soft (services supply and process development) and population macro-systems. The relationship between the assets considered for urban critical contexts (built-up features, road traces, geomorphologic conditions, natural boundaries, critical infrastructures, green systems, socio-economic conditions, etc.) and certain key factors in environmental, governance and socio-economic terms supports the identification of a degree of criticality, associated with the characteristics of the subsystems. High exposure and vulnerability, risks and immaterial assets issues supports the concept of hotspot areas as critical factors in urban contexts, to be verified through index and indicator systems (single or composite), modelling and simulations. The identification of such areas prioritises the application of strategies and actions for adaptation, vulnerability and exposure reduction, and resilience enhancement. In those areas, as reported in Figure 44, multi-criteria assessments should be developed as the operational translation of the research objectives; to reach the targets of such objectives, a proper assessment methodology should be elaborated to measure and compare different alternatives.

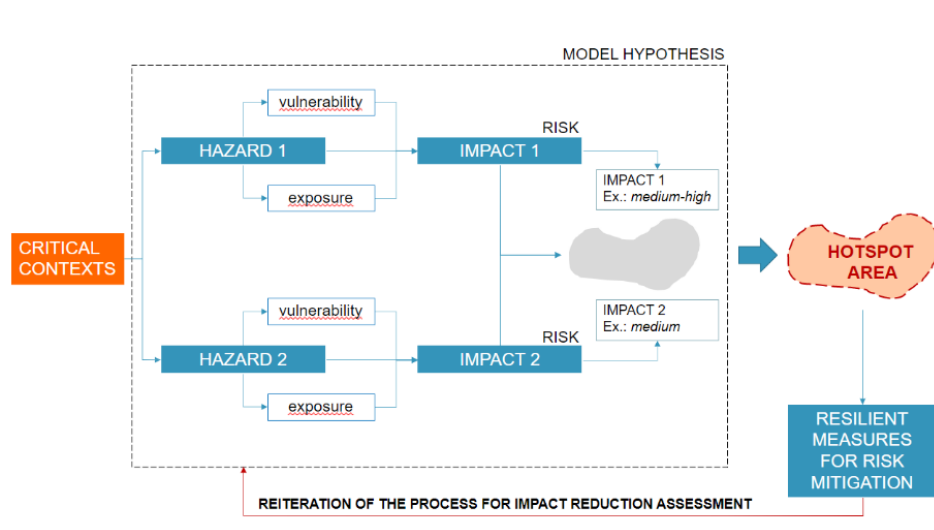


Figure 4545. Process definition and model hypothesis to outline hotspot areas in critical contexts. The application of strategies and actions for risk mitigation (adaptation, vulnerability and exposure reduction, and resilience enhancement) should be tested to assess impact reduction.

Since the common approaches regarding multi-risk methodologies are focused on the quantitative assessment of the multi-risk, a detailed analysis of hazard and vulnerability correlations through indexes and indicators is therefore to be expected (Gallina et al. 2016), taking also into account that the single risks within a multi-risk assessment are usually computed using a common unit of measure (e.g. loss of lives, economic losses, 0-1 normalization). The development of a composite visualization highlights areas affected by different classes of the total risk (e.g., Bell and Glade, 2004b; Wipulanusat et al., 2009) providing a classification of the different areas more affected than other by the investigated hazards in order to provide useful tools for stakeholders and decision makers in the management of risks. These indicators answer the needs of a communication strategy but fail at representing the complexity of multi-risk situations over territories (Carpignano et al., 2009).

Moreover, although multi-risk practices are often used on large scales, regional and local scales remain essential levels for the risk analysis and the adoption of risk management strategies in the perspective of disaster prevention and management (Carpignano et al., 2009). The development of a composite visualisation of the different hazards affecting the same area (Schmidt-Thome e, 2006; Frigerio et al., 2012; Kappes et al., 2012a) and the following multi-hazard assessment at the sub-urban scale would be effective in identifying spatial distribution of principle drivers of risk that might change within a city (Johnson, Depietri, Breil, 2015).

Several authors have contributed to the definition of spatial and analytical criteria to outline hotspot areas (Table 8). Starting from 2001, the World Bank's Disaster Management Facility (DMF, 2001) proposed a global scale multihazard risk analysis focused on identifying key "hotspots" where the disasters risks are particularly high aiming to provide information and methods to inform priorities for reducing disaster risk and making decisions on development investment. Accounting for climatic hazards (drought, flood, storms) and natural hazards (landslides, earthquakes, eruptions) DMF identifies disaster risk hotspots on a global scale based on criticality levels associated to simple indicators (mortality risk and economic losses).

Table 7. Hotspot definitions

YEAR	SOURCES	DEFINITION OF HOTSPOT	HAZARD CONSIDERED
2001	World Bank's Disaster Management Facility (DMF, 2001)	"Cells falling into the highest three deciles for either mortality or economic losses are considered <i>disaster risk hotspots</i> ."	Drought, flood, earthquakes, landslides, storms, eruptions, storms
2005	Natural Disaster Hotspot. A Global Risk Analysis (Dilley et al., 2005)	"Specific area or region that may be at relatively high risk of adverse impacts from one or more natural hazard events" OR "Hotspot countries where more than half of the country's Gross Domestic Product is at risk from two or more hazards"	Geophysical (earthquake, volcanoes), hydrological (flood, landslides, cyclones), drought
2005	Natural disaster hotspots case studies (Arnold, M.)	"where the risks of natural disasters are particularly high"	Drought, landslides, storm surge, floods, cyclones,
2009	A methodological approach for the definition of multi-risk maps at regional level: first application (A. Carpignano, E. Golia, C. Di Mauro, S. Bouchon & J-P. Nordvik)	"Multi-risk maps help understanding of how hazards and vulnerabilities are combined over a territory and give a more accurate representation of the complexity of the risks for an area [...], showing a prioritization of the areas where it is more urgent to take measures to reduce the risks."	earthquakes, Na-Tech, landslides, floods, forest fires
2012	Multi-hazard analysis in natural risk assessment (Bell & Glade, 2012)	"Different areas more affected than other by the investigated hazards. The spatial-oriented maps can be used by different end-users to know specific information in the form of quantifiable risk metrics for the implementation of adaptation measures and planning." (e.g., Bell and Glade, 2004b, Wipulanusat et al., 2009)	Snow avalanches, debris flow, rock falls
2015	Multi-hazard risk assessment of two Hong Kong districts (Johnson, Depietri, Breil)	Where green or grey infrastructures might be needed most. Mapping indicators indicates potentially problematic areas where further investigation and policy action is needed in order to reduce vulnerabilities	Heatwave, landslides, storm surge
2015	A Spatial Framework to Map Heat Health Risks at Multiple Scales (Ho et al., 2015)	"Areas of elevated heat health risks"	Extreme heat events



2016	A multi-disciplinary approach to evaluate pluvial floods risk under changing climate: The case study of the municipality of Venice (Italy) (Sperotto et al., 2016)	"Areas more susceptible to be damaged by pluvial floods"	Pluvial flood
2016	Multi-hazard risk assessment of two Hong Kong districts (Depietri, 2016)	"The identification of hotspots of vulnerability, where more than one potential hazard can have impacts, providing specific indications for disaster preparedness. Under this perspective, the effects of hazards are considered simply additive, with overlapping impacts."	Heat waves, landslides, typhoons
2017	What is a Hotspot Anyway?	"burden hotspot," to denote areas of elevated disease prevalence or incidence; "transmission" or "risk hotspot," to denote areas of elevated transmission efficiency or a higher risk of disease acquisition; and "emergence hotspot," to denote areas with an increased probability of disease emergence or reemergence.	Infectious disease spreading
2017	Integrative assessment of climate change for fast-growing urban areas: Measurement and recommendations for future research (Scheuer et al., 2017)	"Urban land where climate change will likely have a comparatively high impact"	Water scarcity, drought, flooding and heatwaves
2018	Multi-hazard risks in New York City (McPhearson, 2018)	The spatial combination of more than one hazard allows the identification of potential hotspots of risk and vulnerability, accounting the effects of the hazards as additive, with overlapping degrees of impacts in the same locations to be considered jointly.	Heat waves, inland flooding and coastal flooding
2020	Be (and have) good neighbours! Factors of vulnerability in the case of multiple hazards (Pagliacci, Russo, 2020)	"Municipalities with high multi-hazard index, with high socioeconomic and material vulnerability of themselves and of their neighbourhood"	Earthquake, landslide, flood hazard
2020	A Multi-Risk Methodology for the Assessment of Climate Change Impacts in Coastal Zones (Gallina et al., 2020)	"Relevant socioeconomic elements such as infrastructure and population were also considered in the analysis, selected as potential risk hotspots in urban areas" "Vulnerable hotspots where the resilience to multiple hazards (i.e., permanent/temporary inundation and coastal erosion) should be increased."	Sea-level rise, storm surge, coastal erosion
2021	Multi-Risk Climate Mapping for the Adaptation of the Venice Metropolitan Area (Maragno et al., 2021)	"Areas that are less resilient to an impact". "In multi-risk exposed areas, the mix of urban fabric patterns contributes to vulnerability levels, worsening the multi-dimensional conditions that trigger climate impacts. Results show which urban assets have the highest priority in implementing adaptation measures and actions, enabling strategic coordination for multi-hazard management by public decision-makers".	Heatwave, Flooding
2022	Methodology for the Assessment of Multi-Hazard Risk in Urban Homogenous Zones (Mladineo et al., 2022)	Ranked homogenous zones in terms of the relative proneness to coupled seismic, sea floods and extreme sea waves hazards along with exposure and vulnerability analysis	Earthquake, flood and extreme waves

2023	Framework for multirisk climate scenarios across system receptors with application to the Metropolitan City of Venice (Sambo et al., 2023)	"The multirisk maps provide suitable information for setting priorities for further investigations and could be useful during the elaboration of climate change adaptation plans, identifying hotspots where it can be necessary the implementation of risk management actions."	Storm surge, intense precipitations, heat waves, drought
2023	Anthropogenic influence on extremes and risk hotspots (Estrada, 2023)	"Regions for which increased risk of extreme events and high exposure in terms of either high Gross Domestic Product (GDP) or large population are both present.	Extreme precipitation and temperatures
	Munich Re's Risk Management Partners	"Where natural hazard impacts may be largest"	River flood, flash flood, storm surge, typhoons, eruption, earthquake, tsunami, wildfires, extreme weather

4.1.1. Challenges and methods to hotspot assessment

The identification of hotspot areas within urban critical contexts is a key aspect to support decision makers in multi-risk scenarios. Whereas spatial overlap among different risks presents still a degree of uncertainty, a common approach (Sperotto, 2016; Depietri, 2016; Depietri, 2018; Mladineo, 2022; Sambo, 2023) has been developed, consisting in the definition of aggregated risk indexes derived from the combination of scenarios–damage indicators. The multi-risk assessment comprises both multi-hazard and multi-vulnerability concepts, considering possible hazards and vulnerability interactions (Carpignano et al., 2009; Garcia-Aristizabal and Marzocchi, 2012a, 2012b). Each risk is analysed separately, and then the aggregation allows a multi-risk index evaluation. The methodological steps can be summarised as follows:

1. Hazard assessment;
2. Exposure assessment of elements at risk;
3. Vulnerability assessment;
4. Single-risk assessment;
5. Multi-risk assessment.

Climate change related issues and challenges for the multi-risk assessment	
Application context	<ul style="list-style-type: none"> - Identify the objective of the analysis; - Define the time frame; - Distinguish the scale of analysis; - Detect the most appropriate resolution; - Review the available data sources for multi-hazards and associated risks; - Define the approach to be used (multi-hazard, multi-hazard risk, multi-risk); - Consider the involved uncertainties of input information.
Multi-hazard	<ul style="list-style-type: none"> - Improve climate models and analysis; - Define the temporal window to be considered; - Identify appropriate climate variables; - Assess cumulative effects of hazards; - Consider cascade and triggering effects in different scenarios; - Provide climate change scenarios with an associated probability and uncertainty; - Differentiate between short-term triggers and long-term changes.
Exposure	<ul style="list-style-type: none"> - Identify the elements potentially at risk (e.g. population, agriculture, infrastructures, buildings); - Consider the spatiotemporal dimensions for each element at risk (e.g. night-/daytime population); - Provide an ecosystem approach in order to integrated different sectors and their interrelationships; - Provide future scenarios of the elements potentially at risk.
Vulnerability	<ul style="list-style-type: none"> - Identify vulnerability factors for the characterization of the exposure; - Calculate vulnerability functions for each element at risk and the corresponding hazards; - Consider herein also a changing resilience towards a given impact – may in–or decrease; - Provide future scenarios of the vulnerability factors that should be considered to be dynamic (e.g. vegetation cover, population density); - Provide a coupling model land-use/climate model; - Provide a common scale of comparison for a suitable aggregation of the vulnerability factors.
Multi-risk	<ul style="list-style-type: none"> - Identify a common scale of comparison; - Consider the different data requirements for the variety of processes and elements at risk; - Identify the most suitable aggregation method: qualitative, semi-quantitative and quantitative approach.
Facing the challenges	<ul style="list-style-type: none"> - Identify the final users; - Increase the awareness of the stakeholders; - Involve stakeholders and final users at an early stage in the multi-risk process; - Managing the huge amount of data with different, hazard and elements at risk dependent units of measurements; - Aggregate these different unit of measurements; - Communicate the uncertainty of the assessment due to the uncertainty associated to climate models and to the error propagation; - Explain openly the assumptions and limitations of each assessment in order to avoid misjudgement; - Provide an easy-visualization of the outputs in a climate service perspective for management purposes.

Figure 4646. Climate change related issues and challenges for the multi-risk assessment (Source: Gallina et al., 2016).

The elements potentially at risk are identified in the exposure phase that allows the representation of different features of the territory. The multi-risk assessment approaches consider commonly in literature the exposure as referred to the following elements: population, socioeconomic and cultural assets, infrastructures and environment. Moving to integrated exposure of element at risk (see par. 2.3) a multi-risk methodology requires a multidimensional approach, also addressing vulnerability together with exposure to ensure effectiveness in disaster management measures allowing thus to know the distribution of exposed asset at territorial level and their characteristics that mostly affect their performance against one or more hazards.

Accounting for the difficulties while aggregating different indexes relevant to the multi-risk assessment, different approaches (qualitative, semi-qualitative, quantitative) could support the process through different phases. To this extent, to tackle the issues related to different measurement units Carpignano et. al. adopted a quantitative approach; overlapping hazards spatial representations on vulnerability maps related to territorial elements, outlining single risk maps. Once risk indexes related to a single-risk scenario are combined, an overall risk index could be defined as comprehensive of the potential effects of more hazards on the same exposed asset. Editing of the maps allows introduction of political criteria to evaluate aggregated indicators in such way that it is possible to attribute a level of importance to each damage indicator, allowing to highlight the most critical aspects of a territory in agreement with politic strategies carried out by authorities (Carpignano et al., 2009). As well, the spatial-oriented maps can be used by different end-users to know specific information in the form of quantifiable risk metrics for the implementation of adaptation measures and planning (e.g., Bell and Glade, 2004b, Wipulanusat et al., 2009). To weight comprehensively hazards and aspects of vulnerability and define relations between the single hazard and exposure levels, the need of collaboration with stakeholders is also underlined by Johnson, Depietri, Breil (Johnson et al. 2015). To the extent of the present research, once defined a Proof of Concept to be tested in Urban Living Labs, the set of damage indicators as selected could be further refined in an iterative process.

Regarding multi-risk issues, to account for the effect of uncertainty of climate change simulation on the hazard indicators, and consequently on the final risk estimates, an ensemble of scenarios based on a multimodel approach has been proposed by Sambo et al. (Sambo et al., 2023). Therefore, to obtain a prioritization of risk level in the considered areas a combination of climate-change-related hazards approximated by anomalies of climate indexes with high-resolution exposure and vulnerability indicators of targets representative for the economic, social, natural, cultural, and manufactured capitals of the region of interest has been carried out.

The identification of priority receptors (i.e., element at risk) and the assessment of their predisposition to be adversely affected by a climate-related extreme event given their intrinsic physical and socio-economic features has been proven to be an effective strategy to outline focus areas.

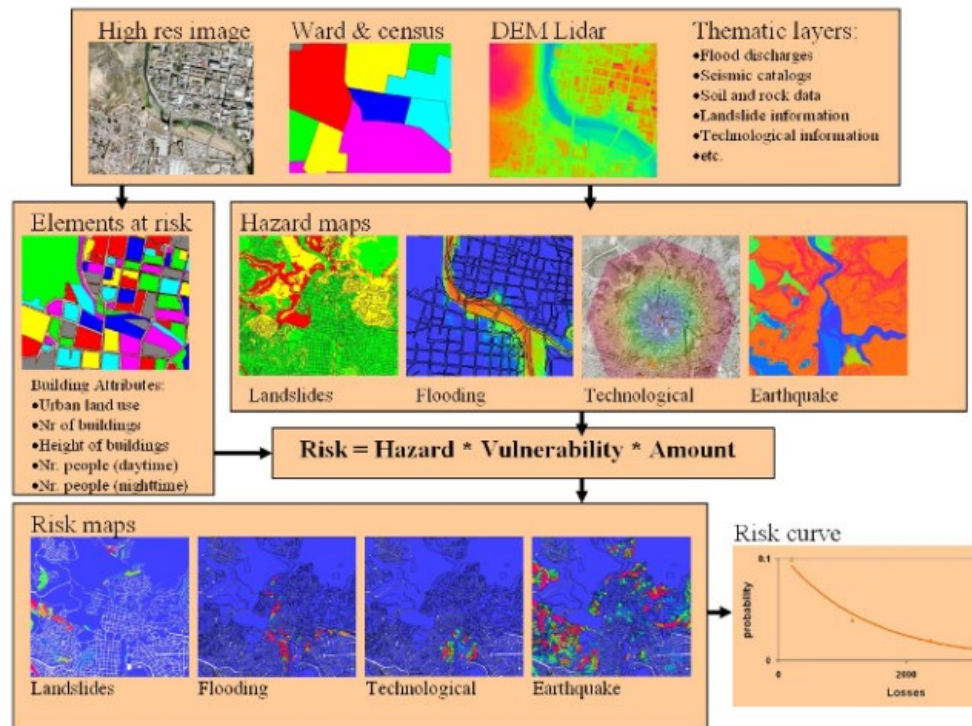


Figure 4747. Multi-risk assessment process. The definition of risk curves depends on the combination of different indexes related to single risks. The risk assessment process is developed using spatial information on hazards, elements at risk and vulnerability with the use of GIS based tools and remote sensing. (Source: Risk City Application of GIS for multi-hazard risk assessment in an urban environment Cees van Westen, ISL, 2004).

4.1.2. Relevant implications for hotspot assessment

Based on the results derived from the scoping review (see 4.1.1), aiming to propose a shared methodology for the assessment of risk hotspots in urban and metropolitan settlements, the following criteria can be considered:

- **multi-risk issues, considering also climate change**, should be prioritized. Despite the interest about the multirisk assessment is increasing, still few examples of applications are found (Gallina et al., 2016);
- **priority receptors** (i.e. element at risk) should be identified assessing their predisposition to be adversely affected by extreme events, including the climate-related ones, given their intrinsic physical and socio-economic features; receptors belong to five different capital typologies commonly used in climate risk and sustainability assessment (Goodwin, 2003): Manufactured Capital (MC), Social Capital (SC), Cultural Capital (CC), Natural Capital (NC), Economic Capital (EC).
- **GIS-based approach** could support decision-makers due to the relevant insight derived from mapping and analyzing geographical data in multi-risk scenarios;
- **composite indicators** could be derived from the combination of scenarios–damage indicators to outline hotspot areas, defining **thresholds** for integrated indicators (see par. 6.1). Since the result is sensitive to the hazard, exposure, and vulnerability indicators selection and assessment scores, changing them has consequences on the final risk and multirisk assessment. For such reason, a sensitivity analysis on indicators choice should be provided.
- **integrated vulnerability and exposure** need to be defined as assessment methodologies, possibly including dynamic aspects often non included in risk assessment (de Ruiter & van Loon, 2022)

- **decision-making methods** combining **risk and decision analytics** need to be defined, involving the use of proxy variables (to be weighted and tested) that correlate with underlying hazard-exposure-vulnerability factors of interest.
- **interactions among hazards** should be analysed by means of **cause-effects matrix** (De Pippo et al., 2008; Garcia-Aristizabal and Marzocchi, 2012c; Kappes et al., 2012), allowing a semi-quantitative estimate of the relationships between agents and processes in the evolution of a system, or from the **probabilistic analysis of historical databases** that already take into account triggering and cascade events (e.g. tsunami databases that already included the possibility of an earthquake triggered tsunamis) (Marzocchi et al., 2012).
- **final users and stakeholders identification** (e.g. researches, public local administrations, national institutions) is required to implement a comprehensive multirisk assessment, taking into account also climate change, into management strategies. The early involvement of stakeholders in the process through the Urban Living Lab and risk storylines setting could help the identification of their needs and the communication of the result.
- **uncertainties** need to be accounted and communicated to provide **results** capable of prioritize systemic adaptation strategies related to the elaboration of multirisk scenarios.

4.2. The use of indicators to identify urban critical context/hotspots taking into account heatwaves and air pollution

An Air Quality Index (AQI) is an indicator that takes into account all typical sources of air pollution. These sources are mostly gaseous pollutant, such as ozone O₃, nitrogen oxides NO_x, carbon monoxide CO, carbon dioxide CO₂, sulphur dioxide SO₂, trace elements or compounds such as lead Pb, arsenic As, nickel Ni, cadmium Cd, and PAH (Polycyclic Aromatic Hydrocarbons), and Particulate Matter. Environmental Agencies define single indicators and guidelines for monitoring and regulating concentrations of each pollutant within urban areas. For example, WHO defined guidelines for the maximum values of 24-hour averaged PM_{2.5} and PM₁₀, and of 8-hour or 24-hour averaged concentrations of gaseous pollutants (WHO, 2021). However, in order to have a clear representation of air quality within an area, the concentration levels of other pollutants need to be quantified and aggregated to PM concentrations.

Each Environmental Agency has defined a different Air Quality Index. These indexes are examples of composite indicators that take into consideration the combined effects of different sources of air pollution within a city and other populated areas. There is not a standard way to define an AQI. For example, the AQI defined by the European Environment Agency (EEA, www.eea.europa.eu/) comprises six qualitative categories describing the air quality over an area (Good, Fair, Moderate, Poor, Very poor, Extremely poor); each category is defined by range values of up to five air pollutants, and by health messages that provide recommendations to the general population and to more sensible groups (www.airindex.eea.europa.eu/, see also the following Figure). Range values for each considered pollutant are based on the report by WHO about the Health Risks of Air Pollution in Europe project (HRAPIE project report: WHO, 2013), taking PM_{2.5} as a basis for driving the index. The current AQI for a certain location is compiled from hourly ground-based measurements from EEA member countries, or from the European Union's Copernicus Atmosphere Monitoring Service (CAMS) if they are missing; modelled values from CAMS are also used to forecast AQI for the following 24 hours.

Pollutant	Index level (based on pollutant concentrations in µg/m ³)						AQ index	General population	Sensitive populations
	Good	Fair	Moderate	Poor	Very poor	Extremely poor			
Particles less than 2.5 µm (PM _{2.5})	0-10	10-20	20-25	25-50	50-75	75-800	Good	The air quality is good. Enjoy your usual outdoor activities.	The air quality is good. Enjoy your usual outdoor activities.
Particles less than 10 µm (PM ₁₀)	0-20	20-40	40-50	50-100	100-150	150-1200	Fair	Enjoy your usual outdoor activities	Enjoy your usual outdoor activities
Nitrogen dioxide (NO ₂)	0-40	40-90	90-120	120-230	230-340	340-1000	Moderate	Enjoy your usual outdoor activities	Consider reducing intense outdoor activities, if you experience symptoms.
Ozone (O ₃)	0-50	50-100	100-130	130-240	240-380	380-800	Poor	Consider reducing intense activities outdoors, if you experience symptoms such as sore eyes, a cough or sore throat	Consider reducing physical activities, particularly outdoors, especially if you experience symptoms.
Sulphur dioxide (SO ₂)	0-100	100-200	200-350	350-500	500-750	750-1250	Very poor	Consider reducing intense activities outdoors, if you experience symptoms such as sore eyes, a cough or sore throat	Reduce physical activities, particularly outdoors, especially if you experience symptoms.
							Extremely poor	Reduce physical activities outdoors.	Avoid physical activities outdoors.

Figure 4848. Left, European Air Quality Index categories and related pollutant range values; right, health messages associated with each category (source: European Environment Agency)

4.2.1. Heatwave

The World Meteorological Organization (WMO) has not adopted yet a standard and mathematically rigorous definition for heat waves, although heat waves are generally understood as “periods of abnormally high temperatures recorded over a long period of time” (Ramis and Amengual, 2019). These high temperatures refer not only to maximum temperatures, but also to minimum night temperatures. Thermal stress to people can be further exacerbated by high levels of humidity and reduced wind intensities. As such, though heat waves are meteorological events, they cannot be assessed without referring to human impacts (Robinson, 2001). Physiological aspects are related to the general thermoregulation of the human body and depend on several factors including age, sex, health condition, prior conditioning through living in a particular climate and/or recent exposure to extreme warm conditions.

A variety of metrics have been introduced based on temperature thresholds, synoptic patterns, thermal stress indices and also holistic indicators to define heat waves. In addition, among temperature or thermal indices, definitions can be based on relative (e.g., Alexander et al., 2006; Fischer and Schär, 2010) or absolute thresholds (e.g., Baccini et al., 2008), or even on their combination (e.g., Beniston et al., 2007). The choice of a specific metric depends on the scope and subject of the work, with absolute thresholds more convenient for analyzing extreme events of a fixed intensity, and relative ones used for the identification of extreme episodes of a fixed rarity.

Indeed, heat waves and more generally extremely high temperatures impact not only on human and animal health, but also on worker productivity, agricultural production, ecosystems and economies (Zuo et al., 2015). In addition, adverse effects extend to the built environment and critical infrastructure such as buildings, water, transportation and energy systems (Boyle et al., 2010).

Thus, according to the subjects exposed to the extremely high temperatures of interest, there are different definitions that can be adopted. As for the factors that can have a major impact on people, there are many indicators using bio-meteorological or holistic approaches such as:

- Bio-meteorological indices: heat index, humidex, apparent temperature, excess heat index, human energy-budget based indices (e.g., standard effective temperature, perceived temperature, physiological equivalent temperature, universal thermal climate index) (Zare et al., 2018).
- Holistic approach: wet-bulb globe temperature, health-related assessment of the thermal environment, Heat Stress Index, Excess Heat Index-acclimatization, Excess heat factor (Zare et al., 2018).

In detail, we describe in the following a list of indicators that are significant to represent the hazard potential of high temperatures.

Heat index: The heat index, also known as the apparent temperature, is what the temperature feels like to the human body when relative humidity is combined with the air temperature. This has important considerations for the human body's comfort. When the body gets too hot, it begins to perspire or sweat to cool itself off. If the perspiration is not able to evaporate, the body cannot regulate its temperature. Evaporation is a cooling process. When perspiration evaporates off the body, it effectively reduces the body's temperature. When the atmospheric moisture content (i.e. relative humidity) is high, the rate of evaporation from the body decreases. In other words, the human body feels warmer in humid conditions. The opposite is true when the relative humidity decreases because the rate of perspiration increases. The body actually feels cooler in arid conditions. There is direct relationship between the air temperature and relative humidity and the heat index, meaning as the air temperature and relative humidity increase (decrease), the heat index increases (decreases). This is particularly important during moist heat waves, when temperatures alone are not sufficient to assess the heat stress experienced by the human body (Cvijanovic et al. 2023). The original definition and calculation of the index was developed in the US with temperatures expressed in °F, but this definition is now adopted also in Europe and following is a table showing its calculation, while on the web different calculators are also available.

		Umidità relativa															
		20%	25%	30%	35%	40%	45%	50%	55%	60%	65%	70%	75%	80%	85%	90%	
T E M P E R A T U R E	41°C	41	43	45	48	51	54										
	39°C	38	39	41	43	46	49	52	55								
	37°C	35	36	38	39	41	43	46	49	51	55						
	35°C	33	34	35	36	37	39	41	43	45	48	50	53				
	33°C	31	31	32	33	34	35	36	38	40	41	44	46	48	51	54	
	31°C	29	29	30	30	31	32	33	34	35	36	38	39	41	43	45	
	29°C	27	28	28	28	29	29	30	30	31	32	33	34	35	36	37	
	27°C	26	26	26	27	27	27	27	28	28	28	29	29	30	30	31	
Conseguenze																	
27-31°C		Possibile affaticamento, crampi di calore															
32-39°C		Forte affaticamento, difficoltà nella respirazione															
40-54°C		Possibile colpo di calore, insolazione															
oltre 54°C		Colpo di calore altamente probabile															

Figure 4949. Heat index calculation and consequences on human health. Green refers to possible fatigue, and heat cramp. Light orange refers to high fatigue, and respiratory difficulties. Dark orange refers to possible heat stroke and insolation. Red refers to highly probable heat stroke.

Humidex: on a similar approach and based on an empirical formula considering air temperature and vapor tension instead of the relative humidity, this index calculates a perceived temperature taking into account temperature and humidity conditions.



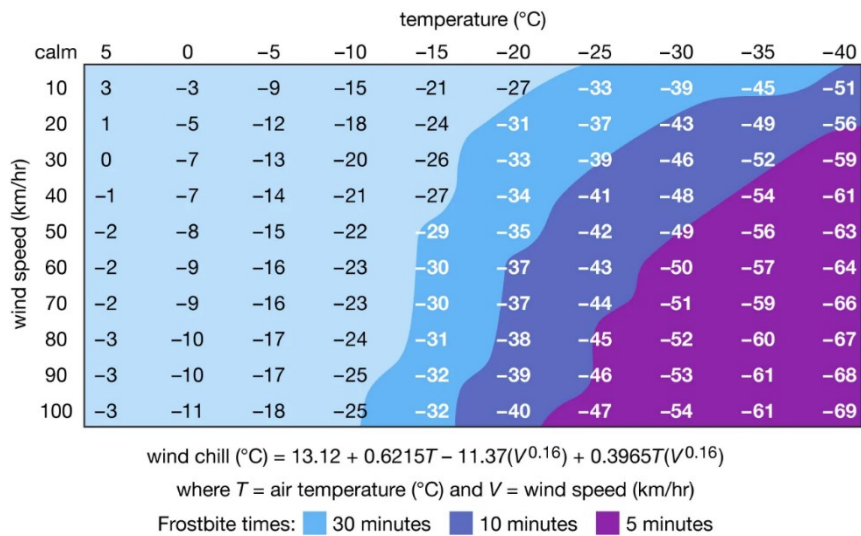
	25%	30%	35%	40%	45%	50%	55%	60%	65%	70%	75%	80%	85%	90%	95%	100%
42°	48	50	52	55	57	59	62	64	66	68	71	73	75	77	80	82
41°	46	48	51	53	55	57	59	61	64	66	68	70	72	74	76	79
40°	45	47	49	51	53	55	57	59	61	63	65	67	69	71	73	75
39°	43	45	47	49	51	53	55	57	59	61	63	65	66	68	70	72
38°	42	44	45	47	49	51	53	55	56	58	60	62	64	66	67	69
37°	40	42	44	45	47	49	51	52	54	56	58	59	61	63	65	66
36°	39	40	42	44	45	47	49	50	52	54	55	57	59	60	62	63
35°	37	39	40	42	44	45	47	48	50	51	53	54	56	58	59	61
34°	36	37	39	40	42	43	45	46	48	49	51	52	54	55	57	58
33°	34	36	37	39	40	41	43	44	46	47	48	50	51	53	54	55
32°	33	34	36	37	38	40	41	42	44	45	46	48	49	50	52	53
31°	32	33	34	35	37	38	39	40	42	43	44	45	47	48	49	50
30°	30	32	33	34	35	36	37	39	40	41	42	43	45	46	47	48
29°	29	30	31	32	33	35	36	37	38	39	40	41	42	43	45	46
28°	28	29	30	31	32	33	34	35	36	37	38	39	40	41	42	43
27°	27	27	28	29	30	31	32	33	34	35	36	37	38	39	40	41
26°	26	26	27	28	29	30	31	32	33	34	34	35	36	37	38	39
25°	25	25	26	27	27	28	29	30	31	32	33	34	34	35	36	37
24°	24	24	24	25	26	27	28	28	29	30	31	32	33	33	34	35
23°	23	23	23	24	25	25	26	27	28	28	29	30	31	32	32	33
22°	22	22	22	22	23	24	25	25	26	27	27	28	29	30	30	31

Figure 5050. Humindex calculation: relative humidity in the abscissa and temperature on the ordinate axis.

Thom discomfort index: it indicates the level of discomfort as a result of high temperature and the combined effect with relative humidity. It is based on dry-bulb and wet-bulb temperature (Thom 1957, Epstein and Moran 2006).

Wind chill index: it is a measure of the rate of heat loss from skin that is exposed to the air. It is based on the fact that, as wind speeds increase, the heat loss also increases, making the air “feel” colder. Wind chill is usually reported as a “wind chill temperature” or “wind chill equivalent”—that is, the temperature under calm air at which heat loss would be equal to the loss actually being experienced because of higher wind speeds. For example, a temperature of -25°C in calm air would have a wind chill temperature equal to the actual air temperature. Under these conditions, exposed skin would freeze in 30 minutes. At a wind speed of 40 km per hour, however, the wind chill temperature would be -41°C , and skin would freeze in less than 10 minutes. Wind chill indices, the formulas and assumptions used to calculate wind chill temperatures, have varied over the years. For the second half of the 20th century, weather forecasts in North America commonly used the Siple-Passel index, based on wind speeds measured by an anemometer 10 metres (33 feet) above the ground. During the winter of 2001–02, the U.S. National Weather Service (see also weather bureau) and the Meteorological Service of Canada introduced a new index based on heat lost from the exposed faces of 12 volunteers in a chilled wind tunnel. Calm air is considered to have winds of 5 km (3 miles) per hour or less. Clear night sky conditions are assumed, eliminating any warming effect of the Sun.

Wind chill chart (Celsius)



Sources: U.S. National Weather Service and Meteorological Services of Canada.

Figure 5151. Wind chill calculation and value. Source: Britannica, 2023.

Heat index: it is an index that combines air temperature and relative humidity, in shaded areas, as an attempt to determine the human-perceived equivalent temperature, as how hot it would feel if the humidity were some other value in the shade. The heat index was developed in 1978 by George Winterling as the "humiture" and was adopted by the USA's National Weather Service a year later. It is derived from work carried out by Robert G. Steadman. Like the wind chill index, the heat index contains assumptions about the human body mass and height, clothing, amount of physical activity, thickness of blood, sunlight and ultraviolet radiation exposure, and the wind speed. Significant deviations from these will result in heat index values which do not accurately reflect the perceived temperature.

Standard effective temperature: Standard effective temperature (SET) is a commonly used index in thermal comfort evaluation. It was established based on two-node model which could reflect thermal regulation process of human body. SET has advantages in environment evaluation compared with ET (only considered the air temperature and relative humidity), in which six parameters, air temperature, radiation temperature, relative humidity, air velocity, metabolic rate and clothing insulation, are converted into a SET index. In the paper published in 1986 (Gagge et al., 1986), Gagge et al. presented the new effective temperature (ET*) and the new standard effective temperature (SET*). Due to its complex definition and calculation method, SET has been revised many times since proposed, and it is necessary to analyse and unify the application of SET index thoroughly (Ji et al., 2022).

Perceived temperature: it is an equivalent temperature based on a complete heat budget model of the human body. It has proved its suitability for numerous applications across a wide variety of scales from micro to global and is successfully used both in daily forecasts and climatological studies (Staiger et al., 2013). PT (°C) is the air temperature of a reference environment in which the thermal perception assessed by PMV would be the same as in the actual environment. PT enables an adjustment of clothing from wintry, $I_{cl}=1.75$ clo, to summery, $I_{cl}=0.50$ clo, in order to achieve thermal comfort ($PMV=0$). If this is not possible, cold stress or heat stress will occur. In the reference environment, t_{mrt} equals t_a , and wind velocity is reduced to a slight draught. Water vapour pressure is the same as in the actual environment. In case of condensation in the reference environment, the dew point temperature is set to PT.

Physiological equivalent temperature: PET is defined as the air temperature at which, in a typical indoor setting (without wind and solar radiation), the heat budget of the human body is balanced with the same core and skin temperature as under the complex outdoor conditions to be assessed (Höppe, 1999).

Universal thermal climate index: The universal thermal climate index (UTCI) is an equivalent temperature (°C), it is a measure of the human physiological response to the thermal environment. The universal thermal climate index (UTCI) describes the synergistic heat exchanges between the thermal environment and the human body, namely its energy budget, physiology and clothing. UTCI takes into consideration the clothing

adaptation of the population in response to actual environmental temperature. There are four variables required to calculate the UTCI: 2m air temperature, 2m dew point temperature (or relative humidity), wind speed at 10m above ground level and mean radiant temperature (MRT). Verification metrics has demonstrated that UTCI city point thresholds at the 95th percentile, exceeded for at least 3 consecutive days both at day- and nighttime ($15 \pm 2^\circ\text{C}$ and $34.5 \pm 1.5^\circ\text{C}$, respectively), are successful in identifying the number of the days with excess mortality while minimizing misses and false alarm (Di Napoli et al., 2019).

Wet-bulb globe temperature: The WetBulb Globe Temperature (WBGT) is a measure of the heat stress in direct sunlight, which takes into account: temperature, humidity, wind speed, sun angle and cloud cover (solar radiation). This differs from the heat index, which takes into consideration temperature and humidity and is calculated for shady areas.

Heat Stress Index: a quantitative composite measure which integrates into a single number one or more of the thermal, and/or physical, and personal factors affecting heat transfer between the person and the environment. Many heat stress indices have been developed and these can be classified as those based on: physical factors of the environment, thermal comfort assessment, "rational" heat balance equations, and physiological strain (Witherspoon and Goldman, 1974).

Relative strain index: The relative strain index (RSI) was developed by Lee and Henschel (Lee, 1965). It is also a measure of discomfort resulting from the combined effect of temperature and humidity. It assumes a person dressed in a light business suit, walking at a moderate pace in a very light air motion. It is applicable to assess heat stress of manual workers under shelter at various metabolic rates.

Mora's threshold: The deadliness threshold is a product of a classification model based on heat-related mortality data from around the world and the associated climatic data, it is simple to use since the threshold can be represented using only dry bulb temperature and relative humidity (Mora et al., 2017). With regard to adding more environmental variables to the model, Mora et al. (2017) was only able to marginally increase classification accuracy when other variables (such as mean daily wind speed, and/or mean daily solar radiation) are added. One of the limitations of this metric is the classification model is only trained with mortality and climatic data, in which other factors such as age and socio-economic conditions are not considered.

Excess heat factor: it is a health-relevant heatwave (HW) indicator (Oliveira et al., 2022). The rationale supporting the EHF definition is to identify and quantify extreme temperatures as the three-day mean air temperature deviation from the long-term percentile-based climatology, in a given day of the year (DOY), multiplied by the past month acclimatization index (if > 1) (Nairn and Fawcett, 2013). As a result, the EHF is a quadratic function of both the long-term and short-term air temperature anomalies, and its magnitude reflects the human acclimatization to the local climate. Although the EHF does not include humidity in its calculation, it uses daily mean temperature (TM) as the simple average between the daily maximum (TX) and minimum (TN) temperature values, which is implicitly affected by relative humidity changes; hence, according to the authors (Nairn and Fawcett, 2013), the EHF provides local public health stake-holders with a simpler but efficient method to estimate potential human excess heat exposure levels, compared to other bioclimatic indices, such as the Universal Thermal Climate Index (UTCI) (Zare et al., 2018), the Physiological Equivalent Temperature (PET) (Matzarakis et al., 1999) or Apparent Temperature (AT), which require additional weather variables in their calculations (this are usually used in thermal comfort studies).

Excess Heat Index-acclimatization: An acclimatisation index (EHIACC) is brought into play to capture sudden rises in temperature in relation to the recent past.

In spite of the widespread use of heat stress indicators, epidemiological studies considering multiple indicators have often found comparable predictive skills of the different indicators (e.g., Barnett et al., 2010; Burkart et al., 2011; Vaneckova et al., 2011), with variations also based on geographic locations, seasons or age groups (Barnett et al., 2010; Rodopoulou et al., 2015). In addition, the choice of the indicators may also depend on the particular endpoints, sometimes and as a consequence, most health studies are based on statistical methods using temperature and humidity data to assess the effects of heat stress on morbidity and mortality (Armstrong et al., 2019; Gasparrini et al., 2016). The Lancet has recently launched a new platform which allows users to engage with findings and data on health impacts at country specific, regional and income group level (<https://www.lancetcountdown.org/data-platform/health-hazards-exposures-and-impacts>): a section is dedicated to health and heat (Section 1.1) and another one is dedicated to health and extreme weather-related events (Section 1.2). As for heat, the platform reports plots and data for exposure to heating (Section 1.1.1),

exposure of vulnerable population to heatwaves (Section 1.1.2), heat and physical activity, change in labour capacity and heat-related mortality.

As previously noted, apart from relevant direct health outcomes including excess mortality (e.g., Gasparrini and Armstrong, 2011; Gosling et al., 2007; Rocklöv et al., 2011), respiratory and cardiovascular diseases (Anenberg et al., 2020; Cosselman et al., 2015; Chang et al., 2022; Kenney et al., 2014; Hifumi et al., 2018; Löhms, 2018), renal diseases (El-Sharkawy et al., 2014; Wang et al., 2014), skin diseases (Rendell et al., 2020), eye diseases (Echevarría-Lucas et al., 2022), gastroenteritis (Manser et al., 2013), infectious diseases (Huang et al., 2018; Semenza and Bettina, 2009), preterm births and stillbirths (Wang et al., 2013; Smith and Hardeman, 2020; Chersich et al., 2020), impacts of such events also encompass indirect health and social impacts such as residential segregation (Mitchell and Chakraborty, 2018) and economic losses in the healthcare system (Wondmagegn et al., 2019; Adélaïde et al., 2022), as well as on heritage, infrastructure, ecosystems and society. To quantify those, a Heat Wave exposure value represents a community's building value (in euros), population (in both people and population equivalence), and agriculture value (in euros) exposed to Heat Waves. As for buildings, for instance, the city vulnerability to heat waves depends heavily on city morphology and shape, but also on the presence of vegetation, proportion of impervious coverage (e.g., Lemonsu et al., 2015). Some metrics have been previously defined and used to describe thermal resilience of passive buildings during heat events (Flores-Larsens et al., 2023). These include: IOD (Indoor Overheating Degree), AWD (Ambient Warmness Degree), α_{IOD} (Overheating Escalation Factor), which can be calculated for long (annual/monthly) or short (weekly/daily) periods to evaluate the resilience of different cooling technologies for buildings; WUTP (weighted unmet thermal performance) to evaluate thermal resilience concerning building characteristics (i.e., building envelope and systems) and occupancy, and identify the building resilience class of an improved building via a comparison with its base case; the solar radiation factor (β_{IOD}) and the Accumulation Factor (g_{IOD}) that account for the previous history and solar radiation in the resilience analysis of massive buildings under free-running conditions. Other indicators used to evaluate the thermal resilience of a building design are:

- Metrics evaluating ability to prevent buildings from reaching critical levels: One common metric to indicate a building's ability to prevent indoor environment from reaching critical levels is “time to reach critical level”. “Time to reach critical level” measures the elapsed time following a disruptive event where the design environment degrades to a critical level of thermal stress (Siu et al., 2023)
- Metrics evaluating ability to reduce occupants' exposure to thermal stress:
 - Time of exceedance is used to evaluate the amount of time indoor thermal conditions are beyond a defined critical limit. This is useful in identifying the proportion of time where an indoor space is not habitable in a defined timeframe. This is applied in thermal autonomy analysis to determine the passive performance of the building envelope (O'Brien and Bennet, 2016; Ozkan et al., 2019), as well as occupant hour loss (OHL) in office buildings, which is aimed to assess the amount of productive time lost for business/building owners (Mathew et al., 2021). However, the time of exceedance does not account for the magnitude of thermal stress, in which a short-term exposure to extreme heat could be hazardous to occupants.
 - The time integral of exposure (often expressed in degree-hours) is the product of the magnitude of exceeded thermal stress and time of exceedance. This could be useful for building designers to evaluate the cumulative effects over a defined timeframe. For example, the LEED passive survivability credit recommends an exposure limit expressed in degree-hours. However, applying degree-hours over a long time period (annual) does not reflect the acute exposure to heat events, which may have a significant impact on occupant health. (Siu et al., 2023)
 - To account for the varying levels of impact during different phases of disruptive events, Homaei and Hamdy (2021) proposed a new metric called weighted unmet thermal performance (WUMTP). This metric applies weighted factors to degree hours over the critical limit. The idea is to assign penalty factors based on three components: 1) different phases of disruptive event (from beginning of disruptive event to the recovery to normal state); 2) the hazard level; and 3) the exposure time during each phase of the event (Homaei and Hamdy, 2021). Then, a time-integrated metric can be calculated by multiplying the degree hours exceeding critical limit with the different penalty factor components (Homaei and Hamdy, 2021). Since this metric covers all stages of a disruptive event, it is theoretically the most

comprehensive metric in the reviewed studies. However, while the proposed metric and framework shows promise, it still requires significant research and refinement. In particular, the authors noted the penalty factors are only based on logical assumptions and validated definitions from physiological experts are needed. It is also unclear whether this framework could be applied to summer conditions (Homaei and Hamdy, 2021). Hence this is still under development, and not ready for industry use yet.

- Metrics evaluating ability to return to normal state: Only one study discussed about metric which incorporated the return to normal state. Homaei and Hamdy (2021) used the amount of time it takes for buildings to return to a normal operating state from critical state after disruptive event as a metric.

So, all in all, in order to quantify hazard and exposure with respect to heat waves, it is important not only to have data on different meteorological variables, but also data on population (not only inhabitants number, but also gender, age, presence of comorbidity, this population census data possibly), building structure, presence of vegetation, land use. To this purpose, previously, D'Ambrosio et al. (2023) have proposed a GIS-based approach (see previously) a GIS-based platform aimed at the analysis of heatwave scenarios risks produced in urbanised environments, applied to assess vulnerability and impact heatwave scenarios. Alternatively, numerical simulation methods together with measurements via ground-based and satellite-based instrumentation can be effectively used to conduct thorough assessment of the above mentioned variables. Following, we report a Table presenting a list of indicators useful to assess heat hazard, vulnerability and exposure, proposed recently by Tuomimaa et al. (2023).

Table 8. List of indicators for assessment of heat hazard, vulnerability and exposure (Tuomimaa et al., 2023).

Factors	Preliminary list of indicators	Component of risk affected by indicator
Social vulnerability	Number of residents with health insurance	-
	Number of people in need of home care in the risk area	Vulnerability Exposure
	Regional distribution of social vulnerability	Vulnerability Exposure
Infrastructure	Area of cool surfaces in the district	Exposure
	Number of dwellings/premises without a cooling device	Exposure
	Number of dwellings/premises with district cooling / possibility for district cooling	Exposure
Blue-green infrastructure	Number of green roofs in the district	Exposure Hazard
	Number of green areas in the district	Exposure Hazard
	Number of green walls in the district	Exposure Hazard
	Number of water areas in the district	Exposure
	Number of trees in the district	Exposure Hazard
State of environment	Nitrogen dioxide content in the district	Exposure
	Temperature differences between districts	Exposure
	Humidity and temperature in neighborhoods	Exposure
	Temperature of building roofs	Exposure
Economic resources	City financial contribution to X	Exposure Vulnerability Hazard
Knowledge and awareness	Number of early warning systems	Vulnerability

4.2.2. Aerosol pollution

Aerosols, also known as particulate matter (PM), are defined as a set of liquid or solid particles suspended in a gaseous or liquid medium. Aerosols are made up of a wide range of chemical species and their chemical composition is extremely variable depending on the proximity of the emission sources (marine, terrigenous, urban, or industrial). In general, an aerosol can consist of an organic fraction including carbonaceous derivatives and elementary carbon, and an inorganic fraction (Pöschl, 2006; Satheesh, 2012). Characterizing the chemical and physical properties of aerosols helps to determine source emissions, elucidate the mechanism of long-range transport of anthropogenic pollutants, and validate both regional and global atmospheric models (e.g., Prospero et al. 2002; Ginoux et al. 2012; Estefany et al. 2023). Furthermore, information on the chemical composition of aerosols constitutes a useful resource to evaluate the impact and the risk of air pollution on human health and the environment (EPA 2004). The size ranges of aerosols generally observed in the atmosphere range from a few nm to a few tens of μm . This great diversity in aerosol size implies that they do not have the same sources (and therefore not the same chemistry), nor the same dynamics of evolution. However, not all these sizes contribute equally to aerosol mass.

As for heat waves, exposure to particulate matter has several impacts on human health (e.g., Cohen et al. 2005) including premature death in people with heart or lung disease, nonfatal heart attacks, irregular heartbeat, aggravated asthma, decreased lung function, increased respiratory symptoms, such as irritation of the airways, coughing or difficulty breathing, and visibility impairment (e.g., Lelieveld et al. 2015; Gurgueira et al. 2002; Chen and Hoek, 2020; Anderson et al. 2012; Yuan et al. 2006). The World Health Organization (WHO) has collected enough scientific evidence to state that the most harmful exposure to particulate matter is long-term exposure to fine particles (WHO, 2021). High levels of particulate matter can also cause environmental damage, including making lakes and streams acidic, changing the nutrient balance in coastal waters and large river basins, depleting the nutrients in soil, damaging sensitive forests and farm crops, affecting the diversity of ecosystems, contributing to acid rain effects (e.g., Hoover and Mackenzie 2009; Grantz et al. 2003; Luo et al. 2019; Alloway 2004), and materials damage on stone, concrete and other building materials, including culturally important objects such as statues and monuments, some of which are related to acid rain effects on materials (e.g., Smith et al. 2008; Ferm et al. 2005; Ozga et al. 2011). Aerosols also affect the weather and climate by their impact on energy transfer (cooling or warming the Earth), and on cloud microphysics (by favouring or preventing clouds from forming) (e.g., Li et al. 2022; Haywood and Boucher 2000).

Amount of aerosol pollution is historically monitored through mass concentrations (PM₁₀, i.e. PM smaller than 10 μm , PM_{2.5}, i.e. PM smaller than 2.5 μm and recently also PM₁, i.e. PM smaller than 1 μm) (e.g., Chate, S.T.D., et al 2012; Keskinen, H.M., et al 2020). Those indicators are generally measured by ground-based stations or estimated through numerical simulations at different scales (e.g., chemical transport models and dispersion models at neighborhood, urban scale, mesoscale, regional scale). Generally, official monitoring networks at ground are managed by country or regional agencies responsible for air quality monitoring (e.g., Environmental Protection Agencies). For example, the following Figure 61 represents the Geographic coverage of PM₁₀ measurements for the OECD (Organization for economic cooperation and development) and G20 countries in the AirBase European repository from the European Environment Agency (EEA, <https://www.eea.europa.eu/en/datahub/datahubitem-view/3b390c9c-f321-490a-b25a-ae93b2ed80c1>). The World Health Organization also publishes data and figures about modelled exposure to particulate matter air pollution (<https://www.who.int/data/gho/data/themes/air-pollution/modelled-exposure-of-pm-air-pollution-exposure>).

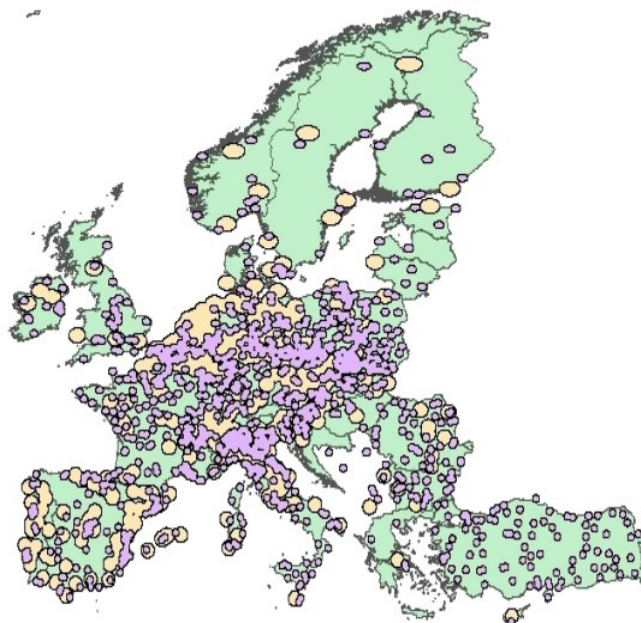


Figure 5252. Geographic coverage of PM10 measurements for the OECD and G20 countries in AirBase.
(Turner et al., 2016).

While regulatory standards, and also the latest WHO global air quality guidelines (WHO, 2021), are based on mass concentrations, it is well known that the associations between air pollution and human health outcomes and the evaluation of the efficacy of air quality legislation and emissions standards are tightly linked with urban aerosol Particle Size Distributions (PSDs), whose knowledge enables the characterization of size-dependent processes that govern a particle's transport, transformation, and fate in the urban atmosphere, and also deposition in the respiratory system and inhalation toxicity (Wu and Boor, 2021). However, in spite of large geographical and intracity variations of PSDs, infrastructure for routine and long-term monitoring of urban aerosol PSDs spanning the nucleation to coarse mode is still lacking (Wu and Boor, 2021), and data on PSDs are generally available only at some particular point locations from mass spectrometers.

Apart from these, several indicators exist also from remote sensing satellite, sunphotometers and LIDAR (Light Detection and Ranging) measurements, based on the scattering and absorbing properties of incoming sunlight from aerosols (King et al. 1999), including the Aerosol Optical Depth, Aerosol Index, Fine Mode Fraction, Ångström Exponent, and Aerosol Layer Height.

Aerosol Optical Depth (AOD): Aerosol Optical Depth (AOD) (or Aerosol Optical Thickness) is an optical parameter which indicates the level at which particles in the air (aerosols) prevent light from traveling through the atmosphere (through absorption and scattering processes). From an observer on the ground, an AOD of less than 0.1 is “clean” - characteristic of clear blue sky, bright sun and maximum visibility, transmissivity is $\exp(-0.1)=0.9$ meaning that over than 90% of light passes through the medium. As AOD increases to 0.5, 1.0, and greater than 3.0, aerosols become so dense that the sun radiation is strongly attenuated (Wei et al. 2020)

Ångström Exponent: The absorption Ångström exponent (AAE) is an aerosol optical property describing the wavelength variation in aerosol absorption. Because aerosol absorption normally decreases exponentially with wavelength over the visible and near-infrared spectral region (Ångström, 1929; Bond, 2001; Lewis et al., 2008), the AAE is defined as

$$C_{\text{abs}}(\lambda) = C_o \lambda^{-\text{AAE}} \quad \text{or} \\ \ln(C_{\text{abs}}(\lambda)) = \ln(C_o) - \text{AAE} \ln(\lambda)$$

where λ , C_{abs} , and C_o denote wavelength, the aerosol absorption coefficient, and a wavelength-independent constant (which equals the absorption coefficient at the wavelength of $1 \mu\text{m}$). Instead of the absorption coefficient, some studies use the aerosol absorption optical depth in the previous equation, because the two are proportional.

Fine Mode Fraction (FMF) and Fine-Mode AOD (fAOD): FMF is defined as the fraction of the fine-mode aerosol (that is, aerosols with diameter between 0.1 and 1 μm) amount to the total aerosol amount. The fine-mode AOD (contribution of fine-mode aerosols to the total AOD) can be derived by multiplying FMF to the total AOD. As most anthropogenic aerosols are fine-mode aerosols, these indicators can characterize the amount of aerosol pollution within an urban area (Yan et al. 2017).

Aerosol Index: Satellite-derived Aerosol Index (AI) products are useful for identifying and tracking the long-range transport of volcanic ash from volcanic eruptions, smoke from wildfires or biomass burning events and dust from desert dust storms, even tracking over clouds and areas of snow and ice. The Aerosol Index (AI) is a qualitative index indicating the presence of elevated layers of aerosols with significant absorption. The main aerosol types that cause signals detected in the AI are desert dust, biomass burning and volcanic ash plumes (Hsu et al. 1999). An advantage of AI is that it can be derived for clear as well as (partly) cloudy ground pixels. The relatively simple calculation of the AI is based on wavelength-dependent changes in Rayleigh scattering in the UV spectral range where ozone absorption is very small. For a given wavelength pair a ratio is calculated from measured Top Of Atmosphere (TOA) reflectance and calculated theoretical reflectance for a Rayleigh scattering-only atmosphere and results in a residual value. Positive values of this residual indicate the presence of UV-absorbing aerosol.

Aerosol Layer Height: Aerosol Layer Height (ALH) products define the average height of aerosol plumes, in the case of vertically localized layers of desert dust, biomass burning or volcanic ash aerosols. The height of the plume is calculated from the retrieval of mid-layer pressure, assuming a constant pressure gradient between top and bottom of the layer. The retrieval algorithms typically use TOA radiance measurements within the oxygen absorption band between 760 and 770 nm (O₂-A band). Together with AI, ALH can characterize the presence of absorbing aerosols above a specific area (Sanders et al. 2015).

The fact that aerosols exert an effect on insolation at ground level was associated also with an effect on Physiological Equivalent Temperature (PET) and human thermal comfort (Wai et al., 2017), thus suggesting the connection of aerosols indicators with those previously outlined for heat waves.

Mapping of exposure to ambient PM has been often conducted also in this case through GIS-based methods (e.g., Diem and Comrie, 2002; Stedman et al., 2008), although the use of satellite observations is clearly emerging as very popular (Zhang et al., 2021). Indeed, recent research has suggested that the combination of ground-based aerosol monitoring with remote sensing can form the key for an integrated air quality characterization and exposure (Stoyanov et al., 2019; Nguyen et al., 2015; Nguyen et al., 2020) or a combination of ground based data together with chemical transport or dispersion models and a generalized additive model to translate remotely-sensed AOD measurements (e.g., Alvarado et al., 2019; Le et al., 2022) can be used to overcome the data paucity and low resolution of ground-based monitoring networks.

4.2.3. Relevant indicators to characterize heat waves and aerosol pollution hazards and exposure

The following Table synthesizes the relevant indicators used in for the different types of hazards: heat waves, aerosol pollution.

Table 9. Indicators to characterize heatwaves and aerosol pollution hazards

Exposed element	Hazard	Indicators
Population	Heat wave	Long term and short term records of: Air temperature (mean, minimum, maximum) Humidity Wind speed Boundary layer height Land surface temperature Solar irradiance Number of inhabitants and distribution of social characteristics Distribution of cooling devices Distribution of green/blue infrastructure elements NDVI

Building	Heat wave	Long-term and short-term records of: Air temperature (mean, minimum, maximum) Relative Humidity Wind speed Boundary layer height Land surface temperature Solar irradiance Distribution of green/blue infrastructure elements Building envelope characteristics (exterior walls, interior walls, roofs, glazing area, technical plenum, global loss coefficient) Thermal mass of the buildings Building materials, geometry, physical properties
Population	Aerosol pollution	Long term and short term records of: PM10, PM2.5 Black Carbon(BC) Aerosol number concentration (ANC) AOD, AI, AAE Boundary layer height Humidity Wind speed Number of inhabitants and distribution of social characteristics (gender, age, presence of comorbidity, ...) Distribution and characteristics of green/blue infrastructure elements NDVI
Building	Aerosol pollution	Long-term and short-term records of: PM10, PM2.5 AOD, AI, AAE Humidity Wind speed Distribution of green/blue infrastructure elements Ventilation effectiveness Number of occupants Dampness and moisture damage Material condition Water damage Exposed surface area Friability Building materials, geometry, physical properties Air plenum or direct air stream

4.2.4. Composite effect of heat waves and air pollution

Several papers have previously suggested how heat waves and air pollution synergistically interact during extreme heat events, and the contemporary exposure to extremely high temperatures and increased air pollution greatly increase the health relevant outcomes especially for vulnerable population and increased ozone, but sometimes also mentioning also PM (e.g., Ebi and McGregor, 2008; Hou and Wu, 2016; Benmarhnia et al., 2014; De Sario et al., 2013; Shaposhnikov et al., 2014; Anenberg et al., 2020; Cosselman et al., 2015). In particular, while epidemiological evidence often focuses on single risk factors, evidence suggests that contemporary exposure to environmental factors may greatly increase the adverse health outcomes, due to their synergistic interaction. Indeed, recent health studies are more and more directed towards the so-called

“exposome” approach, a concept that encompasses the totality of the exposures experienced by an individual throughout life and their changes over time (e.g., Juárez et al., 2020; Ferrante et al., 2022).

In particular, the following Figure 52 extracted from (De Sario et al., 2013) suggests possible ways of interaction between climate change, its influence on extreme weather events, air pollution and aeroallergens.

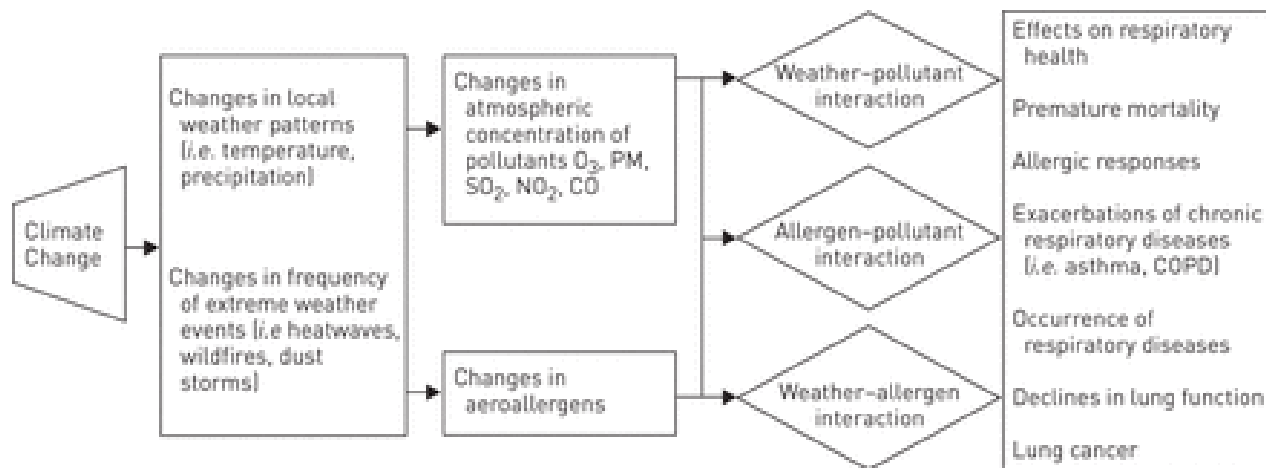


Figure 53 53. Climate change: its influence on extreme weather events, air pollution and aeroallergens, and effects on respiratory health. PM: particulate matter; COPD: chronic obstructive pulmonary disease. (De Sario et al. 2014)

The fact that aerosols exert an effect on insolation at ground level was associated also with an effect on Physiological Equivalent Temperature (PET) and human thermal comfort (Wai et al., 2017), thus suggesting the connection of aerosols indicators with those previously outlined for heat waves in Section 4.2.2.

In spite of the evidence of this interaction between heat waves and air (aerosol) pollution, however, no previous study has suggested the introduction of compound indicators describing simultaneous exposures, and the studies continue to adopt the single exposure indicators listed and described in Section 4.2.2.

4.3. Hotspot example identification and assessment using GIS based approaches

The concept of hotspots has been used in various disciplines (e.g. urban development, economy and criminology) in order to indicate the concentration or the intensity of a certain phenomenon in a limited geographical context (Levine 2002; Van Der Veen and Logtmeijer 2005; Thurstain and Goodwin 2000; Thurstain et al. 2001). With regard to natural phenomena, Dilley et al. (2005) and Arnold et al. (2006) refer to the hotspots as geographic areas where the risks of natural disasters are particularly high. Along the same lines, the flooding risk hotspots can be defined as zones that are relatively more likely to be exposed to flooding. Figure 53 illustrates a schematic representation of a flooding risk hotspot identified as R (standing for risk) as an area in which high probability of occurrence of flooding identified as H (standing for hazard) coincides with areas of high exposure identified as E (see Leader and Wallingford 2009 for a comprehensive discussion on language of risk).

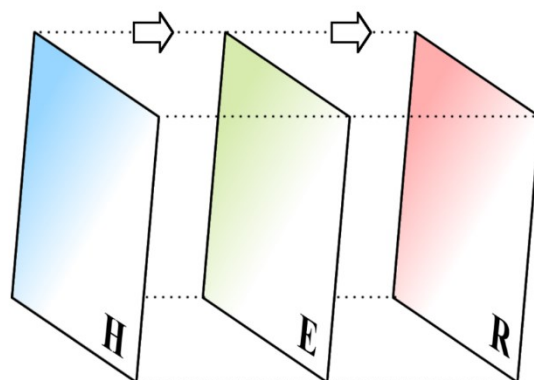


Figure 5454. Hazard (H), exposure (E) and risk (R), the concept of a risk hotspot (Jalayer F, et al. (2014) Probabilistic GIS-based method for delineation of urban flooding risk hotspots).

It is important to underline that the hotspot definition used herein cannot replace a comprehensive evaluation of risk based on accurate hazard and vulnerability assessment on one hand, and evaluation of the socio-economic consequences on the other. In fact, delineation of the hotspots can be seen as an effective screening tool for identifying the zones for a detailed and comprehensive risk assessment. Considering that around half of the world's population lives in urban areas, identifying the urban hotspots is a fundamental preliminary step in urban planning and risk management. Arguably, delineation of urban hotspots does not only provide useful information for policy makers, but it can also be useful as supporting information for indicating future urban dynamics and trends. Mapping of urban risk hotspots provides a screening tool for the urban planner in order to individuate efficiently the zones that need his/her immediate or long-term actions. These actions can include for example adoption of more accurate small-scale risk assessment procedures and undertaking various prevention strategies. The prevention strategies range from planning for structures that help in mitigating the risk, to relocation policies (if advisable), territory restriction measures and actions that aim at increasing public awareness.

4.3.1. Identification of flooding risk hotspots

The proposed procedure employs three GIS-based frameworks for identifying the urban flooding risk hotspots for residential buildings and major roads. This is done by overlaying a map of potentially flood-prone areas [identified by the topographic wetness index (TWI)], a map of urban morphology types (UMT) classified as residential or as urban corridors (i.e. major roads), and a geo-spatial census dataset for demographic information (e.g. population density). Of course, the overlay of land cover and flood-prone area maps is not novel and has been done in various research efforts (see for example, Meyer and Messner 2005; Gwilliam et al. 2006). In a traditional approach towards delineating the urban flooding hotspots, zones of high exposure to flooding are overlaid with areas that are known to be susceptible to flooding or flood-prone areas. These areas are usually identified based on available historical flooding data or by defining a buffer zone around the rivers (see Gall et al. 2007 or Apel et al. 2009 for a comprehensive discussion on identification of flooding risk hotspots). The novelty in the approach proposed herein lies in the use of Bayesian parameter estimation for the characterization of uncertainties in delineating the potentially flood-prone areas. More specifically, these uncertainties are related to the evaluation of the threshold for the TWI. The TWI (Qin et al. 2011) allows for the delineation of a portion of a hydrographic basin, potentially exposed to flood inundation, by identifying all the areas characterized by a topographic index that exceeds a given threshold. The TWI has a purely topographic interpretation (basically measures the capability to accumulate water) and is quite straightforward to calculate in the GIS environment for very large areal extents. On the other hand, accurate hydraulic calculations may involve two-dimensional flood propagation and are more suitable (in terms of computational effort) for limited areal extents (micro-scale, e.g. 1:2,000). The TWI threshold value depends on the resolution of the digital elevation model (DEM), topology of the hydrographic basin and the constructed infrastructure. This threshold value can be calibrated based on the results of detailed delineation of the inundation profile for selected zones (Manfreda et al. 2008, 2011).¹ In this study, the TWI threshold is calibrated based on the calculated inundation profiles for various return periods for selected zones within the basin through a Bayesian parameter estimation framework. Bayesian parameter estimation enables a probabilistic characterization of the

threshold by calculating the complementary probability of false delineation of flood-prone zones as a function of various threshold values. It should be mentioned that the flood-prone areas identified herein are not differentiated with respect to the spatial variation in flood hazard within the area. A recent work by Degiorgis et al. 2012 employs pattern classification techniques for the delineation of flood-prone areas and hazard graduation within these areas based on remote-sensed data. The UMTs (Pauleit and Duhme 2000; Gill et al. 2008; Cavan et al. 2012) form the foundation of a classification scheme which brings together facets of urban form and function. UMTs are distinguished from land use and land cover maps by their specific configuration of built and open spaces. The underlying assumption is that UMTs have characteristic physical features (i.e. land cover) and are distinctive according to the human activities that they accommodate (i.e. land uses). In the assignment/definition of UMT, physical properties and human activities are assumed to be key factors that largely determine the characteristics of urban areas. Once an appropriate UMT classification scheme is established for a particular study area, individual UMT units can be delineated using aerial photography and other geospatial data sources. UMT units are often mapped at a "meso"-scale (i.e. between the city level and that of the individual units). This makes them a suitable basis for the spatial analysis of cities. The flowchart illustrated in Figure 54 provides a schematic diagram of the procedure proposed for the identification of the urban flooding risk hotspots. The flowchart is organized as an overlay of zones of potential high hazard—represented by the TWI values larger than a certain threshold—and specific exposure characteristics—represented by a geo-morphological dataset and/or spatial information about population density. As it can be seen in the flowchart, the TWI threshold is calibrated based on information about flooding extent coming from one or more selected spatial windows. The best-estimate for the TWI threshold can be either a maximum likelihood estimate or a certain percentile (e.g. 16th or 50th) of the probability distribution for the TWI threshold.

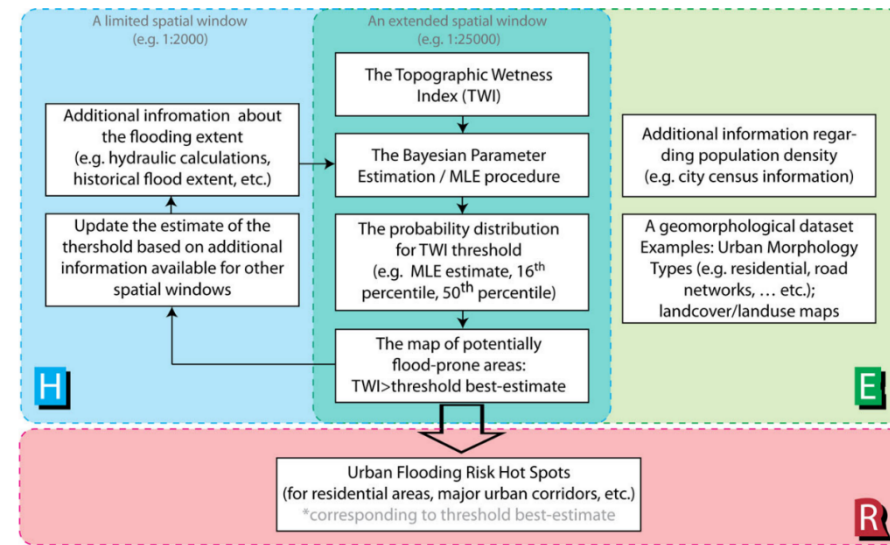


Figure 5555. Flowchart describing the conceptual development of the proposed methodology for delineation of urban flooding hotspots (Jalayer F, et al. (2014) Probabilistic GIS-based method for delineation of urban flooding risk hotspots).

Delineation of flood-prone areas using the topographic wetness index (TWI)

The TWI, initially introduced by Kirkby (1975), has been shown to be strongly correlated to the area exposed to flood inundation (Manfreda et al. 2007, 2008, 2011). The TWI for a given point O within the hydrographic basin is calculated as following:

$$TWI = \log \left(\frac{A_s}{\tan \beta} \right)$$

where A_s is the specific catchment area expressed in metres and is calculated as the local up-slope area draining through point O per unit contour length (A/L). β is the local slope at the point in question expressed in degrees. Figure 55 illustrates the main components used for the calculation of the TWI at a given point O within the hydrographic basin, namely the catchment area A for point O, the length L of the contour line and the specific

catchment area A_s . The TWI allows for the delineation of a portion of a hydrographic basin potentially exposed to flood inundation (referred to herein as flood-prone or more briefly as FP), by identifying all the areas characterized by a topographic index that exceeds a given threshold. The TWI threshold value depends on the resolution of the DEM, the topology of the hydrographic basin and the presence of constructed infrastructures (such as sewage system, bridges and culverts). This threshold is usually calibrated based on the results of detailed delineation of the inundation profile for selected zones.

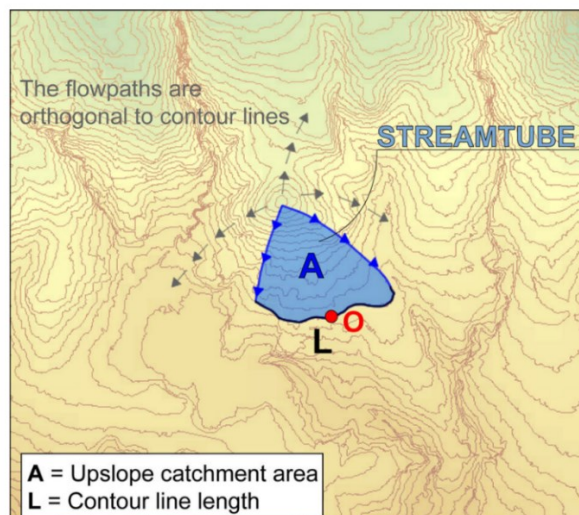


Figure 5656. Main components of the TWI calculation (Jalayer F, et al. (2014) Probabilistic GIS-based method for delineation of urban flooding risk hotspots).

Using the inundation profiles for the calibration of the TWI threshold

As was mentioned in the previous section, the TWI method delineates the flood-prone areas as the portions of the basin for which the topographic index exceeds a prescribed threshold. One way for establishing the TWI threshold is to use the available inundation profile for one (or more) zones of interest within the basin. The inundation profile, reported as the flooding heights (and velocities) for various nodes within a lattice covering a given area for different return periods, can be obtained by means of classic hydraulic routines of various degrees of sophistication and accuracy (Apel et al. 2009). The calculation of the inundation profiles can be summarized in a step-by-step manner as (described in more detail in De Risi et al. 2013): 1. The definition of the rainfall curves for different return periods (TR) based on historic rainfall annual maxima. The acquisition of cartographic information such as, DEM, digital surface model (DSM), the geology map and a representation of land use/land cover for the zone(s) of interest. Calculation of the hydrographs for the various return periods associated with the rainfall curves. The hydrograph refers to the flow discharge as a function of time and constitutes the input for the hydraulic diffusion model. The area under the hydrograph is equal to the total discharge volume for the basin under study. Diffusion of the total discharge volume (area under the hydrograph) based on the general constitutive equations of continuity and fluid dynamics (i.e. one-dimensional or bi-dimensional diffusion models). This can be done by means of various software tools (e.g. FLO2D 2004, HEC-RAS 2010, etc.). The inundation profile, obtained through a procedure similar to the one described above, can be used to delineate the inundated areas (referred to hereafter as IN), for a given return period, as those areas within the zones of interest where the inundation height is greater than zero.

Delineation of geographical functional units using the urban morphology types (UMT)

It has been noted that UMTs form the foundation of a classification scheme which brings together facets of urban form and function. The UMT's are used to develop a geo-spatial dataset containing seamless polygons of UMT units. Each unit is associated with attribute information describing its class and its geometric properties. This geospatial layer provides complete and consistent coverage across the city having used an internally consistent process for unit delineation, data recording and data coding. Linear features such as roads and rivers were used as the outline of UMT units and were matched with administrative units/zones where possible (e.g. for the boundary of the dataset, as shown in Figure 56). In order to build a UMT map, it is necessary to identify the various UMT classes for the specific urban area (e.g. farmland, transport, residential, etc.). These undergo a verification process to establish their appropriateness for the study area. The UMT

classes can then be detected through visual analysis of remote sensing data (ortho-rectified aerial photography) as the primary method of applying the scheme (Gill et al. 2008). Furthermore, for each UMT class, typical images can be captured and kept for reference with a description of its characteristics. Finally, the dataset undergoes field verification and approval. Once a complete UMT layer has been created, through the process of digitization, it is then suitable for further GIS analysis and can be combined with other datasets to produce spatial indicators.

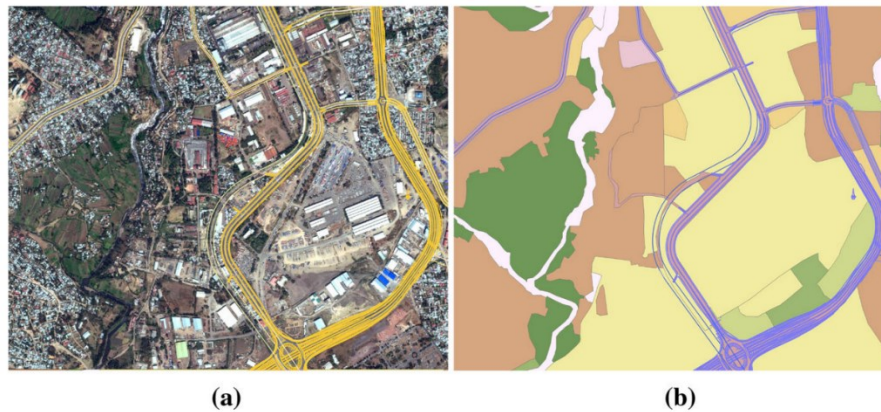


Figure 5757. Mapping UMT units using ortho-rectified aerial photography, an example in Addis Ababa. Note Fig. 4a (source www.bing.it/maps) is not the original orthophoto based on which the UMT in Fig. 4b is generated (Jalayer F, et al. (2014) Probabilistic GIS-based method for delineation of urban flooding risk hotspots).

Identification of urban hotspots by overlaying the TWI, UMT and census population density datasets

The urban hotspots for residential areas and major urban corridors are identified by overlaying the layer of flood-prone areas (identified by TWI values larger than the threshold s), the layers delineating the UMTs (identified as residential and major urban corridor UMT) and a census dataset for demographic information. The urban hotspots are identified taking into account, not just a single value of the TWI threshold, but considering its probability distribution. Obviously, considering the probability distribution for s (in other words, the uncertainty in the evaluation of s) is going to influence the results in terms of the spatial extent of the hotspots and the estimated number of people affected.

4.3.2. Identification of heatwave risk hotspots

Geographic Information Systems (GIS) are essential tools in modern environmental management and planning. They offer powerful capabilities for mapping and analyzing geographical data, enabling experts to visualize, interpret, and understand complex relationships in physical and human landscapes. When it comes to assessing the impacts of heatwaves on physical and socio-ecological systems, GIS provides invaluable insights.

Spatial Analysis of Heatwave Patterns: GIS can effectively map historical heatwave occurrences, highlighting their frequency, duration, and intensity. This spatial analysis is crucial for identifying areas most frequently and severely affected by heatwaves, thereby guiding targeted interventions and resource allocation. Using GIS platforms, and multisource data such ground and remotely sensed data can provide powerful tools to use hierarchical models to assess vulnerability and impact scenarios (D'Ambrosio et al. 2023).

Identification of Vulnerable Populations: By overlaying demographic data onto heatwave maps, GIS helps in pinpointing vulnerable groups within a population. This includes identifying areas with a high density of elderly, children, or low-income groups who might be more susceptible to the adverse effects of heatwaves. This method incorporates different vulnerability dimensions (socio-economic status, extreme age, population density, building obsolescence, etc.) to modify the relationship between heat and health outcomes (e.g., Buscail et al. 2012; Yu et al., 2021).

Infrastructure and Land Use Assessment: GIS analyses land use patterns and the distribution of critical infrastructure such as hospitals, cooling centers, and green spaces. This information is vital in understanding

how urban heat islands exacerbate the effects of heatwaves and identifying areas lacking adequate infrastructure to cope with extreme heat events (e.g., Sidiqui et al. 2022; Schweighofer et al., 2021)

4.3.3. An example of heatwave hotspot assessment

The following contribution has been elaborated by Prof. Federica Dell'Acqua (University of Naples Federico II – Department of Architecture) within her research activity (Programma PON R&I 2014-2020 – Asse IV “Istruzione e ricerca per il recupero – REACT-EU”, Codice Unico di Progetto, CUP 65F21003090003), aiming to present an application case for the identification of heatwave hotspots through GIS-based tools. The application case concerned the municipality of Nola.

The municipality of Nola has an important infrastructure system around the historic centre and links to the system of houses, a historic and archaeological core, and a large agricultural and rural heritage. Nola has, based on the studies of Emilio Sereni in “Storia del paesaggio agrario” (1979), significant traces of the Roman centuriatio (see Figure 57, a), and still traces of farms and the system of farmhouses as productive centres.

The mesh of the Roman centuriatio was a net of mesh of about 700x700m that regulated the rural and urban components of the territory. In Nola, this track is visible in a north-south crossing axis, and around it, the centurial links of the surrounding municipalities oriented according to the morphology of the plain. These traces represent a factor of knowledge of the process of building the rural environment compared to the urban. A knowledge model is necessary to analyse the complexity of these environmental elements, such as environmental values and climatic criticalities.

Nola has specific conditions of vulnerability to climate impacts, due to the orographic characteristics, the infrastructure system and geomorphological limits, the factors of exposure of buildings and outdoor spaces to solar radiation. In the map of the Istituto Geografico Militare 1956 (see Figure 57, b) is visible the system of waters and Regi Lagni that crosses the plain of Nola.



(a)



(b)

Figure 5858. a) Hypothesis of the Roman centuriatio in V. Valerio, “La carta di Napoli e dintorni degli anni 1817/1819, Napoli 1983”. Nola is located in the red square b)

Because of the Regi Lagni water system and the sealed urban surfaces, the hazard of heavy rains (see Figure 58, b) is one of the risk factors. Moreover the built fabric of Nola is dense in some points, with few open spaces and urban voids, and large green areas unrelated to the town. This can aggravate the impacts of heat waves. The two hazards - heavy rains and heat wave- amplify the risk conditions. Therefore, Nola represents a multi-risk case study. In this study, the vulnerability to heat wave is analysed.

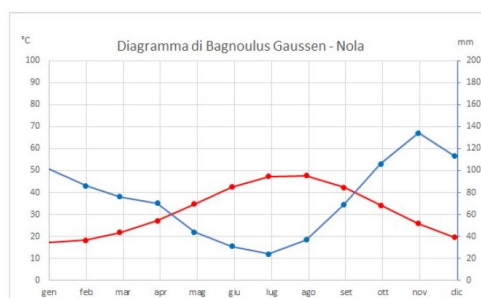
In Nola in the last 5 years, there have been several days of peak heat (see Figure 58, a). In addition, the Bagnoulus Gaussen diagram, through the relationship between average temperatures and average monthly rainfall recorded in Nola from 1991 to 2021, detects a period of dryness from May to August. The difference between the graph of temperatures and that of precipitation returns in a qualitative way a first indication of maximum irrigation needs to be taken into account in strategic planning in relation to any greening (see Figure 58, c).



Due to the non-homogeneous distribution of the population of Nola, an integrated heatwave vulnerability assessment model based on the exposure of the total population and the weak groups is developed.

Località	Data	Inizio	Fine	Durata
Napoli	2019	23/06/2019	25/06/2019	3
		01/07/2019	04/07/2019	4
		06/07/2019	10/07/2019	5
		25/07/2019	27/07/2019	3
		31/07/2019	02/08/2019	3
		10/08/2019	15/08/2019	6
	2020	20/08/2019	03/09/2019	13
		29/06/2020	03/07/2020	5
		09/07/2020	12/07/2020	4
		29/07/2020	03/08/2020	6
		11/08/2020	26/08/2020	16
		10/09/2020	12/09/2020	3
	2021	05/07/2021	07/07/2021	3
		31/07/2021	02/08/2021	3
		16/08/2021	20/08/2021	5
		22/06/2022	25/06/2022	4
		03/07/2022	07/07/2022	5
		15/07/2022	17/07/2022	3
Nola	2022	21/07/2022	31/07/2022	11
		05/08/2022	07/08/2022	3
		24/08/2022	26/08/2022	3
		26/09/2022	08/09/2022	3
		09/07/2023	15/07/2023	6
		18/07/2023	23/07/2023	6
	2023	30/07/2023	01/08/2023	3
		17/08/2023	19/08/2023	3
		23/08/2023	26/08/2023	4

Anno	Dato pluviometrico [mm/h]
2008	23,4
2010	34,5
2011	24,4
2012	24,8
2013	29,4
2014	38,6
2015	35,6
2016	60
2017	44,2
2018	23,8
2019	23,8
2020	26
Media	32,375



	gen	feb	mar	apr	mag	giu	lug	ago	set	ott	nov	dic
Tmed	17,2	18,3	21,8	27,1	34,8	42,4	47,2	47,6	42,3	34,1	25,9	19,5
Pmed	102	86	76	70	44	31	24	37	69	106	134	113

(a)

(b)

(c)

Figure 5959. a) Heat wave days. Data processed from Capodichino weather station data (Source: <https://www.ilmeteo.it/portale/archivio-meteo/Napoli>) b) Historical series of rainfall data recorded in Cicciano from 2008 to 2020 (Source: <http://centrofunzionale.regione.campania.it/#/pages/dashboard>) integrated with data from Annali dell'Ufficio Idrografico e Merografico di Napoli (1928-1999) c) The diagram of Bagnouls Gaussien highlights on Nola a period of dryness, from May to August, coinciding with the stretch of the graph in which the curve of precipitation falls below that of temperatures.

Nola is a metropolitan urban settlement with geomorphological, environmental and non-homogeneous built. For the very variable distribution of both the elements of the physical system (built, outdoor spaces and infrastructure) and the population, it is important to identify the urban critical context.

To find the vulnerability parameters, related to exposure, preliminary environmental analyses are made (map of the green and the water system), technological (year of construction, albedo), and functional-spatial (Schwarzplan) of the territory. To represent the exposure factors, the distribution of the total population and by age groups is analysed.

Since the model is based on exposure, overlapping the maps shows that the historic centre represents a urban critical context (see Figure 59).

In the historic centre, the average albedo index is less than 0.1, green and outdoor spaces are minimal, the urban fabric is dense. Based on the year of construction and construction techniques of the buildings, it is assumed that the building envelope will behave inadequately to heat waves. Although 74% of the surface of the municipal area is permeable, the impermeable surfaces equal to 26% - 10% of which are represented by buildings and 16% by open spaces - are concentrated in the historic core, and in the production area to the north (ZES-CIS of Nola). Regarding exposure, the population 0-9 years is equal to 4.18%, and 60-69 years and over 70 years are equal to 3.35% and 4.37%. The 3 bands, equal to about 12% of the population, are considered weak and therefore more subject to the negative effects on health related to the heat wave phenomena. These values are greater in the old town. In the ZES the environmental and technological values are critical but the exposure is zero. Therefore, the study excludes this area as an urban critical context and considers the historic centre.

CRITICAL URBAN CONTEXT

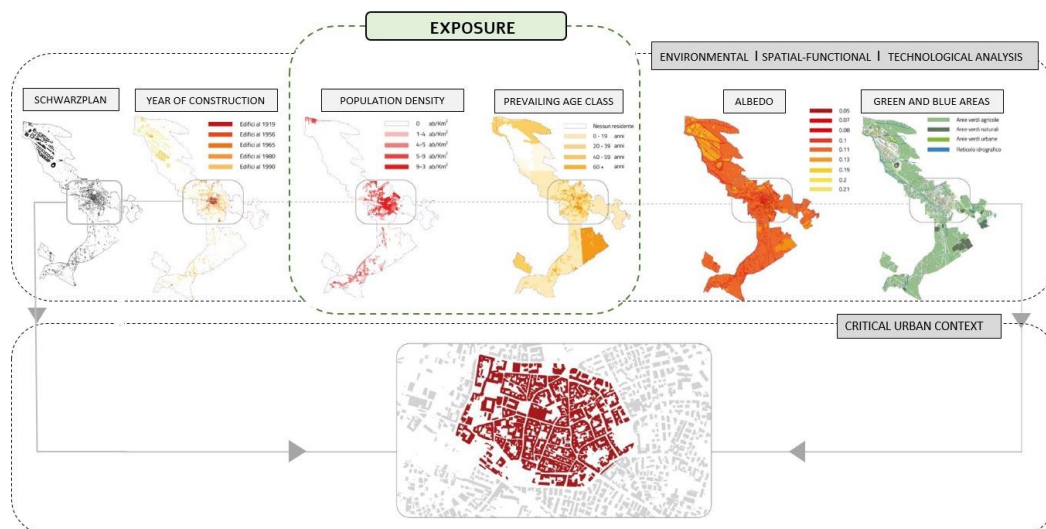


Figure 6060. Conceptual framework for integrated exposure assessment

Once the historical centre has been identified as a critical urban context, the integrated vulnerability assessment model based on exposure can be set (see Figure 60). The workflow represents an application focused on assessing the vulnerability and exposure of urban contexts to hazard heatwave of the model developed within the framework of the research project PLANNER. The model focuses on evaluating the intrinsic vulnerability of the subsystems that make up the physical system (buildings and open spaces). The assessment of the intrinsic vulnerability of the subsystems is based on the evaluation of specific features of each subsystem that could affect their response to heatwave events. Two indicators describe the vulnerability of the subsystems in the study case. The intrinsic vulnerability of buildings is based on the evaluation of the following indicators: thermal lag and thermal decrement factor. The intrinsic vulnerability of outdoor spaces is based on the evaluation of the indicators: Albedo and Normalized Difference Vegetation Index (NDVI). Each indicator is ranked on a scale of 5 classes, where 1 represents a high value of vulnerability to heat wave with respect to the analyzed indicator and 5 represents a low value of vulnerability. The intrinsic vulnerability value of the subsystems (buildings and open spaces) is the result of a weighted average of the intermediate indicators and to each indicator is given 50% of the weight. At the same time, exposure is assessed, by census sections, of the total population and by age groups (see Figure 60).

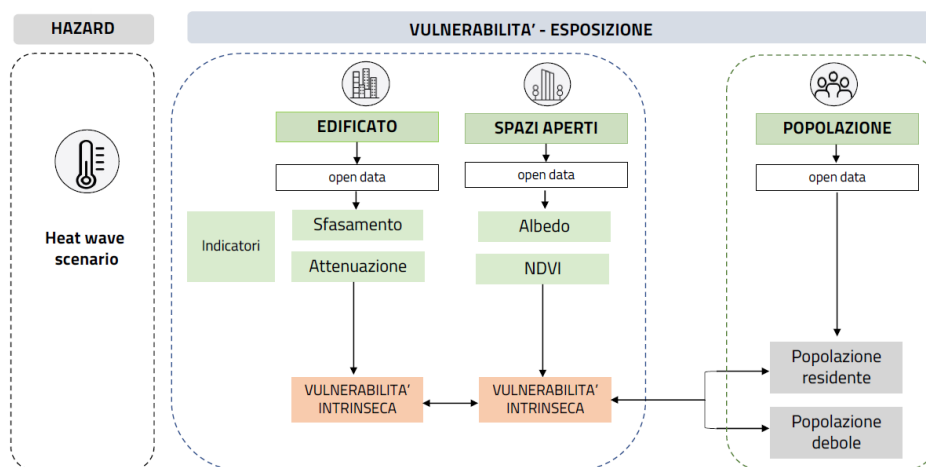


Figure 6161. Integrated exposure assessment for the case of heat wave.

Finally, it is possible to assess, starting from the intrinsic vulnerability values of buildings and open spaces, the integrated exposure also taking into account the exposure of the population and the exposure of the weak groups. The integration of the values of intrinsic vulnerability of buildings and

open spaces and integrated exposure allowed, using aggregation rules calibrated on the study area, to identify urban hotspots, i.e. the areas within the critical urban context of the historic centre that are most vulnerable and exposed to the hazard heat wave. This process represents a framework developed in GIS environment (see Figure 61), based on open-source data of the indicators and population (Sferratore et al., 2024).

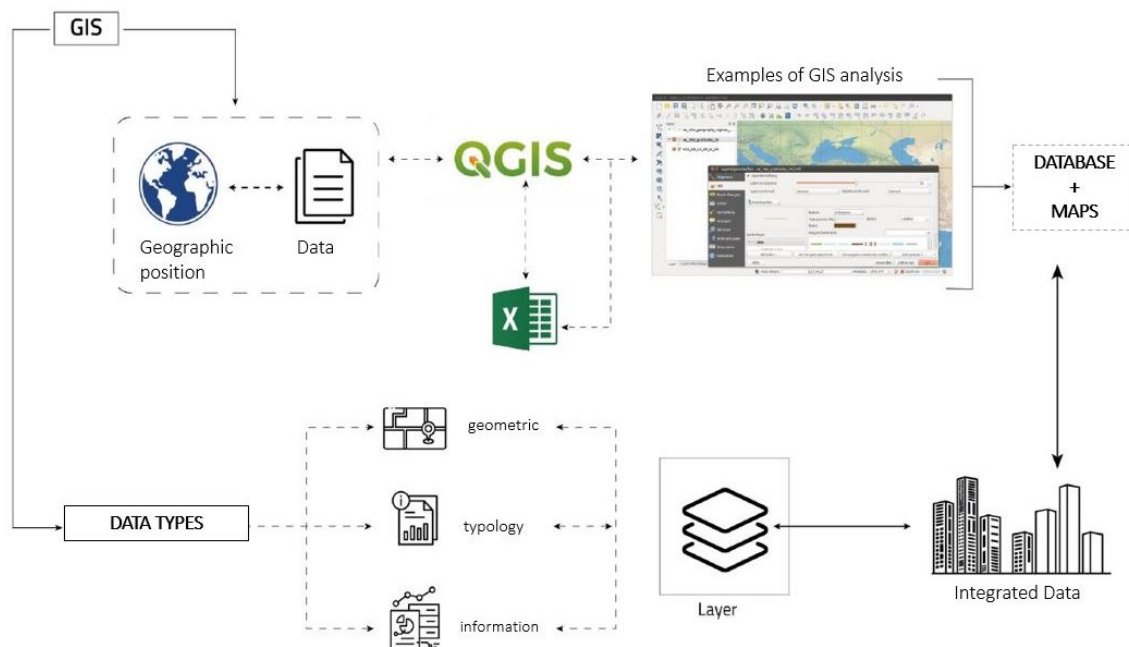


Figure 6262. GIS-based framework.



(a)



(b)

Figure 63. a) population density b) vulnerable population (< 5 years > 65anni).

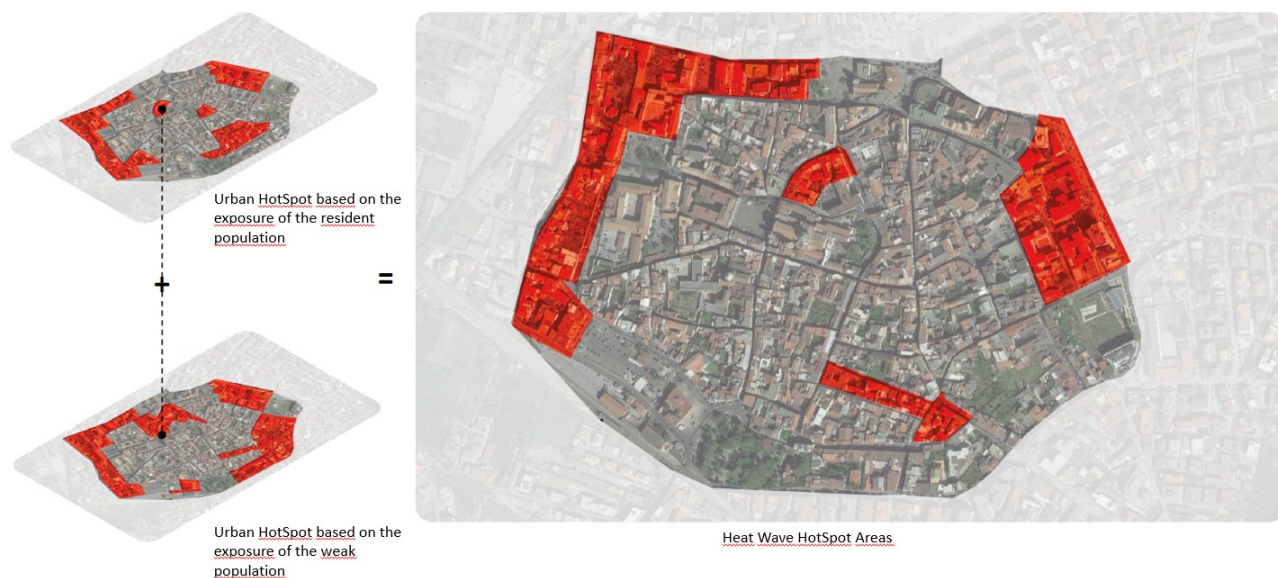


Figure 6364. Heat wave HotSpot Areas Identification based on the exposure value.

The test allows to develop a functional model to the construction of knowledge for the evaluation of the climatic weakness of the critical urban context, and to guide the strategic and meta-design solutions for the reduction of climate vulnerability to the heatwave in relation to the exposed population.

The knowledge of environmental systems in the urban environment – consisting of the interaction between anthropogenic systems and natural systems – is complex because it consists of several elements that composes the system and the interactions that take place on several urban settlements levels, from morphological to functional-spatial. Understanding these interactions is fundamental for sustainable transformations that are based on principles of urban and ecosystem-based regeneration. The GIS-based framework refers to only one hazard. The next research steps will include the assessment of impacts and the identification of hotspot areas based inside the critical urban context.

5. Composite indicators for multi-risk exposure assessment

5.1. Composite indicators

A composite indicator is a mathematical combination of a set of individual sub-indicators that represent different dimensions of a concept and have no common unit of measurement (Nardo, et al., 2005).

The starting point in constructing composite indicators is the definition of a theoretical framework, i.e., the definition of the phenomenon to be measured through the composite indicator. As a matter of fact, the choice of which sub-indicators to use, which weighting method has to be used and as well as how to aggregate information, are subjective choices that can be used to manipulate the results. Thus, the theoretical framework provides the criteria for the selection and combination of variables based on the defined purposes. Once the theoretical framework is established, a number of stages allow the construction of composite index, namely a) the selection of the sub-indicators; b) their normalization; c) the choice of weights of the sub-indicators; d) the choice of aggregation model.

First, the factors that significantly affect the phenomenon are chosen. Based on the theoretical framework, multi-dimensional concepts are divided into several sub-groups (i.e., sets of sub-indicators). Such a nested structure improves the user's understanding of the driving forces behind the composite indicator. Indicators should be selected based on their relevance to the phenomenon being measured and relationship to each other as well as their accessibility and their country coverage. The selection of a group of individual indicators can be based on expert opinion or using analytical approaches, such as principal component analysis, that allows to investigate the relationship among potential indicators in order to retain and use only the most representative ones. Individual indicators selected are then normalized to make them comparable.

Normalization of data is a required step prior to any data aggregation as the indicators often have different measurement units. After normalization, indicators are transformed into pure, dimensionless, numbers. Several normalization techniques can be used. One of the simplest and most common normalization procedures is the maximum-minimum method. It consists in a linear rescaling of each indicator value by subtracting the minimum value and dividing it by the range of the indicator values, so that the minimum value of that factor among all units of analysis is mapped to 0, while the maximum value to 1. Distance to a reference measure is a method that provides the relative position of a given indicator with respect to a reference point. The latter could be a target to be reached in a given time frame (e.g., the reduction target for CO₂ emissions) or a value assumed in a benchmark country. An extensive overview of normalization methods can be found in Nardo et al. (2008).

The definition of the weights to assign and the aggregation procedure to use for combining different dimensions is central in the construction of a composite indicator. The different weights assigned to single indicators should reflect their importance in expressing the considered phenomenon. Thus, for example, if the factors are considered of the same importance, equal weights can be assigned. If a high degree of correlation exists between two or more variables, statistical models such as principal component analysis or factor analysis should be used to overcome the double counting problem of indicators that partially measure the same behaviour (Nardo et al., 2005). Alternatively, participatory methods that incorporate various stakeholders' opinions can be used to assign weights. Subjective weights may be set by a group of experts such as technicians and policy makers or even by citizens through social surveys that allow to get how important individual indicators are for people. In the budget allocation approach, for example, weights are quantified by providing experts a "budget" of N points to distribute over a number of individual indicators; the expert "pays" more for those indicators whose importance they want to place more emphasis on.

Aggregation rules to combine all the components to get the final composite indicator can vary as well. The composite indicator can be obtained by the weighted sum of the sub-indicators (e.g., linear aggregation), their product (e.g., geometric aggregation) or aggregating them using non-linear techniques such as multi-criteria analysis. There is no obvious way of aggregating sub-indicators. The suitable aggregation method should be selected based on the aim of the work and the characteristics of the sub-indicators adopted. Linear aggregation is a compensatory approach that allows full compensability among dimensions, i.e., poor performance in one dimension can be compensated by sufficiently high performance of another (Greco et al., 2018). The geometric



aggregation also implies a certain degree of compensability between individual dimensions. However, while in a linear aggregation the compensability is full and constant, in the geometric aggregation compensability is lower for sub-indicators with lower value (Nardo et al., 2008). Hence, it could be considered as a less compensatory approach. In case compensability among dimensions is not allowed, non-compensatory methods such as the multi-criteria analysis should be used. Some general guidelines for the selection of the most suitable methods for the construction of a composite indicator can be found in Mazziotta & Pareto (2013).

5.1.1. Identification of Critical Urban Context or HotSpot using multi-risk composite-index

The theoretical framework to establish a composite index that can effectively aid in identifying critical urban contexts or hot-spots should address the challenge of integrating crucial physical and social and environmental vulnerability factors in integrated exposure assessment. Indeed, index-based approaches are particularly suitable for measuring multidimensional realities too complex to be summarized by a single indicator (e.g., De Groeve et al., 2013). For this reason, a straightforward risk-oriented exposure index that combines multiple hazards and physical, social and environmental exposure and vulnerability information is proposed herein. More specifically, the index is obtained combining single indicators representative of the aforementioned dimensions. This index can be adopted to evaluate urban critical contexts and hotspots on the territory (see also section 4.1). The context for which the index value is higher can be considered as the critical context, i.e., the context where the considered hazards may generate significant impacts due to characteristics and conditions of the exposed assets that are present in such area.

The proposed integrated multi-risk index for the j th sub-area (e.g. an urban district or census tract) of the urban settlement within a broader area of interest and considering Nh hazards is calculated according to:

$$R_j = \prod_{k=1}^{Nh} [(I_{PH,j}^k)^{w_{ph}} \cdot (I_{SO,j}^k)^{w_{so}} \cdot (I_{EN,j}^k)^{w_{en}}]^{w_k}$$

where the integrated multi-risk index R_j is a composite index for the j th sub-area determined after suitable composition of the risk indices evaluated for different dimensions, namely the physical PH, social SO and environmental EN dimensions. $I_{PH,j}^k$, $I_{SO,j}^k$ and $I_{EN,j}^k$ are the physical, social and environmental risk indices with respect to hazard k and related to the j th sub-area of the urban settlement. These indices define the integrated risk of the physical, social and environmental systems, considering the number of exposed assets to a given hazard (e.g., percentage of buildings located in hazard-prone area) taking into account also their vulnerability features influencing their response to hazards (e.g., the ratio between buildings with the poorest characteristics and the total number of buildings in the urban context) and the hazard intensity level which they are exposed to. w_{ph} , w_{so} and w_{en} are the weights adopted for each dimension of the index, representing the relative importance of individual dimensions in characterizing the risk, while w_k represents the weight associated to hazard k in the multi-risk framework. As discussed before, such weights could be defined by stakeholders based on their objectives and priorities. These weights vary between 0 and 1 and sum to 1. Risk index ranges from 0 and 1, with larger values indicating sub-regions that are prone to hazards of higher intensity, with exposure characterized by highest vulnerability and worst performances in terms of coping capacity.

Note that R is based on a geometric aggregation, that can be considered a partially compensatory approach (e.g., Mazziotta and Pareto, 2013). In other words, compared to a linear aggregation, it is required higher value of risk index related to one dimension (e.g., physical) to compensate as much as for a lower value of risk index related to another dimension (e.g., social). Similarly, a high value of the risk index related to a hazard k does not compensate as much as for a low value of the risk index for hazard $k+1$ (e.g., Nardo et al., 2008). Thus, areas where only one dimension (and one hazard) dominate are de-emphasized, allowing a better representation of the multi-dimensional and multi-risk concept. Ideally, this approach is suitable for the integration of other dimensions, i.e., other parameters and risk drivers affecting the coping capacity (e.g., parameters representative of the institutional and cultural vulnerability of an urban system).

5.1.2. Step-by-step methodology to identify Critical Urban Contexts (CUC) or HotSpots (HS) within an urban settlement

This paragraph exemplifies the methodology introduced in section 7.3 in one application finalized at identification of Critical Urban Contexts (CUC) or HotSpots (HS) within an urban settlement. Note that, while the CUC refers to a broader area (e.g. a district or a part of a district), the HS may be more localized, depending on distinctive features of the hazard and of the integrated exposure. For example, HS may be determined as the union of critical territorial areas identified within a district, e.g. census tracts.

The identification of CUC/HS within an urban settlement can be performed according to the following steps:

- 1) Select relevant hazard(s) to consider
- 2) Establish the set of indicators allowing the characterization of the hazard and its intensity level
- 3) Establish the risk/impact with respect to which the CUC/HS has to be defined
- 4) Establish the exposed assets of the urban system that contribute to the risk/impact
- 5) For each exposed asset select the set of indicators allowing the characterization of integrated exposure (assessment of exposure taking into account the vulnerability)
- 6) For each considered hazard evaluate the risk/impact with suitable combination of hazard and integrated exposure
- 7) Suitably combine the risk/impact evaluated for each hazard to obtain an integrated multi-risk index that is representative for the chosen impact metric

While this approach is suitable to overlay and combine the effects of single hazards on the exposed system, it does not allow to consider the cascading impacts that can be triggered in a complex urban system and the possible interactions that can be activated at the hazard or the vulnerability/impact level when the different parts of the urban system are also interconnected and interdependent. Indeed, even if most relevant hazards in an area, as well as a basic set of exposed elements, are identified, the unfolding of events can trigger unexpected cascading effects activating different types of vulnerabilities and eventually amplifying the final impact. Therefore, the risk-storylines introduced in DV5.2.1, complemented by their representation as impact chains, can be used as a practice-oriented support to guide the selection of the basic elements contributing to the relevant impact scenario, namely hazards, exposed assets and the vulnerabilities, as briefly explained in section 5.1.3.

The following example shows the use of the multi-risk composite index to select Critical Urban Context (CUC) for the case when no hazard interaction occurs and neglecting possible cascading effects. Next, section 5.1.2.1 shows an application to identify urban HotSpot (HS).

5.1.2.1. Example application for identification of CUC

In this section an example of CUC identification using composite index is presented.

The urban settlement selected for the application is the municipality of Somma Vesuviana, in the province of Naples, southern Italy. Somma Vesuviana is a municipality with medium-high population (about 35000 inhabitants, $C_{pop} = 5$), classified as a Town/Suburbs and it is an intermunicipal hubs, according to the classification criteria previously presented (see section 3.3). This municipality is classified as a coastal hill, and it is located on the slope of the Vesuvius volcano. Also, it is characterized by high social vulnerability (see Figure 36, section 3.3). Somma Vesuviana is selected as case study for this application as it is the largest and highly populated municipality in Campania region among ones showing a high value of seismic and flood hazard scores, according to the score-based procedure presented in section 3.4.2.

Preliminary to the application for CUC identification, the urban districts for the municipality should be delimited.

As mentioned before, urban districts are homogeneous areas characterized by homogeneity of urban fabrics, road patterns, buildings' economic value, construction period, and technical-constructive features (section 2.1.1). Their proper identification would require a detailed analysis of urban road patterns, urban fabric and geomorphology of the territory as well as a detailed investigation of buildings features. When such a detailed assessment is missing, a simplified approach for urban district delimitation can be based on historical maps

showing the evolution of the urban settlements or available open-source data. The real estate observatory (Osservatorio del Mercato Immobiliare – OMI – in Italian), for which open source data and maps are available, identifies homogeneous municipal areas based on maximum/minimum market and lease real estate values, expressed in euro per surface unit (square meters), type of property and state of conservation. Also, such maps usually identify areas representing the historical center of the municipality, accounting for the historical evolution of the urban settlements as well. Thus, those areas (OMI zones) are used to delimitate urban districts for this application. Figure 63 shows the delimitation of urban districts based on OMI zones for Somma Vesuviana; the corresponding market and lease real estate values are reported in table 11.



Figure 6465. Delimitation of OMI zones allowing to identify urban districts in Somma Vesuviana. Each zone is identified by an alphanumeric code that categorizes the zone as Central (B), Semi-central (C), Suburb (D) and rural (R).

Zones B2 and B3, which encompass the historical center of the municipality, are associated with the highest real estate market value of residential buildings (between 1,050 and 1,600 Euro/m²), while the lowest market values are associated with the northern (D3) and southern (D4) suburban areas. No market value is associated with zone R1, because it is a rural area on Mont Vesuvius without residential buildings. Therefore, this area is neglected in the analysis.

Table 10. Real estate market value and lease value of residential buildings in each OMI zone of Somma Vesuviana.

OMI zone - denomination	Market value (euro/mq)		Lease value (euro/mq per month)	
	min	max	min	max
B2 – Central (Historical centre)	1050	1600	3.2	4.9
B3 – Central (First belt of historical centre)	1050	1600	3.2	4.9
C3 –Semi central (RIONE TRIESTE - VIA POMINTELLA)	900	1350	2.8	4.2
D3 – North Suburban (STRADA STATALE DEL VESUVIO / SS. 268)	840	1300	2.6	4
D4 – Suburban, slope of mountain Somma (VIA S. MARIA DELLE GRAZIE)	760	1150	2.3	3.5
R1 – Suburban (mountain Somma)	-	-	-	-

Once the districts in the municipalities are delimited, the identification of the CUC is based on the index-based methodology presented in section 5.1 and following the steps listed in 5.1.1.

- 1) The hazardous events considered are earthquakes and riverine floods.
- 2) The seismic hazard indicator is derived from a measure of earthquake-induced ground shaking at the district level, which is quantified according to a selected hazard map. In particular, the PGA value for 475-year return period (or 10% probability of exceedance in 50 years) is selected as measure of ground shaking. The adopted flood hazard indicator is the percentage of OMI zone area expected to be inundated in a medium probability flood scenario (with a mean return period between 100 and 200 years). Below some details on how such indicators are derived.

a. Seismic hazard:

In Italy the official reference for seismic hazard is the MPS04 model proposed by Stucchi et al. (2004; 2011) which presents the hazard in terms of maps showing the value of peak ground acceleration (PGA) and spectral acceleration at reference elastic periods ($S_a(T)$) corresponding to an exceedance probability in a given period of time or, equally, to an assigned return period. PGA value at municipal centroid is assumed as hazard input for all zones. To account for soil amplification effects, the map containing V_s30 values with a spatial resolution of 50×50 m was proposed in Mori et al. (2020) and adopted herein. Criteria for soil category identification adopted are the ones reported in the new Italian building code (NTC18). Five soil categories are identified (A, B, C, D, E), based on topographic characterization and corresponding V_s30 values and for each category soil amplification factors of the spectral acceleration are defined. For each area of analysis (i.e., OMI zone) the percentage occurrence of soil types can be obtained as weighted average of all grid points (V_s30 map) included in the area. Then, the soil factor to apply can be defined as weighted average of soil type factors based on the percentage of soil types in the area. Figure 64 shows the map with V_s30 values for Somma Vesuviana. Based on this map, the soil type B represents the entire municipality. Thus, the soil factors corresponding to such type is applied to amplify the hazard input (PGA) in each zone. In figure 64 the slope map (derived from DEM) is also shown. The latter is used to define topographic amplification factors. The code (NTC18) defines four topographic categories based on the slope (expressed in degrees). A specific topographic amplification factor should be applied if the slope exceeds the 15° . It can be noted that only in few areas of the town the slope is greater than 15° . In such areas amplification factors are considered in the definition of hazard input. Specifically, amplification values to adopt are obtained considering the weighted average of all points that have a given slope and the associated factors, as also describe before for soil factors.

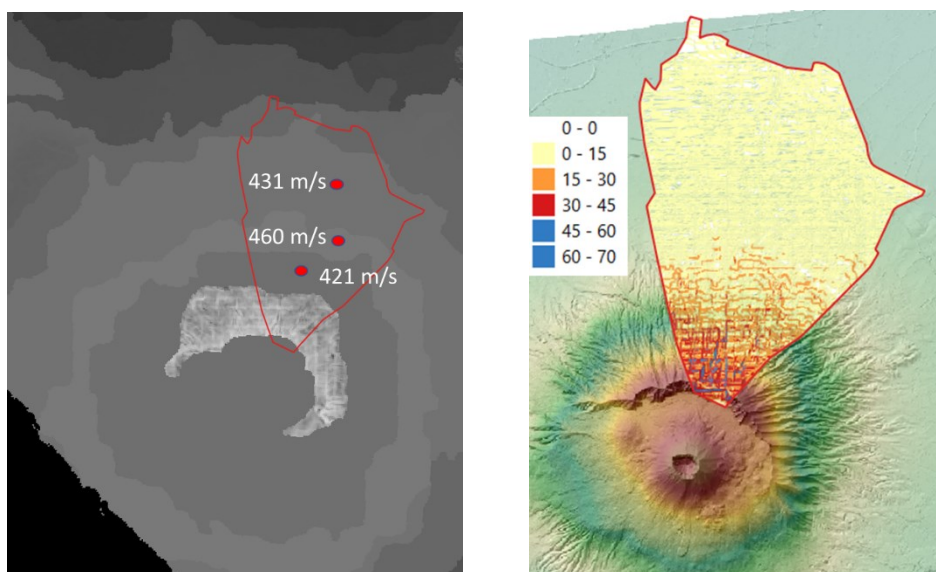


Figure 6566. V_s30 map (left) proposed by Mori et al. (2020) and slope map (right) for the municipality of Somma Vesuviana (bounded with red polyline).

b. Flood hazard:

The percentage of the district area expected to be inundated in a medium probability flood scenario (with a mean return period between 100 and 200 years), is adopted as flood hazard indicator. Such scenario is based on reference flood hazard maps for Italy provided by ISPRA (see also section 3.4.2). Inundation is a reasonable proxy for water depth (the flood hazard intensity measure commonly used) in this case, given their typically close relationship (i.e., the higher the water depth, the larger the inundation area). In figure 65 the hydrogeographic network and flood hazard maps for the medium probability flood scenario provided by ISPRA are reported. It should be noted that inundation maps are highly influenced by the presence of Regi Lagni, that are a network of artificial canals created in XVII century (Tocchi, 2023)

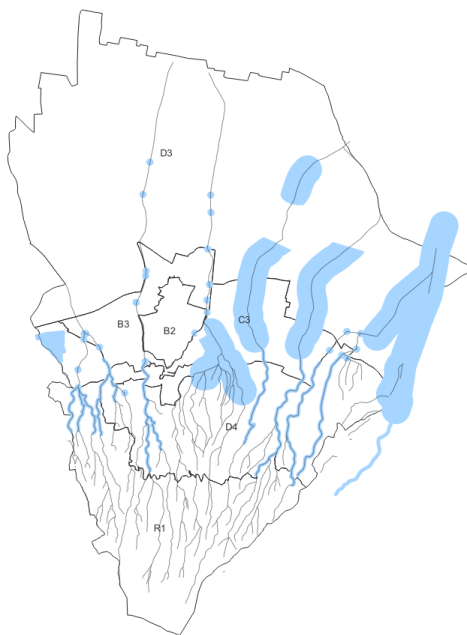


Figure 6667. Hydrogeographic network and flood hazard maps for the medium probability flood scenario provided by ISPRA for Somma Vesuviana

- 3) The risk metric with respect to which the CUC has to be defined is the direct economic loss due to structural/non-structural damages of residential buildings and their contents.
- 4) Thus, as exposed asset for this application only residential buildings are considered.
- 5) To characterize the integrated exposure (assessment of exposure taking into account the vulnerability) the vulnerability indicator of physical assets (in this case of the buildings), expressing the susceptibility of buildings to be damaged by the considered hazardous event, have to be determined.

Concerning earthquake, the Risk-UE index-based approach is adopted to derive seismic Vulnerability Indicator VI (Lagomarsino & Giovinazzi, 2006) for each building typology identified within the district. In such a case the integrated exposure, denoted as VE^s to indicate that it combines both seismic vulnerability and exposure, is obtained as a weighted average of the VI based on the number of buildings of each typology within the district. More details on how to derive building exposure with an integrated inventory approach, combining census data with other sources of information, can be found in (Polese et al. 2019, 2020; Tocchi et al. 2022).

Concerning integrated exposure to floods it should account for the number of buildings belonging to different flood vulnerability classes. Flood vulnerability for buildings is often expressed as a function of the occupancy type, the construction material and building's height, with most vulnerable classes formed by 1 storey buildings (Huizinga et al., 2017; Gentile et al., 2022; FEMA, 2022). Because the material type for residential buildings in southern Italy is mainly Masonry or Reinforced Concrete and for those material no appreciable differences in flood vulnerability is observed, the integrated exposure to floods VE^f can be simply assumed as the number of 1 storey residential

buildings in the district. Such information can be easily derived from census data (ISTAT, 2011) at census tract level. Information at district level is obtained considering all census tracts belonging to it.

- 6) Having determined the hazard and integrated exposure indicators, the risk index for each considered hazard can be determined.

Seismic risk index related to the physical asset considered (i.e., residential buildings) for the j th district (corresponding to OMI zone for this application) is calculated as follows:

$$I_{PH,j}^s = \frac{(H_j^s + VE_{PH,j}^s)}{2}$$

Where:

- PH denotes the physical asset (in this application only residential buildings are considered as physical asset exposed)
- H_j^s is the normalized value of the seismic hazard intensity level in the j th district
- $VE_{PH,j}^s$ is the normalized value of the integrated exposure indicator in the j th district

The min-max transformation is adopted as normalization method. Each variable value is converted to a normalized value by subtracting the minimum value and dividing by the range of the indicator values, according to following equation:

$$NV_j = \frac{V_j - \min_j}{\max_j - \min_j}$$

Where V_j is the value of the variable for the district j , \min_j and \max_j are the correspondent minimum and maximum values over all districts within the municipality, respectively, and NV_j the normalized value of the variable. In this way, each variable is expressed in a standard scale, where 0 indicates the lowest value within the whole sample and 1 the highest one.

Similarly, flood risk index for the j th district is calculated as follows:

$$I_{PH,j}^f = \frac{(H_j^f + VE_{PH,j}^f)}{2}$$

Where:

- PH denotes the physical asset (in this application only residential buildings are considered as physical asset exposed)
- H_j^f is the normalized value of the flood hazard intensity level in the j th district
- $VE_{PH,j}^f$ is the normalized value of the flood integrated exposure indicator in the j th district

Tables 12 and 13 show the values of seismic and flood hazard, and integrated exposure indicators for each district in Somma Vesuviana (corresponding to OMI zones) as well as their normalized values. The last column in each table represents the risk indices calculated for each hazard for each district (zona OMI).

Table 11. Seismic hazard and integrated vulnerability indicators and related normalized value for each urban district (i.e., OMI zone). The final value of the seismic risk index is reported in the last column (R_index).

Earthquake					
Zona OMI	PGA [g]	H^s	VE_Index	VE^s	R_index
B2	0.2064	0.000	0.5778259	0.897	0.448
B3	0.2072	0.071	0.5491046	0.412	0.242
C3	0.2072	0.071	0.527811	0.053	0.062
D3	0.2064	0.000	0.583933	1.000	0.500
D4	0.2180	1.000	0.5246783	0.000	0.500

Table 12. Flood hazard and integrated vulnerability indicators and related normalized value for each urban district (i.e., OMI zone). The final value of the flood risk index is reported in the last column (R_index).

Flood					
<i>Zona OMI</i>	<i>Flooded Area [%]</i>	<i>H^f</i>	<i>VE Index</i>	<i>VE^f</i>	<i>R index</i>
B2	0.01	0.000	0.108	0.000	0.000
B3	0.1	0.231	0.145	0.200	0.215
C3	0.4	1.000	0.193	0.458	0.729
D3	0.12	0.282	0.293	1.000	0.641
D4	0.18	0.436	0.212	0.562	0.499

Note that risk indices are calculated adopting the linear aggregation, i.e., a compensatory approach (Nardo et al., 2008), assuming that hazard and integrated exposure information have the same importance (i.e., without weighting single indicators). This means that a low value of the integrated exposure can be totally compensated by a high value of the hazard and vice-versa.

- 7) Finally, the integrated multi-risk index is obtained combining seismic and flood risk indices as follows:

$$R_j = I_{PH,j}^s \cdot w_s \cdot I_{PH,j}^f \cdot w_f$$

Where w_s and w_f are weights assigned to seismic and flood risk respectively. For this application same weights are adopted for the two risks, i.e., it is assumed that the two risks have the same importance.

Figure 66 shows the value of the integrated multi-risk index in each Somma Vesuviana's districts. It can be noted that district D3 shows the highest integrated risk index value ($R=0.566$) due to the highest value of seismic risk index ($R=0.5$) and a relevant value of the flood risk index (0.641, the highest value excluding D4 district's value). Such high values are mainly influenced by high seismic exposure/vulnerability and high flood exposure/vulnerability of buildings (see Table 12 and Table 13). Therefore, district D3 can be considered the critical urban district for the municipality of Somma Vesuviana. District D4 also shows high value of the integrated risk index, because of high flood risk index ($R= 0.499$, due to both high flood hazard and flood exposure/vulnerability) and high seismic risk index ($R=0.50$, mainly due to high seismic hazard). On the contrary, district B2 shows a value of R equal to zero. This is due to the almost total absence of flood hazard in the area (only the 1% of area is expected to be inundated). As a partially compensatory approach is adopted for the calculation of the integrated risk index, the absence of flood hazard (and flood risk) in the sub-region is not compensated at all by the high value of the seismic risk.

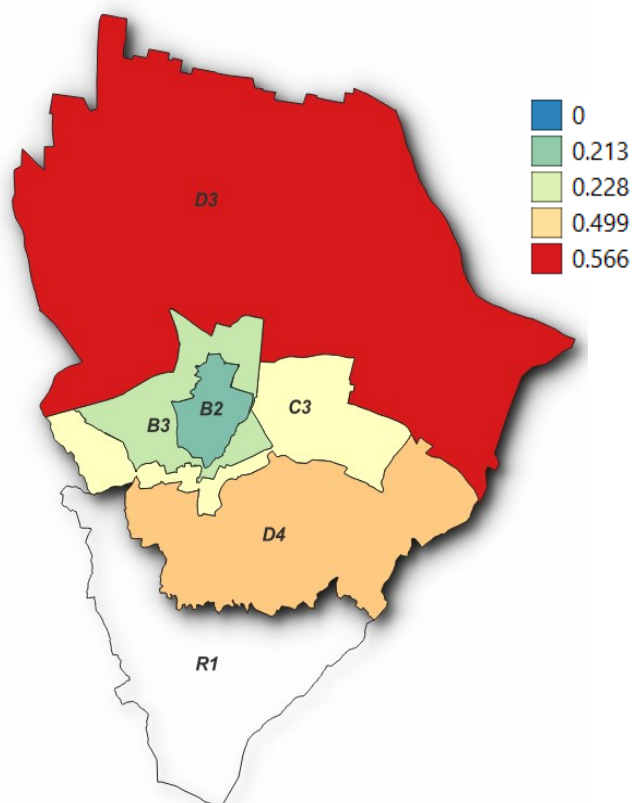


Figure 6768. Integrated risk index values for Somma Vesuviana's districts.

5.1.2.2. Example application for identification of HS

In this section an example of HS identification using composite index is presented. The operational workflow, developed through the use of IT tools (GIS-based), identifies hotspot areas based on the hazard, vulnerability, and exposure characteristics of urban settlements (Verde et al., 2024); the approach presented was further developed in Verde (2024).

The data and the process described for this example application have been developed in former research projects METROPOLIS - Metodologie e Tecnologie integRate e sOstenibili Per l'adattamentO e La sIcurezza di Sistemi urbani (STRESS S.c.a.r.l. - Sviluppo Tecnologie e Ricerca per l'Edilizia Sismicamente Sicura ed ecosostenibile, University of Naples Federico II and University of Sannio and industrial partners and national and international entities such as Municipality of Naples, Civil Protection, River Basin Authority, CMCC – Centro Euro-Mediterraneo sui Cambiamenti Climatici, Scientific Coordinator of the project: prof. G. Verderame, Scientific Coordinator and Scientific director of DiARC Research Team: prof. V. D'Ambrosio - PONREC 2007/2013) and PLANNER-Piattaforma per LA GestioNe dei rischi Naturali in ambiEnti uRbanizzati (EET Spa – Lead Partner, Genesis GI, STRESS S.c.a.r.l. - Sviluppo Tecnologie e Ricerca per l'Edilizia Sismicamente Sicura ed ecosostenibile, Scientific Coordinator of the project: prof. G. Verderame; Scientific Coordinator for climatic aspects: prof. Valeria D'Ambrosio) and partly re-arranged here to show the derivation of HS in a composite-index based framework.

The urban settlement selected for the application is the eastern part of the city of Naples, southern Italy. The minimum territorial areas analyzed towards definition of urban HS are the census tracts, for which open-source information on a number of indicators are available.

Once the minimum territorial areas are established, the identification of the areas contributing to HS is based on the index-based methodology presented in section 7.3 and following the steps listed in 7.3.1.

- 1) The hazardous events considered are heat waves and pluvial flooding.

- 2) For each hazard, a set of indicators has to be implemented to establish the hazard intensity levels. Concerning heat wave, the indicators used to establish its intensity level are: Maximum air temperature, Minimum air temperature, Heat Index and Surface temperature gradient day night. In particular, to assess a hazard scenario, it is necessary to establish for how many consecutive days each of the indicators described exceeds a specified threshold. When all four indicators exceed the threshold values for more than the specified number of consecutive days, a heat wave phenomenon is produced. The projections over time of the identified characteristics are obtained from the RCP (Representative Concentration Pathways) from CMCC (<https://www.cmcc.it/it/scenari-climatici-per-litalia#rcp>) scenarios of greenhouse gas emissions and concentrations for the RCP 4.5 scenario in which emissions are expected to stabilize; RCP 8.5 scenario in which emissions are expected to increase steadily until 2100. Concerning pluvial flooding, the indicators used to establish its intensity level are: Flood Hazard rating and Concentration of distress calls received by Civil Protection (when a heavy rain event causes more danger than an average). In particular, daily precipitation height data (mm) from two different reference periods were considered. Data for the period 2001-2014 were used to simulate current flooding scenarios. Data from 1971-2000 were used for processing in relation to RCP scenarios 4.5 and 8.5.
- 3) The risk metric with respect to which the HS is defined is the increased risk of having a health or safety/livability problem for the population. Referring to heat wave, health problems may be e.g. heat stroke, fainting, shocks, while for pluvial flooding the safety/livability problem is connected to sudden inundation of basements in buildings and rapid water flow in urban areas.
- 4) The exposed assets contributing to such a risk are the population, the buildings and open spaces. While, obviously, the presence itself of the population is necessary for the considered risks to be relevant, the features of buildings and urban spaces, interacting with the hazard, determine the urban conditions for which the hazard can induce more or less critical situation in certain areas.
- 5) To characterize the integrated exposure for the exposed assets (in this case of the population, buildings and open spaces) a set of indicators is identified to allow the assessment and the characterization of the exposure taking into account the vulnerability of each sub-system. Referring to the population, apart from the total population, it is relevant to characterize the social vulnerability that can aggravate the probability of incurring in health or safety/livability problems for both the considered hazards. Some indicators that are usually considered to characterize the social vulnerability are vulnerable groups (number of people with age over 75 and under 4) and fuel poverty population (number of people with low income and family with more than 5 people). All those indicators are retrievable from open-source data such as census databases (available at census tract level). Referring to buildings, the indicators that are relevant to characterize integrated exposure to heat wave are features that, in case of a heat wave, determine their thermal performance such as: Volume, Thermal lag, Thermal decrement factor, Solar exposure of building envelope. Such features allow to characterize the vulnerability of buildings with respect to the heat wave. On the other hand, relevant characteristics of buildings for pluvial flooding, influencing their vulnerability with respect to such hazard, are: Coverage ratio, Percentage of building on pavement, Ground floor activities, Type of coverage. Referring to open spaces, the indicators that are relevant to characterize integrated exposure (and vulnerability) to heat wave are: Albedo, Sky View Factor, Solar exposure of open spaces, Normalized Difference Vegetation Index. Referring to pluvial flooding, the relevant indicators characterizing the vulnerability for open spaces are: Open space area, Soil permeability (based on runoff coefficient of surfaces), Drainage capacity of the sewage system and Degree of maintenance of the sewer system. For each single hazard, the integrated exposure is determined by suitable combination of the population exposure taking into account its vulnerability characterization (e.g. number of people with age over 75) with the vulnerability of buildings and open spaces. In the previous research project (D'Ambrosio et al., 2016; D'Ambrosio et al., 2017; Aprea et al., 2019; D'Ambrosio et al., 2023) the process employed to derive the integrated exposure was as follows: a so-called intrinsic vulnerability of the building and open space system was calculated, obtained by performing a weighted average of the normalized values of the indicators. Such intrinsic vulnerability was classified on a scale 5 classes (1 - high vulnerability level, 5 low criticality level). Next, each

vulnerability value (building intrinsic vulnerability and open spaces vulnerability) was combined with the value of the exposed value (in this case the total number of affected population for each hazard) leading to the estimation, for each unit cell of analysis (the census tract) of a single value (not necessarily lower than one) that integrates both vulnerability and exposure, i.e. the integrated exposure. The combination of intrinsic vulnerability and exposure was performed according to pre-determined aggregation rules (e.g. low exposure + high intrinsic vulnerability of buildings + medium intrinsic vulnerability of open spaces → medium value of integrated exposure).

Although the process just described as used in the previous research works does not follow the normalization and standard rules for aggregation that are employed in composite-index method, it can be logically re-formulated so to allow the calculation of an adimensional index VE.

- 6) Having determined the hazard and integrated exposure indicators, the risk/impact index for each considered hazard can be determined.

In the previous research works, the process employed to derive the impact was as follow:

for each hazard the impact indicator was calculated as a combination of the previously integrated value of vulnerability and exposure and the value of the hazard intensity level considered. Suitable combination rules were employed to establish the impact (e.g. low hazard intensity + high integrated exposure → medium-high value of impact). The impact value was classified in 5 classes (1- high impact level, 5 - very low impact level). The figure below maps the impact calculated with this process with reference to east area of Naples and adopting the census tracts as minimum territorial units.

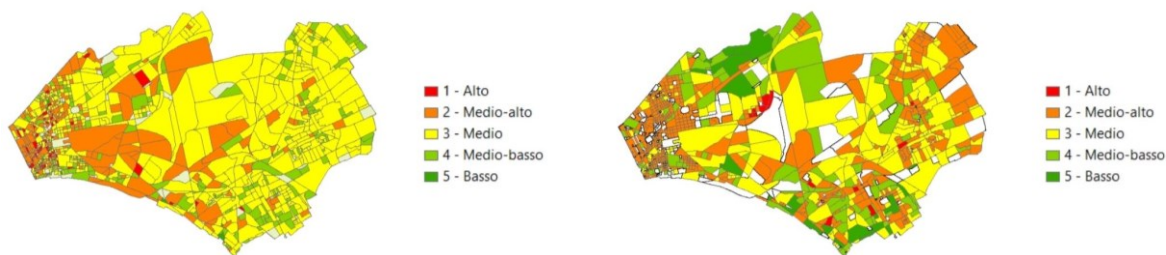


Figure 68.69 Impact scenario of pluvial flooding (on the left) and of heat wave (on the right).

Although the process just described as used in the cited research works does not follow the normalization and standard rules for aggregation that are employed in composite-index method, it can be logically re-formulated so to allow the calculation of an adimensional Risk index for each hazard.

- 7) Finally, the integrated multi-risk index is calculated to identify the HotSpot area

Once the risk/impact scenario is calculated for each hazard, it is possible to obtain an integrated multi-risk index derived from the values pertaining each hazard. In this phase, it is important to remember that both the risk/impact scenarios refer to the same “time scenario”. Indeed, the same RCP 4.5 scenario for medium term is considered for the evaluation of the impact for both hazards.

The process employed to derive the integrated multi-risk indicator was first tested as follow: the areas where the value of the integrated multi-risk index is higher are to be considered urban HotSpots based on the quantitative approach described. In particular, suitable combination rules were employed to establish the value of the multi-risk index based on the value of the heat wave risk/impact index and pluvial flooding risk/impact index.

The figure below maps the urban HotSpots derived with the aforementioned approach.

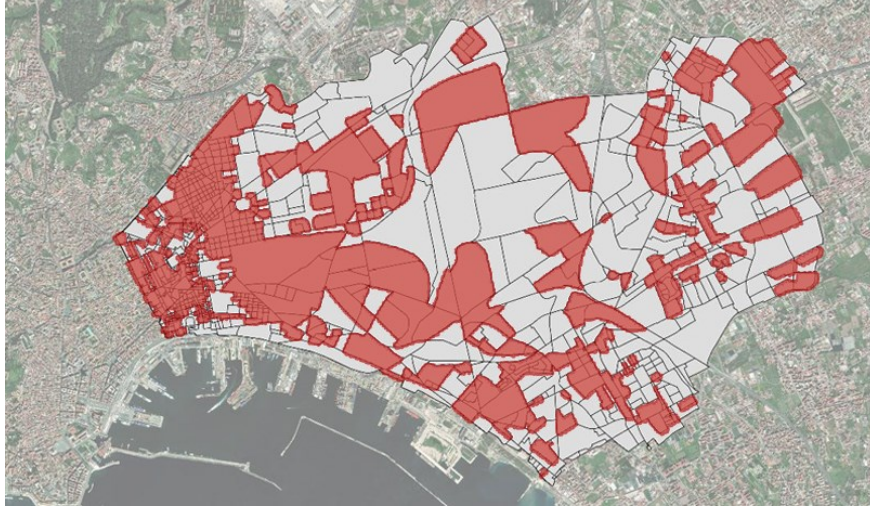


Figure 69.70 Urban hotspots. In the described example the urban hotspots are identified based on a quantitative approach and aggregation rules specific for the study area.

Similarly to what observed for step 6, although the process just described as used does not follow the normalization and standard rules for aggregation that are employed in composite-index method, it can be logically re-formulated so to allow the calculation of an adimensional integrated multi-risk index for each of the unit area j considered in the analysis (in this case the j^{th} census tract). In such a case, each single risk index obtained relative to the single hazard should be normalized considering the values obtained for all the study area. Also, suitable weights w_{hw} and w_{pf} (where subscripts hw and pf refer to heat wave and pluvial flooding, respectively) should be assigned to aggregate the single risk indices $I_{PH,j}^{hw}$ and $I_{PH,j}^{pf}$ in a single integrated multi-risk index R_j :

$$R_j = I_{PH,j}^{hw} w_{hw} \cdot I_{PH,j}^{pf} w_{pf}$$

It should be noted that in the aforementioned application equal weights were assigned to heat wave and pluvial flooding. However, standardized approaches such as multi-criteria, could be used to implement the method for the choice of weights.

5.1.3. Selecting relevant sub-indicators: the use of risk storylines

As previously discussed, the risk-oriented exposure index can be calculated as a function of relevant indicators suitably chosen to represent the exposure of assets to the considered hazards and taking into account the respective vulnerabilities. However, it has to be recognized that the urban settlements and their contextual representation, considering all relevant elements, systems, interrelations and behavioural aspects with respect to multi-hazard conditions, are extremely complex systems and it would be impracticable to capture with a single index the different exposure conditions that could enable the recognition of the so called “urban critical contexts” or “hot-spots”.

A viable approach is to select just the more representative exposure indicators and use them to build the composite risk-oriented exposure index. Indeed, once identified, such indicators are normalized, weighted and aggregated according to the defined approach (section 5.1). For the selection of indicators, it is crucial to define: i) which are the hazardous events of interest; ii) which exposed elements to consider. In fact, the critical district (and hotspots) may change depending on the considered hazards and exposure dimensions (e.g., the exposure to only one hazard or to more than one hazard; the sole physical exposure or also the social exposure etc.). The former issue (point i), concerning the selection of relevant hazards to consider, can be partially solved considering the most relevant hazards (in terms of intensity/frequency) in the urban area; such hazards can be determined adopting a score-based procedure, as proposed in section 3.4.2. On the other hand, the selection of the exposed elements (point ii), suitably considering the respective vulnerabilities, is not so straightforward;

one should recognize that some assets may be considered more relevant with respect to others depending on the impacts and risk that are feared, and different stakeholders may consider more important some assets with respect to others. Moreover, even if most relevant hazards in an area, as well as a basic set of exposed elements, are identified, the unfolding of events can trigger unexpected cascading effects activating different types of vulnerabilities and eventually amplifying the final impact. The understanding and representation of such complex multi-risk scenarios and hazards interactions can be problematic, especially if a rigorous probabilistic approach, taking into account the uncertainties, is applied; as a consequence, even the selection of the exposed elements is more difficult. A practice-oriented support to guide the selection is provided by the so-called risk-storylines (Shepherd et al., 2018; see also DV2.1). Risk storylines are becoming more popular in the field of risk management as a tool to describe the possible impacts of complex phenomena that present a high degree of uncertainty only partially captured by the use of probabilistic models (Sillman et al., 2020). This tool is useful for improving the understanding of risk through an approach oriented more towards representation than probabilistic evaluation of the events themselves. In this context, a Risk Storyline is a scenario that consistently represents the unfolding of a series of past events or chains of future events considered plausible. In the compilation of storylines, the emphasis is placed on understanding the driving factors that intervene during the event and the reliability of these factors.

Representing the risk storylines as impact chains (Zebisch et al., 2022) the basic elements contributing to the scenario, namely hazards, exposed assets, vulnerabilities, the impacts, as well as the causal relations and interdependencies, are clearly identified.

Once that the urban context is identified, i.e. the urban settlement type is chosen and impending hazards are defined, the construction of a risk storyline, complemented by impact chains, allows to i) identify the individual exposure and vulnerability components of the urban system linked to one or more risks; ii) highlight the cascade mechanisms and the set of exposed systems and functions potentially affected by the combined effects of multiple risks; iii) the knowledge of the system's vulnerability factors that influence its ability to respond and adapt to the action of combined risks.

A further step towards selection of the most relevant indicators to define an urban hotspot is the choice of risk that needs to be managed, e.g. through implementation of suitable mitigation strategies. For instance, if the aim is the identification of the urban district most responsible for the economic impacts expected during the events (i.e. the risk is having excessive economic losses), the main exposure/vulnerability elements affecting the direct economic losses can be identified by a bottom-up approach. Through risk storylines and impact chains also the key features of the exposed system that mostly drive a specific type of impact can be identified, for example the not redundant road network that may increase the risk of traffic disruption.

Within this project, some risk storylines were developed involving relevant stakeholders and experts in different fields (from geology to sociology) (Deliverable 5.2.1). Figure 67 shows an example of impact chain showing the sequence of impacts due to the occurrence of a tsunami triggered by an earthquake in an urban context characterized by the presence of an industrial site handling dangerous substances.

SC.03 - Contesto insediativo in area metropolitana sulla linea di costa/Rischi climatici, biologici e no-tech

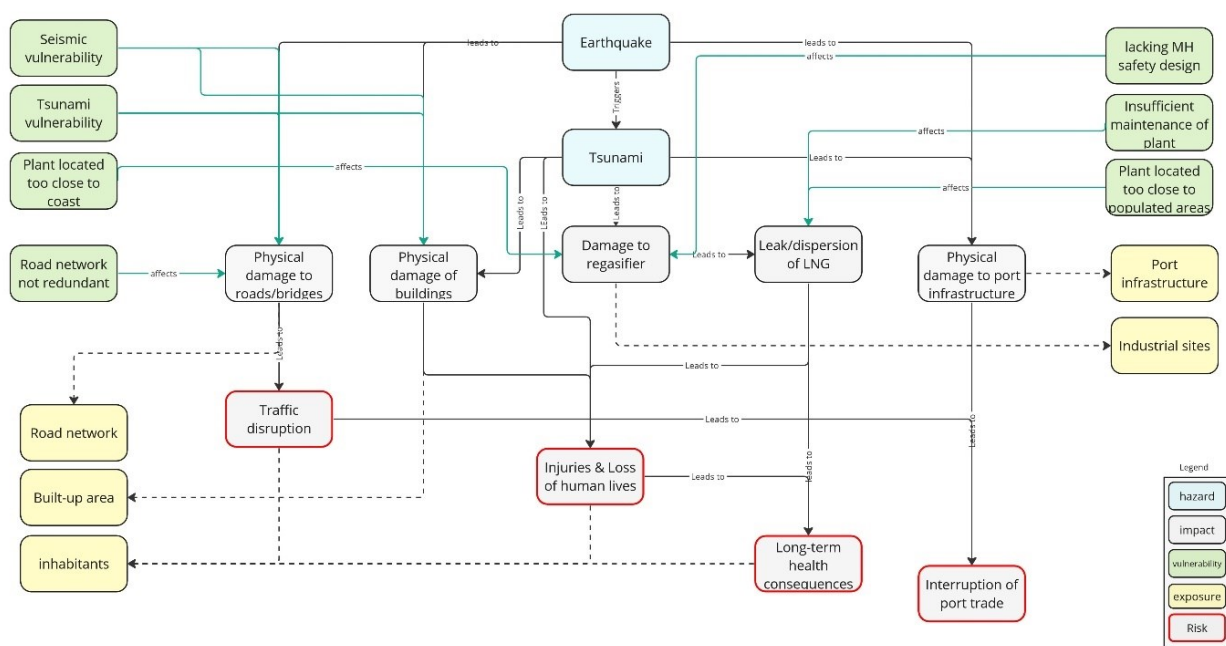


Figure 70 71. Example of impact chain showing the sequence of impacts due to the occurrence of a tsunami triggered by an earthquake in an urban context characterized by the presence of an industrial site handling dangerous substances.

The following sub-paragraph exemplifies the steps for identification of critical urban district (CUD) starting from the risk-storyline shown in Figure 67.

5.1.3.1. Example application for the construction of composite-index based on risk-storyline

The steps listed in section 6.3.3 to identify the critical urban district (CUC) within a municipality can be still applied also in the case the risk-storylines are employed as a support tool. The main differences when using risk-storyline are in steps 1, 3 and 4. Indeed, (step 1) the relevant hazards (and combination) is already established in the risk-storylines. Moreover (step 3) the risk-storyline may unfold several impacts (e.g. direct economic losses, injured/deaths, health issues) and a suitable choice of the impact metric to consider should be performed to be able to proceed with the CUC identification. A possible guiding question for selecting the impact metric is: “With respect to which impact is the HS or CUC defined?”. Once the impact metric is chosen, the exposed assets contributing to such impact, as well as the related vulnerabilities, are identified through the impact chain (step 4). The rest of the approach can be applied in a similar way, with identification of relevant indicators for hazard and vulnerability/exposure as well as for the combination in a final composite indicator representative of the criticality of an urban area.

- 1) Referring to the impact chain shown in Figure 67 the hazardous events considered are earthquake and tsunami.
- 2) Seismic hazard indicator can be evaluated as the PGA value at selected scale (e.g., urban district level or census tract level), derived from Italian seismic hazard maps (MPS04, Stucchi et al., 2004; 2011), taking into account also soil amplification factors (NTC18), as shown in section 5.1.2.1. Indicator for tsunami hazard intensity level can be derived from Tsunami inundation maps and related warning zones provided by ISPRA (see section 3.4.2). For instance, the percentage of expected inundated area under tsunami threat (i.e., tsunami alert buffer zones encompassing both Advisory and Watch levels inundation areas) in each sub-region of analysis can be selected as tsunami hazard indicator.
- 3) The impact chain for this example shows that different impacts and risks can be determined along this storyline. For this first example the risk/impact with respect to which the CUC/HS has to be defined are injuries and loss of human lives.

- 4) Exposed assets that play a crucial role in determining such kinds of impacts can be identified through the impact chain shown in Figure 67. The risk storyline presented in such is developed assuming a context also exposed to Natech risk, i.e., assuming that nearby the urban settlement an industrial site classified as major accident hazard sites is located. However, if there is no hazardous industrial site in the considered context, only two assets have to be considered for the identification of CUC/HS with respect to injuries and loss of human lives:
 - Buildings (e.g., residential buildings, educational buildings, health buildings, etc.)
 - Population (i.e., inhabitants)
- 5) Integrated exposure indicators of physical assets (i.e., buildings) have to be defined. Such indicators represent their exposure accounting for their susceptibility to be damaged by the considered hazardous event. According to urban taxonomy for grey infrastructure proposed in DV5.2.1, buildings can be classified based on their use/occupancy. Thus, integrated exposure indicators for each type of building located in hazards prone areas should be properly defined. For the purposes of this application, it is assumed that in the area potentially hit by earthquake and tsunami only residential and educational buildings are located.

As shown before (section 5.1.2.1), the Risk-UE index-based approach can be adopted to derive a seismic Vulnerability Indicator VI (Lagomarsino & Giovinazzi, 2006) for each building typology identified within the district. In such a case the integrated exposure, denoted as VEs to indicate that it combines both seismic vulnerability and exposure, is obtained as a weighted average of the VI based on the number of buildings of each typology within the district. This approach is specifically developed for residential buildings. A similar approach can be used for educational buildings as well. Although index-based approaches are not available for not residential buildings, vulnerability indices can be derived based on existing fragility models (e.g., Borzi et al., 2013; Perrone et al., 2020). Final integrated exposure values VEs of physical assets can be defined as a function of the integrated exposure indices of residential and educational buildings (e.g. the maximum or the mean value). Tsunami vulnerability depends on buildings typological and structural features as well. The main parameters affecting tsunami vulnerability of buildings (both residential and educational) are the construction material, the lateral load resisting system, the height and the age of construction (Del Zoppo et al., 2022; FEMA, 2017). Further vulnerability factors to take into account for assessing tsunami vulnerability of buildings are ground floor hydrodynamics, foundation type, shape and orientation (with respect to the flow) as well as the presence of natural barriers and large movable objects in the surrounding of buildings (Dall'Osso et al., 2009). For the estimation of tsunami integrated exposure index, available index-based approaches can be used, such as the Papathoma Tsunami Vulnerability Assessment (PTVA) index (Dall'Osso et al., 2016).

Integrated exposure index related to social assets (i.e., population) should consider the people exposure (i.e., number of persons exposed) accounting for their variable susceptibility to be adversely affected by hazardous events as well. To quantify social vulnerability to natural hazards index-based approaches proposed in literature can be used (Cutter et al., 2003; Yoon, 2012; Frigerio et al., 2018).
- 6) The risk index for each considered asset and hazard is determined combining the hazard and integrated exposure indicators.
- 7) The integrated multi-risk index is obtained combining seismic and tsunami risk indices of physical and social assets according to the approach proposed in section 5.1.1.

If a different risk/impact is selected exposed assets contributing to such risk may change and the indicators to represent their exposure should be suitably defined.

Next steps are re-developed starting from a different choice at step 3.

- 3) For this second example the risk/impact with respect to which the CUC/HS has to be defined is the traffic disruption.
- 4) Exposed assets can be determined with the aid of the risk storyline presented in Figure 66. In this case, the road network (including roads and bridges) is the asset that may lead to traffic disruption (and therefore have to be considered for the identification of CUC/HS).
- 5) Integrated exposure indicators for physical assets, i.e., roads network and buildings, exposed to seismic and tsunamis have to be defined. Such indicators express their susceptibility to be damaged due to the hazardous event considered. Buildings seismic and tsunami vulnerability (and related integrated exposure index) can be estimated using procedures and models shown in the previous example. Concerning road network, several vulnerability models are available in literature to evaluate the seismic vulnerability of individual assets and systems such as bridges, tunnels and roads (Andreotti & Lai, 2019; Argyroudis et al., 2020; Dukes et al., 2018; Ghosh et al., 2015; Borzi et al., 2015). An extensive review on available seismic vulnerability models for individual road assets and systems are provided in El-Maissi et al. (2020). In El-Maissi et al., (2023) an index-based approach to evaluate seismic vulnerability of road systems accounting for the “eccentric vulnerability” of the system (function of the damage to buildings surrounding the roads) is also proposed.

Coastal road networks may be damaged or totally destroyed by tsunamis, either by debris impact or erosion of the substrate material (Eguchi et al., 2013; Horspool and Fraser, 2016; Kawashima and Buckle, 2013; Kazama and Noda, 2012; MLIT, 2012). Also, roads level of service may be reduced in the aftermath of a tsunami, not only due to their physical damage but also due to debris litter (Evans and McGhie, 2011). For transportation assets, many studies analyzed bridge structures and proposed tsunami fragility function (Kawashima and Buckle, 2013; Koks et al., 2019; Shoji and Moriyama, 2007). Williams et al. (2019) developed tsunami fragility functions for both roads and road bridges, considering road asset damage data from two recent tsunamis, the 2011 Tohoku earthquake and tsunami, Japan, and the 2015 Illapel earthquake and tsunami, Chile. Together with exposure data, such vulnerability models can be used to derive integrated exposure indices to tsunami for roads and bridges.

The risk storylines shown in Figure 67 points out a further characteristic of the road system that may affect seismic/tsunami impacts and lead to traffic disruption, i.e., the not redundancy of the road network. Indeed, transport robustness and network redundancy ensure road links alternatives when other links in the network are disrupted due to the hazardous events (Jenelius, 2010). A straightforward indicator for evaluating the efficiency of road infrastructures is the Road Density Index, that is quantified comparing the length of roads with the number of inhabitants in the analyzed region (e.g., urban district) (Aljoufie, 2021). However, more refined models can be used to evaluate the network reliability based on the variability in the connection measures between two generic nodes in the network (e.g., Guidotti et al., 2015; Giordano et al., 2021).

Final integrated exposure values VE of physical asset can be defined as a function of the integrated exposure index of roads, bridges and network redundancy index value (e.g. considering the maximum or the mean value of such indices).

- 6) The risk index for each hazard is determined combining the hazard and integrated exposure indicators related to physical system.
- 7) The integrated multi-risk index is obtained combining seismic and tsunami risk indices of physical assets according to the approach proposed in section 5.1.1.

5.2. Multi-criteria Decision Analysis as a tool supporting effective risk management

The use of MCDAs for composite indexing allows for managing the complexity of decision-making processes, explicitly involving stakeholder criteria and preferences, and providing a systemic framework for evaluating alternatives in a comprehensive and transparent manner. The main steps characterising the decision-making process based on the multi-criteria approach are summarised below. They are divided into two macrosteps that concern the knowledge phase and the evaluation process, respectively. In the knowledge phase the data collected concerns the understanding of the actions which have been divided into two main types: type A or soft actions and type B or non-soft or green and grey actions.

The methodological steps of the evaluation process enable the definition of the performance scenarios of the three identified subsystems and are summarised below:

1. Definition of Objectives and Criteria

First, it is necessary to identify the general objectives to be achieved through the composite index. Next, the specific criteria that influence or contribute to the achievement of these objectives are defined. The criteria are the dimensions or aspects that will be evaluated.

2. Allocation of weights to the Criteria

Each criterion is weighted according to its relative importance compared to the others. This step often involves the input of experts or interested stakeholders, who assign weights to the different criteria according to their relevance to the overall objectives.

3. Data Collection

Data related to the individual criteria are collected for each alternative or unit of analysis. This data may be numerical or qualitative, depending on the nature of the criterion.

4. Data normalisation

Data may come from different sources and have different scales of measurement. Normalisation is an important step to bring all data to a common scale, ensuring that no criterion has too much impact on the analysis due to its units of measurement.

5. Construction of the Composite Index

Using the weights assigned to the criteria and the normalised data, a score is calculated for each alternative against each criterion. The composite index can then be obtained by aggregating these scores using the weighted combination of criteria. A common example is the weighted sum of the normalised scores.

6. Sensitivity analyses

Sensitivity analyses can be conducted to assess how variations in the weights assigned to the criteria affect the composite index. This helps to understand the robustness of decisions with respect to variations in stakeholder preferences.

7. Evaluation of Alternatives

Finally, the alternatives are ranked or evaluated according to the composite index obtained. This provides a basis for the decision or ranking of options in relation to the established objectives.

More generally, MCDAs provide a qualitative framework that ensures that evaluation criteria go beyond financial criteria to incorporate social, economic and environmental values of the community. They are seen as a way to simplify decision management in complex scenarios (De Montis et al., 2004). One of the

most recognised advantages of MCDA has been its flexible and systematic approach. In particular, the ability to incorporate quantitative and qualitative data, the possibility of using multiple criteria to acquire a more holistic risk/benefit assessment and the possibility of examining the influence of different scenarios, criteria and stakeholder groups on the prioritisation results. To increase the quality of decisions on measures to be implemented, uncertain stakeholder judgements should be explored and participation in all stages of the decision-making process should be endorsed (de Brito & Evers, 2016). The introduction of the subjective/expert component allows the integration of objective results obtained through mathematical procedures with those based on multi-criteria techniques, making the approaches more inclusive with respect to different scientific expertise (Swart et al., 2012).

However, criteria are often in conflict with each other. For example, different social and environmental criteria may require high costs and too many resources, which may not be possible due to financial and technical constraints. Therefore, it is crucial to find the best possible trade-offs between these conflicting criteria and objectives. In this context, MCDA offers techniques that support decision-making when several conflicting criteria are involved. MCDA has been used in several applications for natural disaster management, such as resilience index estimation (Klonner et al., 2016), flood risk assessment (Khan et al., 2008), hazard index estimation (Yu et al., 2018) and policy development (Kumar, 2010).

For natural disaster emergencies, decisions need to be made to mobilise people. To reduce human loss of life and suffering, disaster management is an important tool in the decision-making process. For this decision-making process, a multi-criteria model is used.

Problem definition is the first step in a risk assessment and involves defining boundary conditions, identifying potential receptors and determining a link between receptor and exposure (DEFRA, 2011). A receptor's exposure to the hazard will be influenced by a number of factors, such as ecology (Mayes et al., 2009), population density (Alvarez-Guerra et al., 2009), etc. Exposure will also be influenced by the character of the hazard (Alvarez-Guerra et al., 2009, 2010), as well as the characteristics of the context in which it operates (Brassington et al., 2007; Carter et al., 2006; Jiang et al., 2016). Decision-makers must also consider broader socio-economic aspects, such as economic resources, social acceptance of decisions, and availability of expertise (Alvarez-Guerra et al., 2009; Apitz & White, 2003). Which elements to include in a prioritisation framework will depend on the needs of the decision-maker, but above all will be influenced by the availability of data. When considering multiple sites, decision-makers must objectively assess and compare a number of physical and socio-economic attributes in a single, unified framework. MCDA techniques provide a framework for organising and integrating data, so they are flexible and can accommodate different types of data (Rosén et al., 2015). MCDA requires datasets to support each identified attribute. If objective data is not available, subjective data can be used, but this introduces an element of uncertainty into the assessment (Goulart Coelho et al., 2017; Hyde, 2006). One approach to overcome this lack of data is to develop a for likelihood, for example, using the proximity of a receptor to a hazard as a surrogate for the probability of exposure (Kingsley et al., 2015). To this end, geographic information systems (GIS) are supportive in assessing the distance between a hazard and a receptor to determine the probability that a receptor is exposed to the hazard (Pizzol et al., 2016; Zabeo et al., 2011).

The combined use of GIS and MCDA offers a powerful approach to address exposure challenges in urban settings, providing a spatial perspective that is essential for understanding the complexity of urban environments and supporting informed decisions.

References

- A.A.V.V., I territori abbandonati, Rassegna 42, giugno 1990.
- A.A.V.V., La città europea del XXI secolo, Skira, Milano, 2002.
- Abijith, D., Saravanan, S., & Sundar, P. K. S. (2023). Coastal vulnerability assessment for the coast of Tamil Nadu, India—a geospatial approach. *Environmental Science and Pollution Research*, 30(30), 75610–75628. <https://doi.org/10.1007/s11356-023-27686-8>
- Adélaïde, L., Chanel, O. & Pascal, M., (2022), Health effects from heat waves in France: an economic evaluation. *Eur J Health Econ* 23, 119–131, <https://doi.org/10.1007/s10198-021-01357-2>
- Aghataher, R., Rabieifar, H., Samany, N. N., & Rezayan, H. (2023). The suitability mapping of an urban spatial structure for earthquake disaster response using a gradient rain optimization algorithm (GROA). *Heliyon*, 9(10), e20525. <https://doi.org/10.1016/j.heliyon.2023.e20525>
- Ahmed, N., Howlader, N., Hoque, M. A.-A., & Pradhan, B. (2021). Coastal erosion vulnerability assessment along the eastern coast of Bangladesh using geospatial techniques. *Ocean & Coastal Management*, 199, 105408. <https://doi.org/10.1016/j.ocecoaman.2020.105408>
- Ainuddin S, Routray JK (2012) Community resilience framework for an earthquake prone area in Baluchistan. *Int J Disaster Risk Reduct* 2(1):25–36.
- Alam MS, Haque SM (2021) Multi-dimensional earthquake vulnerability assessment of residential neighborhoods of Mymensingh City, Bangladesh: a spatial multi-criteria analysis based approach. *J Urban Manag*. <https://doi.org/10.1016/j.jum.2021.09.001>
- Alberico, I., Amato, V., Aucelli, P., D'Argenio, B., Di Paola, G., and Pappone, G. (2012). Historical shoreline changes of the sele plain (southern italy): the 1870-2009 time window. *J. Coast. Res.* 28(6), 1638–1647. doi: 10.2112/J.COASTRES-D-10-00197.1
- Alexander, L. V., Zhang, X., Peterson, T.C., Caesar, J., Gleason, B., et al., 2006. Global observed changes in daily climate extremes of temperature and precipitation. *J. Geophys. Res.*, 111, D05109, doi:10.1029/2005JD006290
- Aljoufie, M. 2021. The Impact Assessment of Increasing Population Density on Jeddah Road Transportation Using Spatial-Temporal Analysis. *Sustainability* 2021, 13, 1455. <https://doi.org/10.3390/su13031455>
- Alloway, A. J., 2004. Contamination of soils in domestic gardens and allotments: a brief overview. *Land Contamination & Reclamation*, 12(3), 179–188, DOI:10.2462/09670513.658
- Alvarado, M.J., et al., 2019. Evaluating the use of satellite observations to supplement ground-level air quality data in selected cities in low- and middle-income countries. *Atmospheric Environment* 218, 117016, <https://doi.org/10.1016/j.atmosenv.2019.117016>
- Alvarez-Guerra, M., Canis, L., Voulvoulis, N., Viguri, J. R., & Linkov, I. (2010). Prioritization of sediment management alternatives using stochastic multicriteria acceptability analysis. *Science of The Total Environment*, 408(20), 4354–4367. <https://doi.org/10.1016/j.scitotenv.2010.07.016>
- Alvarez-Guerra, M., Viguri, J. R., & Voulvoulis, N. (2009). A multicriteria-based methodology for site prioritisation in sediment management. *Environment International*, 35(6), 920–930. <https://doi.org/10.1016/j.envint.2009.03.012>
- Alvioli, M., Poggi, V., Peresan, A., Scaini, C., Tamaro, A., & Guzzetti, F. (2023). A scenario-based approach for immediate post-earthquake rockfall impact assessment. *Landslides*, 1-16. DOI: 10.1007/s10346-023-02127-2.

- Anderson, J.O., Thundiyil, J.G. & Stolbach, A., 2012. Clearing the Air: A Review of the Effects of Particulate Matter Air Pollution on Human Health. *J. Med. Toxicol.* 8, 166–175. <https://doi.org/10.1007/s13181-011-0203-1>
- Andreoli, M. and Tellarini, V. (2000) 'Farm sustainability evaluation: methodology and practice', *Agriculture. Ecosystems and Environment*, 77 (1–2): 43–52.
- Andreotti, G., & Lai, C. G. 2019. Use of fragility curves to assess the seismic vulnerability in the risk analysis of mountain tunnels. *Tunnelling and Underground Space Technology*, 91, Article 103008.
- Anenberg, S.C., Haines, S., Wang, E., Nassikas, N., Kinney, P.L., 2020. *Environ Health* 19, 130 (2020). <https://doi.org/10.1186/s12940-020-00681-z>
- Ångström, A., 1929. On the atmospheric transmission of sun radiation and on dust in the air, I, II, *Geogr. Ann.*, 11, 156–166, <https://doi.org/10.2307/519399>
- Antonelli P., Camorali F., Delpiano A., Dini R. (2012), Di nuovo in gioco. Il progetto di architettura a partire dal capitale fisso territoriale, LIST, Trento.
- Apel H, Aronica GT, Kreibich H, Thielen AH (2009) Flood risk analyses—how detailed do we need to be? *Nat Hazard* 49:79–98
- Apitz, S., & White, S. (2003). A conceptual framework for river-basin-scale sediment management. *Journal of Soils and Sediments*, 3(3), 132–138. <https://doi.org/10.1065/jss2003.08.083>
- Apreda, C., D'Ambrosio, V., & Di Martino, F. (2019). A climate vulnerability and impact assessment model for complex urban systems. *Environmental Science & Policy*, 93, 11–26.
- Argyroudis, S. A., Nasiopoulos, G., Mantadakis, N., & Mitoulis, S. A. 2020. Cost-based resilience assessment of bridges subjected to earthquakes. *International journal of disaster resilience in the built environment*.
- Armaş, I., Toma-Danila, D., Ionescu, R., & Gavriş, A. (2017). Vulnerability to Earthquake Hazard: Bucharest Case Study, Romania. *International Journal of Disaster Risk Science*, 8(2), 182–195. <https://doi.org/10.1007/s13753-017-0132-y>
- Armstrong, B., Sera, F., Vicedo-Cabrera, A. M., Abrutzky, R., Åström, D. O., Bell, M. L., et al. 2019. The role of humidity in associations of high temperature with mortality: A multicountry, multicity study. *Environmental Health Perspectives*, 127(9), 097007. <https://doi.org/10.1289/EHP5430>
- Arnold MI, Chen RS, Deichmann U, Dilly M, Lerner-Lam AL, Pullen RE, Trohanis Z (2006) Natural disaster risk hotspots case studies, disaster risk management series, No. 6, World Bank
- Asghari, M., Nassiri, P., Monazzam, M. R., Golbabaei, F., Arabalibeik, H., Shamsipour, A., & Allahverdy, A. (2017). Weighting Criteria and Prioritizing of Heat stress indices in surface mining using a Delphi Technique and Fuzzy AHP-TOPSIS Method. *Journal of Environmental Health Science and Engineering*, 15(1), 1. <https://doi.org/10.1186/s40201-016-0264-9>
- Baccini, M., Biggeri, A., Accetta, G., et al., 2008. Heat Effects on Mortality in 15 European Cities. *Epidemiology*, 19, 5, 711–719, doi:10.1097/EDE.0b013e318176bfcd
- Aubrecht C, Ozceylan D (2013a) Identification of heat risk patterns in the U.S. National Capital Region by integrating heat stress and related vulnerability. *Environ Int* 56:65–77
- Aubrecht C, Ozceylan D (2013b) Identification of heat risk patterns in the U.S. National Capital Region by integrating heat stress and related vulnerability. *Environ Int* 56:65–77
- AUDIS, GBC Italia & Legambiente, (2011) *Ecoquartieri in Italia: un patto per la rigenerazione urbana. Una proposta per il rilancio economico, sociale, ambientale e culturale delle città e dei territori*, available at: http://upload.legambiente.org/share/ecoquartieri/docs/ecoquartieri_in_italia_documento_di_confronto.pdf
- Barnett, A., Tong, S., & Clements, A. 2010. What measure of temperature is the best predictor of mortality? *Environmental Research*, 110(6), 604–611. <https://doi.org/10.1016/j.envres.2010.05.006>

- AXA, Ipsos (2023) Future Risks Report 2023, Special 10th edition. <https://www.axa.com/en/news/2023-future-risks-report>
- Aymonino C., Lo studio dei fenomeni urbani, Roma, Officina, 1977.
- Aymonino C., Origini e sviluppo della città moderna, Venezia, Marsilio, 1978.
- Aymonino, C. (1977). Tipologia e morfologia. In Lo studio dei fenomeni urbani. Roma: Officina.
- Azhar, G., Saha, S., Ganguly, P., Mavalankar, D., & Madrigano, J. (2017). Heat wave vulnerability mapping for India. *International Journal of Environmental Research and Public Health*, 14(4), 357. <https://doi.org/10.3390/ijerph14040357>
- Azizi, E., Mostafazadeh, R., Hazbavi, Z., Esmali Ouri, A., Mirzaie, S., Huang, G., & Qian, X. (2022). Spatial distribution of flood vulnerability index in Ardabil province, Iran. *Stochastic Environmental Research and Risk Assessment*, 36(12), 4355–4375. <https://doi.org/10.1007/s00477-022-02264-5>
- Azizi, E., Mostafazadeh, R., Hazbavi, Z., Ouri, A. E., & Mirzaie, S. (2022). Screening watersheds of Ardabil province concerning flood vulnerability. *Journal of Rainwater Catchment Systems*, 10(2), 11–26. <https://jircsa.ir/article-1-462-en.html>
- Azizi, E., Nikoo, M. R., Mostafazadeh, R., & Hazbavi, Z. (2023). Flood vulnerability analysis using different aggregation frameworks across watersheds of Ardabil province, northwestern Iran. *International Journal of Disaster Risk Reduction*, 91, 103680. <https://doi.org/10.1016/j.ijdr.2023.103680>
- Babashamsi, P., Golzadfar, A., Yusoff, N. I. M., Ceylan, H., & Nor, N. G. M. (2016). Integrated fuzzy analytic hierarchy process and VIKOR method in the prioritization of pavement maintenance activities. *International Journal of Pavement Research and Technology*, 9(2), 112–120. <https://doi.org/10.1016/j.ijprt.2016.03.002>
- Belete DA (2011) Road and urban storm water drainage network integration in Addis Ababa: Addis Ketema Sub-city. *J Eng Technol Res* 3(7):217–225
- Balica, S., & Wright, N. G. (2010). Reducing the complexity of the flood vulnerability index. *Environmental Hazards*, 9(4), 321–339. <https://doi.org/10.3763/ehaz.2010.0043>
- Barbosa, O., Tratalos, J. A., Armsworth, P. R., Davies, R. G., Fuller, R. A., Johnson, P., & Gaston, K. J. (2007). Who benefits from access to green space? A case study from Sheffield, UK. *Landscape and Urban planning*, 83(2-3), 187-195.
- Barthel, P.-A., Davidson, L., & Sudarskis, M. (2013). Alexandria: Regenerating the city. A contribution based on AFD experiences. https://upfi-med.eib.org/wp-content/uploads/2016/09/Alexandrie_publication_AFD.pdf
- Bassil KL, Cole DC, Moineddin R, CraigAM, LouWY, Schwartz B, Rea E (2009) Temporal and spatial variation of heat-related illness using medical dispatch data. *Environ Res* 109(5):600–606
- Bassolino, E., & Verde, S. (2023). Implementazione di un framework metodologico con strumenti ICT per la gestione sostenibile degli spazi aperti urbani in risposta alle ondate di calore. *BDC*, 23(2), 371-398.
- Bassolino, E., D'Ambrosio, V., & Sgobbo, A. (2021). Data Exchange Processes for the Definition of Climate-Proof Design Strategies for the Adaptation to Heatwaves in the Urban Open Spaces of Dense Italian Cities. *Sustainability*, 13(10), 5694.
- Bell, R., Glade, T., (2004). Multi-hazard analysis in natural risk assessments, in: Brebbia, C.A. (Ed.), *International Conference on Computer Simulation in Risk Analysis and Hazard Mitigation*, pp. 197-206. DOI:10.2495/978-1-84564-650-9/01
- Benevolo L, Le origini dell'urbanistica moderna, Universale Laterza, Bari 1991 (1963).
- Benevolo L., Storia della città, 1-4, Editori Laterza, Bari 2006 (1975).

- Beniston, M., D. B. Stephenson, O. B. Christensen, C. A. T. Ferro, C. Frei, S. Goyette, K. Halsnaes, T. Holt, K. Jylhä, B. Koffi, J. Palutikoff, R. Schöll, T. Semmler, and K. Woth, 2007. Future extreme events in European climate; an exploration of Regional Climate Model projections. *Clim. Change*, 81, 71–95, <https://doi.org/10.1007/s10584-006-9226-z>
- Benmarhnia, T., Oulhote, Y., Petit, C. et al., 2014. Chronic air pollution and social deprivation as modifiers of the association between high temperature and daily mortality. *Environ Health* 13, 53 <https://doi.org/10.1186/1476-069X-13-53>
- Berkes, F., Folke, C., & Colding, J. (Eds.). (2000). Linking social and ecological systems: management practices and social mechanisms for building resilience. Cambridge University Press.
- Bianchetti C. (2003), *Abitare la città contemporanea*, Skira, Milano.
- Birkmann, J., Cardona, O. D., Carreño, M. L., Barbat, A. H., Pelling, M., Schneiderbauer, S., Kienberger, S., Keiler, M., Alexander, D., Zeil, P., Welle, T., 2013, 'Framing vulnerability, risk and societal responses: The MOVE framework', *Natural Hazards*, Vol. 67, pp. 193–211.
- Bisogni S., Renna A., *Il disegno della città*. Napoli, Cooperativa editrice di Economia e commercio, Napoli 1975.
- Blackett, M. (2023). *Climate change could be triggering more earthquakes and volcanic eruptions. Here's how*. World Economic Forum. <https://www.weforum.org/agenda/2023/08/climate-change-trigger-earthquakes-volcanoes/>
- Boeri S., Lanzani A., Marini E., Aim – Associazione Interessi Metropolitani (1993), *Il territorio che cambia. Ambienti, paesaggi e immagini della regione milanese*, Abitare Segesta, Milano.
- Bologna, R., Losasso, M., Mussinelli, E., Tucci, F., (Eds.) (2021), *Dai distretti urbani agli eco-distretti. Metodologie di conoscenza, programmi strategici, progetti pilota per l'adattamento climatico/ From Urban Districts to Eco-districts. Knowledge Methodologies, Strategic Programmes, Pilot Projects for Climate Adaptation*, Maggioli, Santarcangelo di Romagna. ISBN 9788891643216
- Bond, T. C., 2001. Spectral dependence of visible light absorption by carbonaceous particles emitted from coal combustion, *Geophys. Res. Lett.*, 28, 4075–4078, <https://doi.org/10.1029/2001GL013652>
- Borzi B, Ceresa P, Franchin P, Noto F, Calvi GM, Pinto PE. 2015. Seismic Vulnerability of the Italian Roadway Bridge Stock. *Earthquake Spectra*. 2015;31(4):2137-2161. doi:10.1193/070413EQS190M
- Borzi, B., Ceresa, P., Faravelli, M., Fiorini, E., Onida, M. 2013. Seismic Risk Assessment of Italian School Buildings. In: Papadrakakis, M., Fragiadakis, M., Plevris, V. (eds) *Computational Methods in Earthquake Engineering. Computational Methods in Applied Sciences*, vol 30. Springer, Dordrecht. https://doi.org/10.1007/978-94-007-6573-3_16
- Boyle, C., Mudd G., Mihelcic, G.R., Anastas, P., et al., 2010. Delivering Sustainable Infrastructure that Supports the Urban Built Environment. Sustainable living will require megacity-level infrastructural support designs and paradigms. *Environ. Sci. Technol.* 2010, 44, 13, 4836–4840, <https://doi.org/10.1021/es903749d>
- Brassington, K. J., Hough, R. L., Paton, G. I., Semple, K. T., Risdon, G. C., Crossley, J., Hay, I., Askari, K., & Pollard, S. J. T. (2007). Weathered Hydrocarbon Wastes: A Risk Management Primer. *Critical Reviews in Environmental Science and Technology*, 37(3), 199–232. <https://doi.org/10.1080/10643380600819625>
- Breuste, J., Qureshi, S., & Li, J. (2013). Applied urban ecology for sustainable urban environment. *Urban Ecosystems*, 16, 675–680.
- Britannica, The Editors of Encyclopaedia. "wind chill". *Encyclopedia Britannica*, 15 Feb. 2022, <https://www.britannica.com/science/wind-chill>. Accessed 17 November 2023.
- Buckley, J. J. (1985). "Fuzzy hierarchical analysis". *Fuzzy Sets and Systems*, 17(3), pp. 233-247, 12.

- Burkart, K., Schneider, A., Breitner, S., Khan, M. H., Krämer, A., & Endlicher, W. 2011. The effect of atmospheric thermal conditions and urban thermal pollution on all-cause and cardiovascular mortality in Bangladesh. *Environmental Pollution*, 159(8–9), 2035–2043. <https://doi.org/10.1016/j.envpol.2011.02.005>
- Burton C.G. and Silva V. (2014). Integrated Risk Modelling within the Global Earthquake Model (GEM): Test Case Application for Portugal. Proceedings of the Second European Conference on Earthquake Engineering and Seismology, European Association of Earthquake Engineering and European Seismological Commission, Istanbul, Turkey.
- Buscail, C., Upegui, E. & Viel, JF., 2012. Mapping heatwave health risk at the community level for public health action. *Int J Health Geogr* 11, 38 2012. <https://doi.org/10.1186/1476-072X-11-38>.
- Caniggia G. Analisi tipologica: la corte matrice dell'insediamento, a cura di F. Ciccone, Recupero e riqualificazione urbana nel programma straordinario per Napoli, Volumi Cresme 1984.
- Caniggia, G., Maffei, G.L. (1979). Composizione architettonica e tipologia edilizia. Venezia: Marsilio.
- Cao, C., Zhu, K., Cai, F., Qi, H., Liu, J., Lei, G., Mao, Z., Zhao, S., Liu, G., & Su, Y. (2022). Vulnerability Evolution of Coastal Erosion in the Pearl River Estuary Great Bay Area Due to the Influence of Human Activities in the Past Forty Years. *Frontiers in Marine Science*, 9. <https://doi.org/10.3389/fmars.2022.847655>
- Capozzi R., Nunziante P., Orfeo C. (a cura di), Agostino Renna. La forma della città, Clean, Napoli 2016.
- Cardona, O.D., M.K. van Aalst, J. Birkmann, M. Fordham, G. McGregor, R. Perez, R.S. Pulwarty, E.L.F. Schipper, and B.T. Sinh, (2012): Determinants of risk: exposure and vulnerability. In: Managing the Risks of Extreme Events and Disasters to Advance Climate Change Adaptation [Field, C.B., V. Barros, T.F. Stocker, D. Qin, D.J. Dokken, K.L. Ebi, M.D. Mastrandrea, K.J. Mach, G.-K. Plattner, S.K. Allen, M. Tignor, and P.M. Midgley (eds.)]. A Special Report of Working Groups I and II of the Intergovernmental Panel on Climate Change (IPCC). Cambridge University Press, Cambridge, UK, and New York, NY, USA, pp. 65-108.
- Carpignano, A., Golia, E., Di Mauro, C., Bouchon, S., Nordvik, J-P., (2009) A methodological approach for the definition of multi-risk maps at regional level: first application, *Journal of Risk*, Volume 12, pp.513-534. DOI: 10.1080/13669870903050269
- Carreño, M-L., Cardona, O. D., and Barbat, A. H., (2007) Urban seismic risk evaluation: a holistic approach, *Natural Hazards* 40, pp. 137-172.
- Carter, P., Cole, H., & Burton, J. (2006). Bioremediation: successes and shortfalls. *Proceedings of Key International Conference and Exhibition for Spill Prevention, Preparedness, Response and Restoration (Interspill)*. https://www.interspill.org/wp-content/uploads/2021/11/inland_bioremediation_doc.pdf
- Casajus Valles, A., Marin Ferrer, M., Poljansek, K. and Clark, I. editor(s), Science for Disaster Risk Management 2020, EUR 30183 EN, Publications Office of the European Union, Luxembourg, 2021, ISBN 978-92-76-18182-8, doi:10.2760/571085, JRC114026.
- Casson Moreno, V.; Ricci, F.; Sorichetti, R.; Misuri, A.; Cozzani, V. 2019. Analysis of Past Accidents Triggered by Natural Events in the Chemical and Process Industry. *Chem. Eng. Trans.* 2019, 74, 1405–1410.
- Castellari S., Venturini S., Ballarin Denti A., Bigano A., Bindi M., Bosello F., Carrera L., Chiriaco M.V., Danovaro R., Desiato F., Filpa A., Gatto M., Gaudioso D., Giovanardi O., Giupponi C., Gualdi S., Guzzetti F., Lapi M., Luise A., Marino G., Mysiak J., Montanari A., Ricchiuti A., Rudari R., Sabbioni C., Sciortino M., Sinisi L., Valentini R., Viaroli P., Vurro M., Zavatarelli M. (a cura di.) (2014). Rapporto sullo stato delle conoscenze scientifiche su impatti, vulnerabilità ed adattamento ai cambiamenti climatici in Italia. Ministero dell'Ambiente e della Tutela del Territorio e del Mare, Roma

- Castells, N. and Munda, G. (1999) 'International environmental issues: towards a new integrated assessment approach', in M. O'Connor and C. Spash. (eds) *Valuation and the Environment – theory, method and practice*, Cheltenham, UK/Northampton, MA: Edward Elgar: 309–27.
- Catton, W.R. (1982). *Overshoot: The ecological basis of revolutionary change*. Champaign: University of Illinois Press. Public Health Rep 124(1): 167–168).
- Cavan G, Lindley S, Yeshitela K, Nebebe A, Woldegerima T, Shemdoe R, Kibassa D, Pauleit S, Renner R, Printz A, Buchta K, Coly A, Sall F, Ndour NM, Ouee'draogo Y, Samari BS, Sankara BT, Feumba RA, Ngapgue JN, Ngoumo MT, Tsalefac M, Tonye E (2012) Green infrastructure maps for selected case studies and a report with an urban green infrastructure mapping methodology adapted to African cities CLUVA project deliverable D2.7. http://www.cluva.eu/deliverables/CLUVA_D2.7.pdf. Accessed 18 Dec 2012
- Chang, A.Y., Tan, A.X., Nadeau, K.C. et al., 2022. Aging Hearts in a Hotter, More Turbulent World: The Impacts of Climate Change on the Cardiovascular Health of Older Adults. *Curr Cardiol Rep* 24, 749–760 <https://doi.org/10.1007/s11886-022-01693-6>
- Chang, K.-T., Chiang, S.-H. & Hsu, M.-L. 2007. Modeling typhoon- and earthquake-induced landslides in a mountainous watershed using logistic regression. *Geomorphology* 89: 335–347.
- Chate, S.T.D., Ali, P.P.K. and Bisht, D.S. (2012). Variations in Mass of the PM₁₀, PM_{2.5} and PM₁ during the Monsoon and the Winter at New Delhi. *Aerosol Air Qual. Res.* 12: 20-29. <https://doi.org/10.4209/aaqr.2011.06.0075>.
- Chaulagain, D., Ram Rimal, P., Ngando, S. N., Nsamon, B. E. K., Suh, D., & Huh, J.-S. (2023). Flood susceptibility mapping of Kathmandu metropolitan city using GIS-based multi-criteria decision analysis. *Ecological Indicators*, 154, 110653. <https://doi.org/10.1016/j.ecolind.2023.110653>
- Chen, J. and Hoek, G. 2020. Long-term exposure to PM and all-cause and cause-specific mortality: A systematic review and meta-analysis, *Environment International*, 143, 105974, <https://doi.org/10.1016/j.envint.2020.105974>.
- Chen, K., Bi, J., Chen, J., Chen, X., Huang, L., & Zhou, L. (2015). Influence of heat wave definitions to the added effect of heat waves on daily mortality in Nanjing, China. *Science of the Total Environment*, 506–507, 18–25. <https://doi.org/10.1016/j.scitotenv.2014.10.092>
- Chersich, M.F., et al., 2020. Associations between high temperatures in pregnancy and risk of preterm birth, low birth weight, and stillbirths: systematic review and meta-analysis. *BMJ* 2020; 371, <https://doi.org/10.1136/bmj.m3811>
- Churchman, Charles W., Ackoff, Russell L., Smith, Nicolas M. (1954). An approximate measure of value. *Journal of the Operations Research Society of America*, 2(2): 172–187. [doi:10.1287/opre.2.2.172](https://doi.org/10.1287/opre.2.2.172)
- CMCC Foundation (2023), Annual report 2023. Available at: https://files.cmcc.it/Annual_Report/AR_2023_cmcc.pdf
- Cohen, A.J., Anderson, H.R., Ostro, B., Dev Pandey, K., Krzyzanowski, M., Künzli, N., Gutschmidt, K., Pope, A., Romieu, I., Samet, J.M. and Smith, K., 2005. The Global Burden of Disease Due to Outdoor Air Pollution, *Journal of Toxicology and Environmental Health, Part A*, 68:13-14, 1301-1307, DOI: 10.1080/15287390590936166
- Coli, M., Brugioni, M., & Montini, G. (2013, September). Florence and its floods: anatomy of a hazard. In *Proceeding of (Ed.), 18th International Conference on soil mechanics and Geotechnical Engineering (workshop of Geotechnical Engineering for conservation of cultural heritage and historical site)*.
- Conforte, A.J., Tuszyński, J.A., Silva, F.A.B.D., Carels, N. (2019) Signaling complexity measured by shannon entropy and its application in personalized medicine, *Front. Genet.* 10, 930.

- Corbane, C., Pesaresi, M., Politis, p., Syrris, V., Florczyk, A.J., Soille, P., Maffenini, L., Burger, A., Vasilev, V., Rodriguez, D., Sabo, F., Dijkstra, L., Kemper, T., (2017) Big earth data analytics on Sentinel-1 and Landsat imagery in support to global human settlements mapping, Big Earth Data, 1:1-2, pp. 118-144. DOI: 10.1080/20964471.2017.1397899
- Corboz A. (1983), "Le territoire comme palimpseste", Diogene no. 121, pp. 14-35 (ora come Il territorio come palinsesto, in Ordine sparso, saggi sull'arte, il metodo, la città, il territorio, Franco Angeli, Milano 1998).
- Corboz A., Il territorio come palinsesto, in "Casabella", 516, 1985.
- Corrado V., Ballarini I. & Corgnati S.P. (2014). Building Typology Brochure - Italy. Available online: https://episcopo.eu/fileadmin/tabula/public/docs/brochure/IT_TABULA_TypologyBrochure_POLITO.pdf (accessed on 30 May 2023).
- Cosselman, K.E., Navas-Acien, A., Kaufman, J. Environmental factors in cardiovascular disease. Nat Rev Cardiol 12, 627–642 (2015). <https://doi.org/10.1038/nrcardio.2015.152>
- Cruz, A.M.; Krausmann, E. 2008. Damage to Offshore Oil and Gas Facilities Following Hurricanes Katrina and Rita: An Overview. J. Loss Prev. Process Ind. 2008, 21, 620–626.
- Curt, C., (2021) Multirisk: What trends in recent works? A bibliometric analysis, Science of the Total Environment, Volume 763. DOI: 10.1016/j.scitotenv.2020.142951
- Cutter, S. L., & Finch, C. (2008). Temporal and spatial changes in social vulnerability to natural hazards. *Proceedings of the National Academy of Sciences*, 105(7), 2301–2306. <https://doi.org/10.1073/pnas.0710375105>
- Cutter, S. L., Barnes, L., Berry, M., Burton, C., Evans, E., Tate, E. and Webb, J. (2008). A place-based model for understanding community resilience to natural disasters. *Global Environmental Change* 18(4), 598-606.
- Cutter, S. L., Boruff, B. J. and Shirley, W. (2003). Social Vulnerability to Environmental Hazards. *Social Science Quarterly* 84(2), 242-261.
- Cvijanovic I., Mistry M.N., Begg, J.D., Gasparrini, A. & Rodo, X., 2023. Importance of humidity for characterization and communication of dangerous heatwave conditions. npj Climate & Atmospheric Science 6, 33. <https://doi.org/10.1038/s41612-023-00346-x>
- D'Ambrosio, V. & Leone, M. F. (Eds.) (2016). *Progettazione ambientale per l'adattamento al Climate Change 1. Modelli innovativi per la produzione di conoscenza/ Environmental Design for Climate Change adaptation 1. Innovative model for the production of knowledge*. Napoli: Clean.
- D'Ambrosio, V. & Leone, M. F. (Eds.) (2017). *Progettazione ambientale per l'adattamento al Climate Change 2. Strumenti e indirizzi per la riduzione dei rischi climatici/ Environmental Design for Climate Change adaptation 2. Tools and Guidelines for Climate Risk Reduction*. Napoli: Clean.
- D'Ambrosio, V. (2016). Innovazione e sperimentazione nei processi di conoscenza dell'ambiente costruito / Innovation and experimentation in the knowledge processes of the built environment. In D'Ambrosio, V. & Leone, M. F. (Eds.), *Progettazione ambientale per l'adattamento al Climate Change 1. Modelli innovativi per la produzione di conoscenza/ Environmental Design for Climate Change adaptation 1. Innovative model for the production of knowledge* (p. 50-57). Napoli: Clean.
- D'Ambrosio, V., Di Martino, F. & Miraglia, V., 2023. A GIS-based framework to assess heatwave vulnerability and impact scenarios in urban systems. Sci Rep 13, 13073. <https://doi.org/10.1038/s41598-023-39820-0>

- D'Ambrosio, V., Di Martino, F., & Tersigni, E. (2023). Towards Climate Resilience of the Built Environment: A GIS-Based Framework for the Assessment of Climate-Proof Design Solutions for Buildings. *Buildings*, 13(7), 1658. <https://doi.org/10.3390/buildings13071658>
- D'Ambrosio, V., Di Martino, F., & Tersigni, E. (2023). Towards Climate Resilience of the Built Environment: A GIS-Based Framework for the Assessment of Climate-Proof Design Solutions for Buildings. *Buildings*, 13(7), 1658. <https://doi.org/10.3390/buildings13071658>
- Dall'Osso, F., Dominey-Howes, D., Tarbotton, T., Summerhayes, S., Withycombe, G. 2016. *Revision and improvement of the PTVA-3 model for assessing tsunami building vulnerability using "international expert judgment": introducing the PTVA-4 model*. *Nat Hazards* (2016) 83:1229–1256. DOI 10.1007/s11069-016-2387-9.
- Dall'Osso, F., Gonella, M., Gabbianelli, G., Withycombe, G., Dominey-Howes, D. 2009. A revised (PTVA) model for assessing the vulnerability of buildings to tsunami damage. *Nat Hazards Earth Syst Sci* 9:1557–1565. doi:10.5194/nhess-9-1557-2009
- de Brito, M. M., & Evers, M. (2016). Multi-criteria decision-making for flood risk management: a survey of the current state of the art. *Natural Hazards and Earth System Sciences*, 16(4), 1019–1033. <https://doi.org/10.5194/nhess-16-1019-2016>
- De Groeve, T., Poljansek, K. & Ehrlich, D. 2013. Recording Disaster Losses: Recommendation for a European approach, EUR 26111, ENPublications Office of the European Union, Luxembourg, JRC83743.
- De Montis, A., De Toro, P., Droste-Franke, B., Omann, I. and Stagl, S. (2000) 'Criteria for quality assessment of MCDA methods', paper presented at the *3rd Biennial Conference of the European Society for Ecological Economics*, Vienna, 3–6 May 2000.
- De Montis, A., De Toro, P., Droste-Franke, B., Omann, I., & Stagl, S. (2004). Assessing the quality of different MCDA methods. In *Alternatives for Environmental Valuation*. <https://doi.org/10.4324/9780203412879-14>
- De Pippo, T., Donadio, C., Pennetta, M., Petrosino, C., Terlizzi, F., Valente, A., (2008) Coastal hazard assessment and mapping in Northern Campania, Italy. *Geomorphology* 97, pp. 451-466. <http://dx.doi.org/10.1016/j.geomorph.2007.08.015>.
- De Risi R, Jalayer F (2013) Identification of hotspots vulnerability of adobe houses, sewer systems and road networks. CLUVA project deliverable D2.1. http://www.cluva.eu/deliverables/CLUVA_D2.1.pdf. Accessed 25 Jun 2013
- De Risi R, Jalayer F, de Paola F, Iervolino I, Giugni M, Topa ME, Mbuya E, Kyessi A, Manfredi G, Gasparini P (2013) Flood risk assessment for informal settlements. *Nat Hazards* 69(1):1003–1032
- de Rosnay, J., (1977) *Le macroscope: Vers une vision globale*, AC. ISBN 10: 8472880176
- De Rossi A., Durbiano G., Governa F., Reinerio L., Robiglio M. (a cura di), (1999), *Linee nel paesaggio. Esplorazioni nei territori della trasformazione*, Utet, Torino.
- de Ruiter, M. C., & van Loon, A. F., (2022) The challenges of dynamic vulnerability and how to assess it. *iScience*, Volume 25(8), pp. 1–13.
- de Ruiter, M. C., De Bruijn, J. A., Englhardt, J., Daniell, J. E., de Moel, H., Ward, P. J. 2021. The asynergies of structural disaster risk reduction measures: Comparing floods and earthquakes. *Earth's Future*, 9(1), e2020EF001531. <https://doi.org/10.1029/2020EF001531>
- De Sario, M., Katsouyanni, K., Michelozzi, P., 2013. Climate change, extreme weather events, air pollution and respiratory health in Europe. *European Respiratory Journal*, 42 (3) 826-843; DOI: 10.1183/09031936.00074712
- De Seta C, (1989), *I casali di Napoli*, in *Grandi opere*, Editori Laterza. ISBN-10: 8842033332

- Deepika, B., Avinash, K., and Jayappa, K. S. (2013). Shoreline change rate estimation and its forecast: remote sensing, geographical information system and statistics-based approach. *Int. J. Environ. Sci. Technol* 11(2), 395–416. doi: 10.1007/s13762-013-0196-11-22
- DEFRA. (2011). *Guidelines for Environmental Risk Assessment and Management: Green Leaves III*.
- Degiorgis M, Gnecco G, Gorni S, Roth G, Sanguineti M, Taramasso AC (2012) Classifiers for the detection of flood-prone areas using remote sensed elevation data. *J Hydrol* 470–471:302–315
- Del Zoppo, M., Belliazzi, S., Lignola, G.P., Di Ludovico, M., Prota, A. 2022. *Analytical structural vulnerability and classification of Italian residential building stock to tsunami hazard*. Bulletin of Geophysics and Oceanography. Vol. 63, n. 4, pp. 555-574; December 2022. DOI 10.4430/bgo00398
- Dematteis G. (1990), Senso e metodo della descrizione regionale, in C.L. Dematteis (a cura di), Interpretare una regione. Geografia del Piemonte che cambia, Edizioni Libreria Cortina, Torino.
- Demuzere M, Bechtel B, Middel A, Mills G (2019) Mapping Europe into local climate zones. *PLOS ONE* 14(4): e0214474. <https://doi.org/10.1371/journal.pone.0214474>
- Depietri, Y., Dahal, K., McPherson, T., (2018) Multi-hazard risks in New York City, *Natural Hazards and Earth Systems Sciences*, Volume 18, pp. 3363-3381. DOI: 10.5194/nhess-18-3363-2018
- Di Napoli, C., Pappenberger, F., Cloke, H.L., 2019. Verification of Heat Stress Thresholds for a Health-Based Heat-Wave Definition. *Journal of Applied Meteorology and Climatology*, 58, 1177-1194, DOI: 10.1175/JAMC-D-18-0246.1
- Di Salvo, C., Ciotoli, G., Pennica, F., Cavinato, G.P. 2017. Pluvial flood hazard in the city of Rome (Italy). *J. Maps* 2017, 13, 545–553.
- Diem, J.E., Comrie, A.C., 2002. Predictive mapping of air pollution involving sparse spatial observations. *Environmental Pollution*, 119, 1, 99-117 [https://doi.org/10.1016/S0269-7491\(01\)00308-6](https://doi.org/10.1016/S0269-7491(01)00308-6)
- Dilanthi, A., Pournima, S., Richard, H. (2019). Making cities resilient report 2019: A snapshot of how local governments progress in reducing disaster risks in alignment with the Sendai framework for disaster risk reduction. UN Office for Disaster Risk Reduction, Switzerland, Geneva, 2019.
- Dilley M, Chen RS, Deichmann U, Lerner-Lam AL, Arnold M, Agwe J, Buys P, Kjevstad O, Lyon B, Yetman G (2005) Natural disaster hotspots: A global risk analysis. Disaster risk management series, No. 5, World Bank
- Dipartimento della Protezione Civile (2000). Censimento di vulnerabilità a campione dell'edilizia corrente dei Centri abitati, nelle regioni Abruzzo, Basilicata, Calabria, Campania, Molise, Puglia e Sicilia. Gruppo Nazionale per la Difesa dai Terremoti – GNDT. Ministero del Lavoro e della Previdenza Sociale.
- DRMFS (2006) Flash appeal for the 2006 flood disaster in Ethiopia. <http://www.dppc.gov.et/downloadable/reports/appeal/2006/Flood%20Appeal%20II%20MASTER%20Final.pdf>
- Dukes, J., Mangalathu, S., Padgett, J. E., & DesRoches, R. (2018). Development of a bridge-specific fragility methodology to improve the seismic resilience of bridges. *Earthquake and Structures*, 15(3), 253–261
- Duleba, S., Moslem, S., (2019). Examining Pareto optimality in analytic hierarchy process on real Data: an application in public transport service development. *Expert Syst. Appl.* 116, 21–30.
- Duvigneaud P, Denaeyer-De Smet S (1977) L'écosystème urbain Bruxellois. In: Duvigneaud P, Kestemont P (eds) Productivité biologique en Belgique. Duculot, Paris, pp 608–613
- Ebi, K.L., McGregor, G., 2008. Climate Change, Tropospheric Ozone and Particulate Matter, and Health Impacts. *Environmental Health Perspectives*, 116, 11, <https://doi.org/10.1289/ehp.11463>

- Echevarría-Lucas L, Senciales-González JM, Medialdea-Hurtado ME, Rodrigo-Comino J., 2021. Impact of Climate Change on Eye Diseases and Associated Economical Costs. *International Journal of Environmental Research and Public Health*; 18(13):7197. <https://doi.org/10.3390/ijerph18137197>
- Eguchi, R. T., Eguchi, M. T., Bouabid, J., Koshimura, S., and Graf, W. P.: HAZUS Tsunami Benchmarking, Validation and Calibration, Prepared for the Federal Management Agency through a contract with the Atkins, 1–48, available at: <https://nws.weather.gov/nthmp/2013mesmms/abstracts/TsunamiHAZUSreport.pdf> (last access: 13 February 2020), 2013.
- Ellefsen, R., (1991), Mapping and measuring buildings in the urban canopy boundary layer in ten US cities, *Energy and Buildings*, 15–16, 1025–1049.
- El-Maissi, A. M., Argyroudis, S. A., & Nazri, F. M. (2020). Seismic vulnerability assessment methodologies for roadway assets and networks: A state-of-the-art review. *Sustainability*, 13(1), 61.
- El-Maissi, A. M., Argyroudis, S.A., Moufid Kassem, M., Nazri, F. M. 2023. Integrated seismic vulnerability assessment of road network in complex built environment toward more resilient cities, *Sustainable Cities and Society*, Volume 89, 2023, 104363, ISSN 2210-6707, <https://doi.org/10.1016/j.scs.2022.104363>.
- Elmqvist, T., Fragkias, M., Goodness, J., Güneralp, B., Marcotullio, P. J., McDonald, R. I., ... & Tidball, K. (2013). Stewardship of the biosphere in the urban era. Urbanization, biodiversity and ecosystem services: challenges and opportunities: a global assessment, 719-746.
- El-Sharkawy, A.M., Sahota, O., Maughan, R.J., Lobo, D.N., 2013. The pathophysiology of fluid and electrolyte balance in the older adult surgical patient. *Clinical Nutrition*, 33(1), 6-13, <https://doi.org/10.1016/j.clnu.2013.11.010>
- El-Zein, A., & Tonmoy, F. N. (2015). Assessment of vulnerability to climate change using a multi-criteria outranking approach with application to heat stress in Sydney. *Ecological Indicators*, 48, 207–217. <https://doi.org/10.1016/j.ecolind.2014.08.012>
- Emde, C., Buras, R., Mayer, B., and Blumthaler, M., 2010. The impact of aerosols on polarized sky radiance: model development, validation, and applications, *Atmos. Chem. Phys.*, 10, 383–396, <https://doi.org/10.5194/acp-10-383-2010>
- Emmanuel, R. (2005). Thermal comfort implications of urbanization in a warm-humid city: The Colombo Metropolitan Region (CMR) Sri Lanka. *Building and Environment*, 40(12), 1591–1601. <https://doi.org/10.1016/j.buildenv.2004.12.004>
- Ente Nazionale di Normazione [UNI] 2014. UNI/TR 11552. Abaco delle strutture costituenti l'involucro opaco degli edifici. Parametri termofisici.
- EPA, U. S. 2004. Air quality criteria for particulate matter. US Environmental Protection Agency, Research Triangle Park.
- Epidemiology 25(6):781–789 IPCC (2014). *Climate Change 2014: Impacts, Adaptation, and Vulnerability. Part A: Global and Sectoral Aspects*. Contribution of Working Group II to the Fifth Assessment Report of the Intergovernmental Panel on Climate Change [Field, C.B., V.R. Barros, D.J. Dokken, K.J. Mach, M.D. Mastrandrea, T.E. Bilir, M. Chatterjee, K.L. Ebi, Y.O. Estrada, R.C. Genova, B. Girma, E.S. Kissel, A.N. Levy, S. MacCracken, P.R. Mastrandrea, & L.L. White (Eds.)]. Cambridge and New York: Cambridge University Press (1132 pp.).
- Epstein Y, Moran, D.S. 2006. Thermal comfort and the heat stress indices. *Industrial health* 44.3: 388-398, <https://doi.org/10.2486/indhealth.44.388>
- Estefany, C., Zhenli Sun, Zijin Hong, Jingjing Du, Raman spectroscopy for profiling physical and chemical properties of atmospheric aerosol particles: A review, *Ecotoxicology and Environmental Safety*, Volume 249, 2023, 114405, ISSN 0147-6513, <https://doi.org/10.1016/j.ecoenv.2022.114405>

- Estoque, R. C., Ooba, M., Seposo, X. T., Togawa, T., Hijioka, Y., Takahashi, K., & Nakamura, S. (2020). Heat health risk assessment in Philippine cities using remotely sensed data and social-ecological indicators. *Nature Communications*, 11(1), 1–12. <https://doi.org/10.1038/s41467-020-15218-8>
- Estrada, F., Perron, P. & Yamamoto, Y. (2023) Anthropogenic influence on extremes and risk hotspots, *Scientific Report* 13 (35). DOI: <https://doi.org/10.1038/s41598-022-27220-9>
- European Commission (EC), Disaster Risk Management Knowledge Centre DRMKC – INFORM, <https://drmkc.jrc.ec.europa.eu/inform-index/>.
- Evans, N. L. and McGhie, C. 2011. The Performance of Lifeline Utilities following the 27th February 2010 Maule Earthquake Chile, in: 9th Pacific Conference on Earthquake Engineering, Building an Earthquake-Resilient Society, 14–16 April 2011, Auckland, New Zealand, 2011.
- Falzett A., (2017) *La città in estensione*, Gangemi editore.
- Farinelli F. (1991), *L'arguzia del paesaggio*, Casabella no. 575-576.
- Fattoruso, G. (2022). Multi-Criteria Decision Making in Production Fields: A Structured Content Analysis and Implications for Practice. *Journal of Risk and Financial Management*, 15(10), 431. <https://doi.org/10.3390/jrfm15100431>
- FEMA. 2022. Hazus 5.1, Hazus Flood Technical Manual. Federal Emergency Management Agency, Washington, D.C.
- FEMA; 2017: Hazus tsunami model technical guidance. NiyamIT Inc., Herndon, VA, USA, Contract n. HSFE60-17-P-0004, 183 pp.
- Ferlenga A., Bassoli N., (2018) *Ricostruzioni. Architettura, Città, Paesaggio nell'epoca delle distruzioni*, Silvana Editoriale
- Ferm, M., De Santis, F. and Varotsos, C. 2005. Nitric acid measurements in connection with corrosion studies. *Atmospheric Environment*, 39, 35, 6664–6672, <https://doi.org/10.1016/j.atmosenv.2005.07.044>
- Ferrante, G., Fasola, S., Cilluffo, F., Piacentini, G., Viegi, G., La Grutta, S., 2022. Addressing Exposome: An Innovative Approach to Environmental Determinants in Pediatric Respiratory Health. *Front. Public Health*, Sec. Environmental health and Exposome, Volume 10 - 2022 | <https://doi.org/10.3389/fpubh.2022.871140>
- Fischer, E.M., Schär, C., 2010. Consistent geographical patterns of changes in high-impact European heatwaves. *Nature Geoscience* volume 3, 398–403, <https://doi.org/10.1038/ngeo866>
- Fleming, C. S., Regan, S. D., Freitag, A., & Burkart, H. (2023). Indicators and participatory processes: a framework for assessing integrated climate vulnerability and risk as applied in Los Angeles County, California. *Natural Hazards*, 115(3), 2069–2095.
- Fleming, C.S., Regan, S.D., Freitag, A. et al. (2023), Indicators and participatory processes: a framework for assessing integrated climate vulnerability and risk as applied in Los Angeles County, California. *Nat Hazards* 115, 2069–2095 <https://doi.org/10.1007/s11069-022-05628-w>
- FLO-2D Software, Inc (2004) FLO-2D® user's manual, Nutrioso, Arizona, www.flo-2.com
- Flores K.L., Escudero C.R., Zamora-Camacho A. (2021). Multicriteria seismic hazard assessment in Puerto Vallarta metropolitan area, Mexico. *Nat Hazards* 105(1):253–275. <https://doi.org/10.1007/s11069-020-04308-x>
- Flores-Larsens, S., Filippin, C., Bre, F., 2023. New metrics for thermal resilience of passive buildings during heat events. *Building and Environment*, 230, 109990, <https://doi.org/10.1016/j.buildenv.2023.109990>
- Foissard, X., Dubreuil, V., & Quénol, H. (2019). Defining scales of the land use effect to map the urban heat island in a mid-size European city: Rennes (France). *Urban Climate*, 29, 100490. <https://doi.org/10.1016/j.uclim.2019.100490>

- Frank, B., Delano, D., & Caniglia, B. S. (2017). Urban systems: A socio-ecological system perspective. *Sociol. Int. J.*, 1(1), 1-8.
- Frich, A.; L.V. Alexander; P. Della-Marta; B. Gleason; M. Haylock; A.M.G. Klein Tank; T. Peterson (January 2002). "Observed coherent changes in climatic extremes during the second half of the twentieth century" (PDF). *Climate Research*. 19: 193–212. Bibcode:2002ClRes..19..193F. doi:10.3354/cr019193
- Frigerio, I., Carnelli, F., Cabinio, M. & De Amicis, M. 2018. Spatiotemporal Pattern of Social Vulnerability in Italy. *Int J Disaster Risk Sci* (2018) 9:249–262. <https://doi.org/10.1007/s13753-018-0168-7>.
- Fu, G., Cao, C., Fu, K., Song, Y., Yuan, K., Wan, X., Zhu, Z., Wang, Z., & Huang, Z. (2022). Characteristics and evaluation of coastal erosion vulnerability of typical coast on Hainan Island. *Frontiers in Marine Science*, 9. <https://doi.org/10.3389/fmars.2022.1061769>
- Funtowicz, S.O. and Ravetz, J. (1990). *Uncertainty and Quality in Science for Policy*, Dordrecht: Kluwer.
- G. Tocchi, M. Polese, M. Di Ludovico, A. Prota, (2022), REGIONAL BASED EXPOSURE MODELS TO ACCOUNT FOR LOCAL BUILDING TYPOLOGIES, *Bulletin of earthquake engineering*, 20: 193–228, doi.org/10.1007/s10518-021-01242-6
- Gabriel, N. (2014). Urban political ecology: Environmental imaginary, governance, and the non-human. *Geography Compass*, 8(1), 38-48.
- Gagge, A.P., Fobelets, A.P., Berglund, L.G., 1986. A standard predictive index of human response to the thermal environment. *Build. Eng.*, 92 (2B), pp. 709-731
- Galar, D. Kumar, U. (2017). *EMaintenance: Essential Electronic Tools for Efficiency*, Academic Press.
- Galderisi, A.; Limongi, G., (2021) "A Comprehensive Assessment of Exposure and Vulnerabilities in Multi-Hazard Urban Environments: A Key Tool for Risk-Informed Planning Strategies". *Sustainability*, 13, 9055. <http://doi.org/10.3390/su13169055>
- Gall M, Boruff BJ, Cutter SL (2007) Assessing flood hazard zones in the absence of digital floodplain maps: comparison of alternative approaches. *Nat Hazards Rev* 8(1):1–12
- Gallina, V., (2020) A Multi-Risk Methodology for the Assessment of Climate Change Impacts in Coastal Zones, *Sustainability*, Volume 12 (9). DOI: 10.3390/su12093697
- Gallina, V., Torresan, S., Zabeo, A., Critto, A., Glade, T., Marcomini, A., (2016) A review of multi-risk methodologies for natural hazards: Consequences and challenges for a climate change impact assessment, *Journal of Environmental Management*, Volume 168, pp.123-132. DOI: 10.1016/j.jenvman.2015.11.011
- Gao, Z., Hou, Y., & Chen, W. (2019). Enhanced sensitivity of the urban heat island effect to summer temperatures induced by urban expansion. *Environmental Research Letters*, 14, Article 094005. <https://doi.org/10.1088/1748-9326/ab2740>
- Garcia-Aristizabal, A., Di Ruocco, A. & Marzocchi, W. 2013. Naples test case. European Commission project MATRIX, Project No.265138, D7.3.
- Garcia-Aristizabal, A., Marzocchi, W., (2012a) Dictionary of the Terminology Adopted. Deliverable 3.2. MATRIX project (Contract n 265138).
- Garcia-Aristizabal, A., Marzocchi, W., (2012b) Bayesian Multi-risk Model: Demonstration for Test City Researchers. Deliverable 2.13. CLUVA project (Contract n 265137). http://www.cluva.eu/deliverables/CLUVA_D2.13.pdf.
- Garnier T., Une cité industrielle, 1918, ed. Mariani R. a cura di, Tony Garnier una città industriale, riproduzione completa delle tavole in bianco e nero dell'edizione 1932, Jaka Book, Milano 1990.
- Gasparini, A., and Armstrong, B., 2011. The impact of heat waves on mortality. *Epidemiology* 22(1):68-73. doi: 10.1097/EDE.0b013e3181fdcd99.

- Gasparri, A., Guo, Y., Hashizume, M., Kinney, P. L., Petkova, E. P., Lavigne, E., et al. 2015. Temporal variation in heat–mortality associations: A multicountry study. *Environmental Health Perspectives*, 123(11), 1200–1207. <https://doi.org/10.1289/ehp.1409070>
- Gentile, R., Cremen, G., Galasso, C., Jenkins, L.T., Manandhar, V., Menteş, E.Y., Guragain, R., McCloskey, J. Scoring, selecting, and developing physical impact models for multi-hazard risk assessment, *International Journal of Disaster Risk Reduction*, Volume 82, 2022, 103365, ISSN 2212-4209, <https://doi.org/10.1016/j.ijdr.2022.103365>.
- Ghajari YE, Alesheikh AA, Modiri M, Hosnavi R, Abbasi M (2017) Spatial modelling of urban physical vulnerability to explosion hazards using GIS and fuzzy MCDA. *Sustainability (switzerland)* 9(7):1–29. <https://doi.org/10.3390/su9071274>
- Ghased, H., Roozbahani, A., & Shahedany, M. H. (n.d.). Evaluation of Inter-basin Water Transfer Project Scenarios to Central Plateau of Iran Employing COPRAS Multi-criteria Decision Making Method. *Journal of Water and Soil*, 34(2), 317–332. <https://doi.org/10.22067/JSW.V34I2.81708>
- Ghorbanzadeh, O., Valizadeh Kamran, K., Blaschke, T., Aryal, J., Naboureh, A., Einali, J., et al., 2019c. Spatial prediction of wildfire susceptibility using field survey GPS data and machine learning approaches. *Fire* 2 (3), 43. <https://www.mdpi.com/2571-6255/2/3/43>.
- Ghosh, J., Padgett, J. E., & S´anchez-Silva, M. (2015). Seismic damage accumulation in highway bridges in earthquake-prone regions. *Earthquake Spectra*, 31(1), 115–135.
- Ghosh, S., & Mistri, B. (2022). Analyzing the multi-hazard coastal vulnerability of Matla–Bidya inter-estuarine area of Indian Sundarbans using analytical hierarchy process and geospatial techniques. *Estuarine, Coastal and Shelf Science*, 279, 108144. <https://doi.org/10.1016/j.ecss.2022.108144>
- Giammarco C., Isola A. (a cura di), (1993), Disegnare le periferie. Il progetto del limite, La Nuova Italia Scientifica, Roma.
- Giedion S. (1941). *Space, Time and Architecture. The Growth of a New Tradition*, Harvard: Harvard University Press.
- Gill SE, Handley JF, Ennos AR, Pauleit S, Theuray N, Lindley SJ (2008) Characterising the urban environment of UK cities and towns: a template for landscape planning in a changing climate. *Landsc Urban Plan* 87:210–222
- Gill, J. & Malamud, B. 2014. Reviewing and visualising the interactions of natural hazards. *Reviews of Geophysics* 52, 680.
- Ginoux, P., Prospero, J. M., Gill, T. E., Hsu, N. C., & Zhao, M. 2012. Global-scale attribution of anthropogenic and natural dust sources and their emission rates based on MODIS Deep Blue aerosol products. *Reviews of Geophysics*, 50(3), <https://doi.org/10.1029/2012RG000388>
- Giordano, P.F., Limongelli, M. P., Iannacone, L., Gardoni, P. (2021). Value of Information analysis for degrading engineering systems. 10.1201/9780429343292-87.
- Girgin, S. The Natech Events during the 17 August 1999 Kocaeli Earthquake: Aftermath and Lessons Learned. *Nat. Hazards Earth Syst. Sci.* 2011, 11, 1129–1140.
- Goodwin, N. R. (2003). *Five kinds of capital: Useful concepts for sustainable development*. Tufts University Medford, MA.
- Gosling, S.N., McGregor, G., Pády, A., 2007. Climate change and heat-related mortality in six cities Part 1: model construction and validation. *Int J Biometeorol* 51, 525–540 (2007). <https://doi.org/10.1007/s00484-007-0092-9>
- Goulart Coelho, L. M., Lange, L. C., & Coelho, H. M. (2017). Multi-criteria decision making to support waste management: A critical review of current practices and methods. *Waste Management & Research: The Journal for a Sustainable Circular Economy*, 35(1), 3–28.

<https://doi.org/10.1177/0734242X16664024>

- Grantz, D.A., Garner, J.H.B., Johnson, D.W., 2003. Ecological effects of particulate matter. *Environment International*, 29, 2–3, 213–239, [https://doi.org/10.1016/S0160-4120\(02\)00181-2](https://doi.org/10.1016/S0160-4120(02)00181-2)
- Gravagnuolo B., *La progettazione urbana in Europa. 1750-1960*, Editori Laterza 1991.
- Greco, S., Ishizaka, A., Tasiou, M. & Torrisi, G. 2019. On the Methodological Framework of Composite Indices: A Review of the Issues of Weighting, Aggregation, and Robustness. *Soc Indic Res* 141, 61–94 (2019). <https://doi.org/10.1007/s11205-017-1832-9>
- Gregotti V., *Il territorio dell'architettura*, Feltrinelli, Milano, Paper back, USA2008 (1986).
- Gregotti, V. (1965), *La forma del territorio*, Edilizia Moderna no. 87-88.
- Grove, J. M., Pickett, S. T., Whitmer, A., & Cadenasso, M. L. (2013). Building an urban LTSE: The case of the Baltimore Ecosystem Study and the DC/BC ULTRA-Ex Project. *Long Term Socio-Ecological Research: Studies in Society-Nature Interactions Across Spatial and Temporal Scales*, 369–408.
- Gudiyangada Nachappa, T., Tavakkoli Piralilou, S., Gholamnia, K., Ghorbanzadeh, O., Rahmati, O., & Blaschke, T. (2020). Flood susceptibility mapping with machine learning, multi-criteria decision analysis and ensemble using Dempster Shafer Theory. *Journal of Hydrology*, 590, 125275. <https://doi.org/10.1016/j.jhydrol.2020.125275>
- Guidotti, R., Gardoni, P., Chen, Y. 2017. Network reliability analysis with link and nodal weights and auxiliary nodes. *Structural Safety*. 65 (2017) 12–26.
- Gujansky, G., Carmen, M., & Belderrain, N. (2014). Aplicação do método AHPSort para aquisição de um automóvel. *Revista gestão em engenharia*, 1(1), 1–17. Retrieved from <http://www.mec.ita.br/~cge/RGE/ARTIGOS/v01n01a01.pdf>
- Guo Y, Gasparrini A, Amstrong B, Li S, Tawatsupa B, Tobias A, Lavigne E, Coelho M d ZS, Leone M, Pan X, Tong S, Tia L, Him H, Hashizume M, Honda Y, Guo YL, Wu CF, Punnasiri K, Yi SM, Michelozzi O, Saldiva PH, William G (2014) *Global variation in the effects of ambient temperature on mortality: a systematic evaluation*.
- Gurgueira S.A., Lawrence J., Coull B., Murthy G.K., González-Flecha B.. 2002. Rapid increases in the steady-state concentration of reactive oxygen species in the lungs and heart after particulate air pollution inhalation. *Environ Health Perspect* 110:749–755 <https://www.ncbi.nlm.nih.gov/pubmed/12153754>
- Gwilliam J, Fedeski M, Lindley S, Theuray N, Handley J (2006) Methods for assessing risk from climate hazards in urban areas. *Proc ICE-Munic Eng* 159(4):245–255
- Hawley, A.H. (1950). *Human Ecology- A Theory of Community Structure*. New York
- Haywood, J., & Boucher, O., 2000. Estimates of the direct and indirect radiative forcing due to tropospheric aerosols: A review. *Reviews of geophysics*, 38(4), 513–543. DOI 10.1029/1999RG000078
- HEC-RAS 4.1 (2010) Hydrological Engineering Center (HEC) river analysis system (RAS). United States Army Corps of Engineering (USACE). www.hec.usace.army.mil
- Hidalgo, J., Dumas, G., Masson, V., Petit, G., Bechtel, B., Bocher, E., Foley, M., Schoetter, R., Mills, G. (2019), Comparison between local climate zones maps derived from administrative datasets and satellite observations, *Urban Climate*, 27, 64–89.
- Hifumi, T., Kondo, Y., Shimizu, K. et al., 2018. Heat stroke. *J Intensive Care* 6, 30 (2018). <https://doi.org/10.1186/s40560-018-0298-4>
- Ho, H.C., Knudby, A., Huang, W., (2015) A Spatial Framework to Map Heat Health Risks at Multiple Scales, *International Journal of Environmental Research and Public Health*, 12(12). DOI: <https://doi.org/10.3390/ijerph121215046>

- Homaiei, S., Hamdy, H., 2021. Thermal resilient buildings: How to be quantified? A novel benchmarking framework and labelling metric. *Building and Environment*, 201., 108022, <https://doi.org/10.1016/j.buildenv.2021.108022>
- Hoover, D.J., Mackenzie, F.T., 2009 Fluvial Fluxes of Water, Suspended Particulate Matter, and Nutrients and Potential Impacts on Tropical Coastal Water Biogeochemistry: Oahu, Hawai'i. *Aquat Geochem* 15, 547–570. <https://doi.org/10.1007/s10498-009-9067-2>
- Höppe, P., 1999. The physiological equivalent temperature - a universal index for the biometeorological assessment of the thermal environment. *Int J Biometeorol* 43(2), 71-5, doi:10.1007/s004840050118.
- Horspool, N. A. and Fraser, S. 2016. An Analysis of Tsunami Impacts to Lifelines, GNS Sci. Consult. Rep. 2016/22, GNS Science, Lower Hutt, New Zealand, 1–87, 2016.
- Hossain, S. A., Mondal, I., Thakur, S., & Fadhil Al-Quraishi, A. M. (2022). Coastal vulnerability assessment of India's Purba Medinipur-Balasore coastal stretch: A comparative study using empirical models. *International Journal of Disaster Risk Reduction*, 77, 103065. <https://doi.org/10.1016/j.ijdrr.2022.103065>
- Hou, P., Wu, S., 2016. Long-term Changes in Extreme Air Pollution Meteorology and the Implications for Air Quality. *Sci Rep* 6, 23792 <https://doi.org/10.1038/srep23792>
- Hsu, N. C., Herman, J. R., Torres, O., Holben, B. N., et al., (1999). Comparisons of the TOMS aerosol index with Sun-photometer aerosol optical thickness: Results and applications. *Journal of Geophysical Research: Atmospheres*, 104(D6), 6269-6279, <https://doi.org/10.1029/1998JD200086>
- Huang C, Barnett AG, Wang X, Vaneckova P, FitzGerald G, Tong S (2011) Projecting future heat-related mortality under climate change scenarios: a systematic review. *Environ Health Perspect* 119, 1681– 1690.
- Huang, C., et al., 2018. Mortality burden attributable to heatwaves in Thailand: A systematic assessment incorporating evidence-based lag structure. *Environment International* Volume 121, Part 1, December 2018, Pages 41-50, <https://doi.org/10.1016/j.envint.2018.08.058>
- Huizinga, H., de Moel, H. & Szewczyk, W. 2017. Global Flood Depth-Damage Functions - Methodology and the Database with Guidelines. Joint Research Centre, 2017, <https://doi.org/10.2760/16510>. EUR 28552 EN.
- Hwang, C.L. and Yoon, K. (1981) *Multiple Attribute Decision Making: Methods and Applications*. Springer-Verlag, New York. <http://dx.doi.org/10.1007/978-3-642-48318-9>
- Hyde, K. M. (2006). *Uncertainty analysis methods for multi-criteria decision analysis*.
- Iannaccone, L., Gentile, R., & Galasso, C. 2023. Simulating interacting multiple natural-hazard events for lifecycle consequence analysis. 14th International Conference on Applications of Statistics and Probability in Civil Engineering, ICASP14.
- Inter-agency Network for Education in Emergencies – INEE, <https://inee.org/>.
- IPCC (2014), 'Summary for policymakers', in: Field, C.B., V.R. Barros, D.J. Dokken, K.J. Mach, M.D. Mastrandrea, T.E. Bilir, M. Chatterjee, K.L. Ebi, Y.O. Estrada, R.C. Genova, B. Girma, E.S. Kissel, A.N. Levy, S. MacCracken, P.R. Mastrandrea, and L.L. White (eds.), *Climate Change 2014: Impacts, adaptation, and vulnerability. Part A: Global and sectoral aspects – contribution of Working Group II to the Fifth Assessment Report of the Intergovernmental Panel on Climate Change*, Cambridge University Press, Cambridge, United Kingdom and New York, NY, USA, pp. 1-32.
- IPCC (2022), *Climate Change 2022: Impacts, Adaptation and Vulnerability. Contribution of Working Group II to the Sixth Assessment Report of the Intergovernmental Panel on Climate Change*. Cambridge University Press, Cambridge, UK and New York, NY, USA. <https://doi.org/10.1017/9781009325844>

- IPCC (2022), *Climate Change 2022: Impacts, Adaptation, and Vulnerability. Contribution of Working Group II to the Sixth Assessment Report of the Intergovernmental Panel on Climate Change*, Cambridge University Press, Cambridge, UK and New York, NY, USA, 3056.
- IPCC (2023), Summary for policymakers. In *Climate Change 2023: Synthesis Report. A Report of the Intergovernmental Panel on Climate Change. Contribution of Working Groups I, II and III to the Sixth Assessment Report of the Intergovernmental Panel on Climate Change*; Lee, H., Romero, J., Eds.; IPCC: Geneva, Switzerland, 2023; 36. Available online: <https://www.ipcc.ch/assessment-report/ar6> (accessed on 01-05-2023).
- Ishizaka, A., Pearman, C., & Nemery, P. (2012). AHPSort: An AHP-based method for sorting problems. *International Journal of Production Research*, 50(17), 4767–4784. <https://doi.org/10.1080/00207543.2012.657966>
- Jalayer F, De Risi R, De Paola F, Giugni M, Manfredi G, Gasparini P, Topa M E, Yonas N, Yeshitela K, Nebebe A, Cavan G, Lindley S, Printz A, Renner F., (2014) Probabilistic GIS-based method for delineation of urban flooding risk hotspots, *Nat Hazards* 73:975–1001
- Janssen, R. (1992). *Multiobjective Decision Support for Environmental Management*, Dordrecht: Kluwer Academic.
- Januadi Putra, M. I., Yoga Affandani, A., Widodo, T., & Wibowo, A. (2019). Spatial Multi-Criteria Analysis for Urban Sustainable Built Up Area Based on Urban Heat Island in Serang City. *IOP Conference Series: Earth and Environmental Science*, 338(1), 012025. <https://doi.org/10.1088/1755-1315/338/1/012025>
- Jaynes ET (1995) Probability theory: the logic of science. Book.
- Jena, R., & Pradhan, B. (2020). Integrated ANN-cross-validation and AHP-TOPSIS model to improve earthquake risk assessment. *International Journal of Disaster Risk Reduction*, 50, 101723. <https://doi.org/10.1016/j.ijdrr.2020.101723>
- Jenelius, E. 2010. Redundancy importance: Links as rerouting alternatives during road network disruptions. *International Conference on Evacuation Modeling and Management*. Published by Elsevier Ltd doi:10.1016/j.proeng.2010.07.013
- Jenks G.F. (1977). *Optimal data classification for choropleth maps*. Occasional paper No. 2. Lawrence, Kansas: University of Kansas, Department of Geography.
- Ji, W., Zhu, Y., Du, H., et al., 2022. Interpretation of standard effective temperature (SET) and explorations on its modification and development. *Building and Environment*, 108714, <https://doi.org/10.1016/j.buildenv.2021.108714>
- Jiang, Y., Brassington, K. J., Prpich, G., Paton, G. I., Semple, K. T., Pollard, S. J. T., & Coulon, F. (2016). Insights into the biodegradation of weathered hydrocarbons in contaminated soils by bioaugmentation and nutrient stimulation. *Chemosphere*, 161, 300–307. <https://doi.org/10.1016/j.chemosphere.2016.07.032>
- Johnson, D. P., Stanforth, A., Lulla, V., & Luber, G. (2012). Developing an applied extreme heat vulnerability index utilizing socioeconomic and environmental data. *Applied Geography*, 35(1–2), 23–31. <https://doi.org/10.1016/j.apgeog.2012.04.006>
- Johnson, K., Depietri, Y., Margareta, B., (2016) Multi-hazard risk assessment of two Hong Kong districts, *International Journal of Disaster Risk Reduction*, Volume 19, pp. 311-323. DOI: 10.1016/j.ijdrr.2016.08.023
- Jolliffe, I.T. (2002). *Principal Component Analysis*. Series: Springer Series in Statistics, Springer, NY, pp. 50e70

- Juarez, P.D., Hood, D.B., Song, M-A, Ramesh, A., 2020. Use of an Exposome Approach to Understand the Effects of Exposures From the Natural, Built, and Social Environments on Cardio-Vascular Disease Onset, Progression, and Outcomes. *Front. Public Health*, 12 August 2020, Sec. Exposome, Volume 8 - 2020 | <https://doi.org/10.3389/fpubh.2020.00379>
- Ju-Long, D. (1982). Control problems of grey systems. *Syst. Control Lett.*, (1), 288–294. doi: 10.1016/S0167-6911(82)80025-X
- Kappes, M.S., Gruber, K., Frigerio, S., Bell, R., Keiler, M., Glade, T., (2012) The MultiRISK platform: the technical concept and application of a regional-scale multi hazard exposure analysis tool. *Geomorphology* 151-152, pp. 139-155. <http://dx.doi.org/10.1007/s11069-012-0294-2>
- Kawashima, K. and Buckle, I. 2013 Structural performance of bridges in the Tohoku-oki earthquake (SUPPL. 1), *Earthq. Spectra*, 29, S315–S338, <https://doi.org/10.1193/1.4000129>, 2013.
- Kazama, M. and Noda, T. 2012. Damage statistics (Summary of the 2011 off the Pacific Coast of Tohoku Earthquake damage), *Soils Found.*, 52, 780–792, <https://doi.org/10.1016/j.sandf.2012.11.003>, 2012.
- Kennedy, C., Pincetl, S., & Bunje, P. (2011). The study of urban metabolism and its applications to urban planning and design. *Environmental pollution*, 159(8-9), 1965-1973.
- Kenney, W.L., Craighead, D.H., Lacy, A., 2014. Heat Waves, Aging, and Human Cardiovascular Health. *Medicine & Science in Sports & Exercise* 46(10): 1891-1899, October 2014. | DOI: 10.1249/MSS.0000000000000325
- Keskinen, H.-M., et al 2020. Long-term aerosol mass concentrations in southern Finland: instrument validation, seasonal variation and trends, *Atmos. Meas. Tech. Discuss.* [preprint], <https://doi.org/10.5194/amt-2020-447>
- Khan, H., Vasilescu, L. G., & Khan, A. (2008). Disaster management cycle—A theoretical approach. *Journal of Risk Management*, 6, 43–50.
- Khosravi K., Shahabi H., Pham B.T., Adamowski J., Shirzadi A., Pradhan B., Dou J., Ly H.B., Grof G., Ho H.L., Hong H., Chapi K., Prakash I. A comparative assessment of flood susceptibility modeling using Multi-Criteria Decision-Making Analysis and Machine Learning Methods (2019). *J. Hydrol.*, 573, 311-323, 10.1016/j.jhydrol.2019.03.073
- King, M. D., Kaufman, Y. J., Tanré, D., & Nakajima, T. (1999). Remote sensing of tropospheric aerosols from space: Past, present, and future. *Bulletin of the American Meteorological society*, 80(11), 2229-2260.
- Kingsley, S. L., Eliot, M. N., Whitsel, E. A., Wang, Y., Coull, B. A., Hou, L., Margolis, H. G., Margolis, K. L., Mu, L., Wu, W.-C. C., Johnson, K. C., Allison, M. A., Manson, J. E., Eaton, C. B., & Wellenius, G. A. (2015). Residential proximity to major roadways and incident hypertension in post-menopausal women. *Environmental Research*, 142, 522–528. <https://doi.org/10.1016/j.envres.2015.08.002>
- Kirkby MJ (1975) Hydrograph modelling strategies. In: Peel RF, Chisholm MD, Haggett P (eds) *Progress in physical and human geography*. Heinemann, London, pp 69–90
- Klonner, C., Marx, S., Usón, T., Porto de Albuquerque, J., & Höfle, B. (2016). Volunteered Geographic Information in Natural Hazard Analysis: A Systematic Literature Review of Current Approaches with a Focus on Preparedness and Mitigation. *ISPRS International Journal of Geo-Information*, 5(7), 103. <https://doi.org/10.3390/ijgi5070103>
- Koks, E. E., Rozenberg, J., Zorn, C., Tariverdi, M., Voudoukas, M., Fraser, S. A., Hall, J. W., and Hallegatte, S. 2019. A global multihazard risk analysis of road and railway infrastructure assets, *Nat. Commun.*, 10, 1–11, <https://doi.org/10.1038/s41467-019-10442-3>, 2019.
- Koolhas R, Junkspace, Quodlibet, Macerata 2006.

- Kotharkar, R., Bagade, A., & Singh, P. R. (2020). A systematic approach for urban heat island mitigation strategies in critical local climate zones of an Indian city. *Urban Climate*, 34, 100701. <https://doi.org/10.1016/j.uclim.2020.100701>
- Kovacs, Y., Doussin, N., & Gaussens, M. (2017). *Flood risk and cities in developing countries*. AFD - Agence Française de Développement. <https://www.afd.fr/en/ressources/flood-risk-and-cities-developing-countries>
- Krausmann, E.; Cruz, A.M. 2013. Impact of the 11 March 2011, Great East Japan Earthquake and Tsunami on the Chemical Industry. *Nat. Hazards* 2013, 67, 811–828.
- Kumar, D. N. (2010). *Multicriterion Analysis in Engineering and Management*. PHI Learning.
- Lagomarsino, S. & Giovinazzi, S. 2006. Macroseismic and mechanical models for the vulnerability and damage assessment of current buildings. *Bulletin of Earthquake Engineering* volume 4, pages415–443.
- Lallemant, D., Hamel, P., Balbi, M., Lim, T. N., Schmitt, R., & Win, S. (2021). Nature-based solutions for flood risk reduction: A probabilistic modeling framework. *One Earth*, 4(9), 1310–1321. <https://doi.org/10.1016/j.oneear.2021.08.010>
- Lanzani A. (1991), Il territorio al plurale. Interpretazioni geografiche e temi di progettazione territoriale in alcuni contesti locali, Franco Angeli, Milano.
- Lanzani A., I paesaggi italiani, Meltemi editore roma 2003.
- Le Cozannet, G., Garcin, M., Bulteau, T., Mirgon, C., Yates, M. L., Méndez, M., Baills, A., Idier, D., & Oliveros, C. (2013). An AHP-derived method for mapping the physical vulnerability of coastal areas at regional scales. *Natural Hazards and Earth System Sciences*, 13(5), 1209–1227. <https://doi.org/10.5194/nhess-13-1209-2013>
- Le, H.A., Khoi, N.Q., Mallick, J., 2022. Integrated emission inventory and modelling to assess the distribution of particulate matters from rice straw open burning in Hanoi, Vietnam. *Atmospheric Pollution Research*, 13, 5, 101416, <https://doi.org/10.1016/j.apr.2022.101416>
- Leader T, Wallingford HR (2009) Language of risk. Deliverable D32.2. FLOODsite project. http://floodsite.net/html/partner_area/project_docs/T32_04_01_FLOODsite_Language_of_Risk_D32_2_v5_2_P1.pdf. Accessed 25 June 2013
- Lee, C.-T., Huang, C.-C., Lee, J.-F., Pan, K.-L., Lin, M.-L., Dong, J.-J. 2008. Statistical approach to earthquake-induced landslide susceptibility. *Engineering Geology* 100: 43–58.
- Lee, D.H.K., 1965. Climatic stress indices for domestic animals. *Int J Biometeorol* 9, 29–35. <https://doi.org/10.1007/BF02187306>
- Lelieveld, J., Evans, J., Fnais, M. et al., 2015. The contribution of outdoor air pollution sources to premature mortality on a global scale. *Nature* 525, 367–371. <https://doi.org/10.1038/nature15371>
- Lemonsu, A., Vigié, V., Daniel, M., Masson, V., 2015. Vulnerability to heat waves: Impact of urban expansion scenarios on urban heat island and heat stress in Paris (France). *Urban Climate* 14, 586–605, <http://dx.doi.org/10.1016/j.uclim.2015.10.007>
- Lessler, J., Azman, A.S., McKay H.S., Moore, S.M., (2017) What is a Hotspot Anyway? *Am J Trop Med Hyg.*, Volume 96 (6). DOI: 10.4269/ajtmh.16-0427
- Levine N (2002) CrimeStat II: A spatial statistics program for the analysis of crime incident locations, CrimeStat Manual, Ned Levine & Associates, TX, National Institute of Justice, Washington DC
- Manfreda S, Sole A, Fiorentino M (2007) Valutazione del pericolo di allagamento sul territorio nazionale mediante un approccio di tipo geomorfologico. *L'Acqua* 4:43–54 (in Italian)
- Levlovics, E., Gál, T., Unger, J. (2013), Mapping local climate zones with a vector-based GIS method. *Aerul și Apa: Componente ale Mediului*, 423–430.

- Lewis, K., Arnott, W. P., Moosmüller, H., and Wold, C. E., 2008. Strong spectral variation of biomass smoke light absorption and single scattering albedo observed with a novel dual-wavelength photoacoustic instrument, *J. Geophys. Res.*, 113, 280–288, <https://doi.org/10.1029/2007JD009699>
- Li, J., Carlson, B.E., Yung, Y.L. et al., 2022. Scattering and absorbing aerosols in the climate system. *Nat Rev Earth Environ* 3, 363–379. <https://doi.org/10.1038/s43017-022-00296-7>
- Li, Z., Guo, X., Yang, Y., Hong, Y., Wang, Z., & You, L. (2019b). Heatwave trends and the human exposure over China in the 21st century as well as under 1.5 °C and 2.0 °C global warmer future scenarios. *Sustainability*, 11, 3318. <https://doi.org/10.3390/su11123318>
- Li, Z., Hu, J., Meng, R., He, G., Xu, X., Liu, T., Zeng, W., Li, X., Xiao, J., Huang, C., Du, Y., & Ma, W. (2021). The association of compound hot extreme with mortality risk and vulnerability assessment at fine-spatial scale. *Environmental Research*, 198, 111213. <https://doi.org/10.1016/j.envres.2021.111213>
- Li, Z., Zhang, X., Ma, Y., Feng, C., & Hajiyev, A. (2019a). A multi-criteria decision making method for urban flood resilience evaluation with hybrid uncertainties. *International Journal of Disaster Risk Reduction*, 36, 101140. <https://doi.org/10.1016/j.ijdrr.2019.101140>
- Likens, G. E. (1992). The ecosystem approach: its use and abuse. Excellence in ecology, 3, VII-XXIV. Oldendorf/Luhe, Germany: Ecology Institute.
- Liu, A., Ma, X., Du, M., Su, M., Hong, B. (2023), The cooling intensity of green infrastructure in local climate zones: A comparative study in China's cold region, *Urban Climate*, 51, 101631. <https://doi.org/10.1016/j.uclim.2023.101631>
- Liu, A., Ma, X., Du, M., Su, M., Hong, B. (2023), The cooling intensity of green infrastructure in local climate zones: A comparative study in China's cold region, *Urban Climate*, 51, 101631. <https://doi.org/10.1016/j.uclim.2023.101631>
- Loftus, A. (2012). Everyday environmentalism: creating an urban political ecology. Minneapolis: University of Minnesota Press, USA.
- Löhmus M., 2018. Possible Biological Mechanisms Linking Mental Health and Heat—A Contemplative Review. *International Journal of Environmental Research and Public Health*, 15(7):1515. <https://doi.org/10.3390/ijerph15071515>
- Lolli, F., Ishizaka, A., & Gamberini, R. (2014). New AHP-based approaches for multi-criteria inventory classification. *International Journal of Production Economics*, 156, 62–74. <https://doi.org/10.1016/j.ijpe.2014.05.015>
- Losasso, M. (2013), *Progettazione ambientale e caratteri della disciplina architettonica*, in Rigillo, M. (Ed.), *Oltre la siepe. Scenari di ricerca per il progetto ambientale*, Editoriale Scientifica, Napoli, pp. 237-241.
- Lu Y., He T., Xu X. and Qiao, Z. (2021) "Investigation the Robustness of Standard Classification Methods for Defining Urban Heat Islands," in *IEEE Journal of Selected Topics in Applied Earth Observations and Remote Sensing*, vol. 14, 11386-11394, doi: 10.1109/JSTARS.2021.3124558
- Luhmann, N. (1984). *Soziale systeme* (Vol. 478). Frankfurt am Main: Suhrkamp. trad. it. *Sistemi sociali: Fondamenti di una teoria generale*, Bologna: Il Mulino, 1990.
- Lundgren, L., & Jonsson, A. C. (2012). *Assessment of social vulnerability: a literature review of vulnerability related to climate change and natural hazards*. Centre for Climate Science and Policy Research. <https://www.diva-portal.org/smash/get/diva2:552075/FULLTEXT01>
- Luo, X., Haijian, B., Zhuanxi, L., Yujun W-, Ling J., 2019. Impacts of atmospheric particulate matter pollution on environmental biogeochemistry of trace metals in soil-plant system: A review, *Environmental Pollution*, Volume 255, Part 1, 113138, ISSN 0269-7491, <https://doi.org/10.1016/j.envpol.2019.113138>

- Mabrouk, M., & Haoying, H. (2023). Urban resilience assessment: A multicriteria approach for identifying urban flood-exposed risky districts using multiple-criteria decision-making tools (MCDM). *International Journal of Disaster Risk Reduction*, 91, 103684. <https://doi.org/10.1016/j.ijdrr.2023.103684>
- Mahapatra, M., Ramakrishnan, R., & Rajawat, A. S. (2015). Coastal vulnerability assessment using analytical hierarchical process for South Gujarat coast, India. *Natural Hazards*, 76(1), 139–159. <https://doi.org/10.1007/s11069-014-1491-y>
- Maharoor, N., Emmanuel, R., Thomson, C., (2020), Compatibility of local climate zone parameters for climate sensitive street design: Influence of openness and surface properties on local climate, *Urban Climate*, Volume 33, 100642. <https://doi.org/10.1016/j.uclim.2020.100642>.
- Mahdiyar, A., Tabatabaee, S., Abdullah, A., & Marto, A. (2018). Identifying and assessing the critical criteria affecting decision-making for green roof type selection. *Sustainable Cities and Society*, 39, 772–783. <https://doi.org/10.1016/j.scs.2018.03.007>
- Manfreda S, Di Leo M, Sole A (2011) Detection of flood-prone areas using digital elevation models. *J Hydrol Eng* 16(10):781–790
- Manfreda S, Sole A, Fiorentino M (2008) Can the basin morphology alone provide an insight on floodplain delineation? On flood recovery innovation and response. *WIT, Southampton*, pp 47–56
- Manser, C.N., Paul, M., Rogler, G., Held, L., Frei, T., 2013. Heat Waves, Incidence of Infectious Gastroenteritis, and Relapse Rates of Inflammatory Bowel Disease: A Retrospective Controlled Observational Study. *American Journal of Gastroenterology* 108(9):p 1480-1485, DOI: 10.1038/ajg.2013.186
- Manyaga, F., Nilufer, N., & Hajaoui, Z. (2020). A systematic literature review on multi-criteria decision making in disaster management. *International Journal of Business Ecosystem & Strategy* (2687-2293), 2(2), 1–7. <https://doi.org/10.36096/ijbes.v2i2.197>
- Maragno, D., dall'Olmo, C., Pozzer, G., Musco, F., (2021) Multi-Risk Climate Mapping for the Adaptation of the Venice Metropolitan Area, *Sustainability*, Volume 13 (3). DOI: 10.3390/su13031334
- Marin-Ferrer, M., Vernaccini, L. and Poljansek, K., (2017) Index for Risk Management INFORM Concept and Methodology Report — Version 2017, EUR 28655 EN. DOI:10.2760/094023
- Martins, L. C. R. (2018). *Earthquake damage and loss assessment of reinforced concrete buildings* [Universidade do Porto]. <https://core.ac.uk/download/pdf/302909299.pdf>
- Marzocchi, W., Garcia-Aristizabal, A., Gasparini, P., Mastellone, M.L., Di Ruocco, A., (2012) Basic principles of multi-risk assessment: a case study in Italy. *Nat. Hazards* 62, 551-573. <http://dx.doi.org/10.1007/s11069-012-0092-x>.
- Mathew P, Sanchez L, Lee SH, Walter T. 2021. Assessing the Energy Resilience of Office Buildings: Development and Testing of a Simplified Metric for Real Estate Stakeholders. *Buildings*, 11(3):96. <https://doi.org/10.3390/buildings11030096>
- Matthews, T. (2018). Humid heat and climate change. *Progress in Physical Geography*, 42(3), 391–405. <https://doi.org/10.1177/0309133318776490>
- Mavromatidi, A., Briche, E., Claeys, C 2018, “Mapping and analyzing socio-environmental vulnerability to coastal hazards induced by climate change: An application to coastal Mediterranean cities in France”, *ScienceDirect*, volume 27 <https://www.sciencedirect.com/science/article/abs/pii/S0264275116307272>
- Mayes, W. M., Johnston, D., Potter, H. A. B., & Jarvis, A. P. (2009). A national strategy for identification, prioritisation and management of pollution from abandoned non-coal mine sites in England and Wales. *I. Science of The Total Environment*, 407(21), 5435–5447. <https://doi.org/10.1016/j.scitotenv.2009.06.019>

- Mazza L. (a cura di), (1988), *Le città del mondo e il futuro della metropoli*. Partecipazioni internazionali. XVII Triennale di Milano, Electa, Milano.
- Mazziotta, M. & Pareto, A. 2013. Methods for Constructing Composite Indices: One for All or All for One?. *Rivista Italiana di Economia Demografia e Statistica*, Volume LXVII n. 2 Aprile-Giugno 2013.
- McCann, K.S. (2000). The diversity-stability debate. *Nature* 405(11):228-233.
- McCarty JJ, Canziani O, Leary N, Dokken D, White K (2001) *Climate change 2001: impacts, adaptation, and vulnerability*. Contribution of working group II to the Third assessment report of the intergovernmental panel on climate change. Cambridge University Press. Report No.: 0521807689
- Mendoza, G.A. and Prabhu, R. (2000) 'Multiple criteria decision making approaches to assessing forest sustainability using criteria and indicators: a case study', *Forest Ecology and Management*, 131(1-3): 107-26.
- Meyer V, Messner F (2005) National flood damage evaluation methods: a review of applied methods in England, the Netherlands, the Czech Republic and Germany (No. 21/2005). UFZ-Diskussionspapiere
- Nyarirangwe M (2008) The impact of multi-nucleated city morphology on transport in Addis Ababa (2008) In: van Dijk MP, Fransen J (eds) *Managing Ethiopian cities in an era of rapid urbanization*. Eburon, Delft
- Miccoli, F., & Ishizaka, A. (2017). Sorting municipalities in Umbria according to the risk of wolf attacks with AHPSort II. *Ecological Indicators*, 73, 741-755. <https://doi.org/10.1016/j.ecolind.2016.10.034>
- Middel, A., Häb, K., Brazel, A. J., Martin, C. A., & Guhathakurta, S. (2014), Impact of urban form and design on mid-afternoon microclimate in Phoenix Local Climate Zones. *Landscape and urban planning*, 122, 16-28.
- Mills, G., Bechtel, B., Alexander, P., Theeuwes, N., Foley, M., Ching, J., Ren, C., Yong, X., (2017) Using WUDAPT to explore urban exposure to climate risks in selected cities, in Brotas L., Roaf S., Nicol F. (eds.), *Proceedings of 33rd PLEA International Conference: Design to Thrive - PLEA 2017*, Volume 2, pp. 1797 - 1804, NCEUB 2017 - Network for Comfort and Energy Use in Buildings, Edinburgo. ISBN 978-099289575-4.
- Mimura, N., Yasuhara, K., Kawagoe, S., Yokoki, H., Kazama, S. 2011. Damage from the Great East Japan Earthquake and Tsunami-a quick report. Mitigation and adaptation strategies for global change, 16(7), 803-818. <https://doi.org/10.1007/s11027-011-9297-7>.
- Mitchell, B.C., & Chakraborty, J., 2018. Exploring the relationship between residential segregation and thermal inequity in 20 U.S. cities, *Local Environment*, 23:8, 796-813, DOI: 10.1080/13549839.2018.1474861
- Mladineo, N., Mladineo, M., Benvenuti, E., Kekez, T., Nikolic, Z., (2022) Methodology for the Assessment of Multi-Hazard Risk in Urban Homogenous Zones, *Applied Science* 12 (24). DOI: 10.3390/app122412843
- MLIT. 2012. Archive of the Great East Japan Earthquake Tsunami disaster urban reconstruction assistance survey, available at: <http://fukkou.csis.u-tokyo.ac.jp/> (last access: 1 June 2015), 2012.
- Mora, C., Dousset, B., Caldwell, I. et al., 2017. Global risk of deadly heat. *Nature Clim Change* 7, 501-506. <https://doi.org/10.1038/nclimate3322>
- Morabito, M., Profili, F., Crisci, A., Francesconi, P., Gensini, G. F., & Orlandini, S. (2012). Heat-related mortality in the Florentine area (Italy) before and after the exceptional 2003 heat wave in Europe: an improved public health response?. *International journal of biometeorology*, 56, 801-810.
- Morelli, S., Pazzi, V., Tofani, V., Raspini, F., Bianchini, S., & Casagli, N. (2021). Reconstruction of the slope instability conditions before the 2016 failure in an Urbanized District of Florence (Italy), a UNESCO world heritage site. *Understanding and Reducing Landslide Disaster Risk: Volume 1 Sendai Landslide Partnerships and Kyoto Landslide Commitment 5th*, 449-455.

- Mori, F., Mendicelli, A., Moscatelli, M., Romagnoli, G., Peronace, E., Naso, G. 2020. A new Vs30 map for Italy based on the seismic microzonation dataset. *Engineering Geology*, Volume 275, ISSN 0013-7952, <https://doi.org/10.1016/j.enggeo.2020.105745>.
- Munarín S., Tosi M. C. (2001), *Tracce di città. Esplorazioni di un territorio abitato: l'area veneta*, Franco Angeli, Milano.
- Munda, G. (1995) *Multiple Criteria Evaluation in a Fuzzy Environment – theory and applications in ecological economics*, Heidelberg: Physika Verlag.
- Munda, G., Nijkamp, P. and Rietveld, P. (1994) 'Fuzzy multigroup conflict resolution for environmental management', in J. Weiss (ed.) *The Economics of Project Appraisal and the Environment*, Aldershot: Edward Elgar.
- Musco, F., Maragno, D., & Litt, G. (2020). Abaco di azioni di adattamento ai cambiamenti climatici. Disponibile online a: https://air.iuav.it/bitstream/11578/306140/1/Abaco_LAST_low.pdf
- Mysiak, J., Torresan, S., Bosello, F., Mistry, M., & Sperotto, A. (2018). Climate risk index for Italy. *Philosophical Transactions of the Royal Society A: Mathematical, Physical and Engineering Sciences*, 376(2121). <https://doi.org/10.1098/rsta.2017.0305>
- Naga Kumar, K. C. V., Deepak, P. M., Basheer Ahammed, K. K., Rao, K. N., Gopinath, G., & Dinesan, V. P. (2022). Coastal vulnerability assessment using Geospatial technologies and a Multi-Criteria Decision Making approach – a case study of Kozhikode District coast, Kerala State, India. *Journal of Coastal Conservation*, 26(3), 16. <https://doi.org/10.1007/s11852-022-00862-7>
- Nairn, J.R., and Fawcett, R.J.B., 2015. The Excess Heat Factor: A Metric for Heatwave Intensity and its Use in Classifying Heatwave Severity. *International Journal of Environmental Research and Public Health*, 12(1), 227-253, doi:10.3390/ijerph120100227
- Najwer, A., Jankowski, P., Niesterowicz, J., & Zwoliński, Z. (2022). Geodiversity assessment with global and local spatial multicriteria analysis. *International Journal of Applied Earth Observation and Geoinformation*, 107, 102665. <https://doi.org/10.1016/j.jag.2021.102665>
- Nardo, M., Saisana, M., Saltelli, A. & Tarantola, S. 2005. Tools for Composite Indicators Building. Report number: JRC31473 Affiliation: European Commission, Joint Research Centre (JRC).
- Nardo, M., Saisana, M., Saltelli, A., Tarantola, S., Hoffmann, A., Giovannini, E. 2008. Handbook on Constructing Composite Indicators: Methodology and User Guide. Paris (France): OECD publishing; 2008. JRC47008.
- Nath, S. K., Adhikari, M. D., Devaraj, N., & Maiti, S. K. (2015). Seismic vulnerability and risk assessment of Kolkata City, India. *Natural Hazards and Earth System Sciences*, 15(6), 1103–1121. <https://doi.org/10.5194/nhess-15-1103-2015>
- Nazarian, N., Dumas, N., Kleissl, J., Norford, L. (2019). Effectiveness of cool walls on cooling load and urban temperature in a tropical climate. *Energy and Buildings*, 187, 144-162. <https://doi.org/10.1016/j.enbuild.2019.01.022>
- Neuendorf, K. K. (2005). *Glossary of geology*. Springer Science & Business Media.
- Nguyen T.T.N., et al 2015 Particulate matter concentration mapping from MODIS satellite data: a Vietnamese case study. *Environ. Res. Lett.* 10 095016, DOI 10.1088/1748-9326/10/9/095016+
- Nguyen, T.N.T., Luu, V.H., Pham, V.H., Bui, Q.H. and Nguyen, T.K.O. 2020. Particulate Matter Concentration Mapping from Satellite Imagery. In *TORUS 3 – Toward an Open Resource Using Services*, D. Laffly (Ed.). <https://doi.org/10.1002/9781119720522.ch5>
- Nishat, A. (Ed.). (2016). *Assessment of sea level rise on Bangladesh coast through trend analysis*. Climate Change Cell, Department of Environment, Ministry of Environment and Forests.

- Norberg-Schulz C. (1971). *Existence, Space & Architecture. New Concepts of Architecture*, New York: Praeger.
- Nortes Martínez, D., Grelot, F., Brémond, P., Farolfi, S., & Rouchier, J. (2021). Are interactions important in estimating flood damage to economic entities? The case of wine-making in France. *Natural Hazards and Earth System Sciences*, 21(10), 3057–3084. <https://doi.org/10.5194/nhess-21-3057-2021>
- NTC. 2018. Norme Tecniche per le costruzioni. Decreto Ministeriale 17 Gennaio 2018. Supplemento Ordinario n. 8 alla Gazzetta Ufficiale n. 42 del 20 febbraio 2018.
- Nyimbili, P.H., Erden, T. & Karaman, H. Integration of GIS, AHP and TOPSIS for earthquake hazard analysis. *Nat Hazards* 92, 1523–1546 (2018). <https://doi.org/10.1007/s11069-018-3262-7>
- O'Brien, W., Bennet, I., 2016. Simulation-Based Evaluation of High-Rise Residential Building Thermal Resilience. *ASHRAE Transactions*; Atlanta Vol. 122, (2016): 455-468.
- Öberg, H. (2009). Geografiska informationssystem (GIS) som stöd för krisberedskapsarbete - en studie en Växjö kommun. Stockholm: FOI.
- Oke T.R., Mills, G, Christen, A., Voogt, J.A. (2017), *Urban Climates*, Cambridge University Press, Cambridge.
- Oke, T.R. (1988), "Street Design and Urban Canopy Layer Climate", *Energy and Buildings*, Vol. 11, pp. 103-113.
- Oliveira, A., Lopes, A., Soares, A., 2022. Excess Heat Factor climatology, trends, and exposure across European Functional Urban Areas. *Weather and climate extremes*, 36, 100455, <https://doi.org/10.1016/j.wace.2022.100455>
- Oppenheimer, M., Campos, M., Warren, R., Birkmann, J., Luber, G., O'Neill, B., & Takahashi, K. (2014). Emergent risks and key vulnerabilities. In *Climate Change 2014: Impacts, Adaptation, and Vulnerability. Part A: Global and Sectoral Aspects. Contribution of Working Group II to the Fifth Assessment Report of the Intergovernmental Panel on Climate Change* (1046-1050). New York-Cambridge.
- Oswalt P., a cura di, *Shrinking cities*, Hatje Cantz, Bonn 2005.
- Otay, İ., & Kahraman, C. (2022). A novel circular intuitionistic fuzzy AHP-VIKOR methodology: An application to a multi-expert supplier evaluation problem. *Pamukkale University Journal of Engineering Sciences*, 28(1), 194–207. <https://doi.org/10.5505/pajes.2021.90023>
- Ozga, I., Bonazza, A., Bernardi, E., Tittarelli, F., Favoni, O., Ghedini, N., Morselli, L., Sabbioni, C., 2011. Diagnosis of surface damage induced by air pollution on 20th-century concrete buildings. *Atmospheric Environment*, 45, 28, 4986-4995, <https://doi.org/10.1016/j.atmosenv.2011.05.072>
- Ozkan, A., Kesik, T., Zerrin Yilmaz A. & O'Brien W. (2019) Development and visualization of time-based building energy performance metrics, *Building Research & Information*, 47:5, 493-517, DOI: 10.1080/09613218.2018.1451959
- Ozmen, H. B., Inel, M., & Meral, E. (2014). Evaluation of the main parameters affecting seismic performance of the RC buildings. *Sadhana*, 39(2), 437–450. <https://doi.org/10.1007/s12046-014-0235-8>
- Pagano L., Agostino Renna. Rimontaggio di un pensiero sulla conoscenza dell'architettura. *Antologia di scritti e progetti 1964-1988*, Clean, Napoli 2012.
- Pagliacci, F., Russo, M., (2020) Be (and have) good neighbours! Factors of vulnerability in the case of multiple hazards, *Ecological Indicators*, Volume 111. DOI: <https://doi.org/10.1016/j.ecolind.2019.105969>
- Palli, D., Saieva, C., Munnia, A., Peluso, M., Grechi, D., Zanna, I., ... & Masala, G. (2008). DNA adducts and PM10 exposure in traffic-exposed workers and urban residents from the EPIC-Florence City study. *Science of the Total Environment*, 403(1-3), 105-112.
- Pareyson L. (1954). *Estetica. Teoria della formatività*, Edizioni di «Filosofia», Torino.

- Parsons, T. (1951). *The Social System*. England: Routledge.
- Patz, J. A., Campbell-Lendrum, D., Holloway, T., & Foley, J. A. (2005). Impact of regional climate change on human health. *Nature*, 438(7066), 310–317. <https://doi.org/10.1038/nature04188>
- Pauleit S, Duhme F (2000) Assessing the environmental performance of land cover types for urban planning. *Landsc Urban Plan* 52(1):1–20
- Peng, J., & Zhang, J. (2022). Urban flooding risk assessment based on GIS- game theory combination weight: A case study of Zhengzhou City. *International Journal of Disaster Risk Reduction*, 77, 103080. <https://doi.org/10.1016/j.ijdr.2022.103080>
- Peresan, A. & Hassan, H.M. (2022). Tsunami scenarios modelling for selected areas along the Northern Adriatic coast. In *Proceedings of the "3rd European Conference on Earthquake Engineering and Seismology"*. Bucharest, Romania.
- Peresan, A., Scaini, C., & Barnaba, C. (2023). Crowd-Sourced Buildings Data Collection and Remote Training: New Opportunities to Engage Students in Seismic Risk Reduction. *Earth Science, Systems and Society*, 3, 10088.
- Perrone, D., J. O'Reilly, G., Monteiro, R., Filiatrault, A. 2020. Assessing seismic risk in typical Italian school buildings: From in-situ survey to loss estimation, *International Journal of Disaster Risk Reduction*, Volume 44, 2020, 101448, ISSN 2212-4209, <https://doi.org/10.1016/j.ijdr.2019.101448>.
- Piano Nazionale di Adattamento ai cambiamenti Climatici (PNACC), available at: https://www.minambiente.it/sites/default/files/archivio_immagini/adattamenti_climatici/documento_pnacc_luglio_2017.pdf
- Pizzol, L., Zabeo, A., Klusáček, P., Giubilato, E., Critto, A., Frantál, B., Martinát, S., Kunc, J., Osman, R., & Bartke, S. (2016). Timbre Brownfield Prioritization Tool to support effective brownfield regeneration. *Journal of Environmental Management*, 166, 178–192. <https://doi.org/10.1016/j.jenvman.2015.09.030>
- Polese M., Di Ludovico M., Gaetani d'Aragona M., Prota A., Manfredi G. (2020) Regional vulnerability and risk assessment accounting for local building typologies, *International Journal of Disaster Risk Reduction*, 43, 141400, DOI: 10.1016/j.ijdr.2019.101400
- Polese M., Gaetani d'Aragona M., Prota A., (2019) Simplified approach for building inventory and seismic damage assessment at the territorial scale: an application for a town in southern Italy, *Soil dynamics and earthquake engineering*, 121, 405–420, DOI 10.1016/j.soildyn.2019.03.028
- Poljanšek, K., Casajus Valles, A., Marin Ferrer, M., De Jager, A., Dottori, F., Galbusera, L., Garcia Puerta, B., Giannopoulos, G., Girgin, S., Hernandez Ceballos, M., Iurlaro, G., Karlos, V., Krausmann, E., Larcher, M., Lequarre, A., Theocharidou, M., Montero Prieto, M., Naumann, G., Necci, A., Salamon, P., Sangiorgi, M., Sousa, M., Trueba Alonso, C., Tsionis, G., Vogt, J., Wood, M. 2019. Recommendations for National Risk Assessment for Disaster Risk Management in EU , EUR 29557 EN. Publications Office of the European Union, Luxembourg, 2019, ISBN 978-92-79-98366-5 (online), doi:10.2760/084707 (online), JRC114650.
- Pöschl, U., 2005. Atmospheric aerosols: composition, transformation, climate and health effects. *Angewandte Chemie International Edition*, 44(46), 7520–7540, <https://doi.org/10.1002/anie.200501122>
- Prospero, J. M., Ginoux, P., Torres, O., Nicholson, S. E., & Gill, T. E., 2002. Environmental characterization of global sources of atmospheric soil dust identified with the Nimbus 7 Total Ozone Mapping Spectrometer (TOMS) absorbing aerosol product. *Reviews of geophysics*, 40(1), 2-1, <https://doi.org/10.1029/2000RG000095>
- Qin Zc, Zhu AX, Pei T, Li BL, Scholten T, Behrens T, Zhou CH (2011) An approach to computing topographic wetness index based on maximum downslope gradient. *Precision Agric* 12:32–43

- Radinović, D., & Ćurić, M. (2012). Criteria for heat and cold wave duration indexes. *Theoretical and Applied Climatology*, 107, 505–510. <https://doi.org/10.1007/s00704-011-0495-8>
- Rahman N, Ansary MA, Islam I (2015) GIS based mapping of vulnerability to earthquake and fire hazard in Dhaka city, Bangladesh. *Int J Disaster Risk Reduct* 13:291–300. <https://doi.org/10.1016/j.ijdrr.2015.07.003>
- Ramana, K. N. S. V., Krishankumar, R., Trzin, M. S., Amritha, P. P., & Pamucar, D. (2022). An Integrated Variance-COPRAS Approach with Nonlinear Fuzzy Data for Ranking Barriers Affecting Sustainable Operations. *Sustainability*, 14(3), 1093. <https://doi.org/10.3390/su14031093>
- Ramis, C., Ramengual, A. 2019. Climate Change Effects on European Heat Waves and Human Health. In: Encyclopedia of the Anthropocene, Vol. 2, 209-216. Dellasala D.A., Goldstein, M.I. (Eds.) Elsevier, ISBN 978-0-12-813576-1, <https://doi.org/10.1016/B978-0-12-809665-9.09798-6>
- Redman, C. L., Grove, J. M., & Kuby, L. H. (2004). Integrating social science into the long-term ecological research (LTER) network: social dimensions of ecological change and ecological dimensions of social change. *Ecosystems*, 7, 161-171.
- Reid M, O'Neill C, Gronlund S, Brines S, Brown D, Diez-Roux A et al (2009) Mapping community determinants of heat vulnerability. *Environ Health Perspect* 117(11):1730–1736
- Rendell, R., Higlett, M., Khazova, M., O'Hagan, J., 2020. "Public Health Implications of Solar UV Exposure during Extreme Cold and Hot Weather Episodes in 2018 in Chilton, South East England", *Journal of Environmental and Public Health*, vol. 2020, Article ID 2589601, 9 pages, 2020. <https://doi.org/10.1155/2020/2589601>
- Rey G, Fouillet A, Bessemoulin P, Frayssinet P, Dufour A, Jouglu E, Hemon D (2009) Heat exposure and socio-economic vulnerability as synergistic factors in heat-wave-related mortality. *Eur J Epidemiol* 24(9):495–502
- Ricci, F.; Casson Moreno, V.; Cozzani, V. A. 2021. Comprehensive Analysis of the Occurrence of Natech Events in the Process Industry. *Process Saf. Environ. Prot.* 2021, 147, 703–713.
- Rinner, C., Patychuk, D., Bassil, K., Nasr, S., Gower, S., & Campbell, M. (2010). The role of maps in neighborhood-level heat vulnerability assessment for the city of Toronto. *Cartography and Geographic Information Science*, 37(1), 31–44. <https://doi.org/10.1559/152304010790588089>
- Robinson, P.J., 2001. On the Definition of a Heat Wave. *Journal of Applied Meteorology and Climatology*, 40, 4, 762-775, [https://doi.org/10.1175/1520-0450\(2001\)040%3C0762:OTDOAH%3E2.0.CO;2](https://doi.org/10.1175/1520-0450(2001)040%3C0762:OTDOAH%3E2.0.CO;2)
- Rocklöv, J., Ebi, K., Forsberg, B., 2011. Mortality related to temperature and persistent extreme temperatures: a study of cause-specific and age-stratified mortality. *Occup Environ Med*, 68(7):531-6, doi: 10.1136/oem.2010.058818.
- Rodopoulou, S., Samoli, E., Analitis, A., Atkinson, R. W., de 'Donato, F. K., & Katsouyanni, K. 2015. Searching for the best modeling specification for assessing the effects of temperature and humidity on health: A time series analysis in three European cities. *International Journal of Biometeorology*, 59(11), 1585–1596. <https://doi.org/10.1007/s00484-015-0965-2>
- Rolfo D. (2009), L'ingannevole banalità della sommatoria, in A. De Rossi (a cura di), Grande Scala. Architettura politica forma, LIST, Barcellona.
- Rolfo D. (2013), "Bassa densità e buone pratiche in Piemonte", *Urbanistica* no. 152.
- Roozbahani, A., Ghased, H., & Hashemy Shahedany, M. (2020). Inter-basin water transfer planning with grey COPRAS and fuzzy COPRAS techniques: A case study in Iranian Central Plateau. *Science of The Total Environment*, 726, 138499. <https://doi.org/10.1016/j.scitotenv.2020.138499>
- Rosén, L., Back, P.-E., Söderqvist, T., Norrman, J., Brinkhoff, P., Norberg, T., Volchko, Y., Norin, M., Bergknut, M., & Döberl, G. (2015). SCORE: A novel multi-criteria decision analysis approach to

assessing the sustainability of contaminated land remediation. *Science of The Total Environment*, 511, 621–638. <https://doi.org/10.1016/j.scitotenv.2014.12.058>

Rossi A., L'architettura della città, Città Studi Edizioni, 1995 (1 ed. 1966).

Rowe C., Koetter F. (1978). *Collage City*, The MIT Press, Cambridge, Massachusetts and London, England.

Roy, B. (1985). *Méthodologie Multicritère d'Aide à la Décision*. Economica, Paris.

Roy, B. (1996) *Multiple Criteria Methodology for Decision Aiding*. Dordrecht: Kluwer Academic.

Roy, B. The outranking approach and the foundations of electre methods. *Theor Decis* 31, 49–73 (1991). <https://doi.org/10.1007/BF00134132>

Roy, S., Pandit, S., Papia, M., Rahman, M., Ocampo, J.C.O.R., Razi, M.A., Fraile-Jurado, P., Ahmed, N., Al-Amin Hoque, M., Hasan, M., Yeasmin, J., Hossain, S. (2021). Coastal erosion risk assessment in the dynamic estuary: The Meghna estuary case of Bangladesh coast. *International Journal of Disaster Risk Reduction*, 61, 102364. <https://doi.org/10.1016/j.ijdr.2021.102364>

Rufat S, Tate E, Burton, C.G., Sayeed Maroof A. (2015) Social vulnerability to floods: review of case studies and implications for measurement. *International Journal of Disaster Risk Reduction*. DOI:10.1016/j.ijdr.2015.09.013.

Russo, M. (2018). Ripensare la resilienza, progettare la città attraverso il suo metabolismo. [Rethinking resilience, design the city through its metabolism] *TECHNE* 15, 39-44. doi: <https://doi.org/10.13128/Techne-23200>

Saaty, T. L. (1980). *The Analytic Hierarchy Process*. McGraw-Hill, New York. <https://doi.org/10.3414/ME10-01-0028>

Saaty, T. L. (1996). *The Analytic Network Process*. RWS Publications.

Saaty, T. L. (2004). Fundamentals of the analytic network process — Dependence and feedback in decision-making with a single network. *Journal of Systems Science and Systems Engineering*, 13(2), 129–157. <https://doi.org/10.1007/s11518-006-0158-y>

Saaty, T. L., & Ozdemir, M. S. (2003). Why the magic number seven plus or minus two. *Mathematical and Computer Modelling*, 38(3–4), 233–244. [https://doi.org/10.1016/S0895-7177\(03\)90083-5](https://doi.org/10.1016/S0895-7177(03)90083-5)

Sabatini, A.M. (2000). Analysis of postural sway using entropy measures of signal complexity, *Med. Biol. Eng. Comput.* 38, 617e624.

Sadhukhan, B., Chakraborty, S., & Mukherjee, S. (2022). Investigating the relationship between earthquake occurrences and climate change using RNN-based deep learning approach. *Arabian Journal of Geosciences*, 15(1), 31. <https://doi.org/10.1007/s12517-021-09229-y>

Salehi, A., Izadikhah, M. (2014). A novel method to extend SAW for decision-making problems with interval data. *Decision Science Letters*, 3(2), 225-236.

Sambo, B., Bonato, M., Sperotto, A., Torresan, S., Furlan, E., (2023) Framework for multirisk climate scenarios across system receptors with application to the Metropolitan City of Venice, Risk Analysis. DOI: 10.1111/risa.14097

Sanders, A. F. J., De Haan, J. F., Sneep, M., Apituley, A., Stammes, P., Vieitez, M. O., ... & Veefkind, J. P. (2015). Evaluation of the operational Aerosol Layer Height retrieval algorithm for Sentinel-5 Precursor: application to O2 A band observations from GOME-2A. *Atmospheric Measurement Techniques*, 8(11), 4947-4977. <https://doi.org/10.5194/amt-8-4947-2015>

Sangiorgio, V., Fiorito, F., & Santamouris, M. (2020). Development of a holistic urban heat island evaluation methodology. *Scientific Reports*, 10(1), 17913. <https://doi.org/10.1038/s41598-020-75018-4>

- Sangkakool, T., Techato, K., Zaman, R., & Brudermann, T. (2018). Prospects of green roofs in urban Thailand – A multi-criteria decision analysis. *Journal of Cleaner Production*, 196, 400–410. <https://doi.org/10.1016/j.jclepro.2018.06.060>
- Sassen, S. (2008). Urban sociology in the 21st century. In C.D. Bryant & D.L. Peck (Eds.) 21st century sociology (pp. 476–486). Thousand Oaks: Sage Publications, Inc, USA.
- Satheesh, S. K. 2012. Atmospheric chemistry and climate. *Current Science*, 426–439.
- Scaini, C., Peresan, A., Tamaro, A., Poggi, V., & Barnaba, C. (2022). Can high-school students contribute to seismic risk mitigation? Lessons learned from the development of a crowd-sourced exposure database. *International Journal of Disaster Risk Reduction*, 69, 102755.
- Schanze, J. 2018. Pluvial Flood Risk Management: An Evolving and Specific Field. *J. Flood Risk Manag.* 2018, 11, 227–229.
- Scheuer, S., Dagmer, H., Volk, M., in Añel, J.A., (Eds.) (2017) Integrative assessment of climate change for fast-growing urban areas: Measurement and recommendations for future research, PLOS ONE, Volume 12 (12). DOI: 10.1371/journal.pone.0189451
- Schmarzow A. (1894). *Das Wesen der architektonischen Schöpfung*, Karl W. Hiersemann, Leipzig.
- Schmidtlein, M. C., Deutsch, R. C., Piegorsch, W. W., & Cutter, S. L. (2008). A sensitivity analysis of the social vulnerability index. *Risk Analysis*, 28(4), 1099–1114. <https://doi.org/10.1111/j.1539-6924.2008.01072.x>
- Schröder U. (2015). *Pardié. Konzept für eine Stadt nach dem Zeitregime der Moderne*, Köln: Verlag der Buchhandlung Walther König.
- Schröder U. (2023). *Pardié. Idea per una città dopo il regime temporale del Moderno*, edited by Carofiglio N. and Storch M., Firenze: Aión Edizioni.
- Schwarz, N. (2010). Urban form revisited—Selecting indicators for characterising European cities. *Landscape and Urban Planning*, 96(1), 29–47. <https://doi.org/10.1016/j.landurbplan.2010.01.007>
- Schweighofer JAV, Wehrl M, Baumgärtel S, Rohn J., 2021. Calculating Energy and Its Spatial Distribution for a Subsurface Urban Heat Island Using a GIS-Approach. *Geosciences* 11(1):24. <https://doi.org/10.3390/geosciences11010024>
- Secchi B. (2000), *Prima lezione di urbanistica*, Laterza, Roma-Bari.
- Secchi B., *La città del XX secolo*, editori Laterza, Bari 2005.
- Secchi B., *Prima lezione di urbanistica*, editori Laterza, Bari 2004.
- Seidl, D., & Becker, K. H. (Eds.). (2005). *Niklas Luhmann and organization studies* (Vol. 14). Malmö: Liber.
- Seleem, O., Heistermann, M., Bronstert, A. 2021. Efficient Hazard Assessment for Pluvial Floods In Urban Environments: A Benchmarking Case Study for the City of Berlin, Germany. *Water* 2021, 13, 2476. <https://doi.org/10.3390/w13182476>
- Semenza, J.C., Paz, S., 2021. Climate change and infectious disease in Europe: Impact, projection and adaptation. *Series Review VOLUME 9*, 100230, OCTOBER 2021, <https://doi.org/10.1016/j.lanepe.2021.100230>
- Sen M.K., Dutta S., Kabir G., Pujari N.N., Laskar S.A. (2021). An integrated approach for modelling and quantifying housing infrastructure resilience against flood hazard. *J. Clean. Prod.*, 288, Article 125526, 10.1016/j.jclepro.2020.125526
- Serafim, M. B., Siegle, E., Corsi, A. C., & Bonetti, J. (2019). Coastal vulnerability to wave impacts using a multi-criteria index: Santa Catarina (Brazil). *Journal of Environmental Management*, 230, 21–32. <https://doi.org/10.1016/j.jenvman.2018.09.052>

- Sferratore, A., Verde, S., Dell'Acqua, F., and Losasso, M.: From critical urban context to heatwave-related hotspot. An exposure-based application for a study case in the metropolitan area of Naples, EGU General Assembly 2024, Vienna, Austria, 14–19 Apr 2024, EGU24-18465, <https://doi.org/10.5194/egusphere-egu24-18465>, 2024.
- Shahabi, H., Khezri, S., Ahmad, B.B., Hashim, M., 2014. Landslide susceptibility mapping at central Zab basin, Iran: a comparison between analytical hierarchy process, frequency ratio and logistic regression models. *Catena* 115, 55–70.
- Shannon, C.E. (1949). Communication theory of secrecy systems, *Bell Syst. Tech. J.* 28, 656e715.
- Shannon, C.E. (2001). A mathematical theory of communication, *ACM SIGMOB - Mob. Comput. Commun. Rev.* (5), 3e55.
- Shaposhnikov, D. et al., 2014. Mortality Related to Air Pollution with the Moscow Heat Wave and Wildfire of 2010. *Epidemiology* 25(3):p 359-364 DOI: 10.1097/EDE.0000000000000090
- Sharifi, A., Roosta, M., & Javadpoor, M. (2021). Urban Form Resilience: A Comparative Analysis of Traditional, Semi-Planned, and Planned Neighborhoods in Shiraz, Iran. *Urban Science*, 5(1), 18. <https://doi.org/10.3390/urbansci5010018>
- Shepherd, Theodore G., Emily Boyd, Raphael A. Calel, Sandra C. Chapman, Suraje Dessai, Ioana M. Dima-West, Hayley J. Fowler, et al. 2018. “Storylines: An Alternative Approach to Representing Uncertainty in Physical Aspects of Climate Change.” *Climatic Change* 151 (3–4): 555–71. <https://doi.org/10.1007/s10584-018-2317-9>.
- Sheridan, S. C., & Dixon, P. G. (2017). Spatiotemporal trends in human vulnerability and adaptation to heat across the United States. *Anthropocene*, 20, 61–73. <https://doi.org/10.1016/j.ancene.2016.10.001>
- Shoji, G. and Moriyama, T. 2007. Evaluation of the Structural Fragility of a Bridge Structure Subjected to a Tsunami Wave Load, *J. Nat. Disaster Sci.*, 29, 73–81, 2007
- Sidiqui, P., Roös, P.B., Herron, M. et al., 2022. Urban Heat Island vulnerability mapping using advanced GIS data and tools. *J Earth Syst Sci* 131, 266. <https://doi.org/10.1007/s12040-022-02005-w>
- Sillmann, Jana, Theodore G. Shepherd, Bart Van Den Hurk, Wilco Hazeleger, Olivia Martius, Julia Slingo, and Jakob Zscheischler. 2021. “Event-Based Storylines to Address Climate Risk.” *Earth’s Future* 9 (2). <https://doi.org/10.1029/2020EF001783>
- Siu, C.Y., et al., 2023. Evaluating thermal resilience of building designs using building performance simulation – A review of existing practices. *Building and Environment*, 234, 110124, <https://doi.org/10.1016/j.buildenv.2023.110124>
- Smith ML, Hardeman RR., 2020. Association of Summer Heat Waves and the Probability of Preterm Birth in Minnesota: An Exploration of the Intersection of Race and Education. *International Journal of Environmental Research and Public Health*, 17(17):6391. <https://doi.org/10.3390/ijerph17176391>
- Smith, B. J., Gomez-Heras, M., & McCabe, S., 2008. Understanding the decay of stone-built cultural heritage. *Progress in Physical Geography: Earth and Environment*, 32(4), 439-461. <https://doi.org/10.1177/0309133308098119>
- Sorooshian, S. (2018). Group decision making with unbalanced-expertise. Paper presented at the *Journal of Physics: Conference Series*, 1028(1), doi:10.1088/1742-6596/1028/1/012003.
- Sperotto, A., Torresan, S., Gallina V., Coppola, E., Critto, A., Marcomini, A., (2016) A multi-disciplinary approach to evaluate pluvial floods risk under changing climate: The case study of the municipality of Venice (Italy), *Science of The Total Environment*, Volume 562, pp. 1031-1043. DOI: <https://doi.org/10.1016/j.scitotenv.2016.03.150>
- Staiger, H., Laschewski, G., Grätz, A., 2012. The perceived temperature - a versatile index for the assessment of the human thermal environment. Part A: scientific basics. *Int J Biometeorol*, 56(1):165-76, doi: 10.1007/s00484-011-0409-6, DOI: 10.1007/s00484-011-0409-6

- Stedman, J.R., Grice, S., Kent, A., Cooke, S., 2008. GIS-based models for ambient PM exposure and health impact assessment for the UK. Inhaled Particles X, (23–25 September 2008, Manchester), Journal of Physics: Conference Series 151 (2009) 012002, doi:10.1088/1742-6596/151/1/012002
- Stefano, N. M., Casarotto Filho, N., Garcia Lupi Vergara, L., & Garbin da Rocha, R. U. (2015). COPRAS (Complex Proportional Assessment): state of the art research and its applications. *IEEE Latin America Transactions*, 13(12), 3899–3906. <https://doi.org/10.1109/TLA.2015.7404925>
- Stewart, I. D., Oke, T. R., (2012), Local Climate Zones for urban temperature studies. Bulletin of the American Meteorological Society, 1879-1900. DOI: 10.1175/BAMS-D-11-00019.1
- Stillman, J. H. (2019). Heat waves, the new normal: Summertime temperature extremes will impact animals, ecosystems, and human communities. *Physiology*, 34(2), 86–100. <https://doi.org/10.1152/physiol.00040.2018>
- Stoyanov D, Nedkov I, Groudeva V, Cherkezova-Zheleva Z, Grigorov I, Kolarov G, et al., 2020. Long-Distance LIDAR Mapping Schematic for Fast Monitoring of Bioaerosol Pollution over Large City Areas [Internet]. Atmospheric Air Pollution and Monitoring. IntechOpen; Available from: <http://dx.doi.org/10.5772/intechopen.87031>
- Stucchi, M., Akinci, A., Faccioli, E., Gasperini, P., Malagnini, L., Meletti, C., Montaldo, V., Valensise, G. 2004. Mappa di Pericolosità sismica del territorio Nazionale http://zones.ismic.he.mi.ingv.it/documenti/rapporto_conclusivo.pdf (in italian).
- Stucchi, M., Meletti, C., Montaldo, V., Crowley, H., Calvi, G.M., Boschi, E. 2011. Seismic hazard assessment (2003-2009) for the Italian building code. *Bull Seism Soc of Am* 101:1885–1911.
- Sun, X., Sun, Q., Zhou, X., Li, X., Yang, M., Yu, A., & Geng, F. (2014). Heat wave impact on mortality in Pudong New Area, China in 2013. *Science of the Total Environment*, 493, 789–794. <https://doi.org/10.1016/j.scitotenv.2014.06.042>
- Swart, R., Fons, J., Geertsema, W., van Hove, B., Gregor, M., Havranek, M., & Peltonen, L. (2012). *Urban Vulnerability Indicators: A Joint Report of ETC-CCA and ETC-SIA*.
- Tabatabaee, S., Mahdiyar, A., Durdyev, S., Mohandes, S. R., & Ismail, S. (2019). An assessment model of benefits, opportunities, costs, and risks of green roof installation: A multi criteria decision making approach. *Journal of Cleaner Production*, 238, 117956. <https://doi.org/10.1016/j.jclepro.2019.117956>
- Thom EC 1959: The discomfort index. *Weatherwise* 12.2: 57-61.
- Tan X.R., Deng J.L. (1995). Grey correlation analysis: A new method of multi factor statistical analysis. *Stat. Res.*, 12, 46–48.
- Tanim, A. H., Goharian, E., & Moradkhani, H. (2022). Integrated socio-environmental vulnerability assessment of coastal hazards using data-driven and multi-criteria analysis approaches. *Scientific Reports*, 12(1), 11625. <https://doi.org/10.1038/s41598-022-15237-z>
- Thierry, P., Stieltjes, L., Kouokam, E., Nguya, P., Salley, P. M. 2008. Multi-hazard risk mapping and assessment on an active volcano: the GRINP project at Mount Cameroon. *Natural Hazards* 45: 429–456.
- Thurstain M, Batty M, Hacklay M, Lloyd D, Bodt R, Hyman A, Batty S, Tomalin C, Cadell C, Falk N, Sheppard S, Curtis S (2001) Producing boundaries and statistics for town centres. CASA, Center for Advanced Spatial Analysis, London
- Thurstain M, Goodwin DU (2000) Defining and Delineating the central areas of towns for statistical monitoring using continuous surface representations, paper 18. Centre for Advanced Spatial Analysis, London
- Tingsanchali, T., & Promping, T. (2022). Comprehensive Assessment of Flood Hazard, Vulnerability, and Flood Risk at the Household Level in a Municipality Area: A Case Study of Nan Province, Thailand. *Water*, 14(2), 161. <https://doi.org/10.3390/w14020161>

- Tocchi, G. 2023. *Multi-risk assessment for disaster risk reduction: a framework for integrating physical, social and multi-hazard dimensions*. PhD Thesis. University of Naples Federico II, Naples.
- Tocchi, G., Pittore, M., Polese, M. (2025), Identifying urban and rural settlement archetypes: clustering for enhanced risk-oriented exposure and vulnerability analysis, *Natural Hazards and Earth System Sciences*, in press (pre-print available at [10.5194/egusphere-2025-908](https://doi.org/10.5194/egusphere-2025-908))
- Tu, Y., Zhao, Y., Li, Z., Liu, L., & Shen, W. (2023). Regional flood resilience grading based on GEM-AHPSort II method: An objective and managerial factors integrated perspective. *International Journal of Disaster Risk Reduction*, 93, 103766. <https://doi.org/10.1016/j.ijdr.2023.103766>
- Tuomimaa, J., Käyhkö, J., Juhola, S., Räsänen, A., 2023. Developing adaptation outcome indicators to urban heat risks. *Climate Risk Management*, 41, 100533, <https://doi.org/10.1016/j.crm.2023.100533>
- Turchetti, G. (2023). Rome Local Climate Zone (RLCZ): decision-making support tool for the historical city. *TECHNE - Journal of Technology for Architecture and Environment*, (25), 173–181. <https://doi.org/10.36253/techne-13715>
- Turner, J. 2016. "Air Pollution Exposure Indicators: Review of Ground-Level Monitoring Data Availability and Proposed Calculation Method", OECD Green Growth Papers, No. 2016/01, OECD Publishing, Paris, <https://doi.org/10.1787/5jlsqs98gss7-en>.
- UNDRR, 2016, Report of the open-ended intergovernmental expert working group on indicators and terminology relating to disaster risk reduction, <https://www.unisdr.org/we/inform/publications/51748>.
- UN-HABITAT, (2011) *Cities and Climate Change: Global Report on Human Settlements 2011*, Gutenberg Press, Malta. ISBN Number (Volume): 978-92-1-132298-9
- UNISDR, 2009, United Nations International Strategy for Disaster Risk Reduction, Terminology on disaster risk reduction, Geneva.
- UNISDR, 2018. Terminology. <https://www.unisdr.org/we/inform/terminology#letter-u>.
- Van Der Veen A, Logtmeijer C (2005) Economic hotspots: visualizing vulnerability to flooding. *Nat Hazards* 36(1–2):65–80
- Vaneckova, P., Neville, G., Tippet, V., Aitken, P., FitzGerald, G., & Tong, S. 2011. Do biometeorological indices improve modeling outcomes of heat-related mortality? *Journal of Applied Meteorology and Climatology*, 50(6), 1165–1176. <https://doi.org/10.1175/2011JAMC2632.1>
- Verde, S. (2024). “Enhancing climate adaptation design in urban areas: a workflow for climate integrated impact assessment”. *IOP Conf. Ser.: Earth Environ. Sci.* **1402** 012059, DOI 10.1088/1755-1315/1402/1/012059
- Verde, S., Bassolino, E. & Gagliardi, U. (2021). Applicazione di processi di data analysis e data exchange tra strumenti GIS-Based e parametric design tools per la generazione di carte di resilienza climatica del sistema degli spazi aperti urbani. In Sessa F., Di Martino F. & Cardone B. (Eds.), *GISDAY 2020_ Il GIS per la gestione del governo e del territorio - Strumenti e tecnologie GIS di supporto alle decisioni per l'analisi e la gestione complessa dei Sistemi Territoriali, Infrastrutturali ed Urbani*. Areccia (RM): Aracne Editore.
- Verde, S., Clemente, M. F., D'Ambrosio, V., and Losasso, M. (2024). “Multi-hazard conditions in urban settlements: a framework for heatwave and flooding integrated impacts assessment to support climate-oriented design”. *EGU General Assembly 2024*, Vienna, Austria, 14–19 Apr 2024, EGU24-11276, <https://doi.org/10.5194/egusphere-egu24-11276>, 2024.
- Wai, K-M., et al., 2017. Aerosol pollution and its potential impacts on outdoor human thermal sensation: East Asian perspectives. *Environmental Research* 158, October 2017, Pages 753-758, <https://doi.org/10.1016/j.envres.2017.07.036>

- Walker B.B., Schuurman N., Swanlund D., Clague J.J. (2021). GIS-based multicriteria evaluation for earthquake response: a case study of expert opinion in Vancouver, Canada. *Nat Hazards* 105(2):2075–2091. <https://doi.org/10.1007/s11069-020-04390-1>
- Wang Y., Fang Z.C., Hong H.Y., Peng L. (2020). Flood susceptibility mapping using convolutional neural network frameworks *J. Hydrol.*, 582, Article 124482, 10.1016/j.jhydrol.2019.124482
- Wang, J., Williams, G, Guo, Y, Pan, X, Tong, S. 2013. Maternal exposure to heatwave and preterm birth in Brisbane, Australia. *BJOG* 2013; DOI 10.1111/1471-0528.12397.
- Wang, L., Tian, Y., Kim, J., & Yin, H. (2019). The key local segments of human body for personalized heating and cooling. *Journal of Thermal Biology*, 81(19), 118–127. <https://doi.org/10.1016/j.jtherbio.2019.02.013>
- Wang, T., & Chang, T. (2005). Fuzzy VIKOR as an aid for multiple criteria decision making. *Engineering Digital Transformation: Proceedings of the 11th International Conference on Industrial Engineering and Industrial Management*, 352–356. <https://www.worldcat.org/it/title/engineering-digital-transformation-proceedings-of-the-11th-international-conference-on-industrial-engineering-and-industrial-management/oclc/1054092775>
- Wang, XY., Barnett, A., Guo, YM. et al., 2014. Increased risk of emergency hospital admissions for children with renal diseases during heatwaves in Brisbane, Australia. *World J Pediatr* 10, 330–335 (2014). <https://doi.org/10.1007/s12519-014-0469-x>
- Wei, X., Chang, N. B., Bai, K., & Gao, W. (2020). Satellite remote sensing of aerosol optical depth: Advances, challenges, and perspectives. *Critical Reviews in Environmental Science and Technology*, 50(16), 1640–1725, <https://doi.org/10.1080/10643389.2019.1665944>
- White, P., Pelling, M., Sen, K., Seddon, D., Russell, S., & Few, R. (2005). *Disaster Risk Reduction: A Development Concern*. DFID.
- WHO, 2013. Health risks of air pollution in Europe: HRAPIE project: new emerging risks to health from air pollution: results from the survey of experts. Centre for Environment & Health (BON), Living & Working Environments (LWE), Available online at: <https://www.who.int/europe/publications/i/item/WHO-EURO-2013-6696-46462-67326>, last accessed 17 November 2023
- WHO, 2021. WHO global air quality guidelines: particulate matter (PM_{2.5} and PM₁₀), ozone, nitrogen dioxide, sulfur dioxide and carbon monoxide. Air quality and health, Centre for Environment & Health (BON), Environment, Climate Change and Health, Guidelines Review Committee, WP - Asia-Pacific Centre for Environment and Health in WPR (ACE), 290 pp, ISBN: 9789240034228, Available online at <https://www.who.int/publications/i/item/9789240034228>, last accessed 17 November 2023
- Wilhelmi, O. V. and Hayden, M. H. (2010). Connecting people and place: A new framework for reducing urban vulnerability to extreme heat. *Environmental Research Letters*, 5(1), 1–7.
- Williams, H., Wilson, T.M., Horspool, N., Paulik, R., Wotherspoon, L., Lane, E.M., and Hughes, M.W. 2020. *Assessing transportation vulnerability to tsunamis: utilizing post-event field data from the 2011 Tōhoku tsunami, Japan, and the 2015 Illapel tsunami, Chile*. *Nat. Hazards Earth Syst. Sci.*, 20, 451–470, 2020. <https://doi.org/10.5194/nhess-20-451-2020>
- Wilson, E.O. (1992). *The diversity of life*. Cambridge, MA: Belknap Press.
- Wipulanusat, W., Nakrod, S., Prabnarong, P., 2009. Multi-hazard risk assessment using GIS and RS applications: a case study of Pak Phanang Basin, Walailak, *Journal of Science Technologies*, 6 (1), 109–125. DOI: 10.2004/wjst.v6i1.76
- Witherspoon, J.M. and Goldman, R.F., 1974. Indices for thermal stress. *ASHRAE Bull.*, No. LO-73-8: 5-13

- Wondmagegn, B.Y., et al., 2019. What do we know about the healthcare costs of extreme heat exposure? A comprehensive literature review. *Science of the Total Environment*, 657, 606-618, <https://doi.org/10.1016/j.scitotenv.2018.11.479>
- Wu, T. and Boor, B. E., 2021. Urban aerosol size distributions: a global perspective, *Atmos. Chem. Phys.*, 21, 8883–8914, <https://doi.org/10.5194/acp-21-8883-2021>
- Xie, K., Mei, Y., Gui, P., & Liu, Y. (2019). Early-warning analysis of crowd stampede in metro station commercial area based on internet of things. *Multimedia Tools and Applications*. <https://doi.org/10.1007/s11042-018-6982-5>
- Xu, J., Yin, X., Chen, D., An, J., & Nie, G. (2016). Multi-criteria location model of earthquake evacuation shelters to aid in urban planning. *International Journal of Disaster Risk Reduction*, 20, 51–62. <https://doi.org/10.1016/j.ijdr.2016.10.009>
- Xu, K., Zhuang, Y., Yan, X., Bin, L., & Shen, R. (2023). Real options analysis for urban flood mitigation under environmental change. *Sustainable Cities and Society*, 93, 104546. <https://doi.org/10.1016/j.scs.2023.104546>
- Yan, X., Zhanqing Li, Wenzhong Shi, Nana Luo, Taixia Wu, Wenji Zhao, An improved algorithm for retrieving the fine-mode fraction of aerosol optical thickness, part 1: Algorithm development, *Remote Sensing of Environment*, Volume 192, 2017, Pages 87-97, ISSN 0034-4257, <https://doi.org/10.1016/j.rse.2017.02.005>.
- Yang X, Li L, Wang J, Huang J, Lu S (2015) Cardiovascular mortality associated with low and high temperatures: determinants of interregion vulnerability in China. *Int J Environ Res Public Health* 12(6): 5918–1933.
- Yang, Z. X. (2013). Monitoring coastline changes and tidal flat reclamation in jiangsu using remote sensing technology. *Yellow River*, 1, 85–87. doi: 10.3969/j.issn.1000-1379.2013.01.027
- Yao, W., Yao, D., Guo, D., Wang, J. (2020). Shannon entropy and quantitative time irreversibility for different and even contradictory aspects of complex systems, *Appl. Phys. Lett.* 116 (1), 014101.
- Yoon, D. 2012. Assessment of social vulnerability to natural disasters: A comparative study. *Natural Hazards* 63(2): 823–843.
- Yu, J., Castellani, K., Forsysinski, K. et al., 2021. Geospatial indicators of exposure, sensitivity, and adaptive capacity to assess neighbourhood variation in vulnerability to climate change-related health hazards. *Environ Health* 20, 31, <https://doi.org/10.1186/s12940-021-00708-z>
- Yu, M., Yang, C., & Li, Y. (2018). Big Data in Natural Disaster Management: A Review. *Geosciences*, 8(5), 165. <https://doi.org/10.3390/geosciences8050165>
- Yuan, C. S., Lee, C. G., Liu, S. H., Chang, J. C., Yuan, C., & Yang, H. Y. (2006). Correlation of atmospheric visibility with chemical composition of Kaohsiung aerosols. *Atmospheric Research*, 82(3-4), 663-679. <https://doi.org/10.1016/j.atmosres.2006.02.027>
- Zabeo, A., Pizzol, L., Agostini, P., Critto, A., Giove, S., & Marcomini, A. (2011). Regional risk assessment for contaminated sites Part 1: Vulnerability assessment by multicriteria decision analysis. *Environment International*, 37(8), 1295–1306. <https://doi.org/10.1016/j.envint.2011.05.005>
- Zanella P. (a cura di), *Morfologia dello spazio urbano*, Franco Angeli, Milano 1988.
- Zare, S., N. Hasheminejad, H. Shirvan, R. Hemmatjo, K. Sarebanzade and S. Ahmadi, 2018. Comparing Universal Thermal Climate Index (UTCI) with selected thermal indices/environmental parameters during 12 months of the year. *Weather and Climate Extremes*, 19:49-57, <https://doi.org/10.1016/j.wace.2018.01.004>

- Zavadskas, E., & Kaklauskas, A. (2002). Determination of an efficient contractor by using the new method of multicriteria assessment. In *The Organization and Management of Construction* (94–104). Routledge.
- Zebisch, Marc, Stefano Terzi, Massimiliano Pittore, Kathrin Renner, and Stefan Schneiderbauer. 2022. "Climate Impact Chains—A Conceptual Modelling Approach for Climate Risk Assessment in the Context of Adaptation Planning." In *Climate Adaptation Modelling*, edited by Claus Kondrup, Paola Mercogliano, Francesco Bosello, Jaroslav Mysiak, Enrico Scoccimarro, Angela Rizzo, Rhian Ebrey, Marleen de Ruiter, Ad Jeuken, and Paul Watkiss, 217–24. Springer Climate. Cham: Springer International Publishing. https://doi.org/10.1007/978-3-030-86211-4_25
- Zevi B. (1948). *Saper vedere l'architettura*, Torino: Einaudi.
- Zhang, Y. (2013). Urban metabolism: A review of research methodologies. *Environmental pollution*, 178, 463–473.
- Zhang, Y., et al., 2021. Satellite remote sensing of atmospheric particulate matter mass concentration: Advances, challenges, and perspectives. *Fundamental Research* 1, 3, 240–258, <https://doi.org/10.1016/j.fmre.2021.04.007>
- Zhu, Q., Liu, T., Lin, H., Xiao, J., Luo, Y., Zeng, W., ... Baum, S. (2014). The spatial distribution of health vulnerability to heat waves in Guangdong Province, China. *Global Health Action*, 7, 1–10.
- Zhu, S., Li, D., Huang, G., Chhipi-Shrestha, G., Nahiduzzaman, K. M., Hewage, K., & Sadiq, R. (2021). Enhancing urban flood resilience: A holistic framework incorporating historic worst flood to Yangtze River Delta, China. *International Journal of Disaster Risk Reduction*, 61, 102355. <https://doi.org/10.1016/j.ijdrr.2021.102355>
- Zuccaro, G., Cacace, F., Spence, R. & Baxter, P. 2008. Impact of explosive eruption scenarios at Vesuvius. *Journal of Volcanology and Geothermal Research* 178, 416–453.
- Zuo, J., Pullen, S., Palmer, J., et al., 2015. Impacts of heat waves and corresponding measures: a review. *Journal of Cleaner Production*, 92, 1, 1–12, <https://doi.org/10.1016/j.jclepro.2014.12.078>

Cartographic documents

- Carafa, G., (1775) *Mappa topografica della città di Napoli e de' suoi contorni*, Napoli.
- Serra, M. (Eds.) (2022), *LA NUOVA TOPOGRAFIA DI ROMA DI GIAMBATTISTA NOLLI - 1748* (Con L'indice Dei Numeri E L'indice Alfabetico Della Pianta), Edizioni Magna Grecia.

Authors contribution

Even if the Deliverable are unified in their aspects of conception, knowledge framework, methodological approach and experimentation, the contributions have been elaborated as follows:

- "1. Introduction" Mario Losasso, Paola Vannucchi, Maria Polese;
- "2.1. Urban and Metropolitan Settlements: systemic approach and multi-scalar urban components" e "2.1.1. The District scale" Mario Losasso, Maria Fabrizia Clemente;
- "2.2. Hazard, vulnerability and exposure of urban systems" Maria Polese, Gabriella Tocchi, Dario Massabò, Paolo Prati;
- "2.3. From the concept of exposure to integrated exposure", "2.3.1. Definitions and integration factors for exposure under multi-risk conditions", "2.3.2. Vulnerability aspects in characterizing exposure" Mario Losasso, Maria Polese, Gabriella Tocchi;
- "2.3.3. Typo-morphological aspects of urban settlements considering integrated exposure factors", "2.3.3.1. Characteristics of urban settlements", "2.3.3.2. Urban analysis" Bruna Di Palma, Paola Galante, Federica Visconti, Marilena Bosone;
- "2.4. Metrics, index and indicator", "2.4.1. Metrics, index and GIS-based indicators" - Ferdinando Di Martino, Valeria D'Ambrosio, Maria Fabrizia Clemente, Vittorio Miraglia;
- "2.5. Multi-criteria approaches for exposure assessment", "2.5.1. Heat wave", "2.5.2. Flooding", "2.5.3. Coastal erosion", "2.5.4. Earthquake" Pasquale De Toro, Martina Bosone;
- "3.1.1. The urban physical system" Sara Verde, Antonio Sferratore;
- "3.1.2. The socio-ecological systems" Annamaria Zaccaria, Gabriella Tocchi, Antonino Rapicano;
- "3.1.3. The geo-morphological system" Paola Vannucchi, Daniele Maestrelli;
- "3.1.4. Settlement models", "3.1.4.1. Combination of layout patterns and morphological variations of settlements", "3.2. Characterization of urban settlements: typo-morphological, environmental and spatial-functional analysis" Bruna Di Palma, Paola Galante, Marilena Bosone;
- "3.3. Identification of recurring urban patterns of buildings and open spaces", "3.3.1. Buildings", "3.3.2. Open spaces", "3.3.3. Definition of an algorithm in a GIS environment for the recognition of recurring urban patterns in urban settlements" Valeria D'Ambrosio, Enza Tersigni, Sara Verde;
- "3.3.4 Urban settlements knowledge through integrated taxonomies: the contribution of Local Climate Zones" Antonio Sferratore, Vittorio Miraglia;
- "3.4. A clustering proposal of existing urban settlements" Maria Polese, Gabriella Tocchi, Andrea Prota;
- "3.5. The impending hazards in urban context" Sara Verde, Antonio Sferratore;
- "3.5.1. Score-based procedure for the identification of relevant hazards" Maria Polese, Gabriella Tocchi, Carlo Del Gaudio, Antonella Peresan;
- "3.6. Citizen-centered exposure data collection for multi-risk exposure development" Antonella Peresan, Chiara Scaini;
- "4.1. Urban critical context and hotspot identification criteria", "4.1.1. Challenges and methods to hotspot assessment", "4.1.2. Relevant implications for hotspot assessment" Mario Losasso, Antonio Sferratore, Maria Fabrizia Clemente, Sara Verde;
- "4.2. The use of indicators to identify urban critical context/hotspots taking into account heatwaves and air pollution", "4.2.1. Heatwave", "4.2.2. Aerosol pollution", "4.2.3. Relevant indicators to characterize heat waves and aerosol pollution hazards and exposure", "4.2.4. Composite effect of heat waves and air pollution" Tiziano Maestri, Federico Porcù, Erika Brattich, Giorgia Proietti Pelliccia, Shirzad Mohammad Reza;
- "4.3. Hotspot example identification and assessment using GIS based approaches", "4.3.1. Identification of flooding risk hotspots" Francesco De Paola, Giuseppe Speranza;
- "4.3.2. Identification of heatwave risk hotspots", "4.3.3. An example of heatwave hotspot assessment" Mario Losasso;
- "5.1. Composite indicators", "5.1.1. Identification of Critical Urban Context or HotSpot using multi-risk composite-index", "5.1.2. Step-by-step methodology to identify Critical Urban Contexts (CUC) or HotSpots (HS) within an urban settlement", "5.1.2.1. Example application for identification of CUC", "5.1.3. Selecting relevant sub-indicators: the use of risk storylines", "5.1.3.1. Example application for the construction of composite-index based on risk-storyline" Maria Polese, Gabriella Tocchi,
- "5.1.2.2. Example application for identification of HS" Mario Losasso, Sara Verde;

5.2. Multi-criteria Decision Analysis as a tool supporting effective risk management” Pasquale De Toro, Martina Bosone.